Doctoral Dissertation

Automatic Berthing Control Practically Applicable under Wind Disturbances

(風外乱作用下において実用的に適用可能な自動着桟制御に関する研究)

Yaseen Adnan Ahmed

June 2015

Graduate School of Engineering,

Osaka University

Automatic Berthing Control Practically Applicable under Wind Disturbances

(風外乱作用下において実用的に適用可能な自動着桟制御に関する研究)

By

Yaseen Adnan Ahmed

A Dissertation Submitted to the Department of Naval Architecture and Ocean Engineering, Graduate School of Engineering, Osaka University, in Partial Fulfillment of the Requirements for the Degree of

Doctor of Engineering

June 2015

Supervised by

Professor Kazuhiko Hasegawa

TABLE OF CONTENTS

NOMENCLATURE

A_R	Rudder area
A_L	Lateral projected area
A_T	Transverse projected area
A_{OD}	Lateral projected area of superstructure + other tanks on deck
A_{Ref}	Effective rudder area ratio
ANN	Artificial Neural Network
A_n, A_m	Activation value of a unit *n* and *m* in hidden layer, respectively
a_H	Ratio of lateral force induced on hull by rudder to rudder normal force
B	Breath of a ship
b	Breath of a rudder
b_n, b_m	Threshold value of a unit *n* and *m* in the hidden layer, respectively
b_l	Threshold value of a unit *l* in the output layer
CLR	Centre of lateral resistance
C	Distance from midship to centroid of lateral projected area
CG	Centre of gravity
C_{BR}	Distance from midship to centre of superstructure area
C_X	Coefficient of fore and aft component of wind force
C_Y	Coefficient lateral component of wind force
C_N	Coefficient of wind-induced yawing moment
C_1, C_2, C_3	Coefficients for PID controller
DCPA	Distance of the closest point of approach
DCPA'	Non-dimensionalised value of *DCPA*

d_H	Draught moulded at midship
D_p	Propeller diameter
d_1	Distance to imaginary line
d_2	Remained distance to berthing point
e	Vector of network errors
f	Rudder normal force coefficient
F_N	Rudder normal force
GPS	Global positioning system
g	Gravity acceleration
h	Rudder height
H_{BR}	Height from load water line to top of superstructure
H_C	Height to the centre of lateral projected area
I_O	Activation value of a unit o in the input layer
I_{zz}	Mass moment of inertia
J_{zz}	Added mass moment of inertia
J	Advance of propeller ($= u_P/nD_P$)
J_m	Jacobian matrix
k	A constant above water surface
K_T	Thrust coefficient
K_n	Gain constant
L_{pp}	Ship length between perpendiculars
L_{OA}	Length overall
MSE	Mean squared error
M	An assigned integer number
m_x	Added mass in surge direction
m_y	Added mass in sway direction
n	Engine revolution per second
NLP	Nonlinear programming
N_W	Yawing moment due to wind force
O_l	Activation value of a unit l in the output layer
P	Pitch at 0.7 R

p	Pitch ratio at 0.7 R
s	Scale
S_a	Wetted surface area
sg	Sigmoid function
T_u	Time constant
$TCPA$	Time to closes point of approach
$TCPA'$	Non-dimensionalised value of TCPA
T	Propeller thrust force
t_p	Effective thrust deduction factor
u	Surge velocity
$U(t)$	Ship speed
U_{10}	Average wind velocity at 10m high above water surface
U_R	Effective relative inflow velocity to rudder
u_R	Effective relative inflow velocity in longitudinal to rudder
u_P	Effective relative inflow velocity in longitudinal to propeller
v	Sway velocity
V_R	Relative wind speed
W	Point of influence of wind
$W_{n,o}$	Weight on the link form unit o to unit n
$W_{m,n}$	Weight on the link form unit n to unit m
$W_{l,m}$	Weight on the link form unit m to unit l
w_p	Effective wake fraction on straight running
$X_{0m} \sim X_{5m}$, $Y_{0m} \sim Y_{3m}$, $N_{0m} \sim N_{3m}$	Coefficients for Fujiwara wind model
x_H	X-coordinate of centre of lateral force induced on hull by rudder interaction.
x_R	X-coordinate at the position of a rudder

$\acute{x}$	Non dimensional frequency
X_H, Y_H, N_H	Hydrodynamic forces and moments acting on ship hull
X_P, Y_P, N_P	Hydrodynamic forces and moments due to propeller
X_R, Y_R, N_R	Hydrodynamic forces and moments due to rudder
X_w, Y_w, N_w	Aerodynamic forces and moments due to wind
x	Vertical distance to berthing point form present ship position
y	Horizontal distance to berthing point form present ship position
Z	Number of blades
Ψ	Ship heading
ψ_I, ψ_d	Order of course change
ψ_1	Course of the shortest path to the next WP
ψ_2	Course of the shortest path to the second next PP
$\dot{\psi}$	Yaw rate
ψ_{WR}	Realive wind direction
δ_{order}	Order rudder angle
δ	Actual rudder
Δ_a	Displacement
Λ	Aspect ratio of rudder
θ	Encountering angle of way point from vertical axis
α	Bearing angle of waypoint from the ship
λ	Aspect ratio
μ	Scalar value
ρ	Density of water
ρ_a	Density of air

Chapter 1 : INTRODUCTION

1.1 Background and Objectives

The ever-increasing modern technologies often demand a promising solution of highly demanding control problems. The evolution in the control area has been fuelled by three major needs. One for the need to deal with increasingly complex systems, second for accomplishing increasingly demanding design requirements and the last one for the need to attain these requirements under increased uncertainty. Although the conventional approaches have been proposed for such control problems, successful applications can only be found within well-constrained environment. As a result, numerous advancements have been made in developing the intelligent systems. One of them is inspired by human's central nervous system called artificial neural network (ANN).

Since ANN consists of several interconnected simple nonlinear systems that are typically modelled by the transfer function, it has the capability to replicate human brains and perform the same action that a human brain does in any particular situation. Regarding the potential of neural network for learning complicated behaviour of any nonlinear system, researchers from several disciplines are now designing ANN to solve different problems. Considering the advantages of artificial neural network, the first research using ANN as a controller was done by Yamato *et al.* (1) and it was for automatic ship berthing. Later on, Fujii and Ura (2) confirmed the effectiveness of ANN as a controller using both supervised and non-supervised learning system for autonomous under water vehicles (AUVs). After that, ANN was used in different controlling aspect like temperature control (Cui *et al.* 3), process control (Lee *et al.* 4), paper mill wastewater treatment control (Zeng *et al.* 5), engine air/fuel ratio control (Zhau *et al.* 6) etc. The ANN together with Fuzzy logic also created another field of research for hybrid controller as Aoyama *et al.* (7) used it for process control and Di *et al.* (8) used it for arc welding. The ANN was tried for self-tuning control systems by Ponce *et al.* (9) where previous training was not required and some changes in the set point were enough to adjust the learning coefficient. A nice description of controlling

nonlinear system using neural networks was given by Zilkova *et al.* (10) by demonstrating the induction motor control based on the principal of system inverse model. In the same year, an adaptive fuzzy neural network (FNN) was proposed to use for ship course tracking by Zhang *et al.* (11) where he used the FNN estimator to estimate the uncertainties and designed a robust controller to compensate the shortcoming of the FNN back-stepping controller. For the same purpose, Liu *et al.* (12) proposed an adaptive robust controller based on ANN for under actuated surface vessels. Some research studies also found focussing on using robust adaptive NN-based feedback control for a dynamic positioning of ship as explained by Yang *et al*. (13).

For automatic ship berthing, after Yamato *et al*., Hasegawa and Kitera (14) and Im and Hasegawa (15, 16) continued the research. Hasegawa and Kitera proposed the ANN controller combined with expert system to assist ANN, while Im and Hasegawa proposed separate controllers instead of a centralised one for rudder and propeller revolution outputs, respectively. In case of wind disturbances, Im and Hasegawa also proposed a motion identification method using ANN for detecting ship's lateral velocity and yaw rate. Then, based on two rule-based adjusters for the corresponding, the necessary action was taken. Using this procedure, although Im and Hasegawa succeeded to berth the ship in limited wind velocity, in case of wind blowing parallel to the ship's direction, results were not fruitful. Later on, the proposed research theme was tried to upgrade by putting weights on the creation of teaching data. Some adopted human knowledge for creating teaching data and some used standard manoeuvring plan. However, in both cases, the consistency, i.e. similarity in teaching data was not ensured. Thus, the problem regarding to create teaching data in a consistent way and to investigate the capability of a properly trained ANN to cope with any possible wind disturbances remain unsolved. As a continuation of this research, recently Im *et al.* (17) proposed a new algorithm for automatic berthing using selective controller. In the proposed algorithm, Im divided the approaching ship area into several zones and used separately trained ANN to guide the ship from one zone to another. The main intention of this research was to make the ANN independent of particular port shape and predetermined approaching pattern. On the contradictory, Nguyen *et al.* (18) tried non-supervised learning system using adaptive ANN for automatic ship berthing where

the neural network controller was trained online using adaptive interaction technique without any teaching data and off-line training phase. As a conclusion, it is clear that none of the mentioned research studies put weight on the creation of consistent teaching data and judges the effectiveness of consistently trained ANN controller. In the meantime, Ohtsu *et al.* (19) proposed a new minimum time ship manoeuvring method using nonlinear programming (NLP). Using this method, the user can set desired equality and non-equality constraints for any type of ship manoeuvre. The proposed method is then used to create teaching data consistently for berthing by Xu and Hasegawa (20). However, the usage of too many constraints as a termination condition caused fluctuations in the optimised rudder angle output and it also provided difficulties during training the net. Therefore, even in no wind condition, ANN controller resulted some yaw moment left after course changing that was strong enough to divert the ship from its desired path during straight running. Thus, the results were not fruitful during low speed manoeuvre. Moreover, this research also considered limited direction of wind blowing together with uniform wind disturbances up to certain small limit while investigating the effectiveness of the controller in wind condition. In real cases, wind blows in gust form rather than uniform and severe wind may also blow from any possible direction during travelling with reduced manoeuvrability in low speed running, which have not been investigated yet in the case of berthing problem. Nevertheless, in case of wind disturbances, the propeller revolution was adjusted according to the requirement manually rather than by ANN. To improve such shortcomings, this thesis is highly focused on creating consistent teaching data using NLP method and then judge the effectiveness of the controller under wind disturbances without any manual interruption.

1.2 Overview of this Thesis

In this thesis, to ensure a safe and appropriate berthing manoeuvre, the manoeuvring plan is divided into three basic elementary manoeuvres that are course changing, step deceleration and propeller reversing. For course changing manoeuvre, using NLP method a concept named ‘virtual window’ is introduced. Such window

consists of gradually changing ship position as well as ship heading. To ensure minimum time manoeuvre, a ship with its initial heading is expected to start from a desired starting point of that window. Then, by taking the calculated rudder as proposed by the optimal method, it is guaranteed for each ship with different heading to reach the so-called imaginary line well ahead, which is 15 times of ship length (according to the IMO standard) from berthing goal point. Such line is usually imagined by most ship operators during the berthing manoeuvre to ensure safe guidance of their ships. For the first time, Kose and Hashizume (21) mentioned about such strategy in their paper when the authors analysed the manoeuvring of ships in harbours. This imaginary line, then serves as a goal during the optimisation and acts as a reference line for further descent. In this thesis, virtual window is constructed by considering four different rudder angles ±10°, ±15°, ±20° and ±25° as non-equality constraints for minimum time course changing. Thus, each case has its limitation of maximum usage of rudder angle during the optimisation.

After merging to the imaginary line, the ship is commanded to go straight by following the sequential telegraph order made by maintaining the speed response equation. Finally, the engine idling, which is followed by propeller reversing is tuned to stop the ship as close as possible to the berthing goal point. During the berthing manoeuvre, there is a known fact that the ship manoeuvrability reduces drastically in low speed. Therefore, whenever the ship runs straight along with the imaginary line and its velocity gradually reduces due to the drop in propeller revolution, the effect of wind disturbances becomes severe. If a ship motion is considered as signal and environmental disturbances as noises, then in low speed straight running the signal-noise ratio becomes low enough for any controller to separate the noises from actual ship motion. Thus, even ANN is trained to deal with wind disturbances, the differences in ship motion during regular speed and low speed is quiet large and uncertain due to such high noises. As a result, instead of ANN, a more robust feedback controller is preferable to take an adequate rudder angle to guide the ship in such situation. In this thesis, among different types of controllers, a modified version of PID (proportional-integral-derivative) controller is chosen to deal with it. Such controller can correct not only ship heading, but also the distance between the ship's CG (centre of gravity) and the imaginary line.

As a result, even be a conventional PID controller, it plays a significant role due to its robust nature and works effectively than any other controller or rule based adjuster as IM *et al.* (16) used during low speed running. Finally, by combining such course changing and track keeping trajectories, a complete set of consistent teaching data is created.

Using the consistent teaching data, two separate feed-forward multi-layered ANN controllers have been investigated to find the suitable number of hidden layers together with the appropriate number of neurons in each layer for rudder angle and propeller revolution outputs, respectively. Such suitability is determined by considering the minimum squared error (MSE) as evaluation function. The famous back propagation that is gradient descent algorithm is used during training process where the network weights move along the negative of the gradient of the evaluation function.

After proper training, several simulations are done for different staring points on virtual window to judge the effectiveness of the trained controller, considering gust wind up to 1.5 m/s for an Esso Osaka model ship (15 m/s for full scale considering the same Froude number). However, in real cases, it would be extremely difficult to navigate a ship through a given starting point under environmental disturbances to start the berthing approach. Therefore, the networks are also tested for ship staring from some unexpected point within the constructed virtual window area. It means that the ship may start from any point on virtual window that belongs to different initial heading or from any arbitrary point as well. Since the ANN has its inherent interpolation ability and teaching data are consistent in nature, it is expected for the controller of rudder angle to take adequate action even the ship faces any unexpected situation. It is natural that some errors may remain after course changing in such cases. However, the PID controller is believed to make further corrections for heading and minimise the distance between the ship and imaginary line as well throughout its decent. Such cases are investigated in this thesis. Finally, to analyse the success rate of the proposed controller, Monte Carlo simulations are done. The frequency distribution of the success indexes is then plotted to know the tendency.

Although several simulations are done as mentioned above, many unknown situations may arise that cannot be simulated well before to judge the behaviour of the

controller. The first attempt to perform automatic ship berthing experiment using ANN was made by Nakata *et al.* (22) but unfortunately the success rate was very low due to improper training. Considering such fact and to demonstrate the virtual window concept, the consistently trained neural networks are then implemented in the free running experiment system to perform automatic ship berthing experiment. Initially, the experiments are carried out for desired starting points on virtual window. These results are then arranged into some groups depending on the similarities of network's behaviour or the resulting trajectory pattern. The possible reasons of such behaviour are also investigated for different initial conditions as well as wind disturbances. Later on, several experiments are carried out for ship stating from arbitrary points to judge the controller's robust nature. In such cases too, the network for rudder command has found to behave in a similar way as starting from the desired point on virtual window.

In this thesis, the goal point of the proposed controller is set to a temporary berth to ensure the safety. Therefore, to execute the crabbing motion as a last stage of berthing operation, automatic tug assistance is introduced. Initially, to develop a controller for side thrusts/tugs assistance, ANN has been investigated as explained by Tran and Im (23) under no wind condition. However, considering the wind that is mostly unpredictable, there is no other easy way to maintain consistency in teaching data that is very important to ensure the effective ANN controller. As a result, PD controller is given preference over ANN in such cases. Moreover, to control the forward motion, especially in wind, longitudinal thrust is also involved. The proposed controller is then used to shake hands with the current controller to align the ship with pier under maximum allowable wind disturbances.

It is stated that the proposed ANN-PID controller works effectively while starting from any arbitrary point. However, it is better if the ship starts from its desired point on virtual window or near to it to avoid any abrupt behaviour. To do that, i.e. to guide the ship from its current state to a set point on virtual window, a waypoint controller based on fuzzy reasoning is discussed in this thesis. The fuzzy reasoning used for the waypoint controller is similar to that used for marine traffic collision avoidance system by Hasegawa (24, 25, and 26). Here, instead of collision risk, nearness is reasoned by the fuzzy controller. After guiding the ship up to its desired starting point, the proposed

ANN-PID controller is activated. Several experiments are done to judge the compatibility of these two controllers and the results are included.

Finally, the thesis work can be concluded as follows: at first, the fuzzy reasoned waypoint controller is used to guide the ship from its current state to a set desired stating point. Then, the ANN-PID controller is activated to start the berthing approach. At last, the PD controlled thrusters provide relevant side and longitudinal thrusts to execute the crabbing motion and aligning the ship with the actual pier as a final step of berthing operation. All such controllers are found effective enough under wind up to 1.5 m/s for Esso Osaka model 3-m model ship that is 15m/s for full scale considering the same Froude number. This 15 m/s is also considered as maximum limit to get the permission for berthing under windy condition in most ports of Japan

Chapter 2 : SUBJECT SHIP AND MATHEMATICAL MODEL

2.1 Model Ship

In this thesis, among the different types of model available, 'Esso Osaka' 3-m model is chosen. The main reason of choosing this model is the availability of large amounts of captive model test results as well as a physical model itself. Its details are given in Table 2.1.

Table 2.1. Principal particulars of model and full-scale ship

Items			Ship model	Full-scale ship
Scale	s		1/108.33	
Length between perpendicular	L_{pp}	(m)	3.000	325.00
Breadth moulded	B	(m)	0.48925	53.00
Draught moulded at midship	d_H	(m)	0.20114	21.73
Wetted surface area	S_a	(m^2)	2.358	27,680
Displacement	Δ_a		244.4^{kg}	$319{,}040^{t}$
Propeller				
Diameter	D_p	(m)	0.08400	9.100
Pitch at 0.7 R	P	(m)	0.06007	6.507
Pitch ratio at 0.7 R	p	(non)	0.7151	0.7049
Number of blades	Z		5	5
Rudder: Rectangular in shape & Normal type in section				
Breadth	b	(m)	0.08308	9.0
Height	h	(m)	0.1279	13.85
Aspect ratio	Λ	(non)	1.539	1.539
Effective rudder area ratio	A_{Ref}	(non)	1/56.66	1/56.66

The Esso Osaka ship model used for berthing experiment is made of FRP

(fiber-reinforced plastic) and scaled as 1:108.33. Figure 2.1, shows the model used for the experiment purpose.

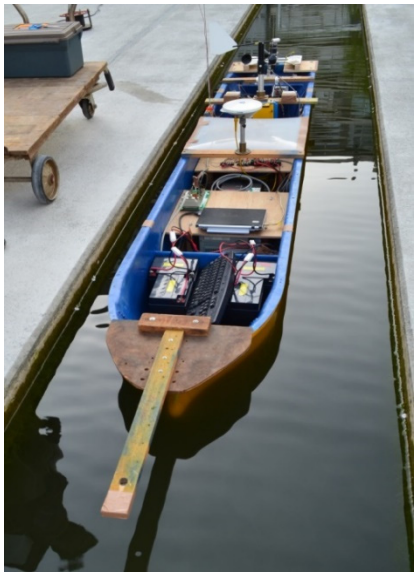

Figure 2.1. Esso Osaka 3-m model

2.2 Mathematical Model

To use precise and accurate mathematical model is very important in this thesis. Based on the model's predictability, the consistent teaching data are crated. Therefore, any inappropriate prediction will directly hamper the effectiveness of the trained controller. In this thesis, a modified version of mathematical model based on MMG is used for describing the ship hydrodynamics in three degrees of freedoms in this thesis. In the MMG model, not only hull, propeller and rudder forces are considered separately, but their interactions are also taken into account. This MMG model can predict both forward and astern motion of ship for any particular rudder angle and propeller revolution. The corresponding equations of motions at CG (centre of gravity) of the ship are expressed in Equation 2.1.

$$\begin{aligned}(m+m_x)\dot{u}-(m+m_y)vr &= X_H+X_P+X_R+X_W\\ (m+m_y)\dot{v}+(m+m_x)ur &= Y_H+Y_P+Y_R+Y_W\\ (I_{ZZ}+J_{ZZ})\dot{r} &= N_H+N_P+N_R+N_W\end{aligned} \tag{2.1}$$

where, X_H, Y_H, N_H are hydrodynamic forces and moments acting on a hull, X_R, Y_R, N_R are hydrodynamic forces and moments due to rudder, X_P, Y_P, N_P are hydrodynamic forces and moments due to propeller and X_W, Y_W, N_W are aerodynamic forces and moments due to wind.

The corresponding expressions for calculating the forces and moments are listed in Appendix A for both forward and astern motion. In case of forward motion, the hydrodynamic coefficients are determined by curve fitting through the captive model test results (27) for drift angle, β =20° to -20°. On the other hand, the reversing mathematical model is prepared by considering a larger drift angle. Details of such mathematical model can be found in the 23rd ITTC meeting report (28) and Ueda and Ueno's (29) paper on Esso Osaka.

To consider the influence of wind disturbances during ship manoeuvring, famous Fujiwara wind model (30) is used for calculating the wind forces and moment. Equation 2.2 is used for such calculation.

$$\begin{aligned} X_W &= \frac{1}{2} C_X \rho V_R^2 A_T \\ Y_W &= \frac{1}{2} C_Y \rho V_R^2 A_L \\ N_W &= \frac{1}{2} C_N \rho V_R^2 A_L L_{OA} \end{aligned} \tag{2.2}$$

where, L_{OA} is length overall of the ship, A_T is transverse projected area of the ship, A_L is lateral projected area of the ship, V_R is relative wind speed, X_W is fore-aft component of wind force, Y_W is lateral component of wind force, N_W is yawing moment and C_X, C_Y, C_N are the coefficients calculated using Fujiwara's model.

A simple way of considering the wind effect on ship manoeuvring motion is to apply uniform wind load. Previous research studies on ship berthing often considered such uniform wind velocity. However, to create a realistic environment in simulation, fluctuating wind pattern, i.e. gust wind should be considered. In this thesis, Equation 2.3 is used to make an irregular wave pattern by using power spectral density function S(ω).

$$\zeta(t) = \sqrt{2I(\infty)/M}\sum_{m=1}^{M}\cos(\omega_m t + \varepsilon_m) \tag{2.3}$$

where, $a_m{}^2 = 2I(\infty)/M$, $I(\omega) = \int_0^{\omega} S(\omega)d\omega$, $\varepsilon_m = 2\pi P_m$ (P_m : random numbers, $0 \leq P_m \leq 1$)

ω_m satisfies $I(\omega_m) = (2m-1)I(\infty)/2M.$

The power spectrum of wind expressed by Davenport (31) is used as follows:

$$S(\omega) = 8\pi k \frac{U_{10}{}^2}{\omega}\frac{x'^2}{(1+x'^2)^{4/3}} \left(= 14.4U_{10}\frac{x'^2}{(1+x'^2)^{4/3}}\right) \tag{2.4}$$

where, M is an assigned integer number, k = 0.003 above the water surface, U_{10} is the average wind velocity at 10m high above the water surface and x' is non dimensional frequency $= \dfrac{600\omega}{\pi U_{10}}$.

Thus, by using inverse Fourier transformation, the time series of fluctuating wind is realised. In order to validate the predictability of the MMG model for course changing and straight running, several speed and turning experiments are carried out with Esso Osaka model ship and compared with the simulation results. Since the virtual window is created for four different rudder angles (used as non-equality constraint), turning tests are also performed for such rudder angles considering both port and starboard turn. Figure 2.2, shows the speed test result for different propeller revolutions where the experiment result seems to diverge from the simulation result with the increment of propeller revolution. However, within half ahead, i.e. propeller rps 14 (used during course changing in this thesis), such deviation is well within considerable limit.

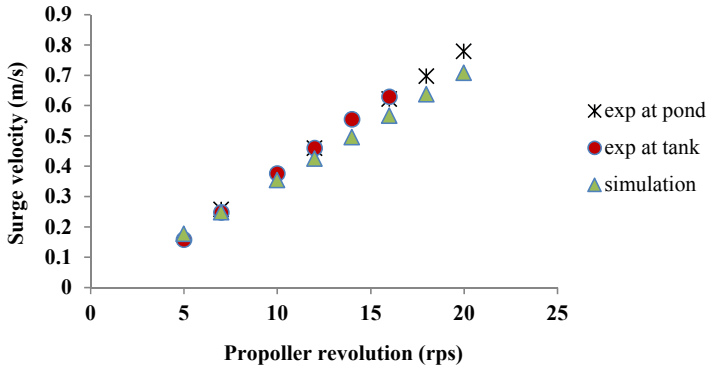

Figure 2.2. Speed test

Figure 2.3 to 2.6 show the turning test results as compared with the simulation one. These tests are carried out for half-ahead speed that is used for course changing part in this thesis.

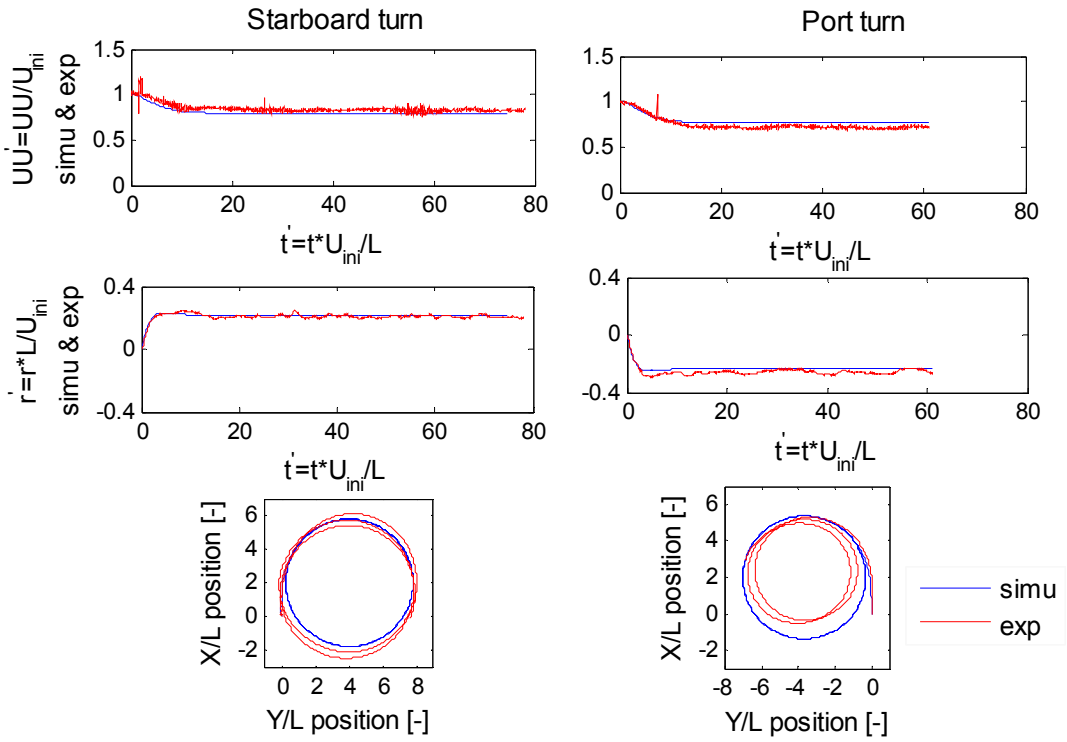

Figure 2.3. Turning circle comparison for ±10°

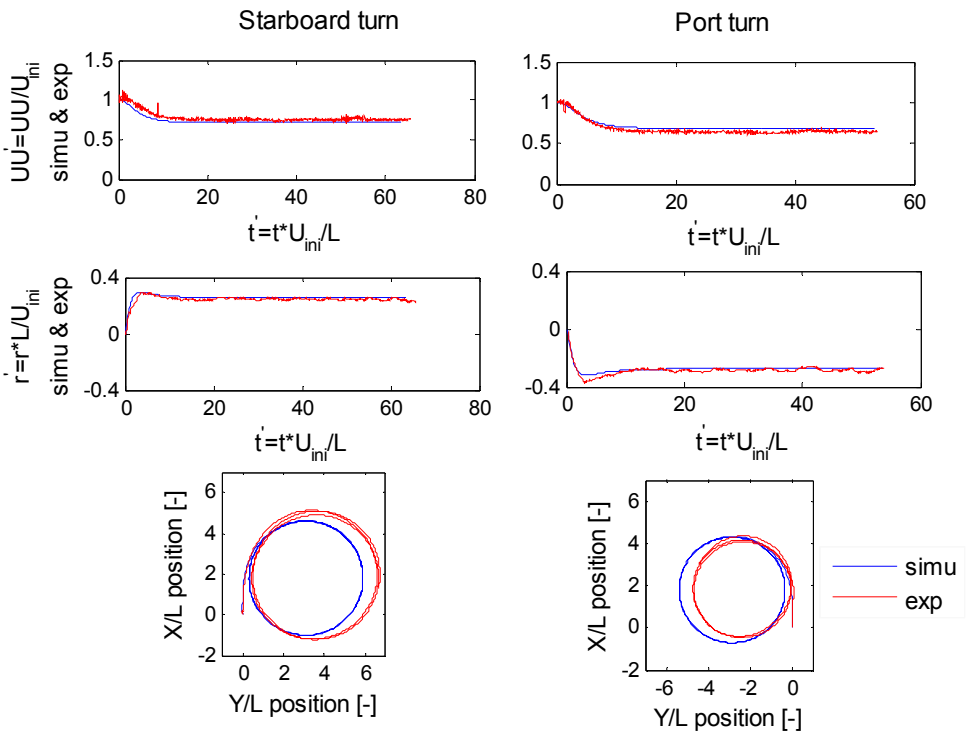

Figure 2.4. Turning circle comparison for ±15°

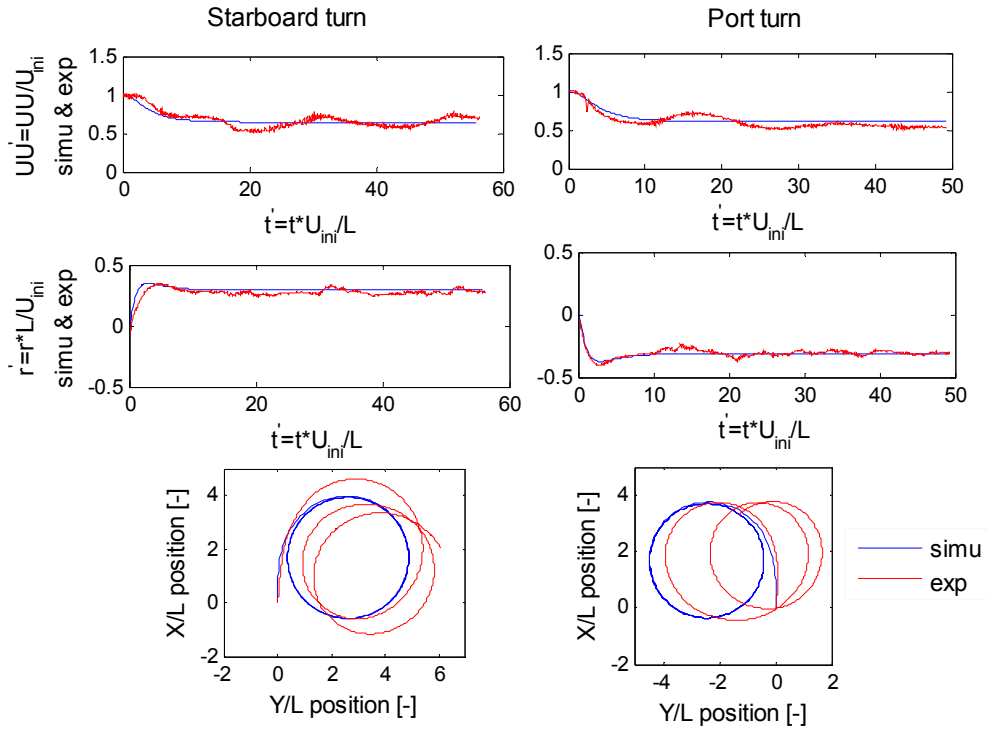

Figure 2.5. Turning circle comparison for ±20°

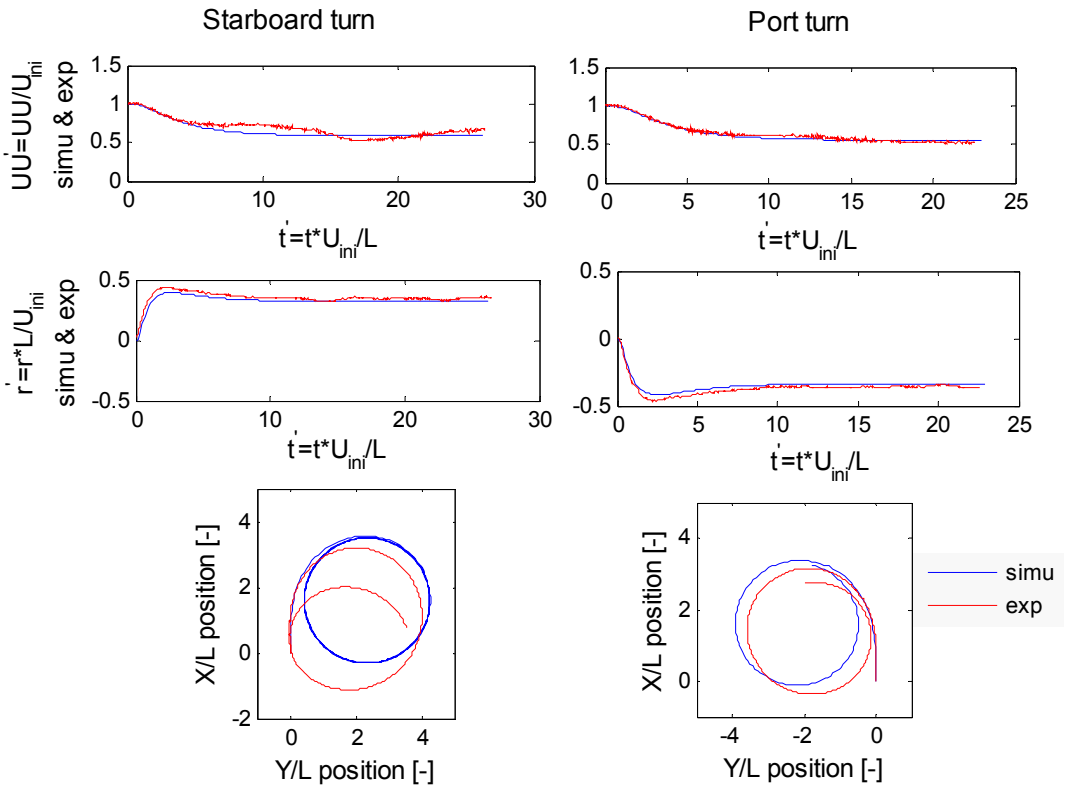

Figure 2.6. Turning circle comparison for ±25°

Here, each comparison contains not only turning trajectory, but also non-dimensional surge velocity and yaw rate for comparing initial transition to a steady state value. Considering Figures 2.3 and 2.4, each of turning circle shows quite promising result as compared with experiment one. However, due to the existence of wind during the experiments showed in Figures 2.5 and 2.6, the ship started to drift and the resulting circular trajectories shifted towards the direct of wind. In such cases, comparison of the tactical diameters proves the predictability of manoeuvring motion while using the mentioned MMG model. Although slight discrepancies exist, they are well within acceptable limit.

Chapter 3 : TEACHING DATA CREATION & TRAINING OF ANN

3.1 Berthing Plan and Execution

In this thesis, similar to aircraft landing, the berthing manoeuvre is planned to make first course changing from any given initial heading to a final desired ship heading. For this purpose, nonlinear programming (NLP) method for minimum time course changing is used. This NPL method for minimum time manoeuvring was also used by Okazaki and Ohtsu (32) for berthing purpose. In that study, a tracking controller was developed to follow the waypoint, target speed and heading in waypoint as a solution of the minimum time berthing problem. However, in this thesis, the NLP is used to ensure the final heading with no sway and yaw angular velocity and these constraints will align the ship to a reference line known as imaginary line. To imagine such reference line during berthing operation is usually a common practice for most ship operators. After merging to this line, the ship will keep its path and drop its speed according to the speed response equation. Then, the engine idling followed by propeller reversing will stop the ship at its desired zone. Since the optimisation is used for the course changing to ensure the final heading with no sway velocity and yaw rate, the ship is expected to go straight along with the reference line if there would no wind disturbances. However, in real situation considering the effect of wind in low speed running, PID is used as a feedback controller to minimise the ship deviation from imaginary line as well as correct the ship heading after course changing.

Kose and Hashizume (21) proposed two concepts by analysing the manoeuvring procedure followed by the captain in case of real large ship to ensure safety. One is that the goal of berthing manoeuvre is supposed to be at some interval distance from pier instead of approaching the pier board to board. The second one is planning a manoeuvre that allows a well-to-do operation in case of any critical situation.

In this thesis, to ensure Kose and Hashizume's two proposed concepts, the berthing goal is assumed to be at a distance 1.5 times of ship length from the actual pier. Moreover, the berthing is considered as successful if the ship stops (surge velocity$\leq$0.05 m/s) within an area of 1.5L around the berthing goal point. During the berthing

manoeuvre, the ship also approaches the pier along with an imaginary line that makes an angle 30° with the pier. Another one is that, to cope with any unexpected situation, rudder angle is restricted within ±10°, ±15°, ±20° or ±25° depending on its initial position on virtual window for course changing. In case of wind disturbances, the PID controller during straight running is also restricted to take rudder angle within ±5°, which is later on modified as ±10°. Figure 3.1 shows the details of the coordinate system used in this thesis together with other valuable information.

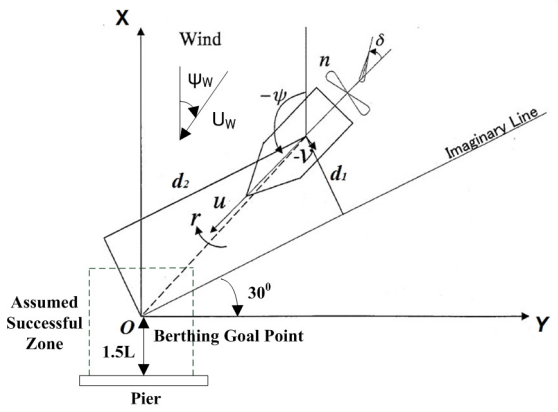

Figure 3.1. Coordinate system and other assumptions during berthing

3.1.1 Virtual Window Concept for Course Changing

Maintaining consistency in the course changing trajectories while training neural network, would be a key factor to increase the robustness of the controller. In this thesis, nonlinear programming (NLP) method is utilised to do so. Lavenberg-Marquardt algorithm is used during the optimisation and the steepest descent method is chosen to update the Hessian matrix. Details of this algorithm can be found in More's (33) paper. The NLP method used in this thesis is to get the optimal steering that satisfies the constraints given in the form of termination conditions during course changing. For such optimisation, the function named 'fmincon' from MATLAB optimisation toolbox is used. The objective function is set as time that ensures minimum time steering and the optimal variable as rudder angle. The constraint conditions used in NLP method are shown in Table 3.1.

Table 3.1. Constraints used in the optimal course changing

Objective function	Course changing time	
Optimal variable	Rudder angle, δ-order	
Initial Conditions	Ship velocity	Half Ahead
	Heading angle	ψ
	Position	*(x, y)*
	Others	v=0; r=0; $\delta = 0$
Equality constraints	Heading Angle	240°
	Position	On the imaginary line
	Ship velocity	Free
Non equality constraints	Rudder restriction	$\lvert\delta\rvert \leq$ 10°/ 15°/ 20°/ 25°

Considering the mentioned constraints, repeated optimisation technique is adopted where in each optimisation the ship's initial heading angle is changed by certain amount keeping the same termination conditions. Figure 3.2 demonstrates the technique used for ship's different initial headings and one particular final heading, which is 240º with no sway and angular velocity. Here, the final heading 240º means making an angle 30º with the pier i.e. the ship will align with the imaginary line after course changing. The final plot of such consecutive trajectories would be the same as shown in Figure 3.3(a), i.e., each trajectory ends with a different endpoint. However, by following the reshuffling process as shown in Figure 3.3(b), it is possible to align the trajectories for a particular endpoint that will coincide with the imaginary line. The reshuffling process results a new set of starting points, each belongs to a particular ship heading and it is possible to draw a curve through such points. Such curvature is named as 'virtual window'. Therefore, the virtual window denotes a safety window that ensures a ship with any particular heading passing through its desired position to reach the imaginary line well ahead to go for further deceleration and make successful berthing. In this thesis, such virtual windows is constructed for four different rudder angles used as constraints during the optimisation technique.

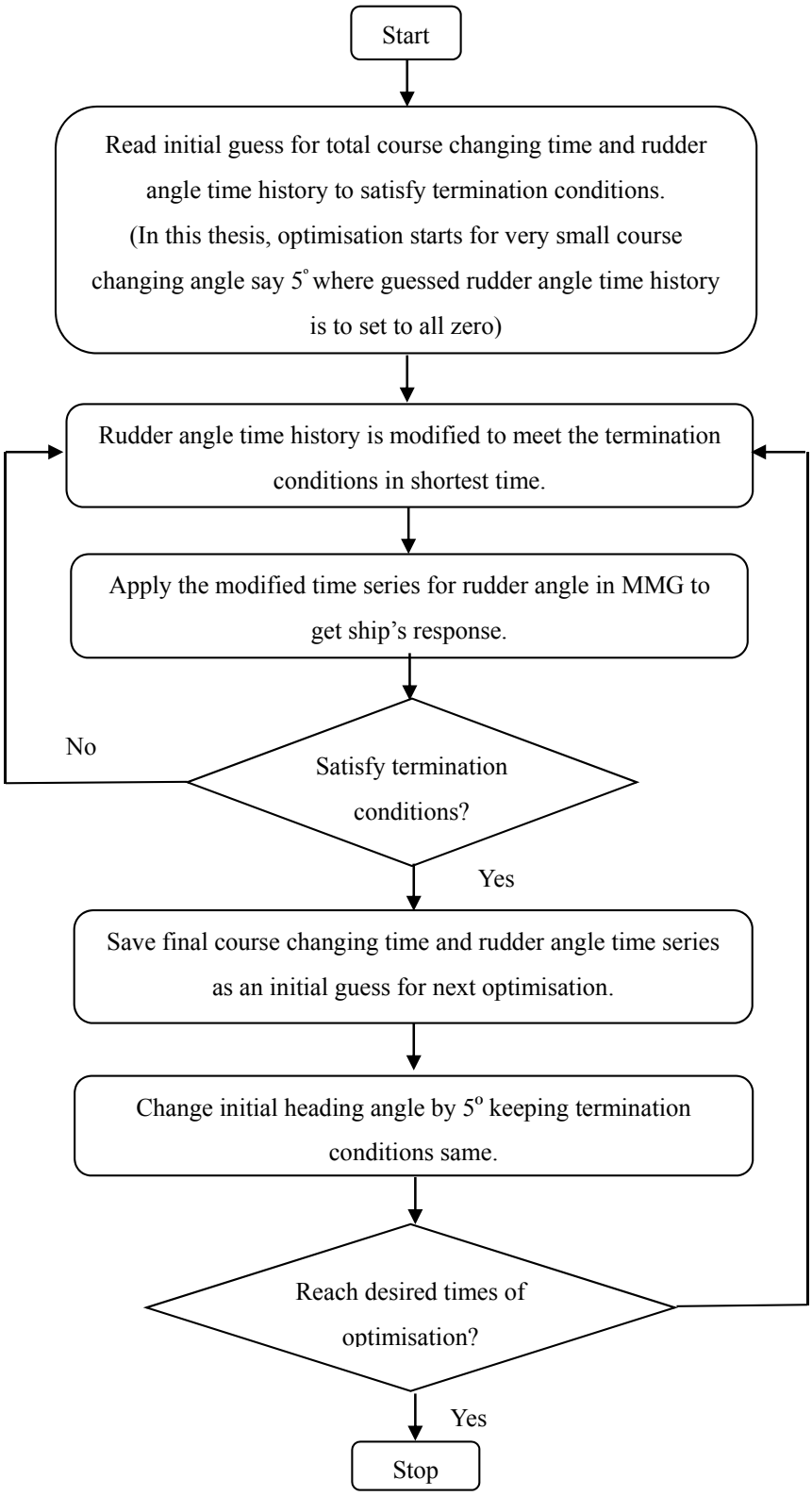

Figure 3.2. Repeated optimisation technique

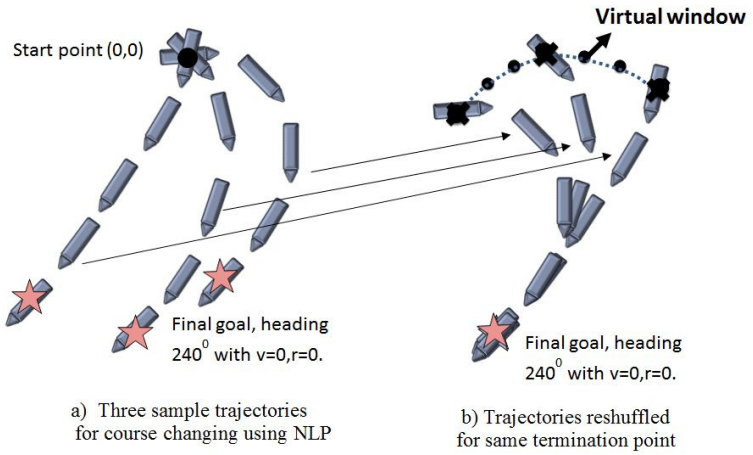

Figure 3.3. Idea of Virtual Window

After getting the points on virtual window, simulations are done for the optimal course changing considering the points as starting positions with their corresponding initial headings. Figure 3.4 and 3.5 show few of such optimal course changing results.

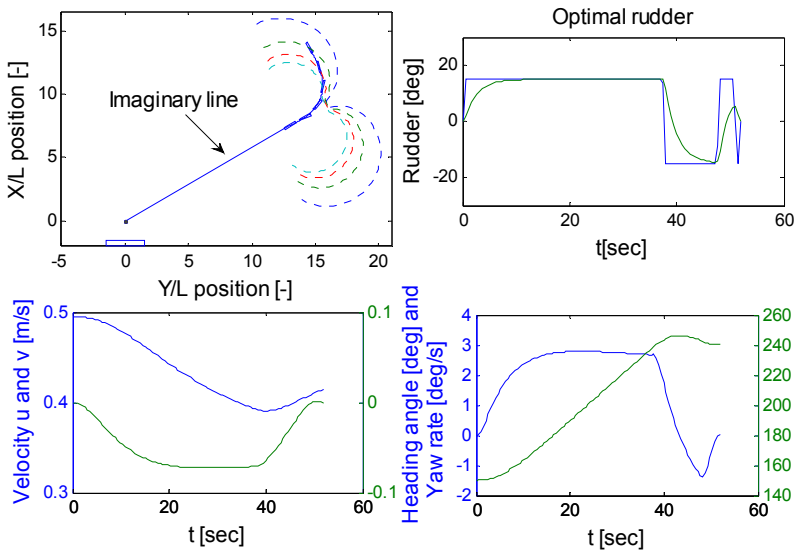

Figure 3.4. Optimal rudder for initial heading 150°, starting from virtual window for rudder constraint ±15°

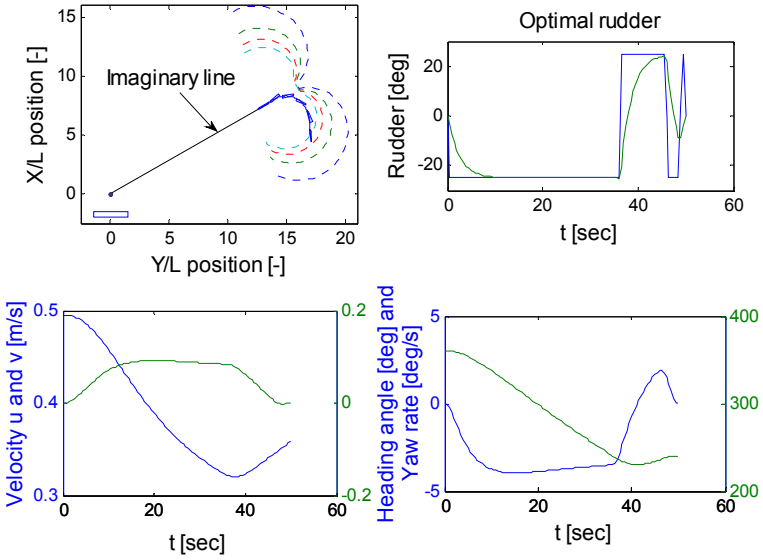

Figure 3.5. Optimal rudder for initial heading 360°, starting from virtual window for rudder constraint ±25°

3.1.2 Track Keeping Using PID Controller

After making a proper course change using the calculated rudder command for minimum time manoeuvre, the ship is expected to go straight if there would no wind disturbances. However, in real cases such disturbances exist. Therefore, after merging to the imaginary line while reducing the speed gradually, slight wind may cause drastic course changes if no action is taken to compensate such disturbances immediately. Moreover, the level of noise under wind disturbances is high enough for the ANN controller to distinguish it from actual ship motion. Considering the difficulties in maintaining the course in low speed under environmental disturbances, in this thesis, as a feedback controller, PID is used instead of ANN that is mentioned in the Equation 3.1. The first term of such expression represents the P controller that provides the necessary correction for maintaining the particular ship heading, second term belongs to the D controller to minimise the yaw rate and the third term is the I controller for ship heading that compensates the ship's deviation from the pre-set imaginary line. The third term mentioned in the following equation is the perpendicular distance of ship's CG (centre of gravity) to the pre-set imaginary line. Therefore, it is calculated from the ship's instantaneous position. This ship position is again calculated by integrating the sine or cosine component of the ship heading multiplied by its velocity.

$$\delta_{order} = C_1 * (\psi_d - \psi) - C_2 * \dot{\psi} - C_3 * d_1$$

$$\Rightarrow if \begin{cases} \delta_{order} > 0^0, \delta_{order} = 5^0 \\ \delta_{order} = 0^0, \delta_{order} = 0^0 \\ \delta_{order} < 0^0, \delta_{order} = -5^0 \end{cases} \tag{3.1}$$

where, ψ_d is desired heading, ψ is current heading, $\dot{\psi}$ is yaw rate, d_1 is a deviation from the imaginary line, C_1~C_3 are coefficients.

Usually, there are two methods available for deciding the coefficients mentioned in Equation 3.1. One of them is step response method and the other is steady response method. The selection of proper method will depend on the system to control. On the other hand, the values of the coefficients fully depend on the response of the system to control. In this thesis, instead of above such mentioned method, a sample set of coefficients is guessed depending on experience and then those are tuned to meet desired system response. The main objective of such tuning is to ensure an earlier response of the controller in case of any deviation takes places. As the controller has three coefficients, thus two coefficients are kept fixed (initial values are guessed as mentioned before) while the remaining one is tuned for the desired response. The same strategy continues until the best suitable three coefficients are got. Therefore, in one word, it would be a trial and error process. The following figures show a demonstration of the ship's response depending on the used (the best set to cope with wind disturbances from different directions) and any arbitrary chosen coefficient values. The black trajectories in the figures show how the ship deviates from its actual path under wind disturbances due to not taking any rudder action.

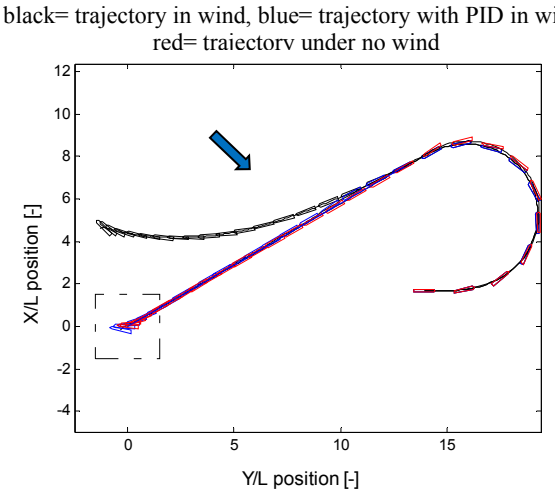

Figure 3.6. Trajectory for best-chosen coefficients

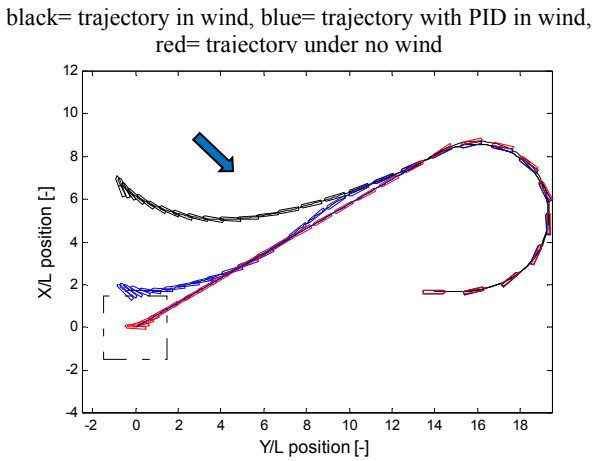

Figure 3.6(cont..). Trajectory for arbitrary chosen coefficient

Maintaining a proper telegraphic order is also important to stop the ship within an available distance. This will provide some inherent consistency while using the teaching data for training ANN for propeller revolution output. Endo and Hasegawa (34) surveyed the contents of deceleration manoeuvring during the real navigation cases and found that the ship usually approaches the berthing goal by dropping the ship velocity gradually as a standard deceleration manoeuvring. In order to find out the ship response, Yoshimura and Nomoto (35) reduced the coupled equations of motions into a simple mathematical model of ship response that is given as Equation 3.2.

$$(\mathrm{m} + m_x)\dot{u} + X_{uu}u^2 + \left(m + c_m m_y\right)I_p\dot{\psi}^2 + X_{\delta\delta}V^2\delta^2 = \rho D^4 n^2 (C_1 - C_2\frac{V}{nD}) \tag{3.2}$$

Now, if the ship travels in a straight path without operating its rudder and no transverse flows with respect to ship exits, then Equation 3.2 can be written as Equation 3.3.

$$m\frac{du(t)}{dt} + X_{uu}u(t)^2 = k_{nn}n(t)^2 \tag{3.3}$$

Let's consider the propeller revolution is changed by Δn (very small value) from its initial value n_0 that causes a change Δu to the initial ship velocity U_0. Now, by substituting u as (u_0+ Δu) and n as (n_0+ Δn) in Equation (3.3) and considering the Taylor expansion by elimination higher order terms results the simplified 1st order semi-linear approximation for resistance force and thrust force terms. The derivation is given as follows:

$$\begin{aligned}
m\frac{d(u_o + \Delta\mathrm{u})}{dt} + X_{uu}(u_o + \Delta\mathrm{u})^2 &= k_{nn}(n_o + \Delta\mathrm{n})^2 \\
m\left(\frac{du_o}{dt} + \frac{d(\Delta\mathrm{u})}{dt}\right) + X_{uu}{u_o}^2(1 + \frac{\Delta\mathrm{u}}{u_o})^2 &= k_{nn}{n_o}^2(1 + \frac{\Delta\mathrm{n}}{n_o})^2 \\
m\frac{du_o}{dt} + m\frac{d(\Delta\mathrm{u})}{dt} + X_{uu}{u_o}^2(1 + 2\frac{\Delta\mathrm{u}}{u_o} + \cdots) &= k_{nn}{n_o}^2(1 + 2\frac{\Delta\mathrm{n}}{n_o} + \cdots) \\
m\frac{d(\Delta\mathrm{u})}{dt} + X_{uu}{u_o}^2 + 2u_o X_{uu}\Delta\mathrm{u} &= k_{nn}{n_o}^2 + 2n_o k_{nn}\Delta\mathrm{n} \\
m\frac{d(\Delta\mathrm{u})}{dt} + 2u_o X_{uu}\Delta\mathrm{u} &= 2n_o k_{nn}\Delta\mathrm{n}
\end{aligned} \tag{3.4}$$

Now, let $X_u = 2u_o X_{uu}$ and $k_n = 2n_o k_{nn}$. Then the above finding can be written as following:

$$m\frac{du(t)}{dt} + X_u u(t) = k_n n(t) \tag{3.5}$$

$$\frac{m}{X_u}\frac{du(t)}{dt} + u(t) = \frac{k_n}{X_u}n(t) \tag{3.6}$$

$$T_u\frac{du(t)}{dt} + u(t) = K_n n(t) \tag{3.7}$$

where, *u(t)* is ship velocity, *n(t)* is propeller revolution, $T_u=m/X_u$ is the time constant and $K_n=k_n/X_u$ is gain.

Finally, Equation 3.7 is the respective simplified equation for ship speed response. The reason of such simplification is understandable. Since the change in the ship velocity is almost proportional to the change in propeller revolution, it is meaningful to simplify the response equation by Taylor expansion and neglecting the higher order terms.

The solution of the above speed response equation is given by:

$$u(t) = u_0 e^{-\frac{t}{T_u}} + K_n n(t)(1 - e^{-\frac{t}{T_u}}) \tag{3.8}$$

where, u_o is initial ship speed during particular engine telegraph step change and $K_n n(t)$ is steady ship speed when propeller revolution keeping at goal step *n(t).*

The sequence of telegraph order considered in this thesis is the half ahead during course changing. Then, it is followed by slow ahead, dead slow ahead, engine idling and at last propeller reversing. In case of stopping manoeuvre, slow astern is used as telegraph order. Here, the step changing time is as much as time constant T_u of the ship speed response equation which is shown in Equation 3.7. Considering t=T_u in Equation 3.8 results *u(t)* as 63.21% of speed drop from its initial speed U_0. Thus, each telegraph order is considered as the ship's speed drops by 63.21% from its initial value. Moreover, since the engine idling is followed by propeller reversing, the engine idling time is also adjusted such that the ship can reach as close as possible to the berthing point during propeller revering stage. The total available distance considered during deceleration and stopping manoeuvre is 15 times of ship length according to IMO standard. Table 3.2 shows the propeller revolution used for the telegraph order in this thesis together with their corresponding steady velocity.

Table 3.2. Rps used for telegraph order and corresponding steady velocity

Stages	Rps	Velocity (m/s)
Half Ahead	14	0.495
Slow Ahead	8	0.2829
Dead Slow Ahead	4	0.1414
Stop Engine	0	--
Slow Astern	-8	--

3.2 Teaching Data Creation

Following the above mentioned procedure i.e. by combining the course changing and track keeping trajectories, the whole set of teaching data for berthing manoeuvre is created. Since optimal steering is considered for course changing, each ship with its particular initial heading can have only one particular starting point on virtual window to satisfy the given constraints. In this thesis, virtual window considering four different rudder angles (used as constraints) is used to create the teaching data. For left hand side approach, total 24 starting points (6 for each rudder angle constraint) are considered in the teaching data for initial heading 90°, 120°, 150°, 180°, 210° and 230°/225°/220°/215° (for rudder constraints ±10º, ±15º, ±20º and ±25º respectively). On the other hand, for right hand side approach, total 32 starting points (8 for each rudder angle constraint) are considered for initial heading -270° or 90°, 60°, 30°, 0° or 360°, 330°, 300°, 270° and 250°/255°/260°/265° (for rudder constraints ±10º, ±15º, ±20º and ±25º respectively). Maximum rudder angle taken in the teaching data is fully dependent on ship's initial position on virtual window. In order to include the wind effect in

teaching data, each successful ship berthing trajectory is consider under three different wind velocities which are 0.2m/s, 0.6m/s and 1.0 m/s for model ship. Each wind velocity is again considered for four different wind directions that are 45°, 135°, 225° and 315°. Therefore, instead of using the wind information directly to the neurons, the influence of wind is considered in way of somewhat deviated ship trajectories and at the same time using PID controller to correct them during low speed running. The resulting set of teaching data considering the wind effect is given in Figure 3.7. Here it is noted that, the effects of wind during course changing are not severe as the ship's speed is comparatively higher than that of wind.

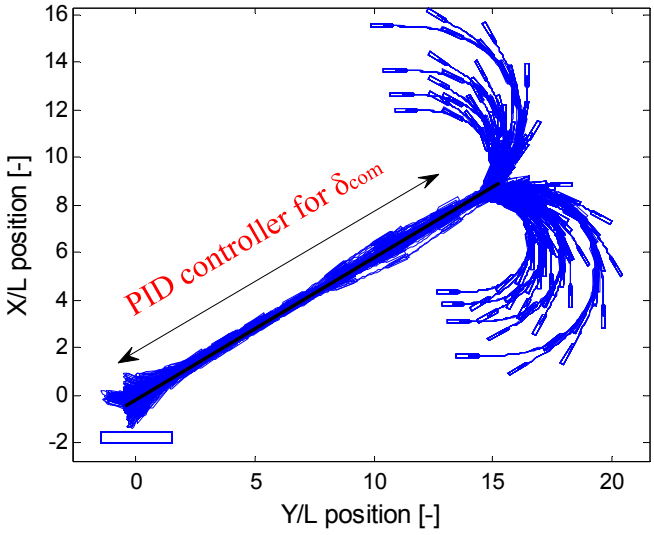

Figure 3.7. Teaching data including wind influence

3.3 Training of ANN Controller

The above mentioned teaching data are divided into two considering the left hand side (LHS) and the right hand side (RHS) approach to ensure similar pattern of course changing trajectories (port or starboard). Then, two multi-layered feed-forward neural networks are constructed for rudder and propeller revolution outputs, respectively instead of centralised controller for each case. The effectiveness of using such separate controllers had already been proved by Im and Hasegawa (15).

3.3.1 Training, Transfer and Performance Function

In order to train the network, famous back propagation technique that is gradient descent algorithm is used where the network weights move along the negative of the gradient of the performance function. In this thesis, MATLAB Neural Network Toolbox is used where varieties of training functions with different basic algorithms are available to train the net. Among them training function based on Lavenberg-Marquardt algorithm is chosen. This algorithm is designed to approach second-order training speed without having to compute the Hessian matrix like in quasi-Newton method. When the performance function has the form of a sum of squares, then the Lavenberg-Marquardt algorithm uses the following approximation to the Hessian matrix in order to follow Newton-like update.

$$x_{k+1} = x_k - [J_m{}^T J_m + \mu I]^{-1} J_m{}^T e \tag{3.9}$$

where, J_m is the Jacobian matrix that contains first derivatives of the network errors with respect to the weights and biases, e is a vector of network errors and μ is a scalar value.

If μ becomes zero, the algorithm is same as Newton's method and when large, it results gradient descent with a small step size. Thus, μ is decreased after each successful step when the performance function is also reduced and vice versa. In this way, the performance function will always be reduced at each iteration of the algorithm.

In case of transfer function, log-sigmoid is found suitable which is given as Equation 3.10.

$$f(x) = \frac{1}{1+e^{-x}} \tag{3.10}$$

In addition, the performance of the trained network is judged depending on calculated mean squared error value (MSE). If the normalized teaching data are considered in the following form:

$$\{p_1, q_1\}, \{p_2, q_2\}, \ldots\ldots\ldots \{p_n, q_n\} \tag{3.11}$$

where, p is input of network and q is target output. Consequently, MSE can be calculated as follows:

$$MSE = \frac{1}{n}\sum_{i=1}^{n} e(i)^2 = \frac{1}{n}\sum_{i=1}^{n} (q(i) - O(i))^2 \tag{3.12}$$

where, O is output of network.

3.3.2 Construction of Networks

In order to construct a well-trained net, appropriate inputs for that net, number of hidden layers and the corresponding number of neurons in each hidden layer are needed to be investigated. In this thesis, in order to determine the suitable inputs, different parameters are tested depending on previous researchers' preference and found the followings as suitable one.

For rudder output, input parameters for the net are u: surge velocity, v: sway velocity, r: yaw rate, ψ : heading angle, (x, y) : ship position, δ: actual rudder angle, d_1:distance to imaginary line and d_2: distance to berthing point.

For propeller revolution, input parameters are u: surge velocity, ψ : heading angle, (x, y) : ship position, d_1: distance to imaginary line and d_2: distance to berthing point.

Since there does not exist any particular rule to select the hidden layers and neurons for the network, in this thesis such numbers are determined by trial and error and observing the minimum MSE value after each training period. In previous research studies very limited set of teaching data were used to train which resulted a very simple neural network construction with single hidden layer. However, in this thesis, to learn the complex pattern of teaching data, two hidden layers are found suitable enough with appropriate neurons to ensure the minimum MSE value. Different combinations of neurons for the two hidden layers are investigated and the particular combination that gives less MSE value is chosen. Table 3.3 shows the necessary information regarding

the network formation during training nets.

Table 3.3. Number of neurons in each layer

Nets		No of hidden layers	No. of Neurons			Transfer function
			Input	Hidden	Output	
Rudder angle	LHS approach	2	9	10,6	1	logsig, logsig, purelin
	RHS approach	2	9	12,8	1	
Propeller revolution	LHS approach	2	6	12,5	1	logsig, logsig, purelin
	RHS approach	2	6	12,8	1	

Epoch, time and performance value after training are given in Table 3.4.

Table 3.4. Other information after training

Net	Epoch (no of iterations)		Time taken for learning (sec)		Performance value	
	Rudder angle	Propeller revolution	Rudder angle	Propeller revolution	Rudder angle	Propeller revolution
LHS approach	233	164	487	310	0.00145	0.00210
RHS approach	177	211	170	217	0.00162	0.00258

The resulting multi-layered ANNs are demonstrated in Figure 3.8. Here, the outputs from the hidden layers are given by:

$$A_n = sig(\sum W_{n,o} I_o + b_n) \tag{3.13}$$

$$A_m = sig(\sum W_{m,n} I_n + b_m) \tag{3.14}$$

Finally, the respective outputs for rudder angle and propeller revolution is given by

$$O_l = purelin(\sum W_{l,m} A_m + b_l) \tag{3.15}$$

where**,** *o* is number of input parameters, *n* is number of neurons in 1st hidden layer, m is number of neurons in 2nd hidden layer, *l* is number of output and *sig* is log sigmoid function.

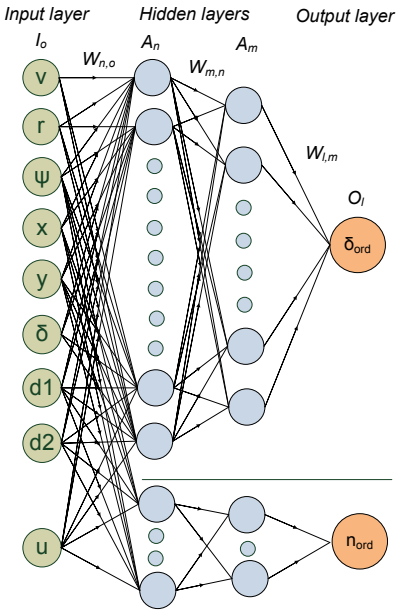

Figure 3.8. Construction of ANNs

In this thesis, the network for rudder command will be used only during course changing. Then, it will be followed up by the PID controller for low speed straight running. Here, the decisive factor to alter the ANN for PID controller is ship position.

Once the PID controller is activated, the rest of task regarding the rudder controller is solely determined by the PID controller itself. On the other hand, the network for propeller revolution will be used throughout the whole berthing process. Therefore, it would be a combined effort of ANN and PID controller while considering wind disturbances. Figure 3.9 shows the control strategy during the whole berthing process.

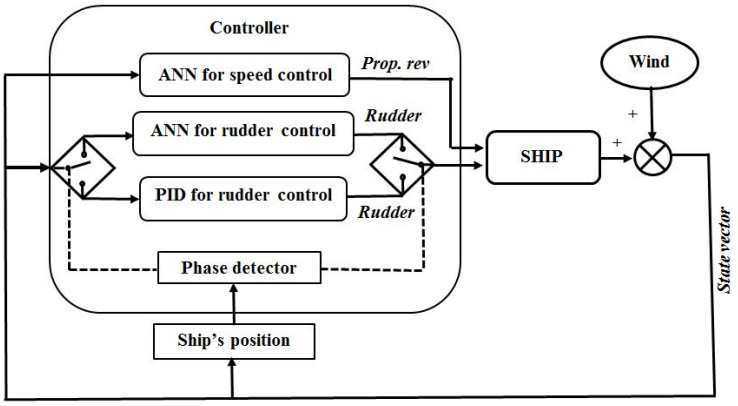

Figure 3.9. Control Strategy

The plant, to be controlled for berthing is the same as for controlling the motion of the ship. Therefore, after proper training, the controllers are used in the plant as shown in Figure 3.10, where they take the required inputs from the outputs of the plant and decide the inputs for desired action.

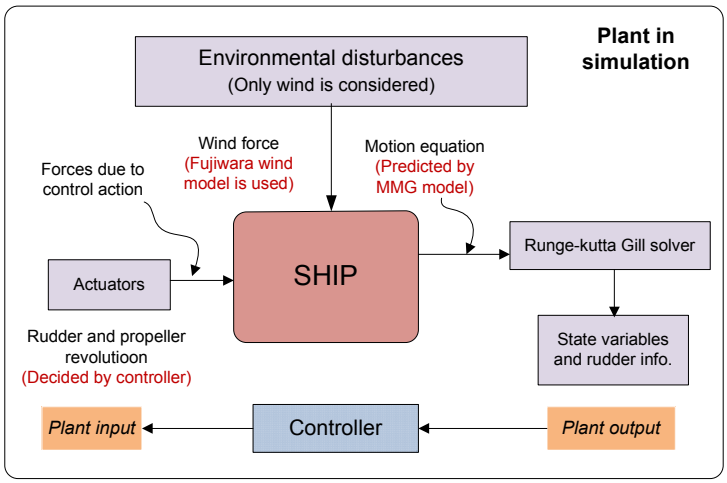

Figure 3.10. Plant to be controlled

Chapter 4 : SIMULATION RESULTS

To judge the effectiveness of trained ANN with PID controller, several types of simulations are carried out. Initially, the teaching and non-teaching data are tested for the ship starting from its expected point on virtual window. Here, the teaching data denotes the ship's identical initial position and heading that are used to train the networks under wind disturbances. On the other hand, in case of non-teaching data, other points on virtual window are tested for their corresponding heading. To judge the capabilities of the controller to cope with wind disturbances, different gusts from different directions are also tested for both teaching and non-teaching data. Robustness of the controller in terms of position flexibility is tested by considering the ship starting from unexpected point on virtual window rather than expected one that belongs to its current heading or any arbitrary point within the constructed virtual window zone. Such simulation results are discussed in the following subsections.

4.1 Ship Starting from Desired Point on Virtual Window

In this thesis, the starting points on virtual window are created for every 5° of heading interval. However, the teaching data include the points at 30° heading interval to prevent overfeeding. Therefore, numbers of points on virtual window are untreated in the teaching data that are necessary to be tested by the trained controller. On the other hand, the teaching data include the trajectories considering wind disturbances up to 1.0 m/s from four different directions. Thus, the other wind directions as well as maximum sustainable wind velocity also need to be investigated for the controller.

Initially, the simulations are done for both LHS and RHS approaches considering the ship starting from its desired point used as teaching data. During the simulation, the wind disturbances are considered up to 1.0 m/s and from different directions. Figure 4.1 and 4.2 illustrate the effectiveness of ANN-PID controller when tested for the same teaching data provided. In such figures, two types of trajectories are plotted. One is for ANN-PID controller in wind and other one is for optimal steering without PID in the wind. It clearly shows that the PID controller succeeds to prevent the ship's deviation in

low speed. On the other hand, the red trajectory results due to not using any controller while straight running and the ship simply deviates from its desired path under wind disturbances. Although in case of course changing, such deviation is not noticeable due to relatively high ship speed. Wind information is shown in the first row-second column of each figure that is experienced by the ship during the berthing. In both cases, the controller successful stops the ship within the desired zone as shown as a blue square box in these figures. The desired zone covers an area of 1.5 times of ship length around the berthing goal point (0, 0).

ANN in real berthing cases is expected to face completely different situation than used to train it. However, due to its interpolation ability, the controller is expected to take necessary actions regardless of any situation. To judge such ability, simulations are also done for different points on virtual window and wind information other than used as teaching data. Figure 4.3 and 4.4 illustrate such results.

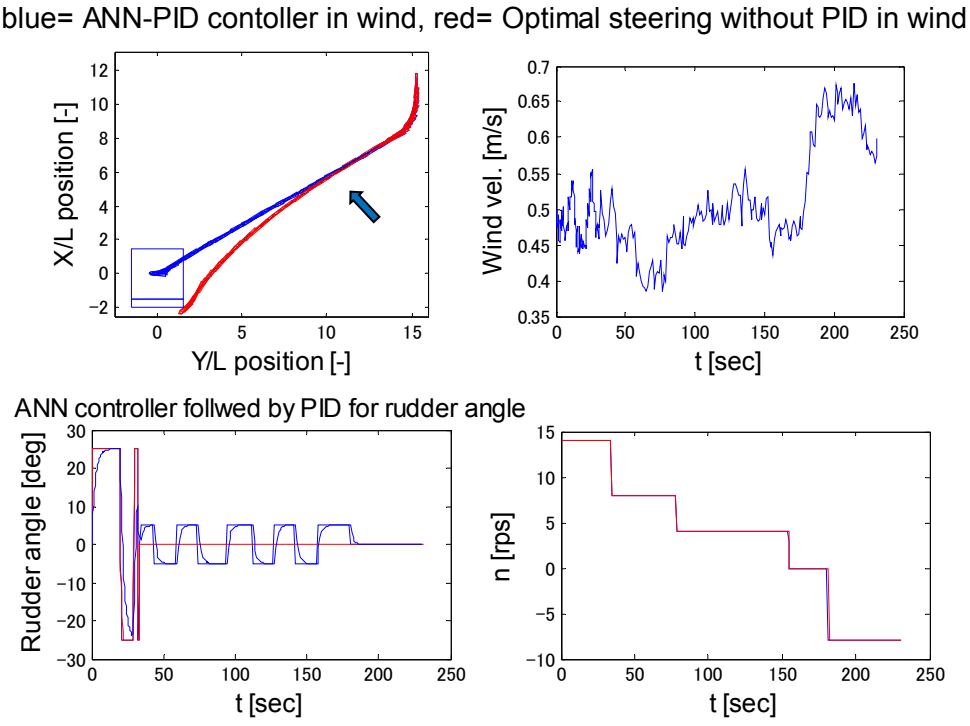

Figure 4.1. Controller tested for teaching data, average wind velocity 0.6 m/s, wind direction 135º, initial ship heading 180º from virtual window for rudder constraint ±25º

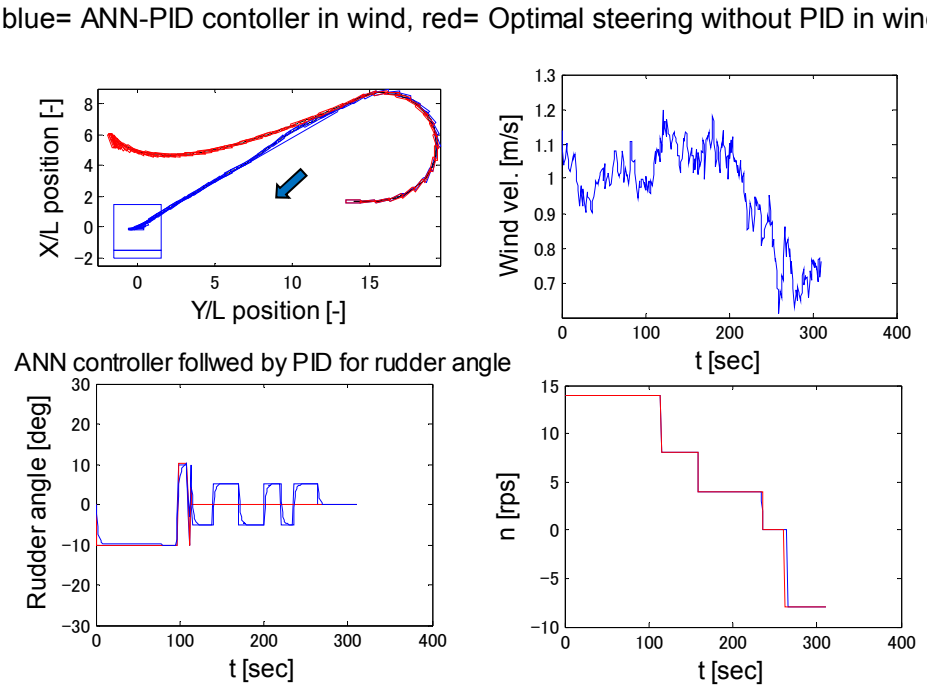

Figure 4.2. Controller tested for teaching data, average wind velocity 1.0 m/s, wind direction 45º, initial ship heading -270º from virtual window for rudder constraint ±10º

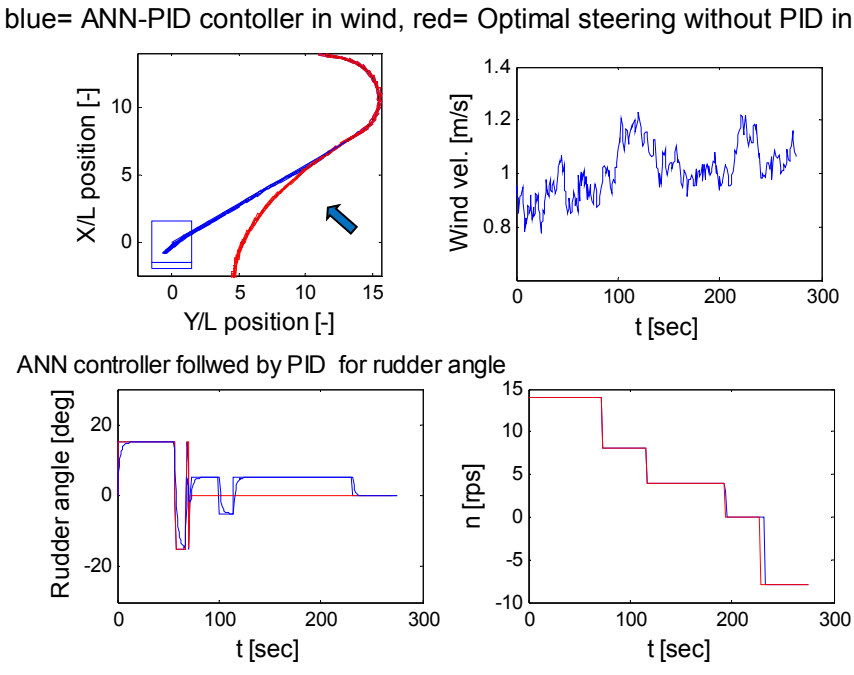

Figure 4.3. Controller tested for non-teaching data, average wind velocity 1.0 m/s, wind direction 135º, initial ship heading 100º from virtual window for rudder constraint ±15º

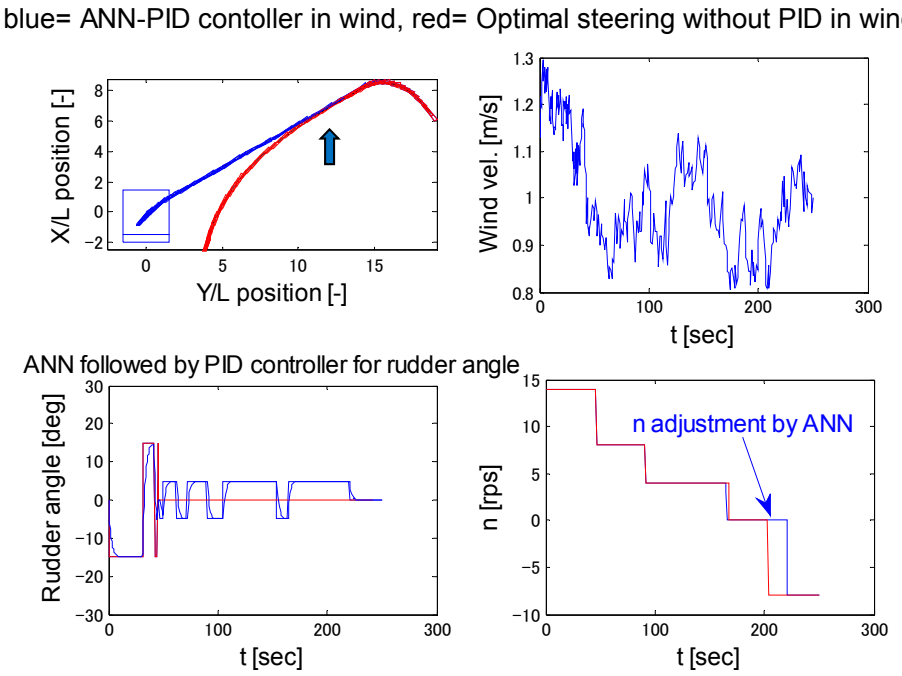

Figure 4.4. Controller tested for non-teaching data, average wind velocity 1.0 m/s, wind direction 180º, initial ship heading 320º from virtual window for rudder constraint ±15º

Considering Figure 4.3, the result looks similar to teaching data provided. However, in Figure 4.4, the second row-second column clearly shows how the ANN adjusts the propeller revolution by elongating the idling time depending on situation demands. Here, the second row-first column shows the rudder angle which is adjusted by ANN during course changing and PID controller during straight running.

In most of previous research studies, consideration of maximum wind velocity was very limited say 1.0 m/s for Esso Osaka model ship. Although in most harbours in Japan, the maximum wind velocity consideration for berthing is 13 or 15 m/s that would be approximately 1.3 and 1.5 m/s in case of Esso Osaka model ship (for the same Froude number). Therefore, in this thesis, one of the most changing tasks is to make the ANN-PID controller able to ensure successful berthing for wind over 1.0 m/s, although the teaching data contain information up to 1.0 m/s. To judge such capability, average wind velocities of 1.3 and 1.5 m/s are tested under different directions. Figures 4.5 and 4.6 demonstrate such illustration where the ANN adjusts the propeller revolution by elongating the idling time or considering engine idling and reversing sequentially and ANN-PID control the rudder command to ensure safe berthing.

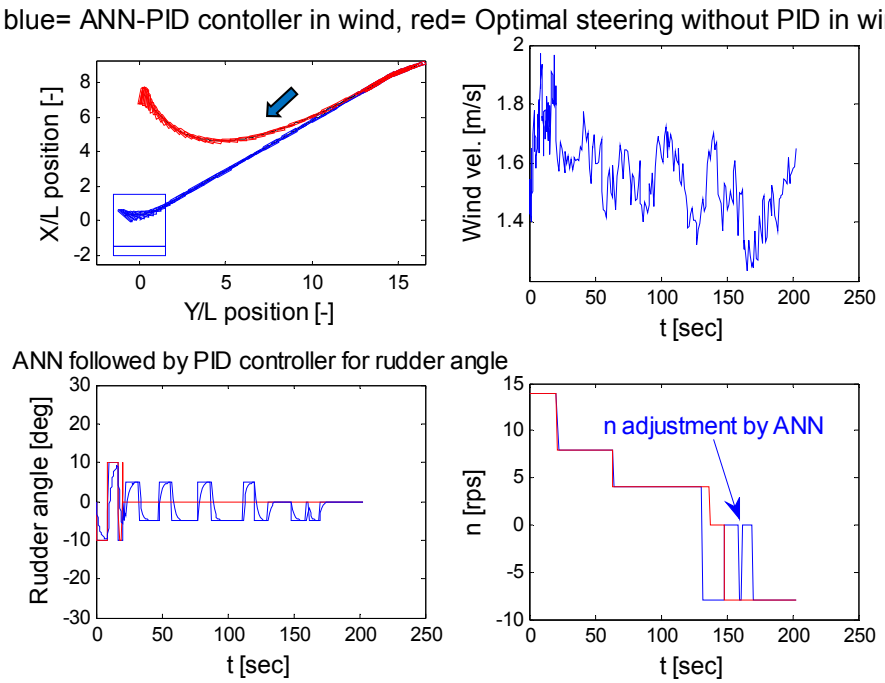

Figure 4.5. Controller tested for wind over 1.0m/s, average wind velocity 1.5 m/s, wind direction 45º, initial ship heading 250º from virtual window for rudder constraint ±10º

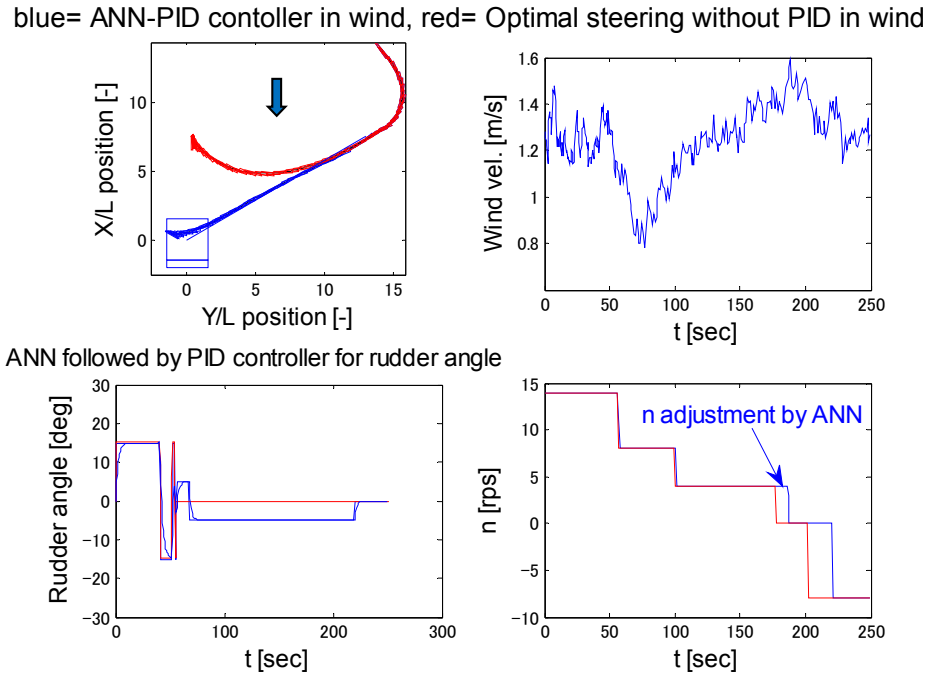

Figure 4.6. Controller tested for wind over 1.0m/s, average wind velocity 1.3 m/s, wind direction 0º, initial ship heading 140º from virtual window for rudder constraint ±15º

Although the above figures show successful berthing results using ANN-PID controller, due to the difficulties in accurate prediction of wind disturbances, further research studies are done where three separate types of investigations are carried out. These are given as follows:

a) The effectiveness of ANN-PID controller is tested for any particular ship's initial state and increasing the wind velocity gradually keeping the direction same in every case.

b) Different gusts for same average wind velocity and direction are tested for ship's same initial state.

c) Eight different wind directions are tested for a particular average wind velocity and ship's initial state.

The following subsections will explain about such investigation results.

4.1.1 Verification for Different Wind Velocities

To verify the effectiveness of the controller for different wind velocities, ship with any particular initial heading starting from its point on virtual window is tested for gradually increasing wind velocities. Many successful results are found during such investigation. However, some rare cases are also found where the ANN provides proper propeller revolution order but due to the inappropriate rudder angle taken by the PID controller during straight running, ship cannot reach to the pier successfully. Figure 4.7 shows one of such examples where the ANN-PID controller is capable enough to guide the ship safely to the berthing zone up to 1.0 m/s but for 1.3 or 1.5 m/s, it fails as shown in row three and four.

To deal with such rare situation that may arise in real cases, an increase in rudder restricting is proposed to use for the PID controller during straight running which is ±10º instead of ±5º as shown in Equation 4.1. This will increase the rudder effectiveness under high wind condition and thus the ship is capable to maintain its track.

$$\delta_{order} = C_1 * (\psi_d - \psi) - C_2 * \dot{\psi} - C_3 * d_1 \tag{4.1}$$

$$\Rightarrow if \begin{cases} \delta_{order} > 0^0, \delta_{order} = 10^0 \\ \delta_{order} = 0^0, \delta_{order} = 0^0 \\ \delta_{order} < 0^0, \delta_{order} = -10^0 \end{cases}$$

Figure 4.8 demonstrates its effectiveness where successful berthing is ensured for the third and fourth cases of Figure 4.7 for average wind velocity 1.3 and 1.5 m/s. Therefore, for further investigation, the ANN controller followed by the modified PID controller is used during straight running to judge the workability of ANN-PID controller.

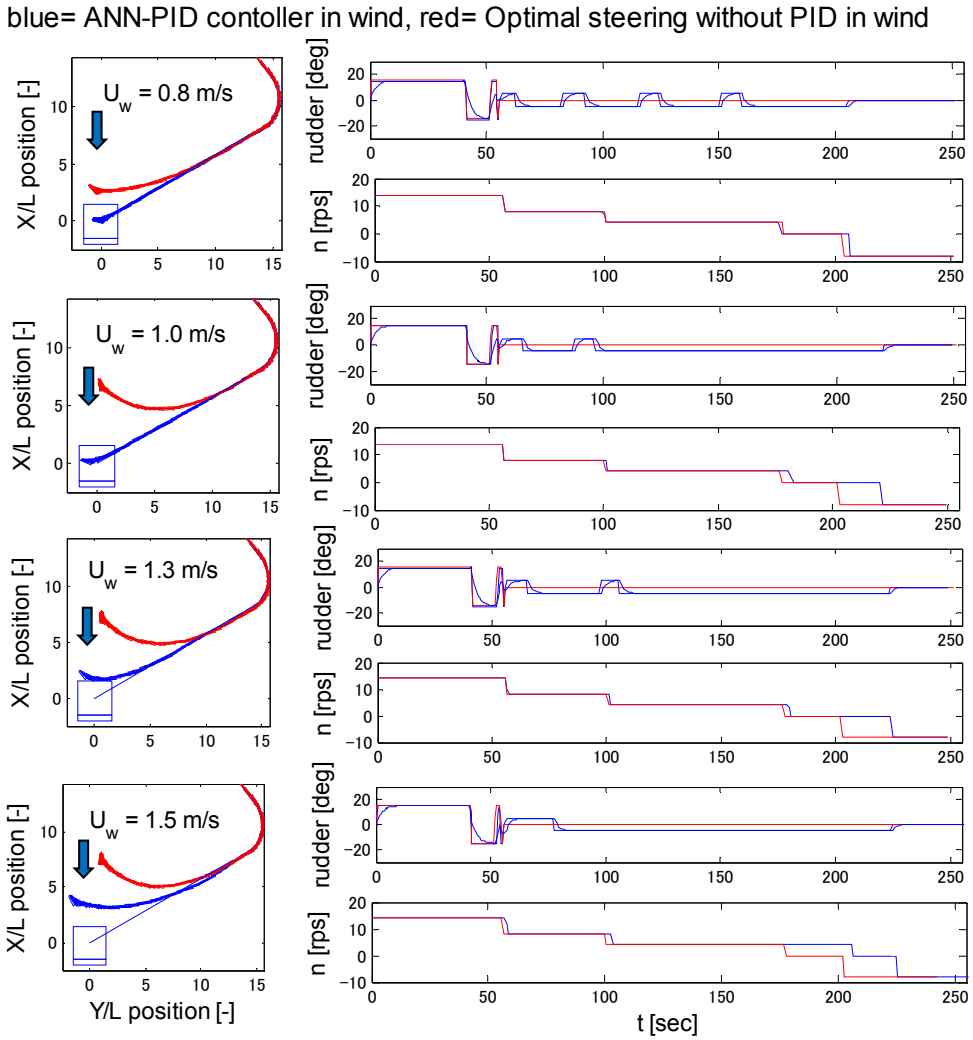

Figure 4.7. Controller under different wind velocities, wind direction 0º, initial ship heading 140º from virtual window for rudder constraint ±15º

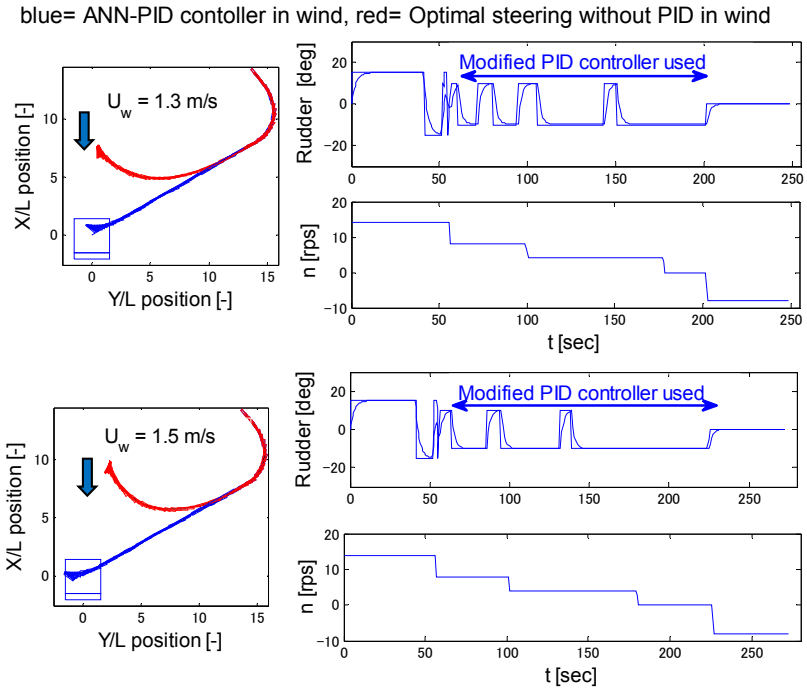

Figure 4.8. Controller with modified PID, wind direction 0º, initial ship heading 140º from virtual window for rudder constraint ±15º

4.1.2 Verification for Different Gust Realisations

Different gust realisations for same average wind velocity are also investigated to judge the controller's effectiveness. Such investigation also provides the importance to consider the gust wind instead of uniform one, as the resulting ship trajectories as well as controlling action may vary drastically in different fluctuating wind patterns of same average velocity. Figure 4.9 and 4.10 illustrate such results for ANN-PID controller. In such figures, first and fourth row of second column shows the different gust realisations although the average is the same.

Here, Figure 4.9 shows almost similar trajectories for different gusts, but the PID controller's output as well as adjustment for propeller revolution by ANN is completely different. On the other hand, noticeable differences in trajectories are found in Figure 4.10. However, in both cases, the ANN-PID controller can ensure successful berthing by taking the proper rudder angle and propeller revolution depending on situation demands.

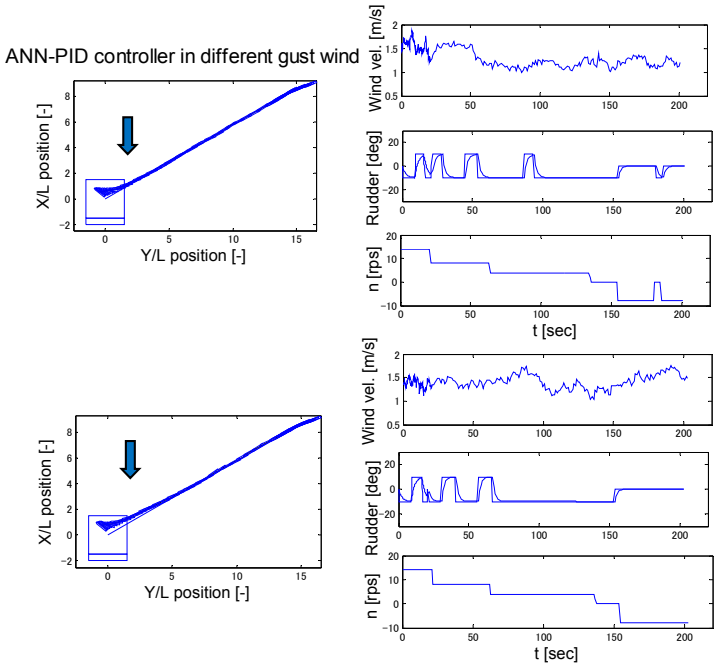

Figure 4.9. Controller under different gusts, average wind velocity 1.5 m/s, wind direction 0º, initial ship heading 250º from virtual window for rudder constraint ±10º

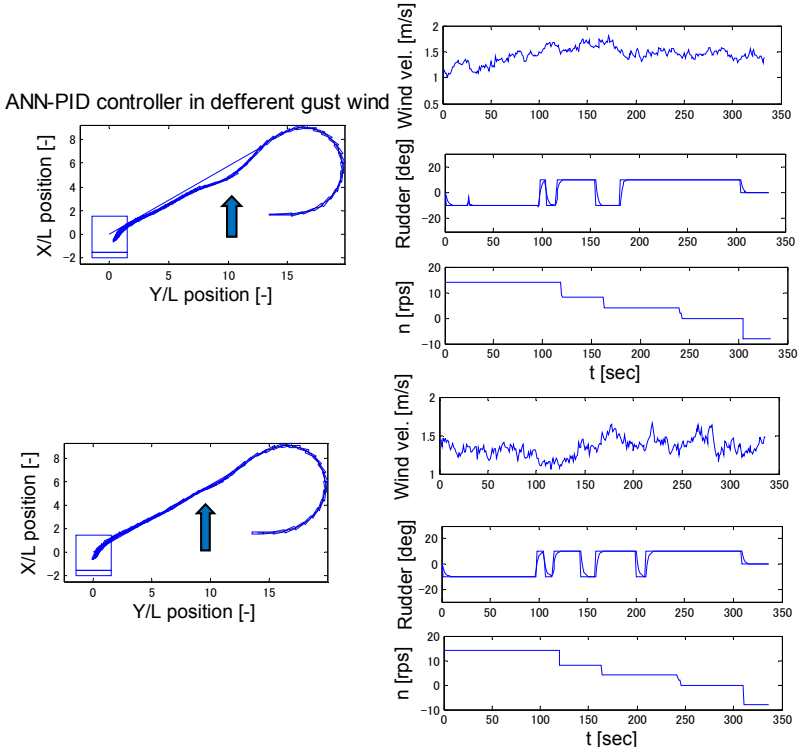

Figure 4.10. Controller under different gusts, average wind velocity 1.3 m/s, wind direction180º, initial ship heading -270º from virtual window for rudder constraint ±10º

4.1.3 Verification for Different Wind Directions

Wind can blow from any possible direction, thus the effectiveness of ANN-PID controller needs to be investigated for different wind velocities together with different directions. In this thesis, to do that, ship with different initial headings and starting points is tested for any particular wind velocity from different directions. The following figure shows one of such results under wind from different directions while keeping the average velocity and ship's initial state similar. During such investigation, maximum average wind velocity of 1.5 m/s is considered for eight different directions at 45º interval.

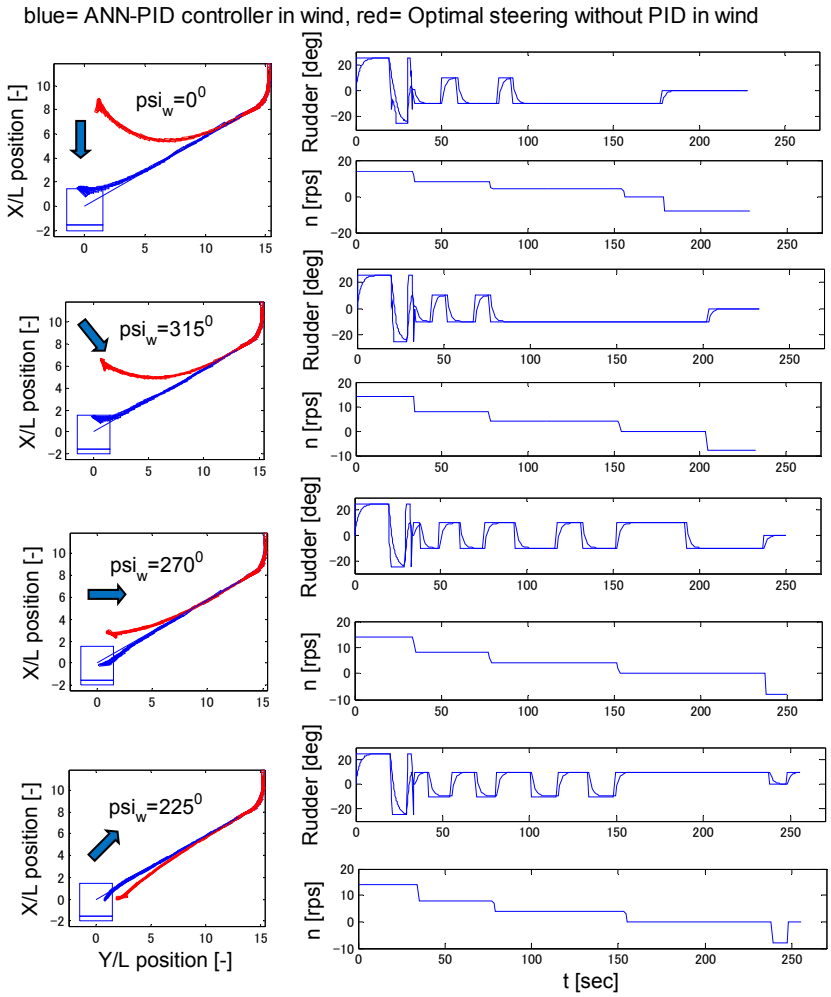

Figure 4.11. Controller under different wind directions, average wind velocity 1.5 m/s, initial ship heading 180º from virtual window for rudder constraint ±25º

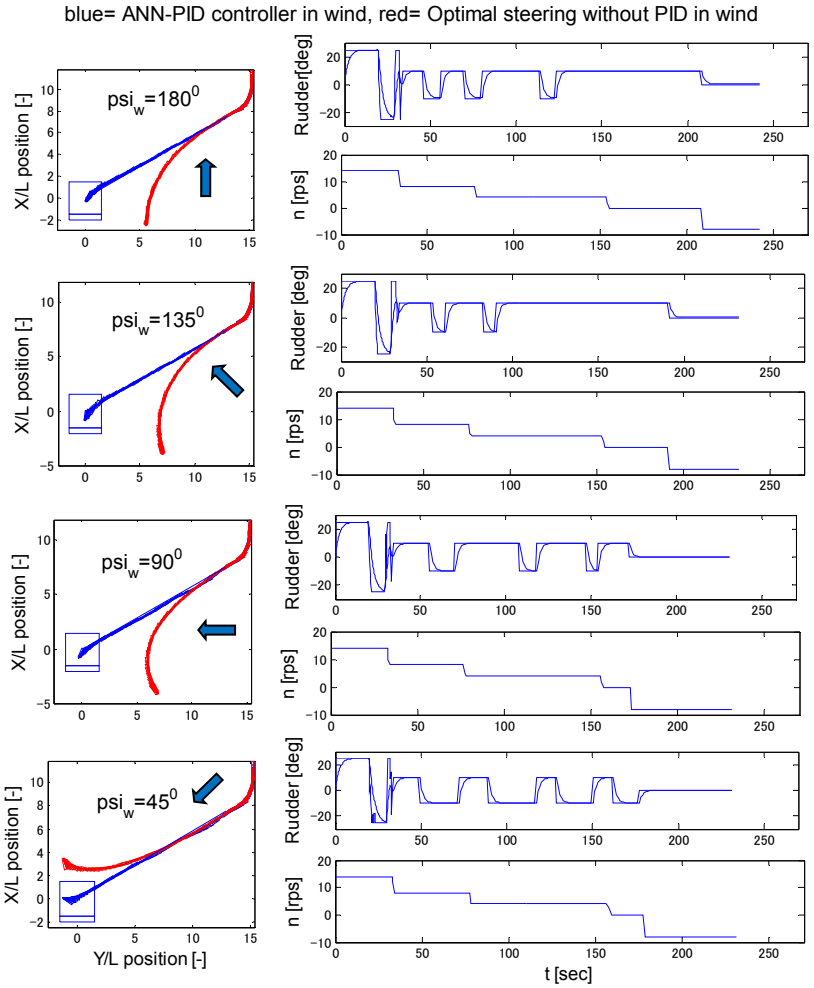

Figure 4.11(cont..). Controller under different wind directions, average wind velocity 1.5 m/s, initial ship heading 180º from virtual window for rudder constraint ±25º

The red trajectories in Figure 4.11 clearly show the effect of wind from different directions. Due to not using any controller during low speed running, the ship deviates from its desired path in different ways depending on the directions of the wind. However, while using the proposed PID controller with ANN, each case ensures successful berthing.

4.1.4 ANN-PID Controller in Severe Wind near Pier

At an earlier stage of this thesis, a PID controller with restricted rudder angle ±5° was proposed to use during straight running. Using that PID controller, it was investigated that stopping with higher reversing propeller revolution may become

necessary in some limited cases, depending on strong wind blowing near pier over 1.0 m/s average velocity. Since the final position to stop the ship in case of berthing is very crucial, such criterion was investigated depending on the ship position before stating reversing and proposed as follows:

If the ship position before reversing propeller becomes less than 0.9 times of ship length from the berthing goal point, then reversing with half astern is better than using slow astern. Thus, in such cases, the ANN results for slow astern are substituted by half astern value.

Considering such modification, Figure 4.12 demonstrates the simulation result for half astern and compared with previous result.

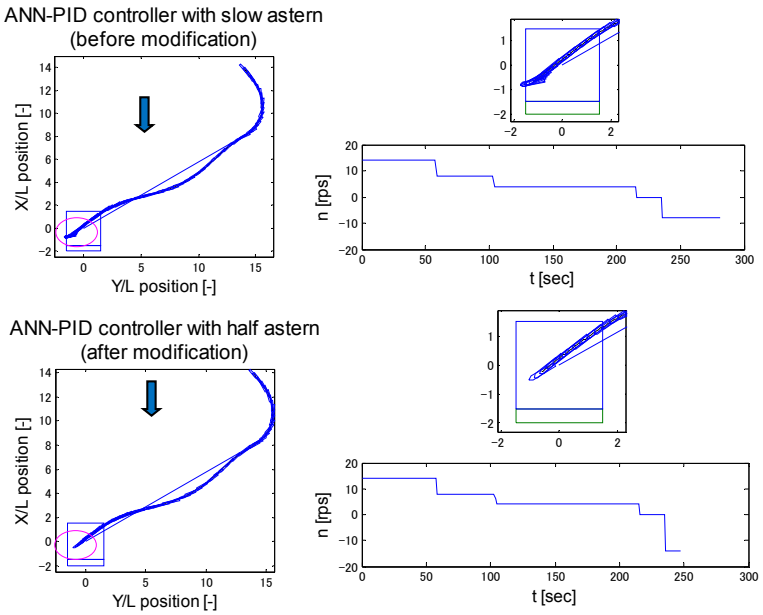

Figure 4.12. Comparison between half astern and slow astern, average wind velocity 1.3 m/s, wind direction 0º, initial ship heading 140º from virtual window for rudder constraint ±15º

This kind of modification is proposed for emergency cases, when the ANN fails to make early reversing and the remaining distance to stop the ship becomes less than 0.9 times of ship length. However, for the further development of this thesis, the same ANN-PID controller is tested for different wind velocities and different ship's initial sates as explained in the previous subsections. Then, it has been found that in some cases even using a PID controller with restricted rudder angle ±5º it may become

difficult to make a successful berth under wind over 1.0 m/s. In this thesis, such cases are investigated with revised restricted rudder for PID controller where ±10º instead of ±5º is used and found satisfactory results as shown in Figure 4.8. Considering the revised rudder for PID controller, cases with severe wind near pier are also investigated where half astern may become necessary if the PID controller with ±5º is used during straight running as shown in Figure 4.12. The following figures demonstrate some results in case of severe wind near pier while modified PID controller is used during straight running with slow astern.

Figure 4.13 and 4.14 clearly slow while using the modified PID controller, there is no need of half astern although severe winds are observed near pier. This is because the modified PID controller is sufficient to take an adequate rudder angle to prevent much deviation. At the same time, ANN adjusts the propeller revolution according to demand to make successful berthing. As a conclusion, ANN controller with modified PID may treat as an alternative solution to avoid any possible higher reversing astern for berthing.

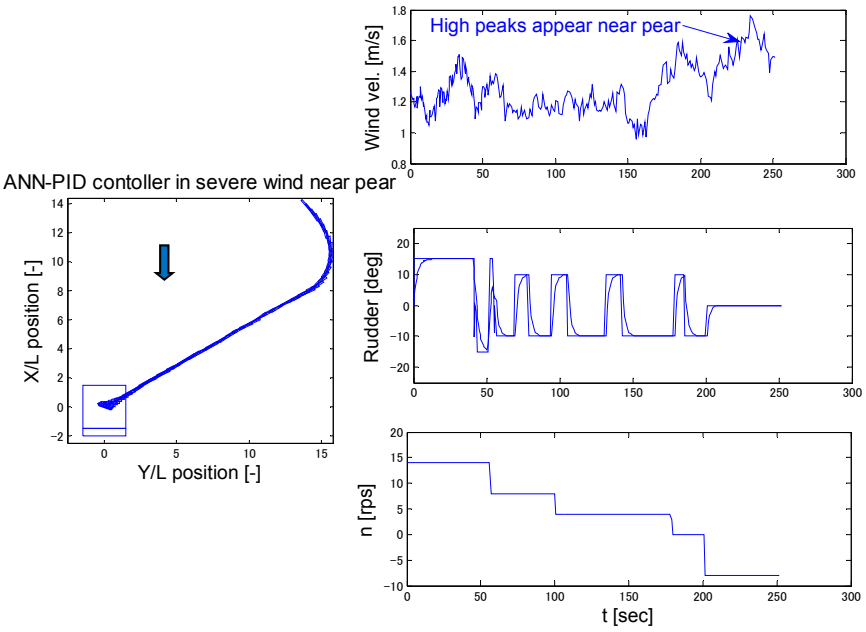

Figure 4.13. Slow astern with modified PID, average wind velocity 1.3 m/s, wind direction 0º, initial ship heading 140º from virtual window for rudder constraint ±15º

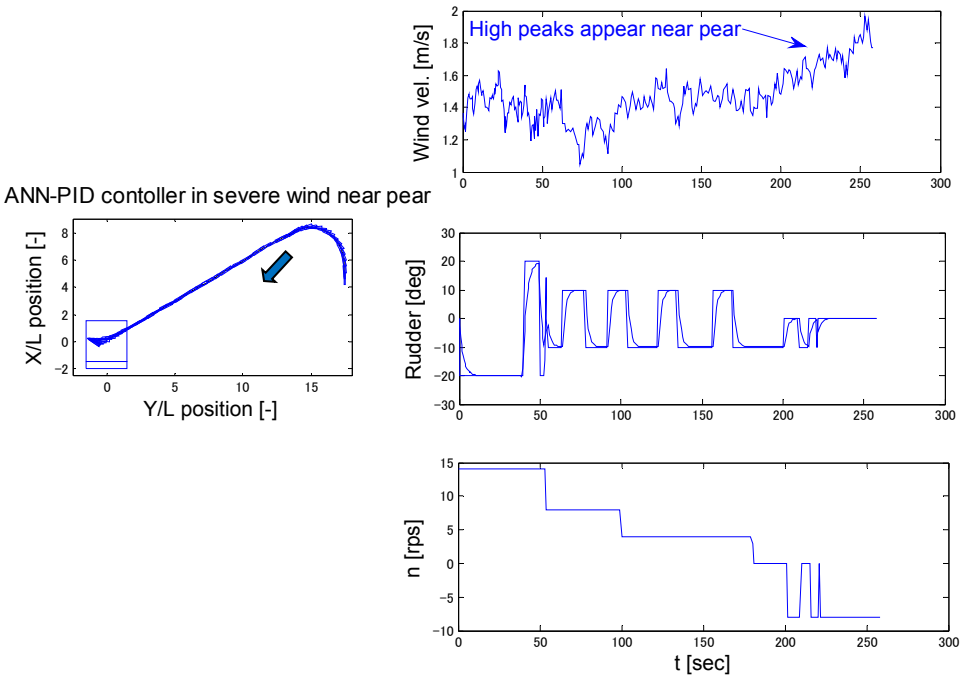

Figure 4.14. Slow astern with modified PID, average wind velocity 1.5 m/s, wind direction 315º, initial ship heading 360º from virtual window for rudder constraint ±20º

4.1.5 PID Controller versus ANN-PID Controller

This kind of comparison emphasises the necessity of using ANN to judge the correct timing of propeller revolution, while only PID controller to adjust the ship's deviation from imaginary line may fail for high wind condition. In this thesis, the created teaching data are so consistent that proper training with such set of teaching data enhances the ability of trained ANN to judge correct telegraph order depending on the ship's velocity and other available input parameters. Therefore, the ANN with PID controller works successfully in most cases where only PID controller for track keeping fails due to the improper judgement of propeller revolution change. Figure 4.15 and 4.16 illustrate such comparison for severe wind disturbances like 1.3 m/s or 1.5 m/s. The difference in the trajectories is shown in enlarged form as first row-second column of each figure.

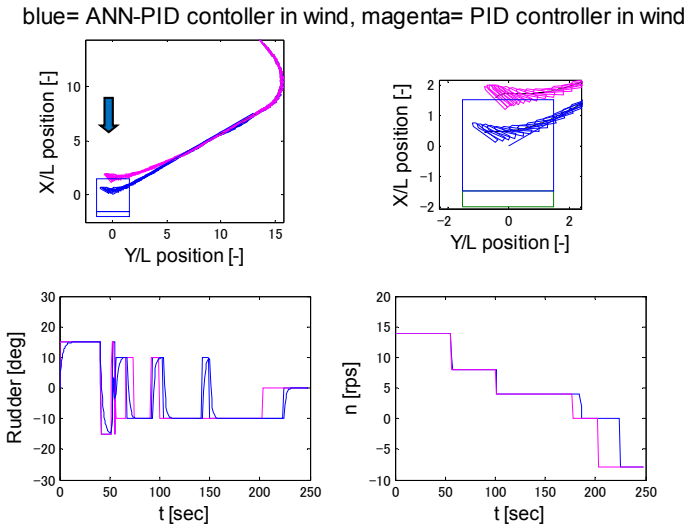

Figure 4.15. Comparison between ANN-PID and PID, average wind velocity 1.5 m/s, wind direction 0º, initial ship heading 140º from virtual window for rudder constraint ±15º

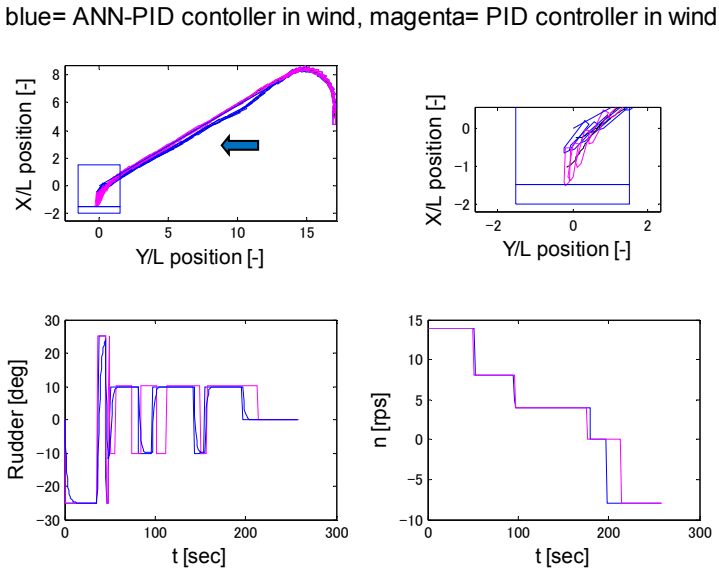

Figure 4.16. Comparison between ANN-PID and PID, average wind velocity 1.3 m/s, wind direction 90º, initial ship heading 360º from virtual window for rudder constraint ±25º

Here, Figure 4.15 shows how the ANN elongates the engine idling time to allow the ship to go further and finally followed by reversing to stop the ship within the successful berthing zone. On the other hand, Figure 4.16 shows the ANN reduces the idling time as the situation demands to make successful berthing. Here in each case, the improper idling time causes berthing failure.

4.2 Ship Starting from Arbitrary Point

Although the simulations mentioned in the previous subsections are done by assuming the ship successfully passes through its desired starting point, in real situation considering the existing disturbances, it is extremely difficult to do so. Therefore, to judge the controller's suitability in real ship operation, the networks are tested for staring point flexibility. This also means to judge the interpolation ability of trained ANN. Figure 4.17 illustrates one of such results.

In Figure 4.17, considering the first row, the red and blue lines indicate the surrounded teaching data and the ANN is tested for an arbitrary point in the middle of virtual window for rudder constraints ±10º and ±15º as shown in black line with the initial ship heading 160º. It is also mentioned that the teaching data contains information regarding the ship heading 150º and 180º as the nearest value of the tested heading. The average wind velocity is set at 1.3 m/s from 45º. Here, it is clearly noticeable that the course changing pattern for the tested point is similar to its surrounded teaching data and the rudder angle shown in the second row-first column is a combination of 10º and 15º for course changing which is expected one.

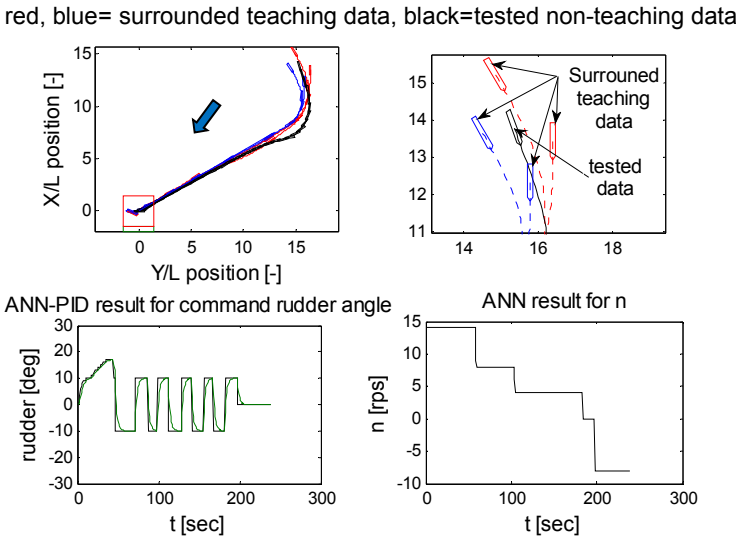

Figure 4.17. Controller's interpolation ability, initial heading 160º from an arbitrary point

To judge the position flexibility, three options are chosen in this thesis. The first is for the ship attaining any undesired point on virtual window, i.e. the current heading is

not matching with the desired one for that starting point. Second is for the ship starting from the middle of virtual window for two different rudder constraints and the third is for the ship starting from any position within the constructed virtual window area with any possible initial heading. The following subsections describe about these in details.

4.2.1 Ship Starting from Undesired Point on Virtual Window

In this category, a ship staring form undesired virtual window point is tested to judge the robustness of the controller. In other words, a ship with its initial heading other than expected is simulated from different virtual window points. Figure 4.18 and 4.19 illustrate the results for LHS approach, when the ship with initial heading 180º and 200º respectively is started from each other's corresponding point in a virtual window.

Considering Figure 4.19, due to starting form unexpected point, although the ANN controller takes necessary action, there exists a certain gap between the ship and imaginary line after course changing. Then, followed by the PID controller, necessary corrections are taken. At last, the ship manages to merge with the imaginary line and the ANN controller controls its speed to stop it within the assumed successfully berthing zone. During the simulation, an average wind of 1.5 m/s from 135º is considered and the combined ANN-PID controller has found to work effectively. On the other hand, considering Figure 4.19 under the same wind disturbances, although starting from an unexpected point, ANN manages to act properly. Thus, the course changing trajectory looks the best possible one. Here, the PID controller just needs to keep the course for low speed running in wind disturbances. Moreover, the ANN controller for propeller revolution tries to make idling and revering sequentially for some times to allow the ship to move more forward as its speed reduces faster than expected.

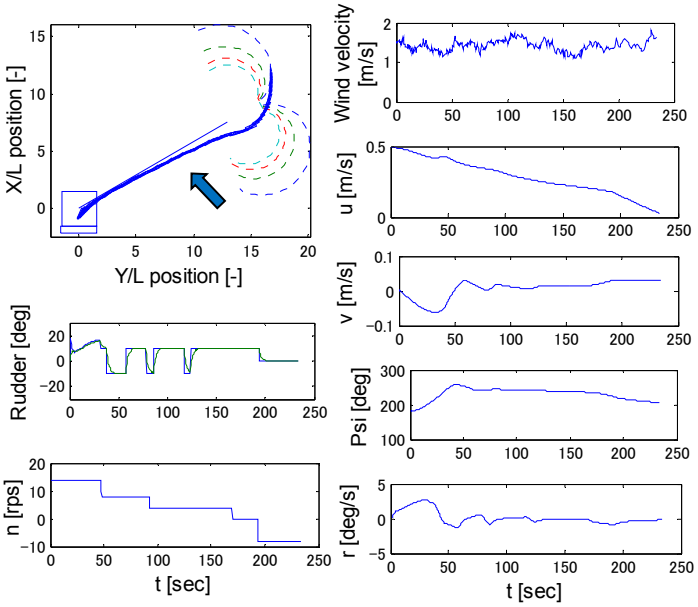

Figure 4.18. Initial heading 180º and starts from point belongs to heading 200º on virtual window for rudder constraint ±10º

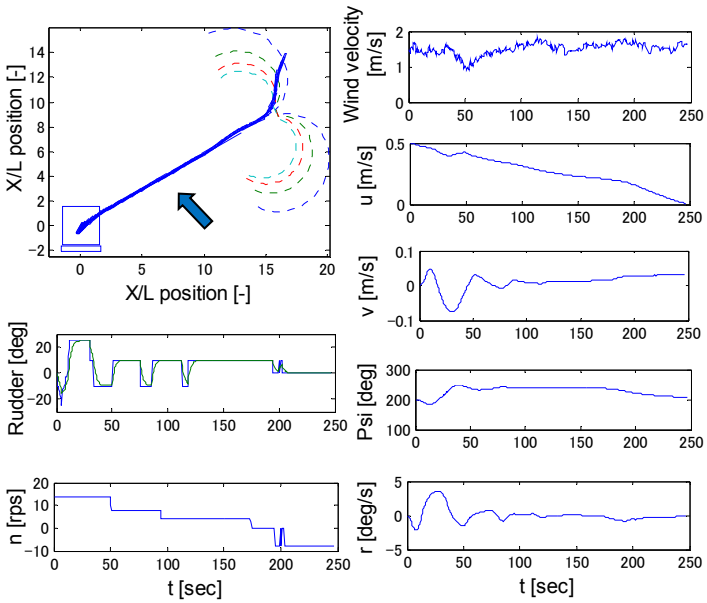

Figure 4.19. Initial heading 200º and starts from point belongs to heading 180º on virtual window for rudder constraint ±10º

Fig 4.20 illustrates the result for the ship starting with initial heading 160º, 180º and 200º respectively, but from the same point on virtual window. Here, the point desired for heading 140º on virtual window for rudder constraint ±15º is chosen. In case of initial heading 160º as shown in the first row of the figure, the ANN first decides to

take a port turn. Later on, it starts its expected starboard turn but gradually. Therefore, the ship follows a long way and there exists a large gap between the ship and imaginary line after course changing. This is a quiet unusual phenomenon and may sometimes occur due to starting from unexpected point. However, the PID controller works effectively to minimise such existing gap and at last, the ship successfully stops within the expected zone. For the other two cases, the ANN controller takes proper decision and after a slight port turn, the ship starts its expected starboard turn. Therefore, it takes a shorter path to travel as well as less time to complete the berthing process. The wind disturbances considered in all three cases are the same, which is average wind velocity of 1.5 m/s from 315º wind direction.

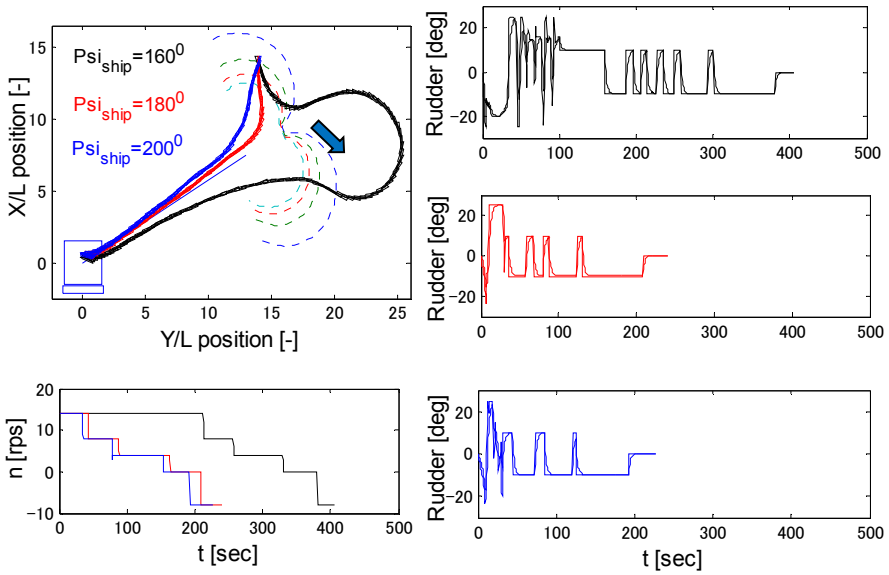

Figure 4.20. Ship with different initial headings and same initial point (LHS)

In a similar way, Figure 4.21 and 4.22 show the results for RHS approach considering the ship starting with initial heading 280º and 300º respectively, but from each other's corresponding point. The wind is considered as 1.5 m/s from 225º. In both cases, the existing gaps between the ship and imaginary line after course changing are minimised successfully by the followed up PID controller. The ANN controller for propeller revolution also increases the speed when the ship tends to stop well beyond entering the successful zone due to the presence of opposing wind.

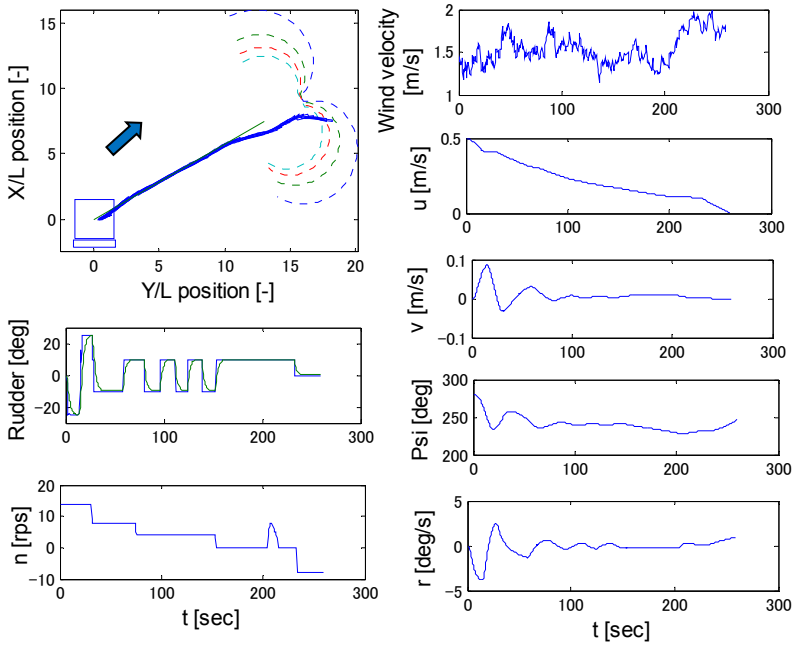

Figure 4.21. Initial heading 280º and starts from point belongs to heading 300º on virtual window for rudder constraint ±20º

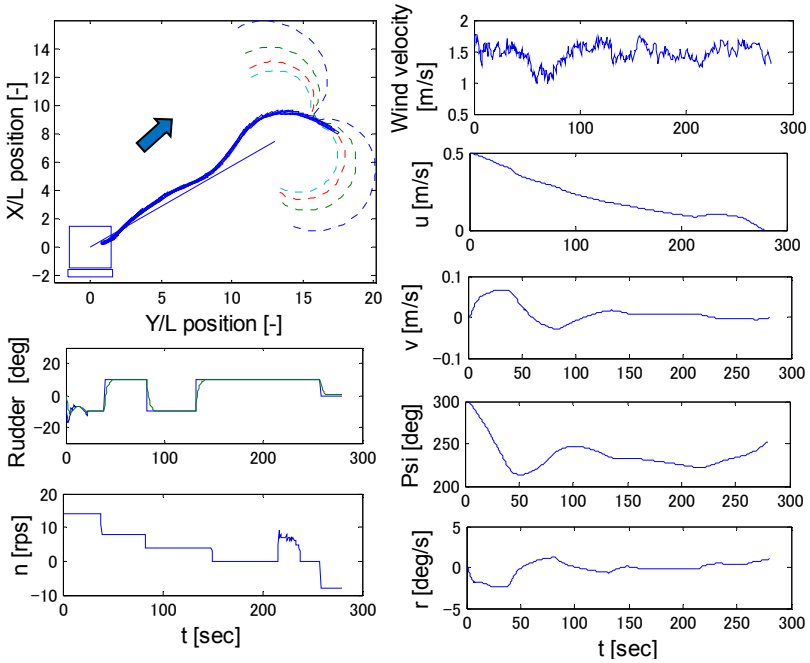

Figure 4.22. Initial heading 300º and starts from point belongs to heading 280º on virtual window for rudder constraint ±20º

Figure 4.23 on the other hand, illustrates the simulation results for ship starting with heading 300º, 320º and 340º respectively, but from the same initial point that is

desired for heading 360º on virtual window for rudder constraint ±25º. The wind disturbances considered here is an average of 1.5 m/s from 180º. In such situation, the ANN controller for propeller revolution allows some boosting like action to accelerate the ship little bit. This also allows increasing the rudder effectiveness in low speed running. Although the overall trajectories are not same, in each case the combined controller ensures successful berthing.

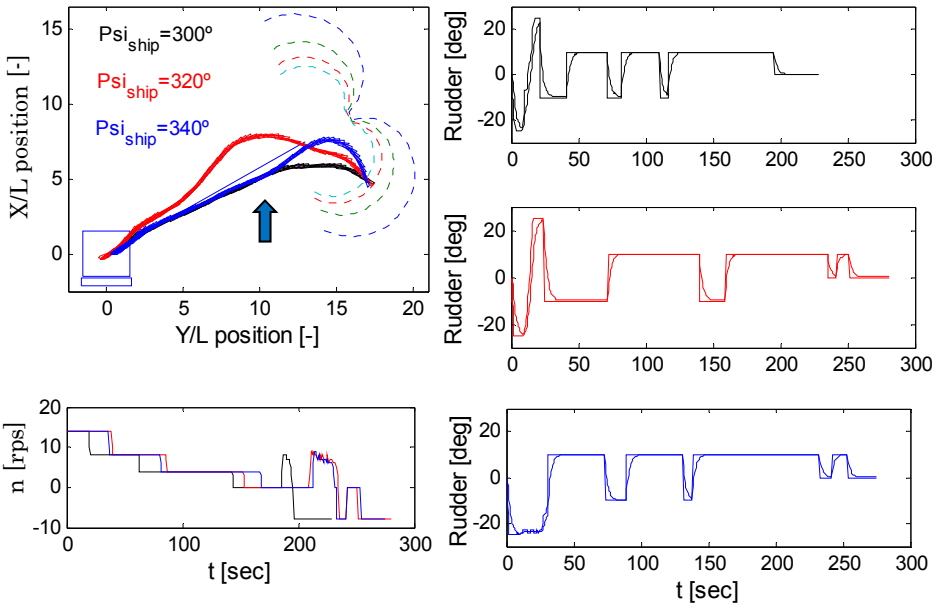

Figure 4.23. Ship with different initial headings and same initial point (RHS)

4.2.2 Ship Starting from Mid of Virtual Window for Two Different Rudder Constraints

The ship having different initial headings and starting from middle of virtual window for two different rudder constraints is tested in this category. Simulations are carried out both for LHS and RHS side approach. Figure 4.24 and 4.25 illustrate the results for the ship starting from mid of virtual window for rudder constraints ±10º ~ ±15º and ±15º ~ ±20º, respectively. In both cases, the ANN controller does the smooth operation during course changing and the ship successfully stops within its desired zone. The wind velocity considered here is 1.5 m/s from 270º and 90º, respectively as shown in the mentioned figures.

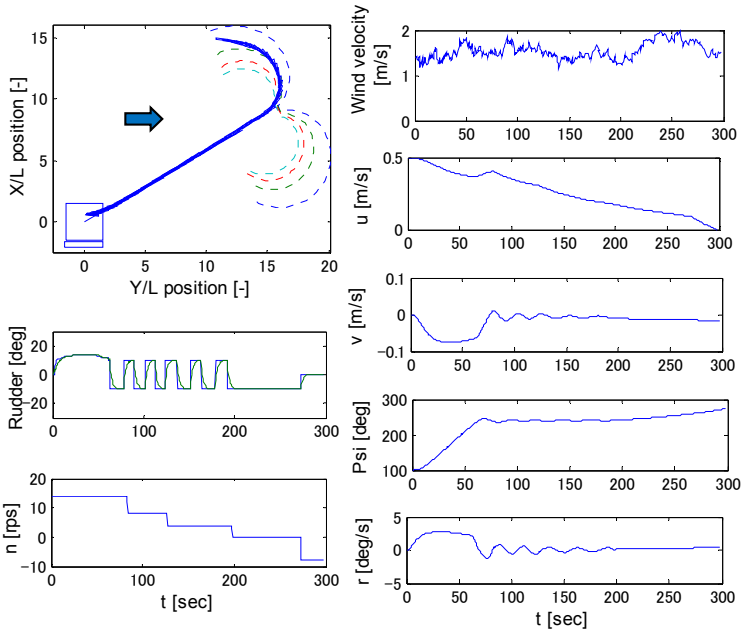

Figure 4.24. Initial heading 100º and starts from mid of virtual window for rudder constraints ±10º and ±15º

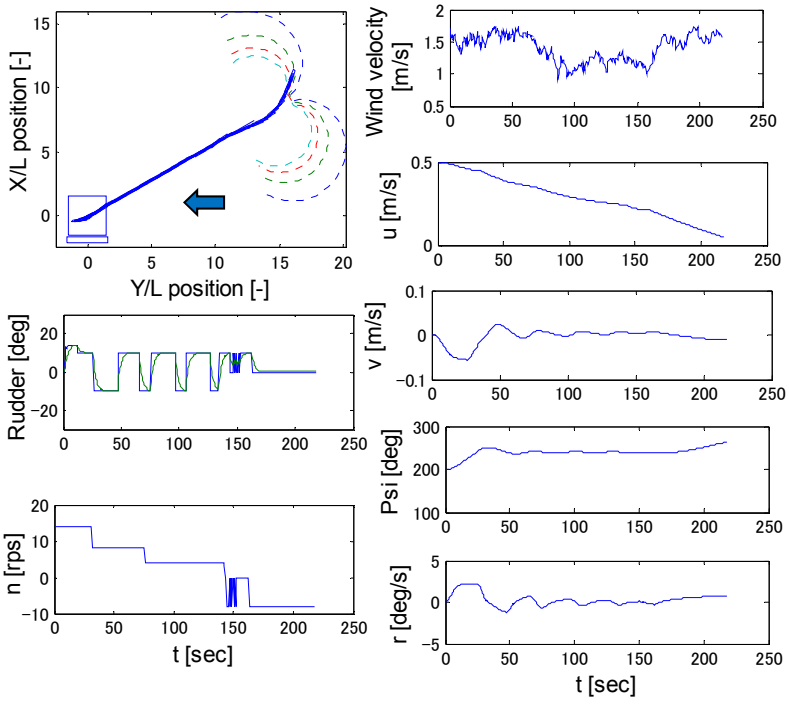

Figure 4.25. Initial heading 200º and starts from mid of virtual window for rudder constraints ±15º and ±20º

On the other hand, Figure. 4.26 and 4.27 illustrate the results for RHS approach.

Figure 4.26 shows the result for the ship starting with heading 450º or 90º from mid of window for rudder constraints ±20º and ±25º under wind disturbances of 1.0 m/s from 0º. Here, the ANN controller for rudder executes the port rudder right from the beginning of coursing changing. Then, followed by the PID controller, the existing gap between ship and imaginary is minimised. Finally, the ship stops successfully as proper propeller revolution is maintained by ANN controller during the whole berthing process. Considering Figure 4.27, ship starting with heading 270º from mid of virtual window for rudder constraints ±10º and ±15º is simulated under wind disturbances of 1.5 m/s from 225º. Here, the ANN-PID controller again proves its effectiveness by successfully guiding the ship up to near the pier.

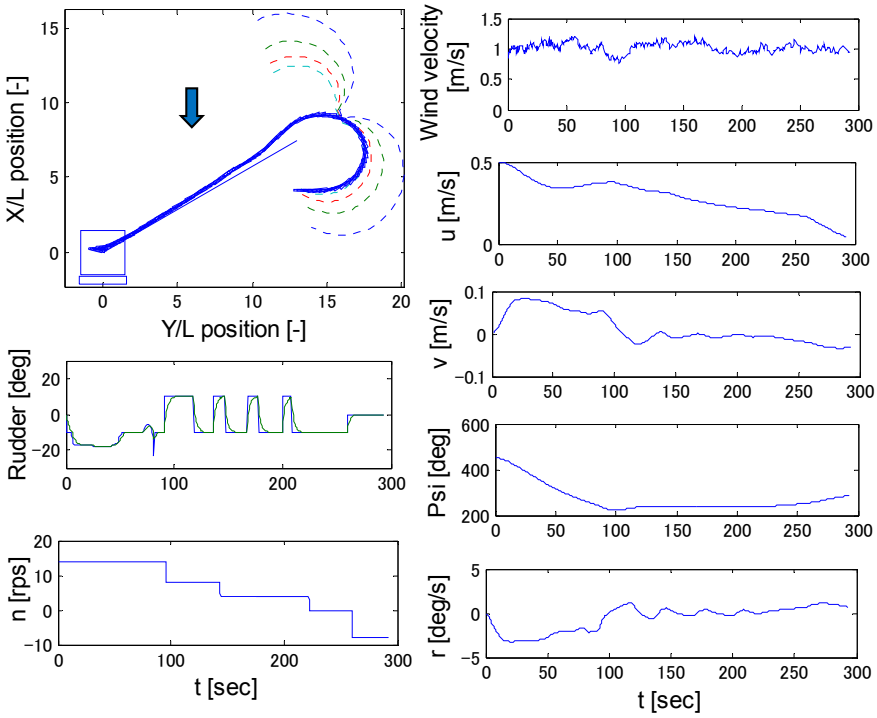

Figure 4.26. Initial heading 90º and starts from mid of virtual window for rudder constraints ±20º and ±25º

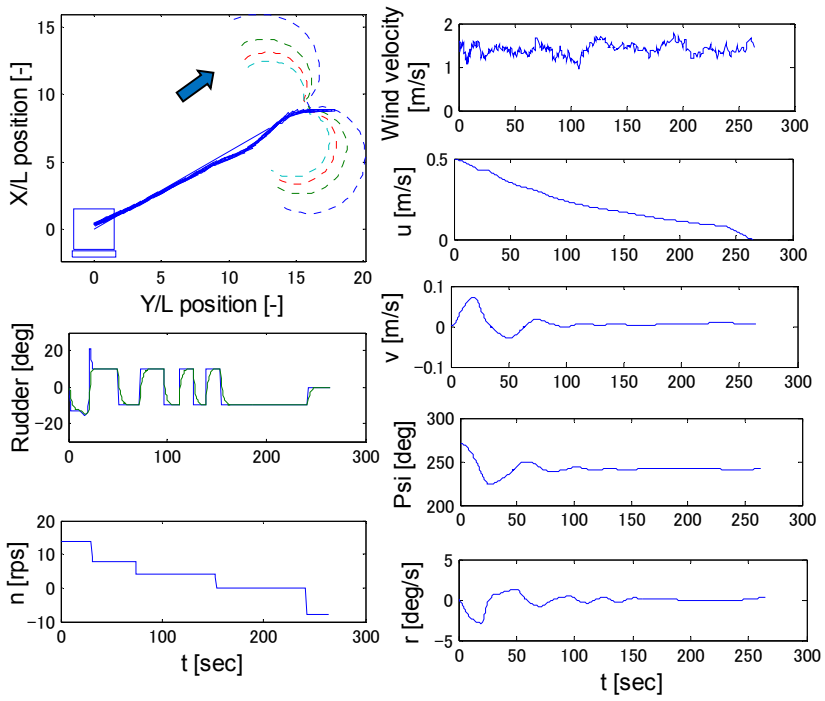

Figure 4.27. Initial heading 270º and starts from mid of virtual window for rudder constraints ±10º and ±15º

4.2.3 Ship Starting from Any Point within the Virtual Window Area

The ship having different initial heading and starting from arbitrarily chosen point is tested in this category for possible successful berthing results. A separate GUI is developed which helps the user to select the starting point of ship by using cursor. Such GUI also displays the virtual window for four different rudder constraints. Thus, the user can judge possible starting point depending on the ship's initial heading. Figure 4.28 and 4.29 illustrate such simulation results for LHS approach.

Considering Figure 4.28, ship starting with initial heading 150º is simulated from an arbitrary point under wind disturbances of 1.5 m/s from 45º. Here, the controller takes slight port rudder first which allows the ship to enter into a convenient space before starting its approach to merge with the imaginary line. Therefore, the trajectory for course changing seems very smooth. Due to having following wind, the ANN controller also executes reversing well before idling stage and then go for final reversing. On the other hand, in Figure 4.29, the operation for propeller revolution

under wind disturbances of 1.5 m/s from 315º looks usual and the ship merges gradually to the imaginary line as the error is minimised by the PID controller during low speed running.

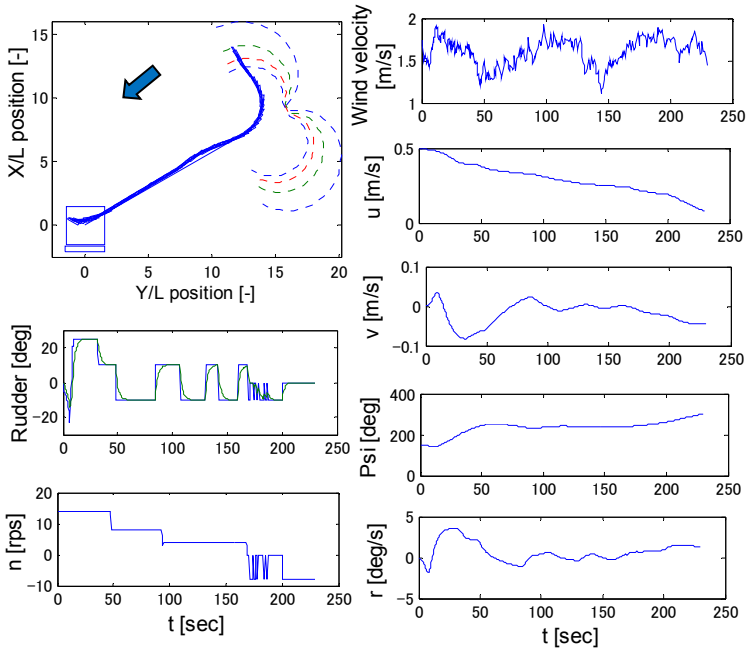

Figure 4.28. Controller for arbitrary starting point, ship starts with heading 150º

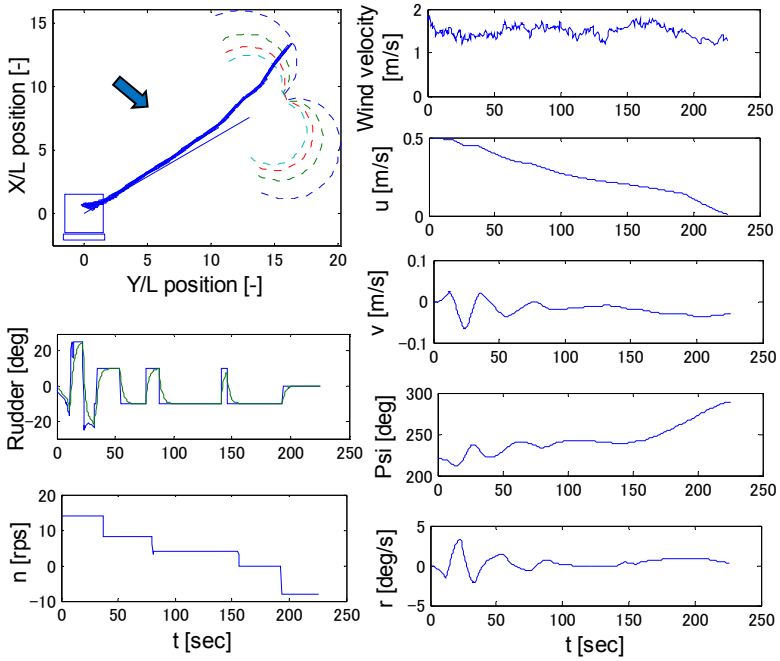

Figure 4.29. Controller for arbitrary starting point, ship starts with heading 220º

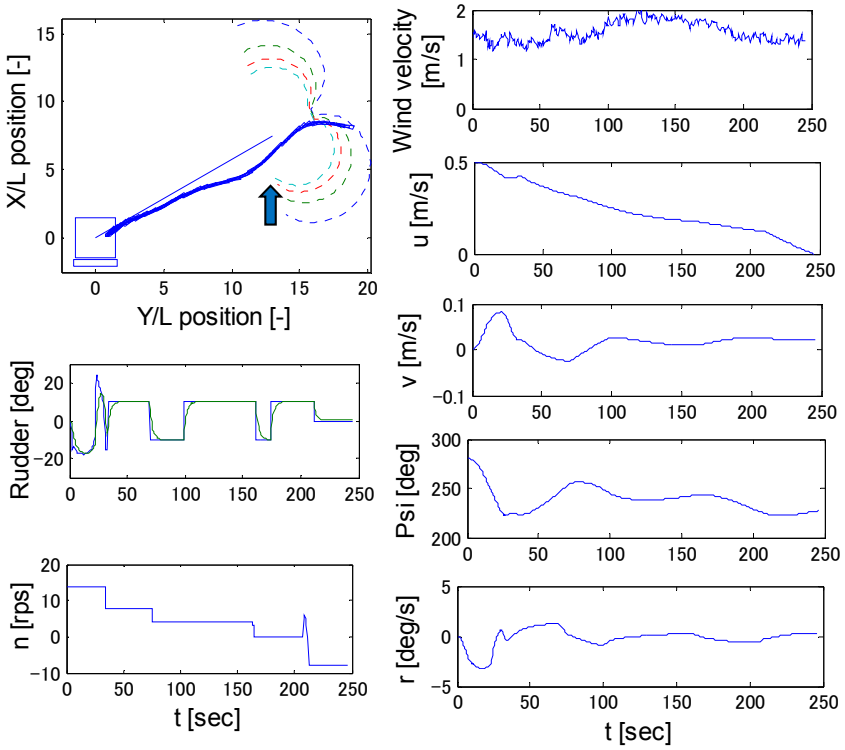

Figure 4.30. Controller for arbitrary starting point, ship starts with heading 280º

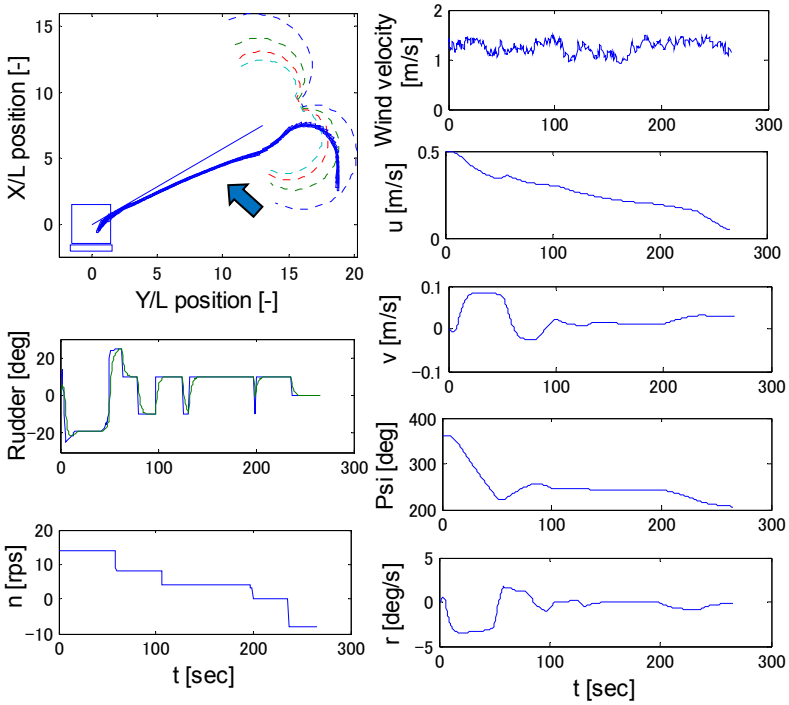

Figure 4.31. Controller for arbitrary starting point, ship starts with heading 360º

In a similar way, simulations are also carried out for the RHS approach as shown in

Figure 4.30 and 4.31. Considering Figure 4.30, ship starting with heading 280º is simulated under wind disturbances of 1.5 m/s from 180º. Here, an arbitrary position near virtual window for rudder constraint ±10º is chosen as a starting point from where the controller guides the ship successfully up to the desired boundary zone. Figure 4.31 also ensures successful berthing result for the ship starting with heading 360º under wind disturbances of 1.5 m/s from 135º.

Figure 4.32 illustrates the simulation results for ship starting with initial heading 280º, but from three different arbitrary points. In all three cases, the controller takes different decisions based on surrounding situation and succeeded to guide the ship up to the expected safety zone. The wind disturbances considered in all three cases are the same, which is average wind velocity of 1.5 m/s from 180º wind direction.

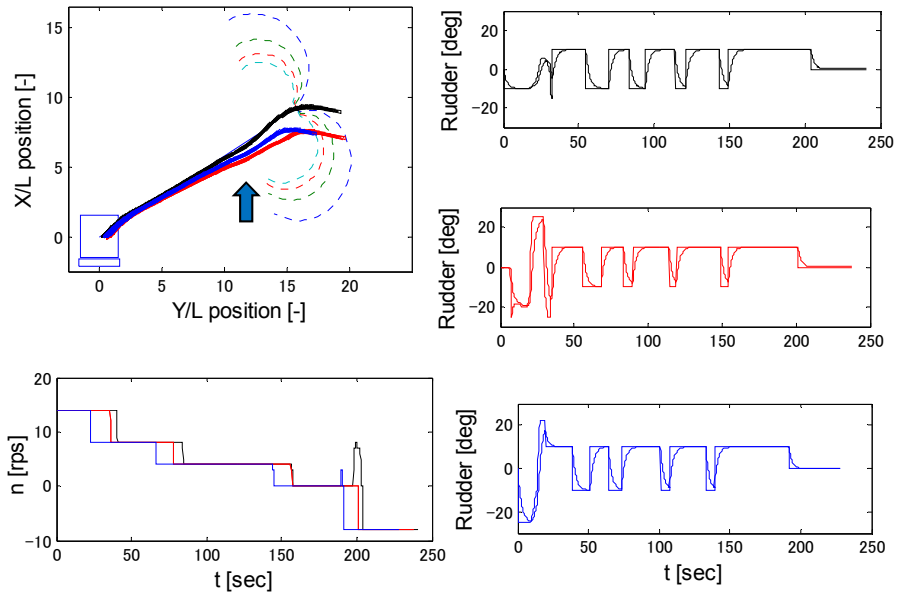

Figure 4.32. Ship with the same initial heading and different initial points

4.3 Stability Analysis using Monte Carlo Simulations

In any closed loop system, it is very important to prove the stability of the controller in order to guarantee the success. In this thesis, supervised neural networks are used with a PID controller for low speed running to ensure automatic ship berthing.

In order to judge the effectiveness of the controller, several simulations are done as mentioned in the previous subsections. However, to analyse the reliability of the controller, Monte Carlo simulations are also performed. To generate the random numbers, uniformly distributed pseudorandom numbers are chosen. Such random numbers are generated for ship's staring point, heading, average wind velocity and wind direction. Then, around 970 cases are investigated which covers all virtual window areas.

As a success index, three parameters are considered. These parameters are sufficient to know the success of the controller in each run. The indexes are: Non-dimensioned distance from the target goal point after stopping, heading error from target value 240º and final surge velocity from target value 0.05 m/s. Analysis of such success indexes is mentioned in the following subsections.

4.3.1 Non-dimensionalised Distance from Final Goal Point

In this thesis, the ship is assumed to be stopped if the surge velocity becomes less than 0.05 m/s. After the termination of each simulation case, error in ship position, i.e. Δx and Δy are calculated based on target goal point (0, 0). Here, the success of each ship berthing counts if the ship stops within the desired successful zone, which is 1.5L area around the goal point. After that, tugs will assist to align it with pier.
The distance as a success index is calculated using Equation 4.2 and non-dimensionalised using Equation 4.3.

$$\Delta d = \sqrt{\Delta x^2 + \Delta y^2} \tag{4.2}$$

$$\Delta d' = \frac{\Delta d}{L_{ship}} \tag{4.3}$$

Then, considering the randomly chosen ship positions, headings and wind disturbances, the results are tabulated for the frequency of each particular interval of non-dimensionalised distance. The corresponding frequency table is given below:

Table 4.1. Frequency table for $\Delta d'$

$\Delta d' = \frac{\Delta d}{L_{ship}}$	frequency	percentage
0-0.1	38	3.91%
0.1-0.19	288	29.66%
0.2-0.29	190	19.57%
0.3-0.39	85	8.75%
0.4-0.49	62	6.39%
0.5-0.59	98	10.09%
0.6-0.69	44	4.53%
0.7-0.79	13	1.34%
0.8-0.89	11	1.13%
0.9-0.99	13	1.34%
1-1.19	10	1.03%
1.2-1.29	6	0.62%
1.3-1.39	6	0.62%
1.4-1.49	3	0.31%
1.5-1.59	4	0.41%
1.6-1.69	5	0.51%
1.7-1.79	1	0.10%
1.8-1.89	4	0.41%
1.9-1.99	0	0.00%
2-2.49	4	0.41%
2.5-2.99	3	0.31%
3-3.49	0	0.00%
3.5-3.59	0	0.00%
	success=	91.45%

The histogram and median value plot for the above frequency table are shown in Figure 4.33. The above frequency table and histogram plot clearly show that the maximum frequency occurs at 0.1L ~ 0.19L interval that is 29.66% of total sample cases. Then, the frequency gradually decreases with the increment of non-dimensionalised distance value. Beyond 1.12L, the percentage gets less than 1.0. Here, the total success rate is 91.45%.

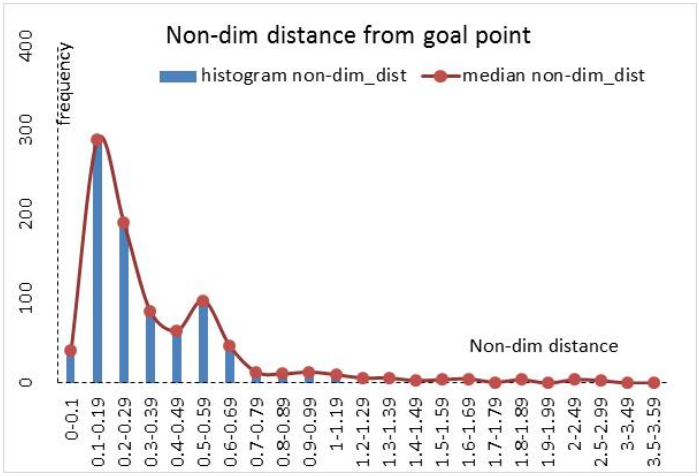

Figure 4.33. Histogram and median value plot for $\Delta d'$

Regarding the unsuccessful cases, these occur for a limited number of starting points and ship headings. In such cases, the neural network confuses and rotates the ship repeatedly instead of guiding it to the imaginary line. However, it is believed that, by including those initial conditions into the teaching data and training the nets again, the existing percentage of error that is 8.55% for unsuccessful berthing cases could be reduced to a lesser value.

4.3.2 Heading Error

After course changing, the expected heading to be kept by the PID controller during low speed running is 240º. However, due to the hydrodynamic properties that are acting on the ship during reversing, the ship with single rudder-single propeller has the natural tendency to turn toward its starboard side. Moreover, in nearly zero speed the effectiveness of rudder also drastically deteriorates. Thus, the wind disturbances also have its large effect. As a result, although the controller successfully attains the target heading during the low speed running, due to reversing, the final heading tends to diverge toward the starboard side. This means, the expected frequency distribution curve should have the tendency to shift towards some positive value. Here, the error in final heading is calculated from the target heading using Equation 4.4.

$$\Delta\psi = \psi_{(final)} - 240 \tag{4.4}$$

Then, considering the randomly chosen ship positions, headings and wind disturbances, the results are tabulated for the frequency of each particular interval of heading error given as Table 4.2.

Table 4.2. Frequency table for $\Delta\psi$

$\Delta\psi$ (deg)	frequency	percentage
-70~-60.1	1	5.46%
-60~-50.1	5	0.51%
-50~-40.1	6	0.62%
-40~-30.1	5	0.51%
-30~-20.1	21	2.16%
-20~-10.1	45	4.63%
-10~-0.1	64	6.59%
0~9.9	91	9.37%
10~19.9	190	19.57%
20~29.9	279	28.73%
30~39.9	121	12.46%
40~49.9	42	4.33%
50~59.9	23	2.37%
60~60.9	14	1.44%

The histogram and the median value plot for the above frequency table are shown in Figure 4.34. The above frequency table and histogram plot clearly show that the maximum frequency occurs at 20º ~ 20.9º interval, which is 28.73% of total sample cases. This will actually make the final ship heading parallel to the pier. Beyond that maximum frequency, in both positive and negative directions, the frequency gradually reduces. Moreover, the histogram plot also shows that the frequency distribution of heading error shifts little bit forward, i.e. towards the starboard side due to the mentioned reason.

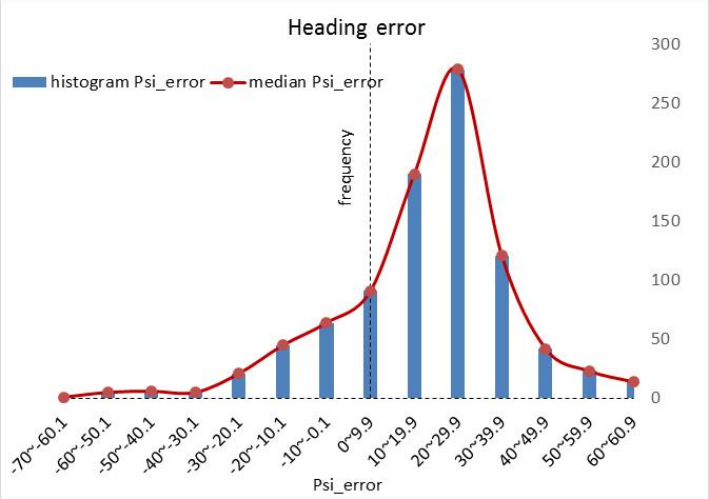

Figure 4.34. Histogram and median value plot for $\Delta\psi$

Since the tugs are expected to assist the ship later to align it with pier, the heading error within the shown limit is allowable for further tug assistance if the vessel is clearly stopped. Thus, analysis of final surge velocity is very important to ensure the success of berthing.

4.3.3 Surge Velocity Error

One of the criteria for considering the berthing as successful in this thesis is the final surge velocity ≤ 0.05 m/s. Thus, for each of the sample cases, the final surge velocity error is calculated to know its frequency distribution using Equation 4.5.

$$\Delta surge = surge_{final} - 0.05 \tag{4.5}$$

Then, considering the randomly chosen ship positions, headings and wind disturbances, the results are tabulated for the frequency of each particular interval of heading error value given as Table 4.3.

Table 4.3. Frequency table for $\Delta surge$

$\Delta surge$	frequency	percentage
≈0	844	86.92%
0-0.09	59	6.08%
0.1-0.19	23	2.37%
0.2-0.29	45	4.63%
0.3-0.39	0	0.00%

The histogram and the median value plot for the above frequency table are shown in Figure 4.35. The above frequency table and histogram plot clearly show that the maximum frequency occurs when the error is almost zero. Such case occurs in 86.92% of total sample cases. This clearly shows the controller is effective enough to stop the ship within the desired zone. Beyond that maximum frequency, it gradually decreases to a smaller value.

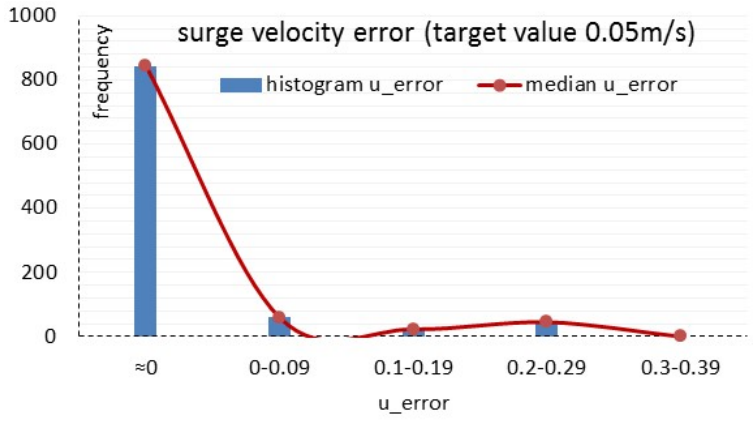

Figure 4.35. Histogram and median value plot for $\Delta surge$

Finally, considering the frequency distribution of the success indexes for randomly chosen samples, i.e. using the Monte Carlo simulations, a clear idea is established about the success rate of the proposed controller under wind disturbances. Regarding the number of unsuccessful cases for the randomly chosen sample, as mentioned earlier, can be decreased by adding those situations in the teaching data and train the network again. Such concern will be considered in the future work of this thesis.

Chapter 5 : EXPERIMENTS FOR AUTOMATIC SHIP BERTHING

5.1 Free Running Experiment System

To validate any research studies on autonomous navigation, it is very important to do the model ship experiment first. Doing such experiments in a basin, often raises questions about the limitation of basin size to fully testing the ship's performances. Therefore, researchers are very keen to do such navigational tests in open spaces like a pond or river that allows the model ship to face the real environmental disturbances. Im and Seo (36) describe elaborately about the free running experiment system. Such unique system usually consists of several sensors that provide ship's navigational information i.e. ship's speed, positions, turning rate etc. Osaka University (OU) has the privilege of having such free running experiment system. Figure 5.1, shows the total configuration of the system that OU has.

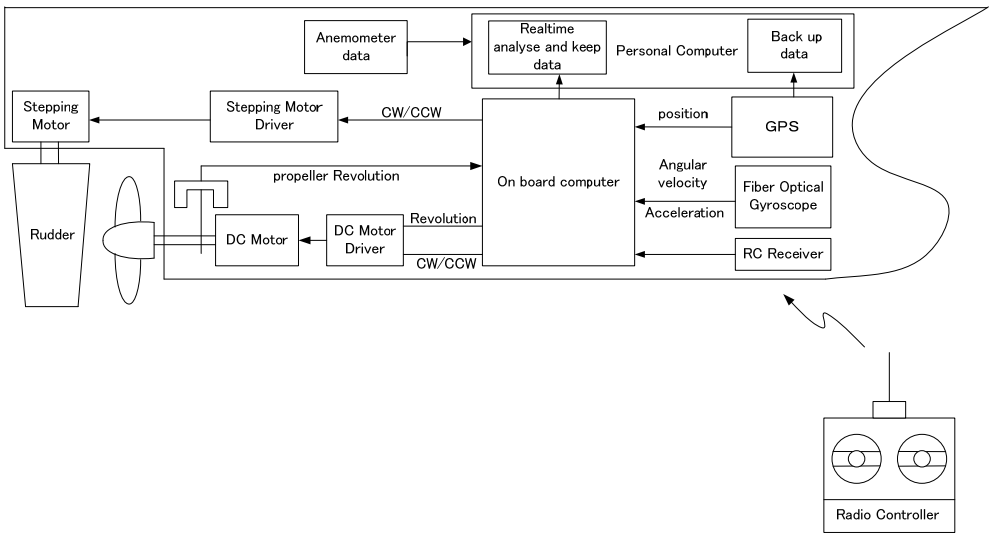

Figure 5.1. Free running experiment system

Here, the whole system consists of three basic and important sensors. One of them is global positioning system (GPS). During the experiment, two real time kinematic (RTK) GPSs are used. One of them is kept fixed on the top of a nearby building and the other one is mounted on model ship. As a result, the model is considered to move with

respect to the fixed RTK GPS. By this way, the fixed RTK GPS provides necessary corrections to get accurate ship position and velocity as compared to using the single GPS unit.

The second important sensor is a gyroscope. It is installed at the centre of gravity (CG) of the ship. The gyroscope is used to measure any type of angular movement. Therefore, this device is responsible for calculating rolling, pitching and yawing motion of the ship during the experiment.

Third and the last sensor in OU's free running experiment system is anemometer. This will calculate the relative wind force as well as wind direction during the experiment.

Having these sensors on board, any types of experiments can be carried out for suitable ship model. In order to maintain particular propeller revolution, pulse width modulation (PWM) mechanism is used for the servo motor. On the other hand, stepping motor is used to maintain precise movement of the rudder. Two 12V batteries are used in series to feed 24V to both servo motor and stepping motor driver. Other devices like on board computer, the gyroscope is provided with 12V by using two batteries in parallel. For GPS on board, 12V is provided through a transformer, which converts the supply voltage to a lower desired value. One personal laptop is also used where all data are kept as backup during each experiment.

5.2 Implementing ANNs in Free Running Experiment Code

After getting satisfactory results from Monte Carlo simulations, the trained ANNs for rudder and propeller revolution are implemented in the free running experiment system. In this thesis, the ANNs used for automatic ship berthing are based on supervised learning. Therefore, after training for minimum MSE value, the weight and the bias matrices of the networks become pre-determined i.e. they will not change during the experiment. Since the networks are created in MATLAB R2009a and the existing free running experiment code is written in C, the desired matrices for the networks need to be read through the C language code. Moreover, virtual window file also needs to be transferred during the berthing experiment to decide the ship's initial

position depending on its heading. The following sub-sections describe elaborately about how the ANNs are implemented in free running experiment system to execute the automatic ship berthing experiment based on virtual window concept.

5.2.1 Pre-processing of Sensors' Outcome for Network's Inputs

Pre-processing is very important while training net in order to remove the scale effects. Therefore, it is often useful to scale the inputs and targets so that they always fall within a specified range. In this thesis, all inputs and targets are scaled within [-1 1] and the following expression is used for the mentioned purpose.

$$y = (y_{\max} - y_{\min}) * (\mathrm{x} - \mathrm{x}_{\min}) / (x_{\max} - x_{\min}) + \mathrm{y}_{\min} \tag{5.1}$$

where, y_{max}=1, y_{min}=-1, x_{max} is the maximum possible value of any particular input for the network, x_{min} is the minimum possible value of that particular input for the network, x is the current value of that particular input for which the conversion is needed and y is the desired converted value of x within [-1 1].

To feed the necessary inputs for pre-processing, GPS provides ship position together with surge and sway velocity. Gyroscope gives the ship heading angle as well as yaw rate. The actual rudder angle is determined by counting pulses sent to the stepping motor for desired angle of rotation. Other parameters like d_1 and d_2 are calculated geometrically depending on the ship position. All such inputs generated by the sensors here represent the value of 'x' in the above expression. Finally, after getting x_{max} and x_{min} for each input from the teaching data, 'y' is calculated for each 'x' to feed to the networks. For any value of 'x' greater than x_{max} will give y=1 and for less than x_{min} will give y=-1.

5.2.2 Reading Virtual Window File and Coordinate Adjustment

Automatic ship berthing experiment using virtual window concept is a completely new era. To initialise the ship position on virtual window, ship's different headings

together with their corresponding points on virtual window for four different rudder constraints are read by the program code. OU's free running experiment system has the privilege to run the model either in manual mode or in auto mode. During manual mode, the rudder angle and the propeller revolution are controlled using radio controller. This mode is usually used to drive the model up to some suitable zone to start the auto mode. When the auto mode is activated, gyroscope detects the ship's current heading and according to that heading, the initial position of the model is sorted out from a given virtual window file. Since the window is created for different rudder constraints, the user needs to select the constraint prior to the experiment depending on interest. The following figure shows one sample data of the virtual window file that is read during the berthing experiment.

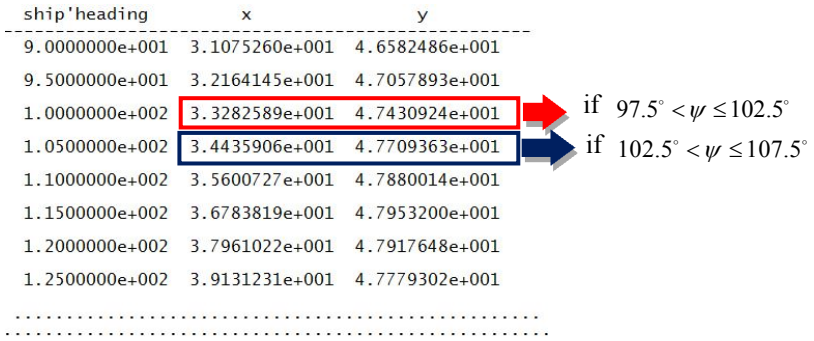

Figure 5.2. Virtual window file

Here, it is noticeable that different points to start the model are given at an interval of 5º of ship heading. However, while activating the auto mode, the current heading angle is detected by gyroscope and the desired starting point needs to be found out for that initial heading. Since the ANN has good interpolation ability, each starting point during the experiment is considered here for a particular range of the ship's initial heading rather than sticking to one particular value. The range of ship heading for each particular starting point is considered as 5º.

Regarding the coordinate adjustment while actuating the auto mode, as mentioned above, a point on the user selected virtual window is sorted out depending on the ship's instantaneous heading. At the same time, GPS also gives a particular ship position. Usually, these two coordinate systems do not coincide with each other. As a result,

relative position with respect to the fixed point on virtual window needs to be calculated on real time to feed the inputs for networks. Equation 5.2 shows the simple calculations done in each time step for such transformation.

$$
\begin{aligned}
x_{diff} &= x_{GPS(\text{at\_VW\_point})} - x_{vw(from\_\text{VW\_file})} \\
y_{diff} &= y_{GPS(\text{at\_VW\_point})} - y_{vw(from\_\text{VW\_file})} \\
x &= x_{GPS} - x_{diff} \\
y &= y_{GPS} - y_{diff}
\end{aligned}
\tag{5.2}
$$

In order to fit the virtual window for different rudder constraints within the available experiment field, the coordinate also needs to be rotated somewhat for both left hand side and right hand side approach. Figure 5.3 shows the arrangement of the coordinate system during berthing experiment. For LHS approach, the imaginary line is set at an angle of 15º from the line perpendicular to the pier. On the other hand, for RHS approach the line is set as perpendicular to the pier.

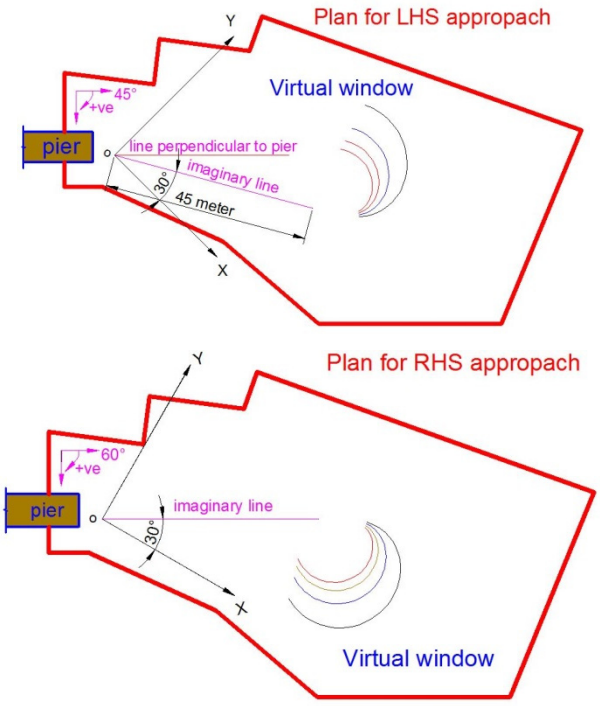

Figure 5.3. Coordinate rotation during berthing experiment

5.2.3 Reading Weight and Bias Matrices for Calculations

It is mentioned earlier that the compilers for the networks are different while being trained and used. Therefore, taking the advantages of supervised learning, the weight and bias matrices are transferred in the form of ASCII values and later on read by the free running system code. In order to perform the desired calculations, proper interlink connections are built among the pre-processed inputs, hidden layers' neurons and pre-processed output. Later on, the pre-processed output is transferred to its actual value before execution by using Equation 5.3.

$$x = (y - y_{min}) * (x_{max} - x_{min}) / (y_{max} - y_{min}) + x_{min} \tag{5.3}$$

Here, the maximum and minimum value of rudder angle during course changing i.e. for the rudder angle output, x_{max}=25° and x_{min}=-25°. On the other hand, propeller revolution varies from half ahead to slow astern. Thus, for the propeller revolution output, x_{max}=14 and x_{min}=-8.

While transferring from one layer to another, the same transfer functions are recreated as used during training net. Since two separate networks are used in this thesis, calculations are done simultaneously on each time for desired rudder and propeller revolution outputs, respectively.

5.3 Initial Conditions during Experiment

A ship may start its approach for berth with different initial speeds. It may also experience different combinations of sway velocities and yaw rates. However, while using the NLP method for creating teaching data, the surge velocity was considered as half ahead without any sway velocity and yaw rate. It means that the ship was assumed to go straight before starting its approach. In real cases, due to the presence of environmental disturbances, it is very difficult to attain so. Moreover, while performing the berthing experiment, there was no arrangement to start the ship from the opposite side of the pier in order to enter the virtual window in a straight course. Therefore, the

model was planned to accelerate first from the pier and then turn to enter the virtual window. As a result, every time while switching to auto mode to enable the ANN controllers, the ship experiences some initial sway velocity as well as yaw rate. Although prior to switching the auto mode the counter rudder is taken to minimise those values, in every run small values of sway velocity and yaw rate always remain. Therefore, it would be a quiet interesting matter to observe how the ANNs behave to such new situation by utilising their robustness. Another important concern is that the points on the virtual window in this thesis do not have any physical existence. As a result, the only option left for the user is to guess the position of the ship by eyes and execute the auto mode when it approaches close to its desired point. Therefore, a good guess provides enough distance for the ship to stop and vice versa. That is why, during the experiment, the whole coordinate is made flexible and positions are calculated relative to each starting point. Figure 5.4 illustrates three possible situations, where case 2 would be the perfect guess to execute the auto mode and its corresponding goal point is about 4.5 m from the pier. Considering case 1, due to starting up from a shorter distance than expected, the final goal point falls over the pier and for case 3, an extended distance to start up the ship allows enough space to stop and this time ship will stop at a distance more than 4.5 m from actual pier. Thus, case 2 and 3 would be the preferable target for executing the automatic ship berthing experiment with reasonable space.

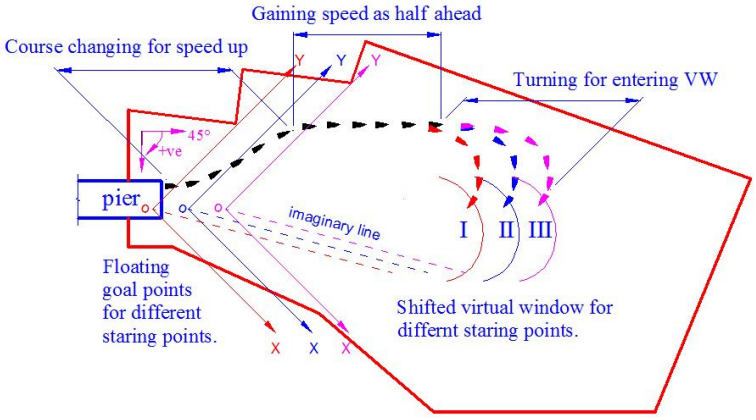

Figure 5.4. Floated goal points with different staring points

5.4 Experiment Results for Points on Virtual Window

In this thesis, the teaching data are categorised into two, depending on the left hand side (LHS) and right hand side (RHS) approach of a ship and the networks are trained based on their approaching pattern. Therefore, two different types of experiments are carried out. One is for LHS approach and another is for RHS approach. Initially, the experiments are carried out by assuming the ship starting from its desired point on virtual window. Conducting the experiments several times, some similarities have been found while observing the behaviour of the controller for berthing manoeuvre. Depending on that, the experiment results are gathered into some groups where the controller behaves in a similar way or the resulting trajectories look like similar. Here, each figure demonstrating the experiment result includes the resulting trajectory in its first row and the corresponding controller's action in the second row. On the other hand, the corresponding details of each figure include the time history of all necessary particulars where the fifth and sixth rows show the relative wind information during the experiment. Although relative wind information is given in the figures, while explaining the figures in the text, the actual wind direction is mentioned for the ease of understanding.

Another important concern is that during the berthing experiment, the program was set to make the rudder neutral, i.e. rudder angle zero during reversing. Therefore, the following results might show some frequent rudder angle change during idling and reversing stages that is inconvenient to use in real ship operation. However, such frequent operation can be eliminated by letting the PID controller to take its action without interfering it. By doing so, although the PID controller is expected to take the rudder during reversing, it will not affect the final resulting trajectory. This is because the rudder has no effect during reversing.

5.4.1 Ship Approaching from Left Hand Side (LHS)

Several experiments are conducted for the ship approaching from LHS. The success of each experiment largely depends on the presence of wind disturbances during

course changing and especially during low speed running along with the imaginary line. However, the ANN-PID controller is expected to work effectively up to the wind that blows on an average of 1.5 m/s, which is 15m/s for full scale (same Froude number). While conducting the berthing experiments, the controller has found to behave in some particular ways based on the initial conditions and existing wind disturbances. Therefore, the experiment results in this thesis, are gathered in some groups rather than showing in a scattered way. In any particular group, the included experiment results do not guarantee a 100% successful ship berthing. However, similarities in the controller's behaviour are clearly visible.

Group 1: Regarding this group, while switching to auto mode, the ANN decides to take the starboard rudder first to ensure the ship's approach from left hand side. This is a usual case for the left hand side approach and ANN's action remains same irrespective of the combination of initial sway velocity or yaw rate. Here, in most cases within reasonable wind, the ship manages to merge with the imaginary line well ahead and proceeds along with the line without much deviation. The resulting trajectories belong to this group look like similar as used in teaching data for LHS approach. Figure 5.5 to 5.7 illustrate such demonstration.

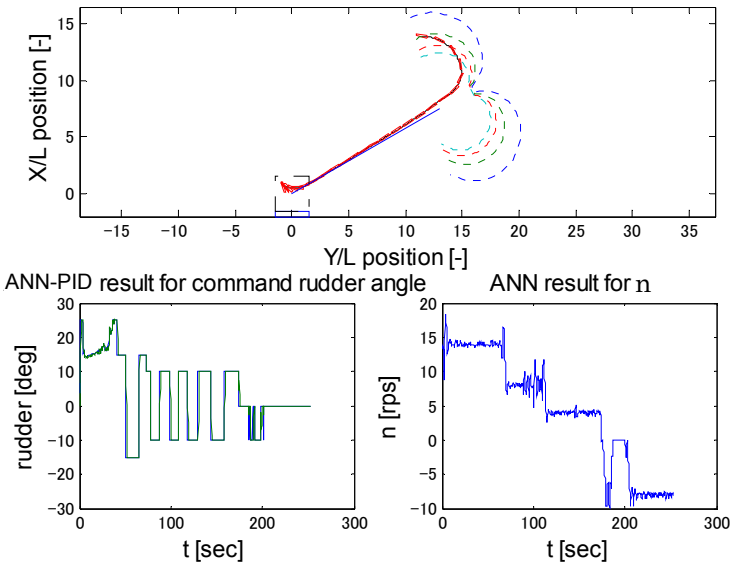

Figure 5.5. Group 1, initial heading 99.3º from virtual window for rudder constraint ±15º

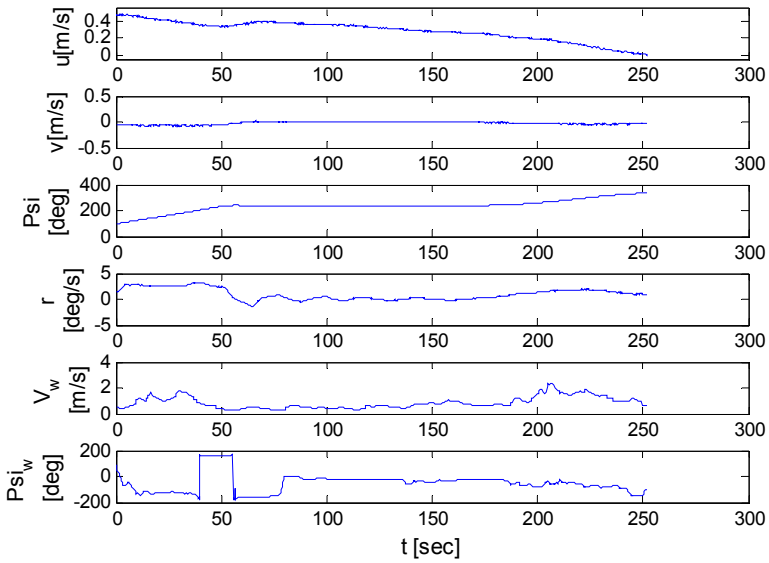

Figure 5.5(cont..). Corresponding details

Among those figures, Figure 5.5 can be considered as a representative illustration belongs to this group. During that experiment, while switching to auto mode, the ANN took the starboard rudder right from the beginning and continued until the ship heading became parallel to the imaginary line. Later on, it executed the counter rudder to minimise the resulting sway velocity and yaw rate i.e. to ensure straight like course. Finally, the PID controller was activated to provide necessary corrections while track keeping along the imaginary line. During such low speed running, the wind was under considerable limit with its almost following direction. Therefore, the ship stopped within the assumed berthing zone and the final surge velocity was 0.004 m/s. Here, the ANN also performed the engine idling and reversing sequentially while controlling ship speed near goal point. Such phenomenon was also observed in simulations for berthing under wind disturbances.

Considering Figure 5.6, the ANN also took the starboard rudder first for the combination of initial sway velocity and yaw rate. However, it maintained a constant rudder angle during the whole course changing which is unlike as Figure 5.5. During the experiment, the auto mode was activated little bit later than the expected. Therefore, the final goal point fell over the pier as explained in Figure 5.4, case 1 and the user was forced to stop the experiment to save the model from being collided with the actual pier.

Although there was not enough space to allow the ship to stop completely, by observing the ANN's action while controlling the propeller revolution, it was clearly seen that the reversing was just started to reduce the velocity. Therefore, it is believed that the existing surge velocity, which is 0.11 m/s in this case would have been drastically reduced if there were enough space to continue the experiment.

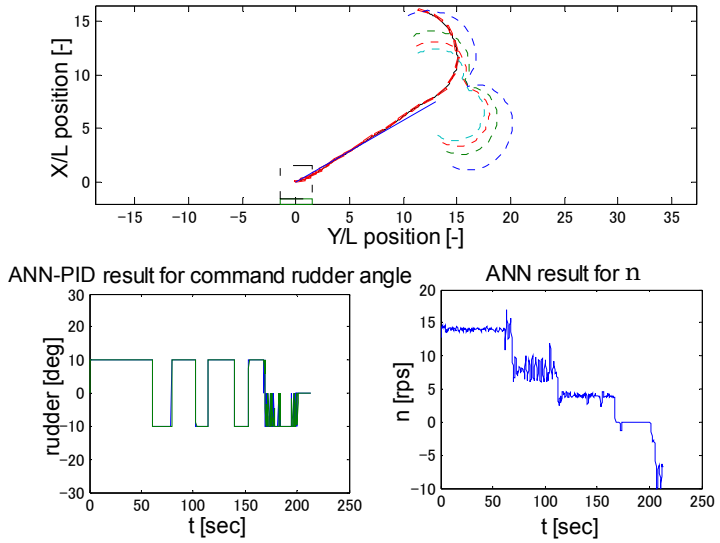

Figure 5.6. Group 1, initial heading 110.9º from virtual window for rudder constraint ±10º

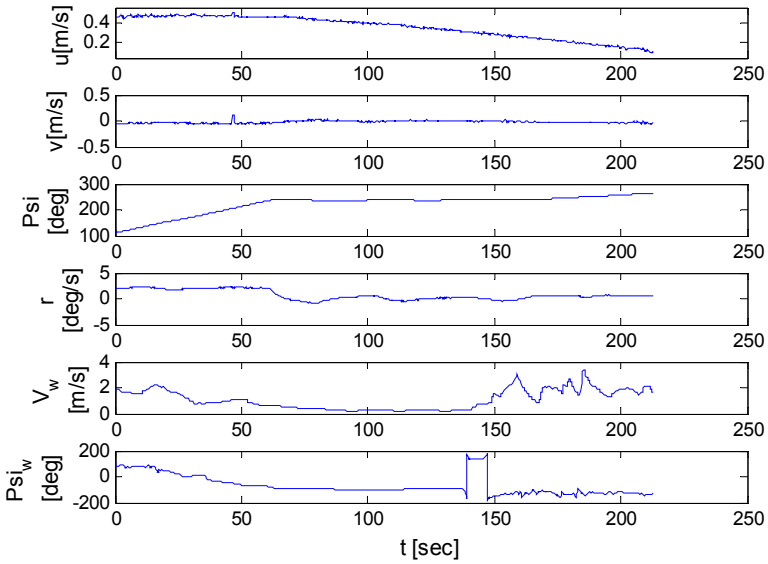

Figure 5.6(cont..). Corresponding details

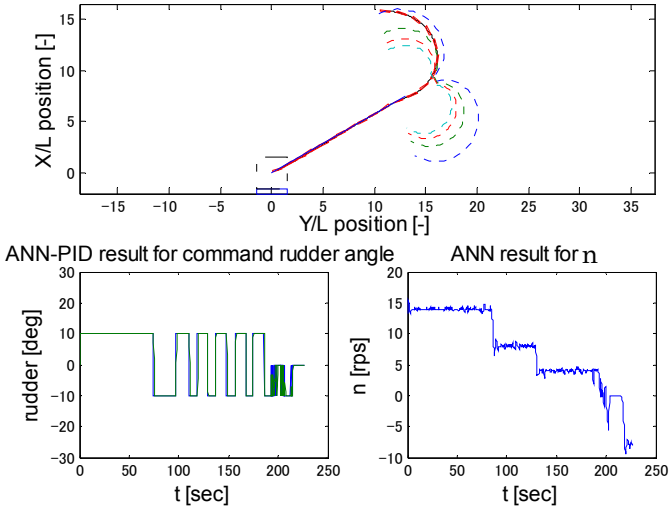

Figure 5.7. Group 1, initial heading 97.7º from virtual window for rudder constraint ±10º

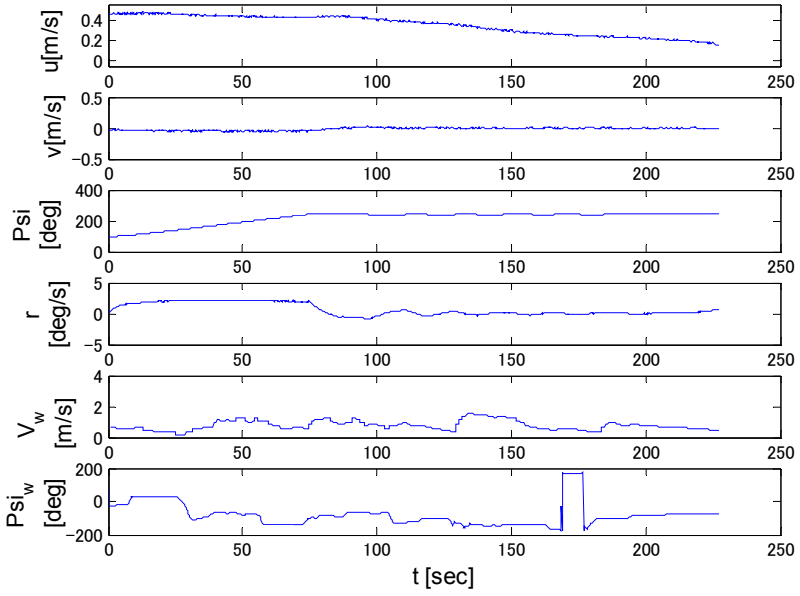

Figure 5.7(cont..). Corresponding details

Figure 5.7 shows a similar type of trajectory where the controller's action is similar as explained in Figure 5.6. The experiment was also stopped due to the same reason as mentioned in Figure 5.6. For this experiment, the existing surge velocity was 0.16 m/s while the ANN continued with reversing.

Group 2: Depending on the combination of initial sway velocity and yaw rate while switching to auto mode, sometimes the ANN first decides to minimise them by taking the counter rudder. Doing so often distracts the ship from its safest place to approach. Therefore, the controller realises such situation and continues with port rudder until the ship makes a complete port turn. At the same time, ANN also tries to adjust the ship position to a safer place. Then, it decides to take the desired starboard rudder to finally starting the approach. During the whole course changing process, ANN for propeller revolution maintains half ahead speed until the ship merges to the imaginary line. This kind of behaviour of ANN has found in several experiments and therefore gathered in this group. The resulting trajectories belong to this group are different from those used to train the net. However, this time the credibility simply goes to the well trained ANN for taking such decision to complete the whole berthing process. Figure 5.8 to 5.10 illustrate such demonstration.

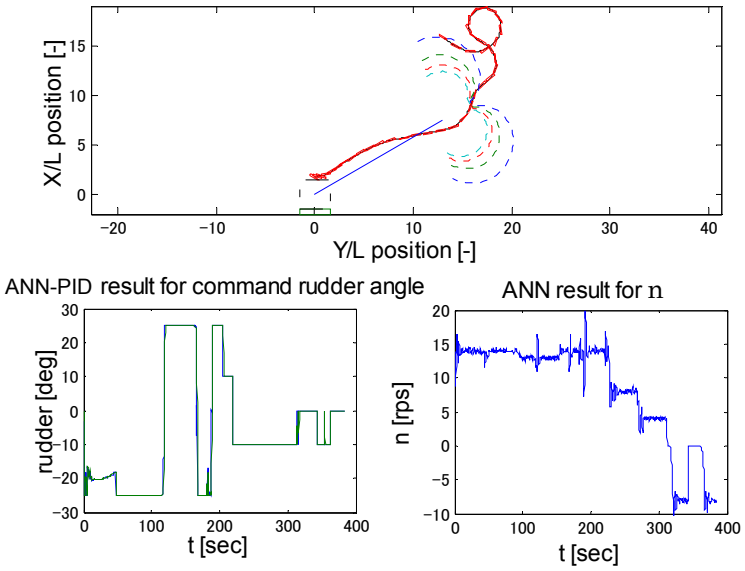

Figure 5.8. Group 2, initial heading 124.2º from virtual window for rudder constraint ±10º

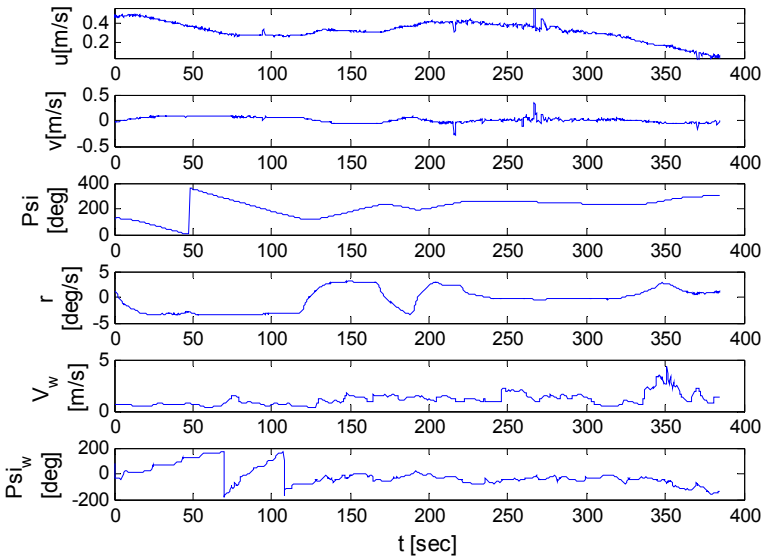

Figure 5.8(cont..). Corresponding details

In case of Figure 5.8, ANN started with port rudder first in order to minimise the unexpected initial sway velocity and yaw rate. Later on, the controller found the existing ship position was not suitable to start the approach. Therefore, by executing the maximum allowed port rudder, it ensured the quickest turn of the ship and at the same time adjusted its position to start the approach again. However, during course changing the fluctuated wind of around 1 m/s from 0º to -45º initiated some difficulties for the ANN to merge with the imaginary line. Later on, the wind altered its direction with an average of 10º to 15º. Finally, due to the presence of high wind up to 4.3 m/s near the pier, the ship deviated from its desired course during reversing and stopped just near to the assumed successful berthing zone.

In Figure 5.9, the controller's action during course changing was almost similar as explained in Figure 5.8. However, due to existing wind, the resulted course changing trajectory shifted towards the right hand side. Later on, when the strong wind started to blow after 260 sec with an average direction of -75º, it again distracted the ship just before merging to the imaginary line. However, the PID controller was sufficient to take adequate rudder and ensure successful berthing.

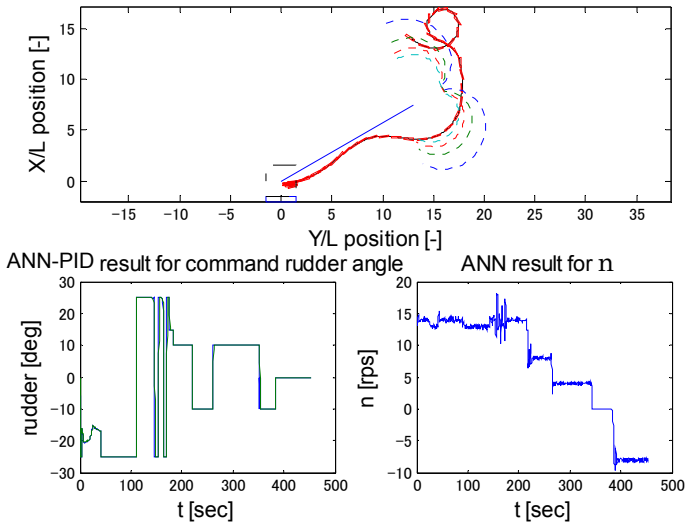

Figure 5.9. Group 2, initial heading 121.8º from virtual window for rudder constraint ±15º

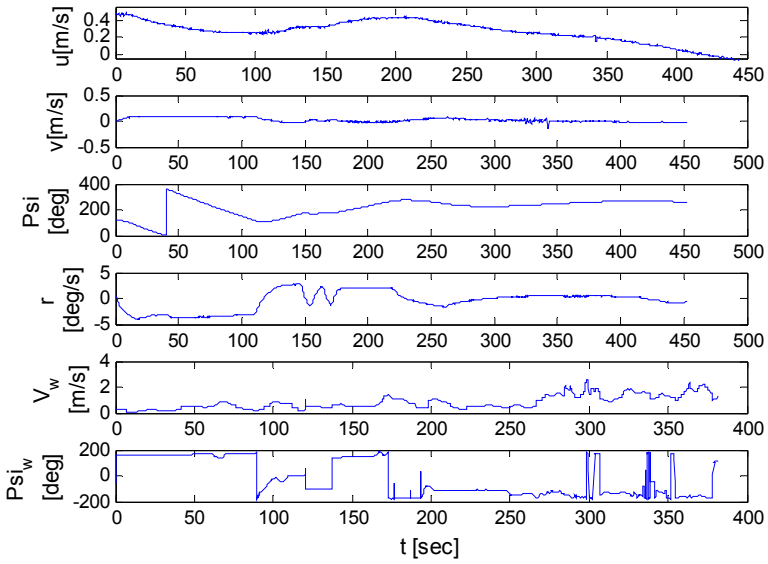

Figure 5.9(cont..). Corresponding details

On the other hand, in case of Figure 5.10, the wind direction was inconsistent and strong wind blew only during some part of course changing. Therefore, such fluctuating wind direction did not have much effect on the resulting ship's trajectory and the ship managed to stop just where it was expected. The final surge velocities in each three cases were less than zero, i.e. the ship was stopped and started to back up due to the reversing of the propeller.

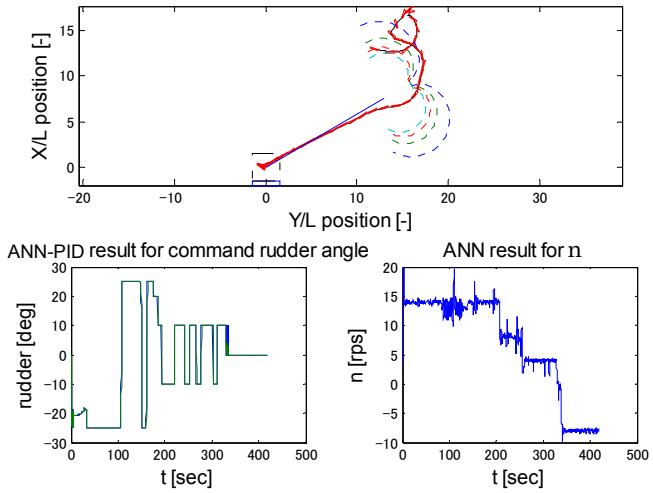

Figure 5.10. Group 2, initial heading 104.8º from virtual window for rudder constraint ±20º

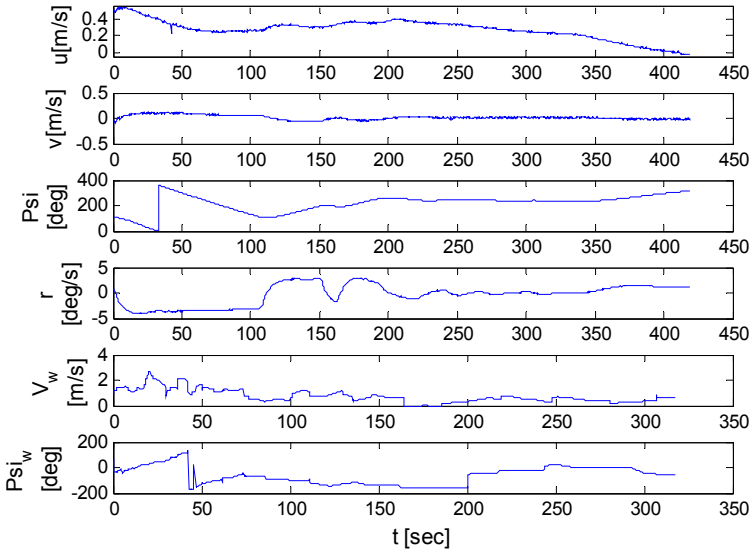

Figure 5.10(cont..). Corresponding details

Group 3: Although in group 2, ANN tries to oppose the existing sway velocity and yaw rate while switching to auto mode, sometimes ANN may want to go with such existing values by taking the expected starboard rudder first like in group 1. By doing so, if such sway velocity or yaw rate reaches some peak value depending on the ship position, then ANN finally decides to take the port rudder to oppose them. But this time, unlike as group 2, ANN prevents the complete turn of ship by taking the starboard rudder again as the ship is believed to be still in suitable positing to start its approaching to merge with the imaginary line. Therefore, all trajectories belong to this group is due

to subsequent starboard to port or port to starboard rudder taken by ANN according to situation demands. Figure 5.11 to 5.13 illustrate such demonstration.

Considering Figure 5.11, ANN behaved in a similar way as explained above. On the other hand, in Figure 5.12 and 5.13, ANN took the port rudder first. However, in each case, ANN prevented the complete turn by taking the starboard rudder. After that, ANN also adjusted the rudder to go for a short straight like path and then began to merge with the imaginary line as shown in Figure 5.11 and 5.12.

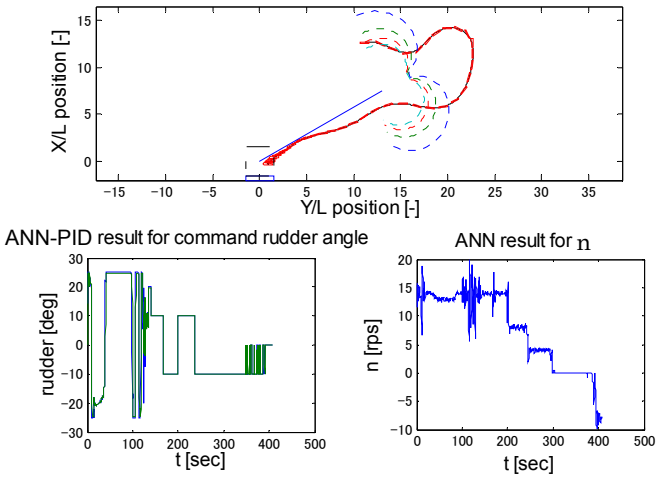

Figure 5.11. Group 3, initial heading 88.8º from virtual window for rudder constraint ±20º

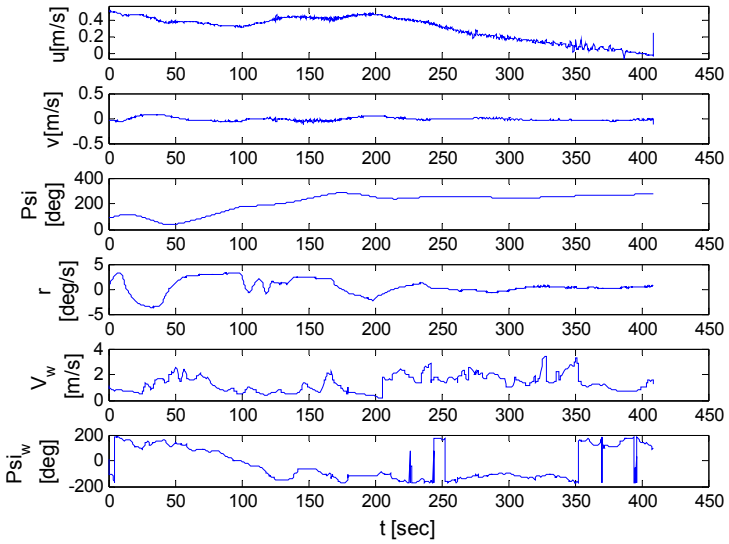

Figure 5.11(cont..). Corresponding details

In Figure 5.11, although the actual wind direction altered in wide range, during low speed running some consistency was noticed within the fluctuating wind ranging from 0º to -50º. Such wind actually delayed the emergence of the ship after course changing. At last, a sudden change of wind from -100º to -120º after 350 sec caused a faster velocity drop. Therefore, just after the reversing started, the final velocity became a negative value and the ship started to drift.

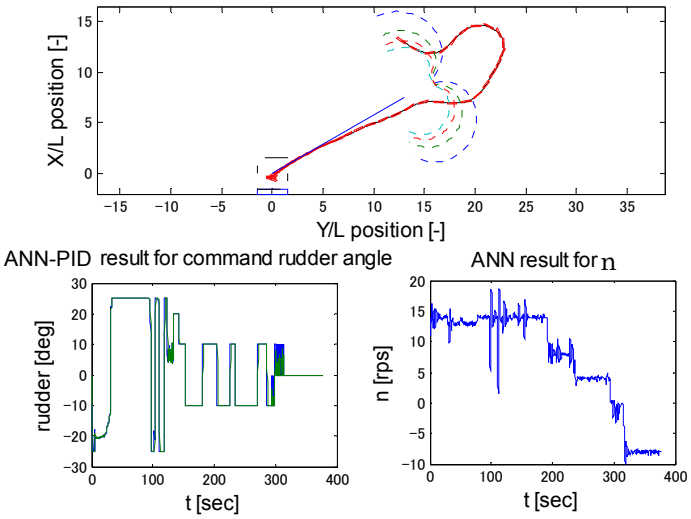

Figure 5.12. Group 3, initial heading 122.3º from virtual window for rudder constraint ±20º

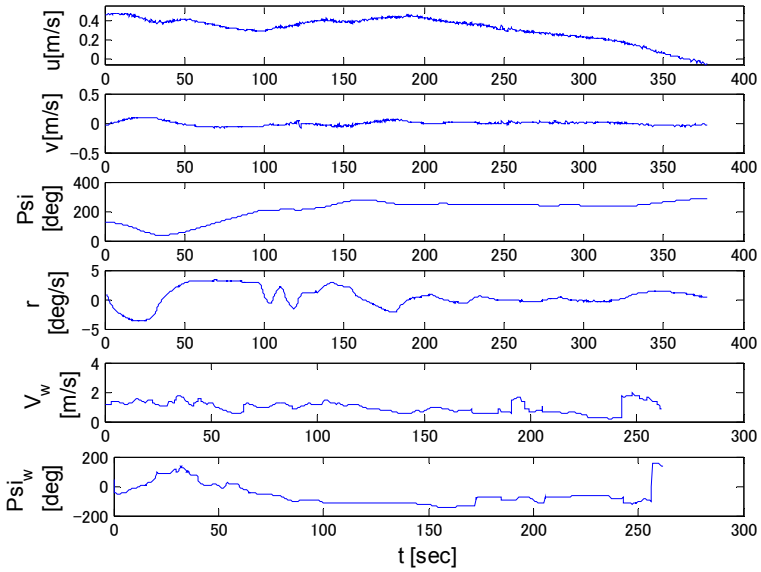

Figure 5.12(cont..). Corresponding details

In Figure 5.12, the wind velocity was low enough as compared to Figure 5.11 and its direction was found consistent during straight running with an average of -75º. Therefore, in such case, the reversing played a vital role to stop the ship near pier. On the other hand, in Figure 5.13, the wind direction looked like similar as in Figure 5.12, but it contained several gusts up to 4 m/s. Therefore, the velocity dropped faster than expected like in Figure 5.11 and the ANN preferred to continue with the idling stage for longer time to allow the ship come closer to the goal point. However, while entering to the berthing zone, the ship was started to drift due to the existing wind.

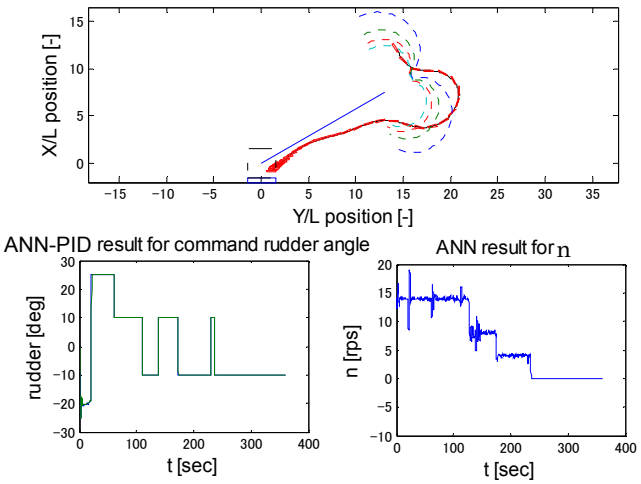

Figure 5.13. Group 3, initial heading 148.7º from virtual window for rudder constraint ±25º

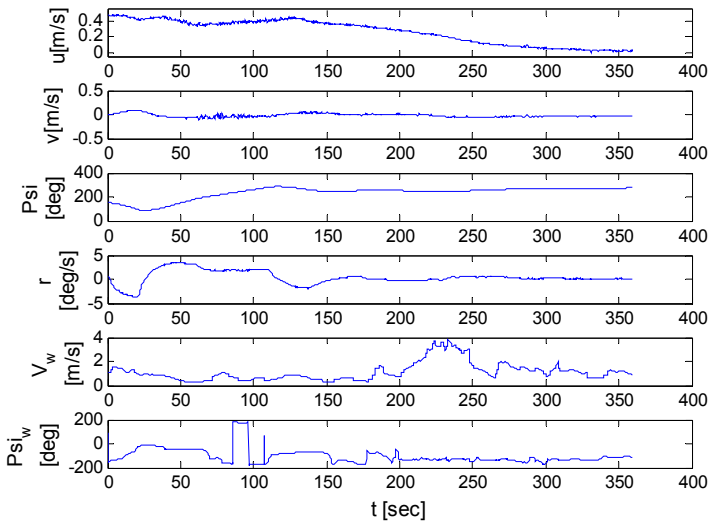

Figure 5.13(cont..). Corresponding details

5.4.2 Ship Approaching from Right Hand Side (RHS)

Several experiments are done for the ship approaching from RHS. Since the networks are different from those used in LHS approach, the controller's behaviour is also investigated for different unknown situations. Unfortunately, due to the presence of heavy wind during the experiment time, the success rate was not high enough as found in LHS approach. Even so, such experiment results can be categorised into several groups depending on the controller's behaviour. Therefore, the trajectories belong to each group have some similarities, although the success for automatic berthing may vary.

Group 1: Considering this group, while switching to auto mode, ANN may take starboard rudder first to oppose the existing sway velocity and yaw rate or it may go with the existing one by taking the port rudder. While taking the port rudder, if sway velocity and yaw rate reach their maximum value as decided by ANN, it takes the starboard rudder to minimise these values. After that, ANN actuates the desired port rudder to start its final approach to merge with the imaginary line. The important concern belongs to this group is that after course changing, ANN in most cases manages to merge the ship with imaginary line without much deviation. As a result, under considerable wind, the ship moves almost along with it. Figure 5.14 to 5.16 illustrate such demonstration for successful berthing.

Considering Figure 5.14 and 5.15, ANN took its maximum allowed starboard rudder first for a very short time and then it was followed by the desired port rudder for course changing. After merging to the imaginary, in both cases ship preceded almost along with it. In figure 5.14, during straight running, most of time the wind blew with an average velocity of 0.5 m/s. However, sudden gusts appeared after 200 sec with an average direction of 170º. On the other hand, in Figure 5.15, the gusts were present right from the beginning of the course changing with an average of 1.5 m/s. Therefore, even using the PID controller, sudden course alteration occurred in both cases during propeller idling and reversing i.e. when the rudder action was not effective enough. The final surge velocities in these cases were -0.006 m/s and 0.05 m/s, respectively.

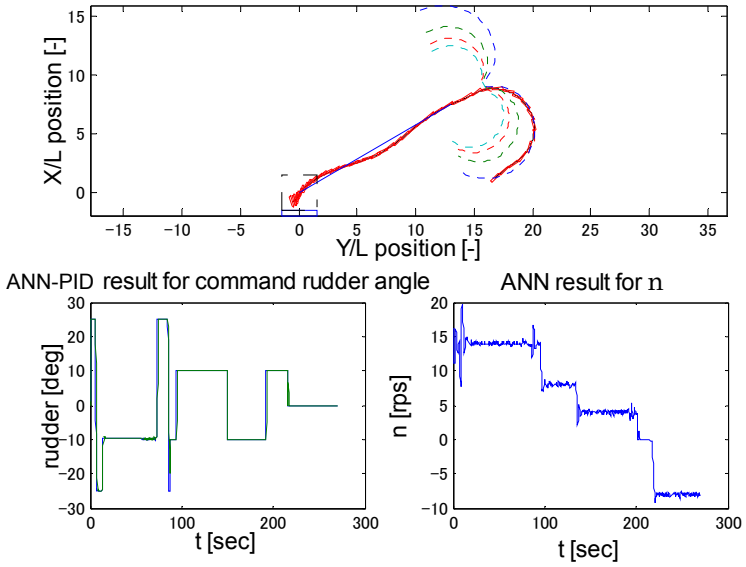

Figure 5.14. Group 1, initial heading 49.9º or 409.9º from virtual window for rudder constraint ±10º

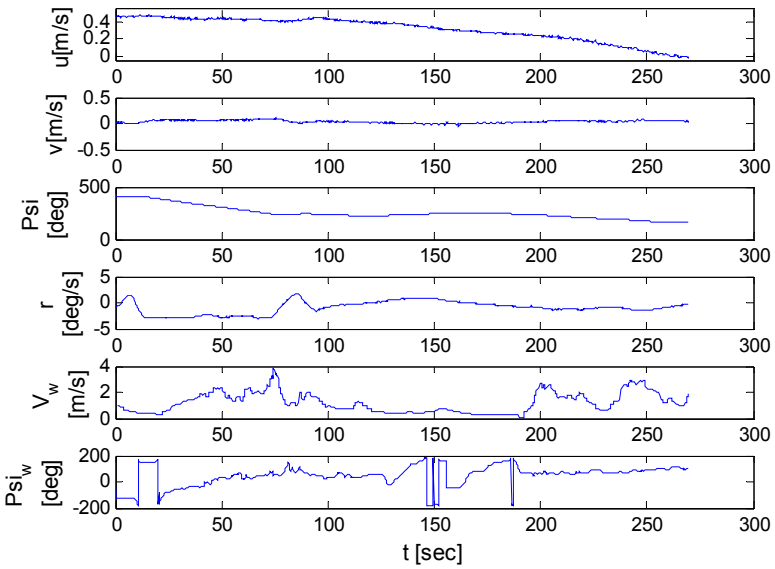

Figure 5.14(cont..). Corresponding details

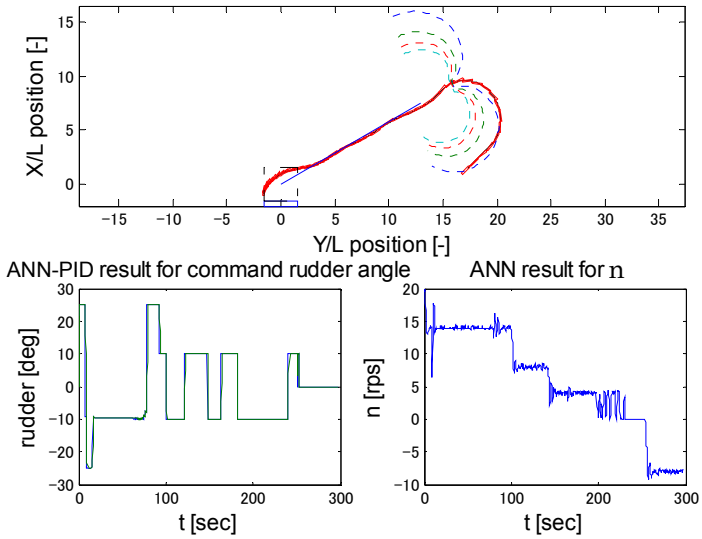

Figure 5.15. Group 1, initial heading 44.1° or 404.1° from virtual window for rudder constraint ±10°

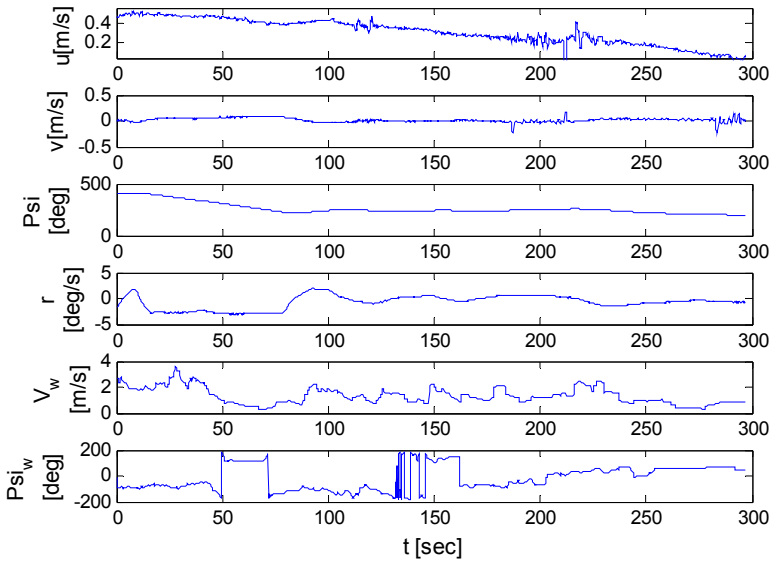

Figure 5.15(cont..). Corresponding details

In Figure 5.16, ANN decided to go with the port rudder first and then followed by subsequent starboard and port rudder for course changing. By doing so, it just missed the imaginary line to merge with it. However, due to having reasonable wind, the PID controller succeeded to make necessary corrections to adjust the ship course and finally the ship was stopped just on the pier. During this experiment, some fluctuations in GPS

reading also provided confusion while calculating propeller revolution by ANN. Therefore, the fluctuations in propeller revolution were due to GPS signal problem.

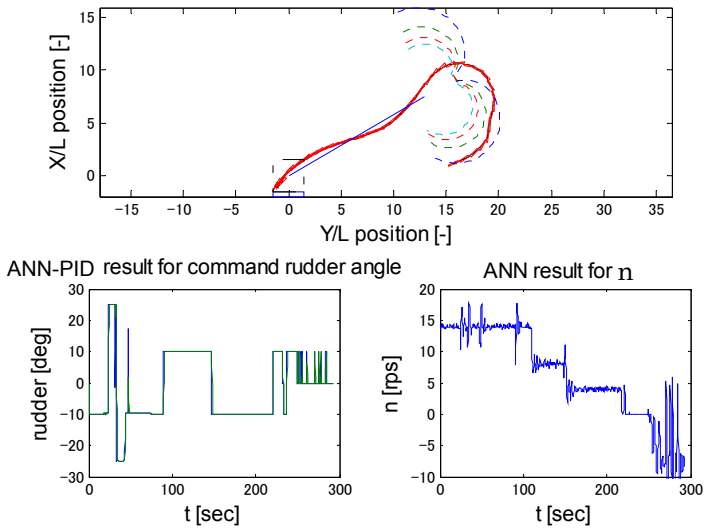

Figure 5.16. Group 1, initial heading 67.1º or 427.1º from virtual window for rudder constraint ±10º

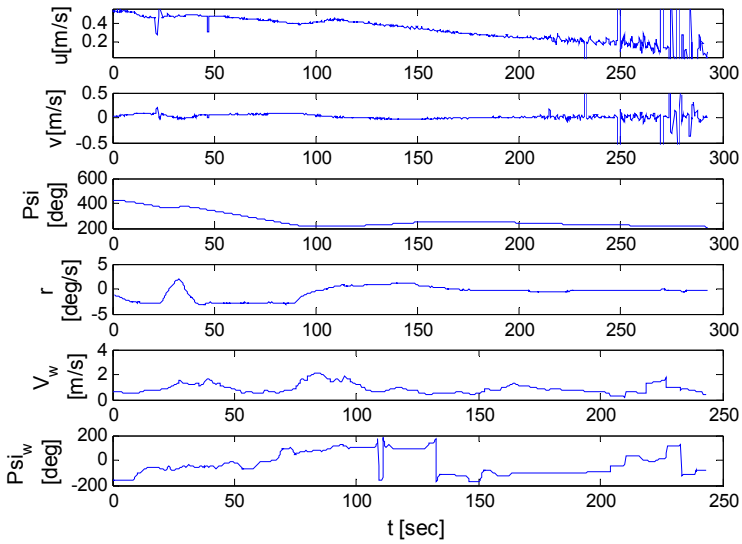

Figure 5.16(b). Corresponding details

Since the experiment day was windy, some experiment results were also found where the ANN behaved in a similar way as mentioned for this group but the ship distracted during low speed running due to having high wind disturbances,. The

following two figures demonstrate such trajectories. Here, although the ship failed to berth successfully, illustrating the result also demonstrates what may happen if the proposed ANN-PID controller is used in the wind that blows beyond the permitted limit.

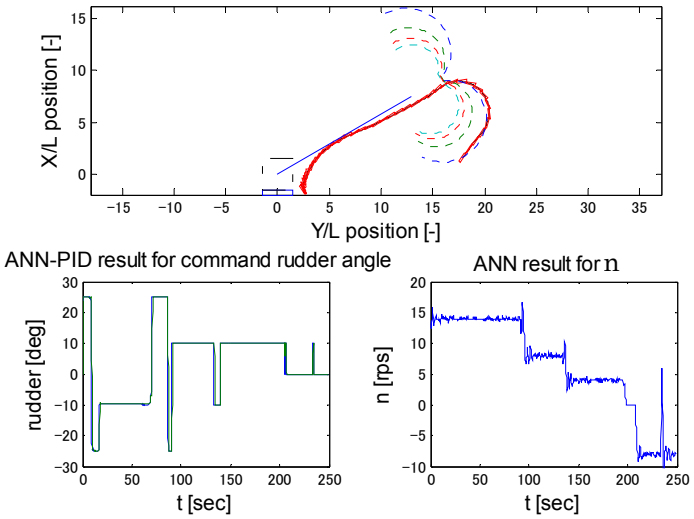

Figure 5.17. Group 1, unsuccessful berthing, initial heading 37.2º or 397.2º from virtual window for rudder constraint ±10º

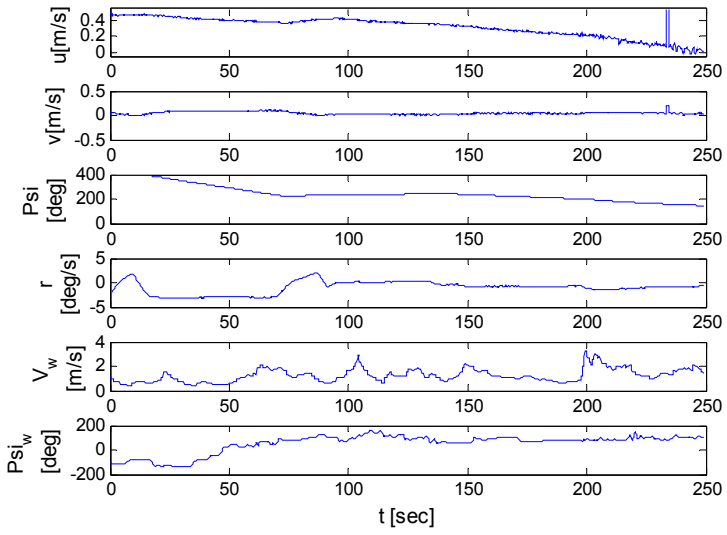

Figure 5.17(cont..). Corresponding details

Considering Figure 5.17, although several gusts were present right after the course changing, due to having enough ship velocity the PID controller was sufficient to

maintain the course. Later on, after 200 sec during reversing, the wind attained its maximum peak velocity as 3.2 m/s and changed its direction to an average of 180º. Due to such crucial change, the ship finally failed to make successful berthing. In Figure 5.18, similar types of phenomenon happened when the high gusts altered its direction from an average of -100º to 160º after 180 sec. Therefore, not only the wind velocity, but also its direction played the role for the success of the controller.

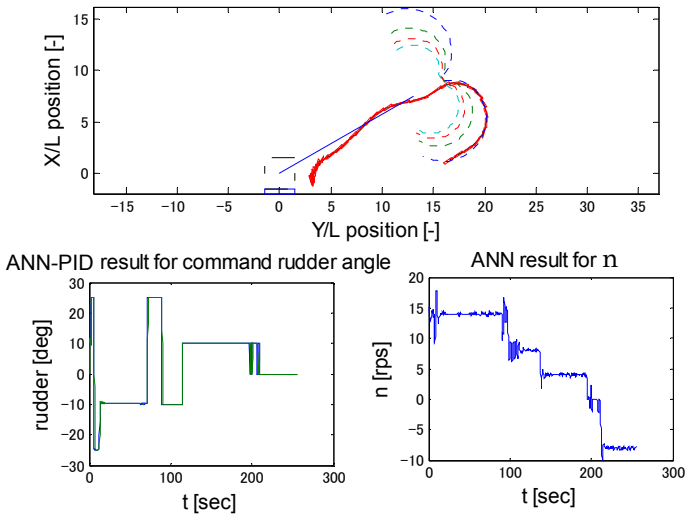

Figure 5.18. Group 1, unsuccessful berthing, initial heading 57.1º or 417.1º from virtual window for rudder constraint ±10º

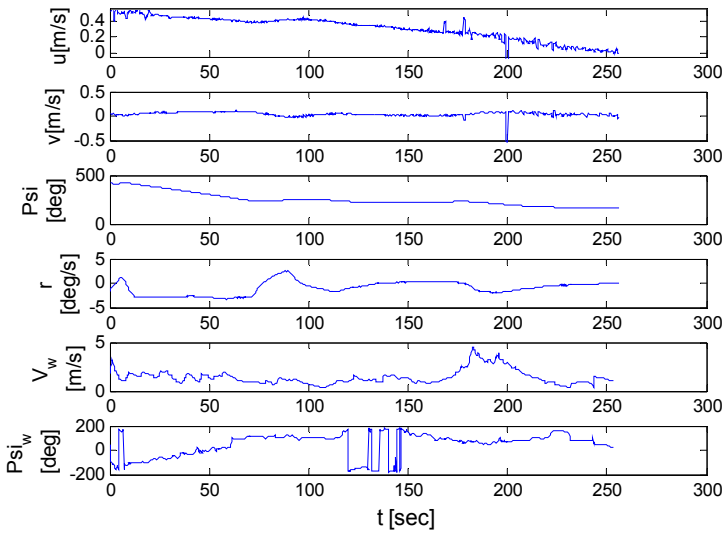

Figure 5.18(con.). Corresponding details

Group 2: Due to the presence of high wind disturbances during course changing or due to improper decision taken by ANN itself, sometimes the ship may fail to merge with the imaginary line in large extent. As a result, the ship deviates from its desired course right from the beginning of the imaginary line. After that, the PID controller takes the counter rudder to compensate such deviation and it succeeds in some extent. This means, neither of such trajectories represents the successful berthing result. However, the trajectories can be gathered into this group by observing the similarities in controlling behaviour or the pattern of resulting trajectories. Figures 5.19 to 5.20 illustrate such demonstration.

In Figure 5.19, several gusts with an average from -125º continuously blew throughout the whole berthing operation. Therefore, the resulting trajectory was shifted a little bit towards upper-right direction. On the other hand, considering Figure 5.20, some initial fluctuations in GPS signal as well as the gusts with an average direction of 100º caused the total course changing trajectory to shift a little bit towards upper-left direction. In both cases, the wind direction remained consistent during the low speed running. Therefore, the PID controller tried to minimise the deviation by taking the starboard rudder and succeeded in some extent. Although in such cases, the ship failed to reach the safety zone, the corresponding surge velocities were 0.01 m/s and -0.03 m/s i.e. they were successfully stopped by the controller.

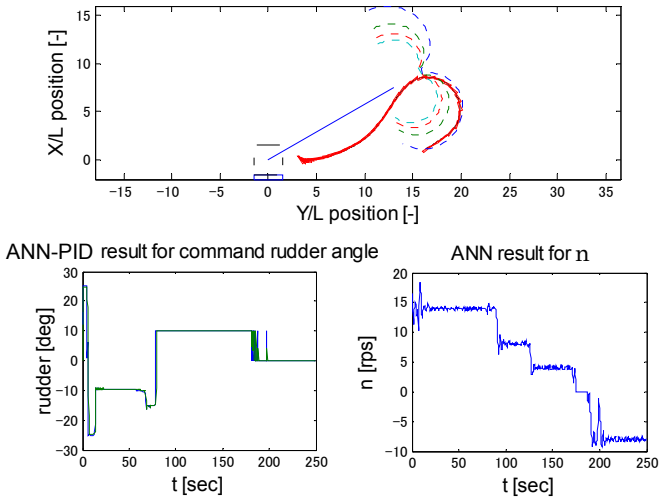

Figure 5.19. Group 2, unsuccessful berthing, initial heading 55.4º or 415.4º from virtual window for rudder constraint ±10º

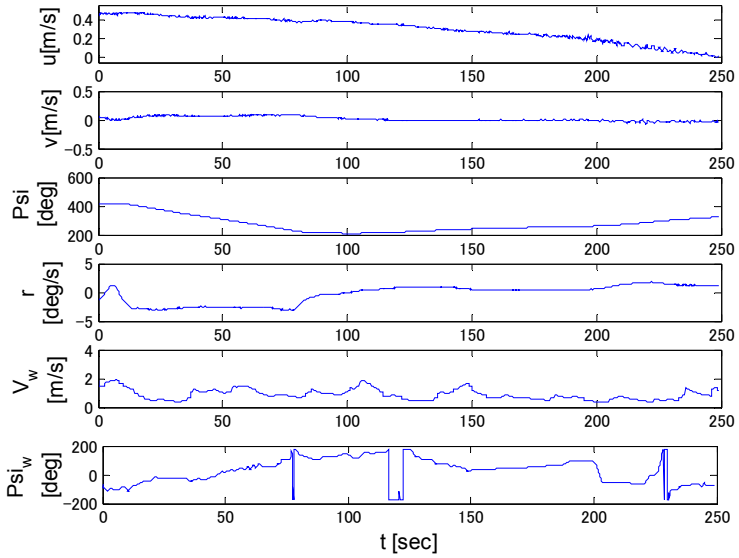

Figure 5.19(cont..). Corresponding details

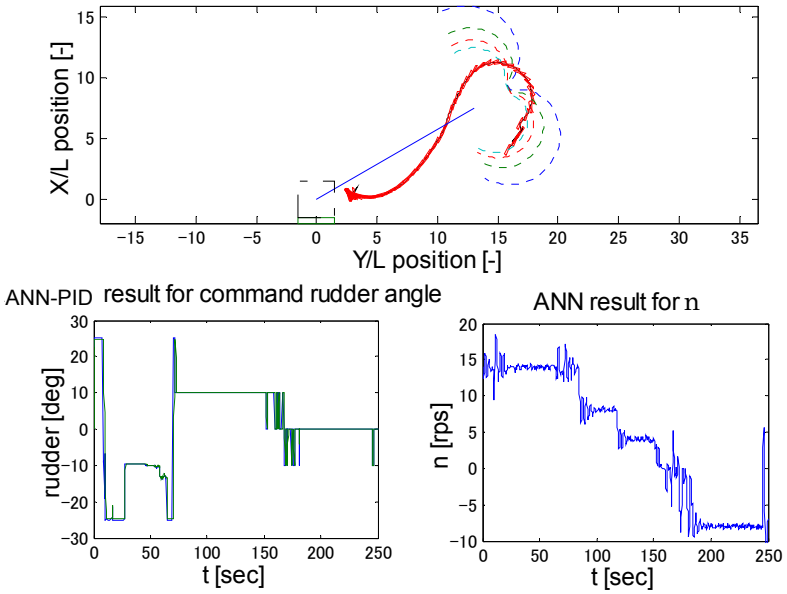

Figure 5.20. Group 2, unsuccessful berthing, initial heading 28.4º or 388.4º from virtual window for rudder constraint ±25º

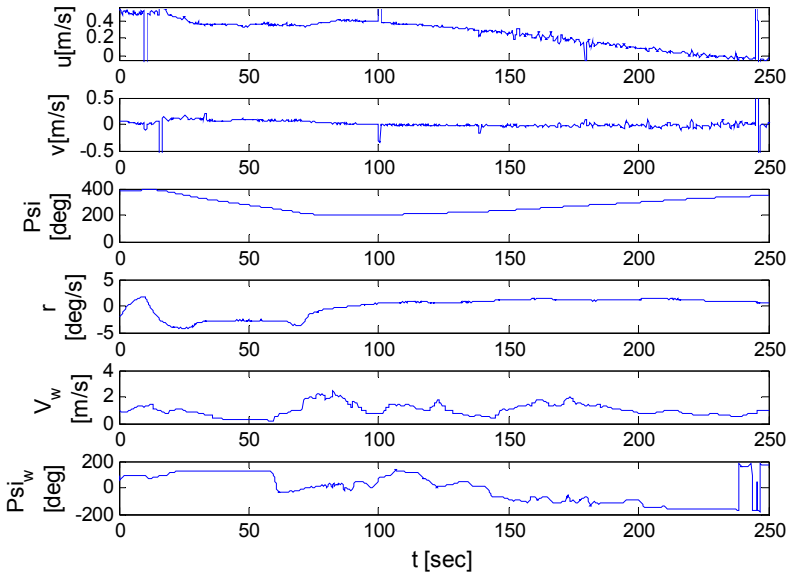

Figure 5.20(cont..). Corresponding details

Group 3: Depending on ANN's response or due to the existence of wind disturbances, sometimes the ship may fail to merge with the imaginary line that is similar to group 2. However, this time the PID controller during step deceleration successfully returns the ship to the imaginary line by taking the starboard rudder and the ship just passes through it. Then, for such overshooting, the controller again takes the port rudder to correct the ship heading and minimise its deviation from the imaginary line. Finally, the completed trajectory looks like 'S' shape. Figure 5.21 illustrates such demonstration.

Considering Figure 5.21, the wind was within considerable limit during course changing and the ship experienced some following wind. Later on, when the ship changed its course to merge with the imaginary line, the following wind became its heading wind. During slow speed running, several small gusts also presented with an average direction of -120º. After 290 sec, high wind started to blow with an average direction of -50º and finally helped the ship to enter the successful berthing zone. Here, during the low speed running, the PID controller behaved in a similar way as mentioned above and the resulting trajectory looks like 'S' shape. The final surge velocity at the end of the experiment was -0.02 m/s.

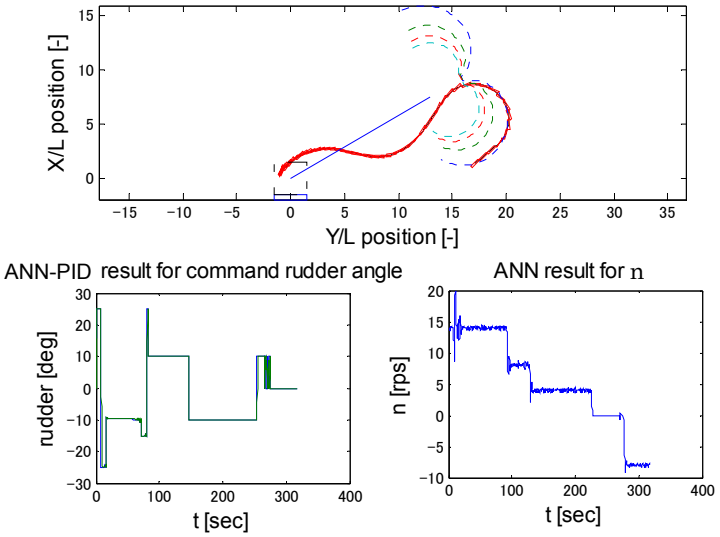

Figure 5.21. Group 3, initial heading 46.9º or 406.9º from virtual window for rudder constraint ±10º

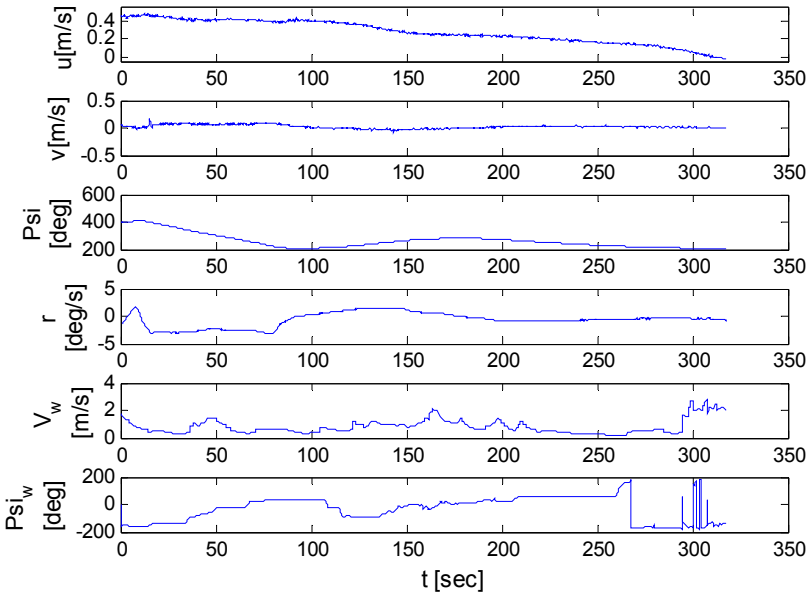

Figure 5.21(cont..). Corresponding details

The other trajectories belong to this category are found in the presence of high wind disturbances. Therefore, such results do not guarantee the successful berthing. However, similarities in the resulted trajectories are clearly visible while using the ANN-PID controller. Figure 5.22 shows one of such results.

Considering Figure 5.22, during course changing, high wind changed its direction

gradually from an average of -100º to 150º. As a result, the course changing trajectory was shifted little bit towards the left side of imaginary line than expected. This is unlike as in Figure 5.21. After that, the PID controller tried to make necessary corrections. Here, during step deceleration, the wind direction was mostly inconsistent and there were sudden gusts during propeller idling and reserving stage. Therefore, the ship just passed over the successful zone due to having improper velocity drop.

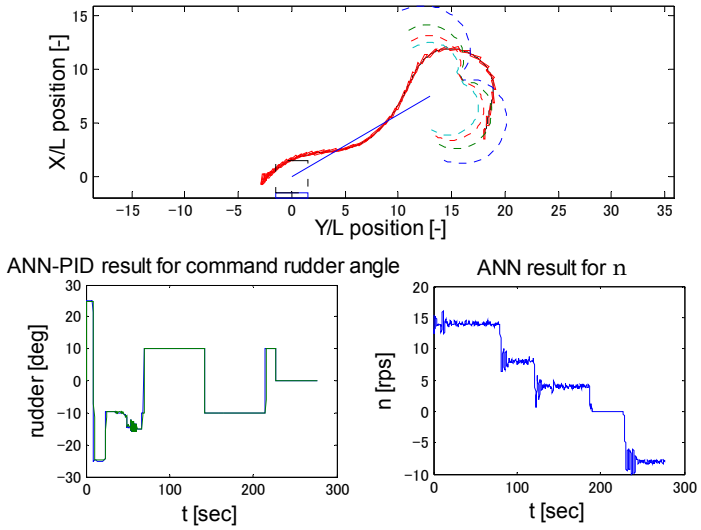

Figure 5.22. Group 3, unsuccessful berthing, initial heading 4.0º or 364.0º from virtual window for rudder constraint ±15º

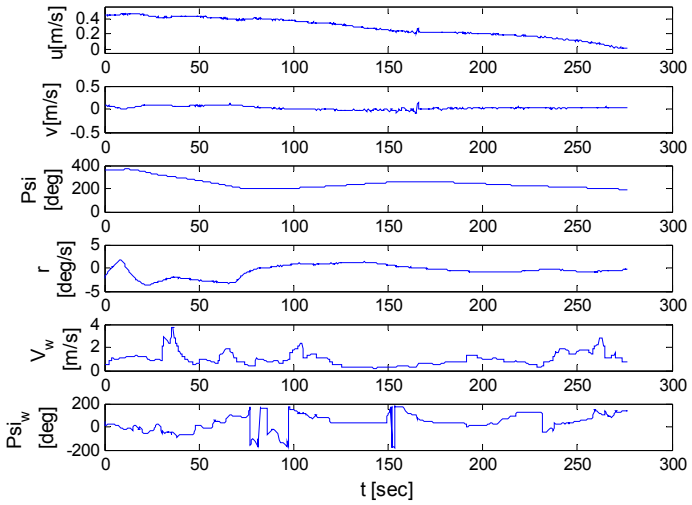

Figure 5.22(cont..). Corresponding details

Group 4: Sometimes wind disturbances or improper controller's action causes a gradual shift of course changing trajectories, but this time ANN manages to attain the final desired heading that is almost parallel to the imaginary. In such cases, PID controller prefers to maintain the same heading and the ship proceeds almost parallel to the imaginary line instead of merging with it. Figure 5.23 illustrates such demonstration.

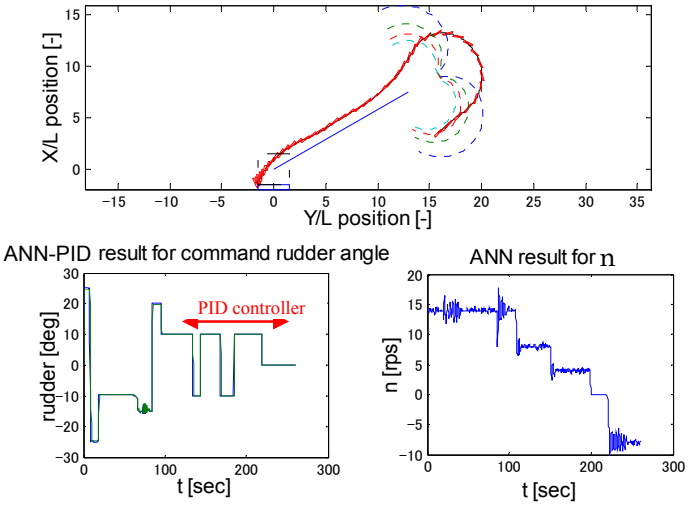

Figure 5.23. Group 4, initial heading 41.3º or 401.3º from virtual window for rudder constraint ±20º

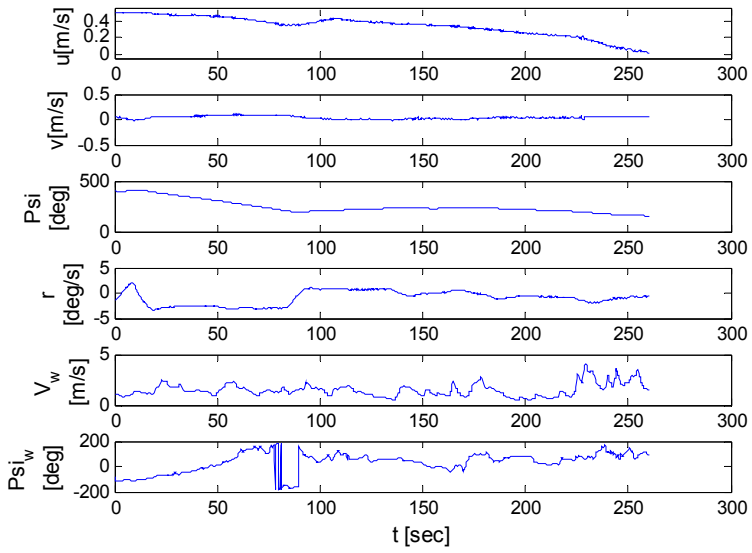

Figure 5.23(cont..). Corresponding details

In Figure 5.23, it is noticeable that the PID controller took consecutive starboard and port rudder to maintain the ship heading which was almost parallel to the imaginary line. Later on, high gusts from an average direction of 180º during propeller idling and reversing altered the course and the ship was stopped with a final velocity of 0.01 m/s.

In some cases, the controller performed in a similar way as mentioned in Figure 5.23. However, due to having some following wind, the reversing with slow astern was not sufficient to stop it. Therefore, the ship moved a little bit forward than the defined successful zone. Figure 5.24 demonstrates such illustration.

In Figure 5.24, the wind was under reasonable limit during course changing. Then, depending on the existing sway velocity and yaw rate, ANN took the starboard rudder first followed by the desired port rudder. Such action provided some shift in turning trajectory, despite the ANN almost successfully attained the desired final heading. Later on, several small gusts in the following direction accelerated the ship after 200 sec. Therefore, even considering reversing by ANN, the velocity drop was not as expected. As a result, the ship exceeded the successful zone and at last considered stopped with a final velocity of 0.01 m/s.

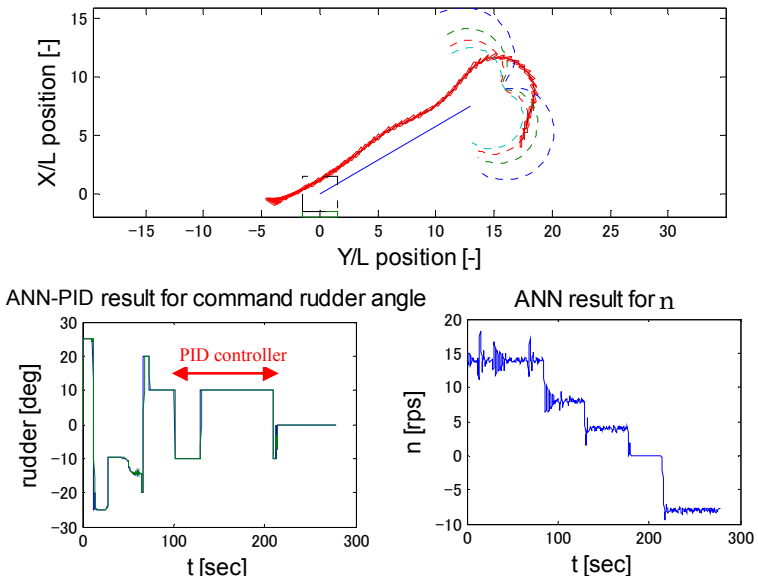

Figure 5.24. Group 4, unsuccessful berthing, initial heading 4.7º or 364.7º from virtual window for rudder constraint ±20º

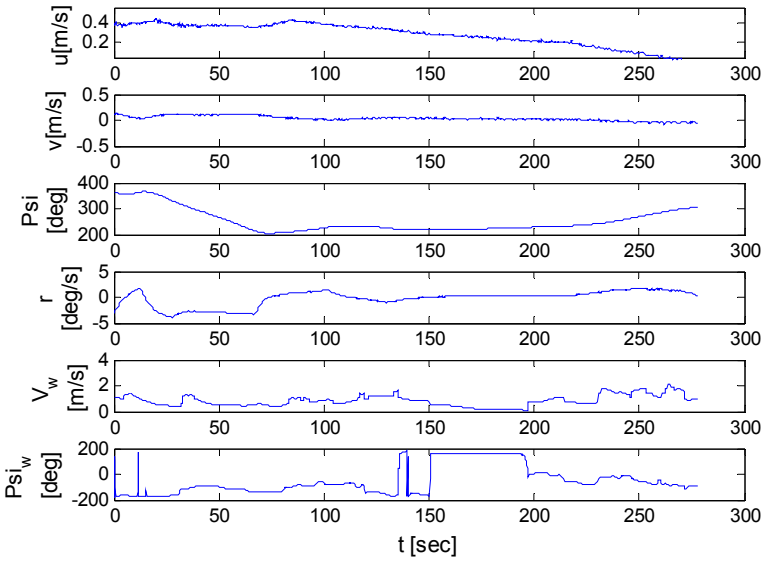

Figure 5.24(cont..). Corresponding details

5.5 Experiment Results for Arbitrary Staring Points

In this thesis, three different types of experiments are carried out to judge the position flexibility of the proposed controller. These are the same as explained for simulations in the previous section. The following subsections include those experiment results.

5.5.1 Experiment for Ship Staring from Undesired Point on Virtual Window

To do such experiment, a ship with its initial heading needs to be started from the other point on virtual window rather than its desired one. Therefore, it is planned to alter the sorted out initial starting point during the activation of auto mode by adding or subtracting some value to the measured actual heading. It means, the ship will start from a point on the virtual window, but it will be different from the expected one as a dummy heading value is considered instead of original one. Thus, the controller will respond not only based on having different initial sway velocity and yaw rate but also due to staring from the undesired point on virtual window. Such experiments are done only for RHS approach due to the limitation of time. The following figures demonstrate such

experiment results.

Considering Figure 5.25, while activating the autonomous control, the initial heading was altered by -5º. As a result, although the actual initial heading was 50.6º, it was assumed to start from a point desired for 45º and the controller took decision relative to that point. During the experiment, the wind was within reasonable limit and the ship was stopped successfully within the successful berthing zone.

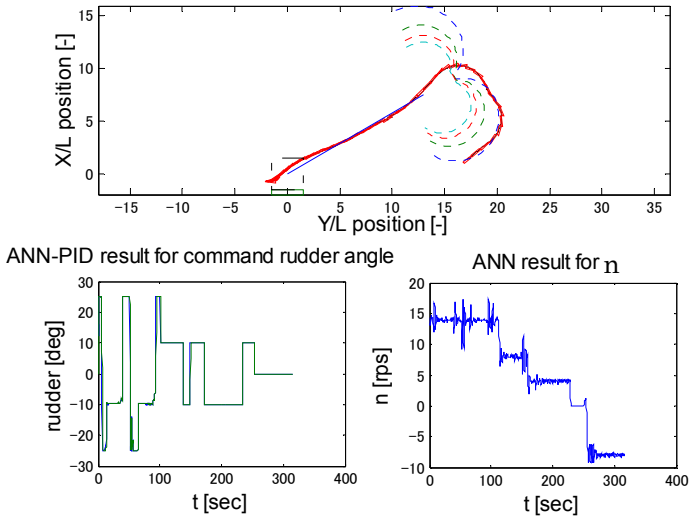

Figure 5.25. Initial heading 50.6º or 410.6º from point desired for 45º on virtual window for rudder constraint ±10º

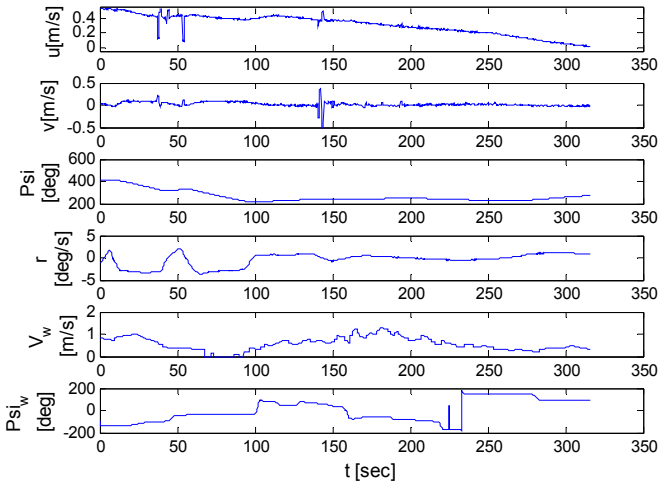

Figure 5.25(cont..). Corresponding details

In Figure 5.26, the ship's initial heading was altered by +20º while sorting out the starting point from virtual window file. Therefore, it was assumed to start from a point desired for 60º although it had its initial heading 39.9º or 40º. On the other hand, Figure 5.27 demonstrates the result for ship with initial heading of 32.8º. However, it started from a point desired for 20º. In both cases, although the small gap exists after course changing by ANN controller, later on it was minimised by activating the PID controller and overall the combined effort ensured successful berthing. Here, the resulting trajectories in Figure 5.25, 5.26 and 5.27 belong to group 1 for RHS approach.

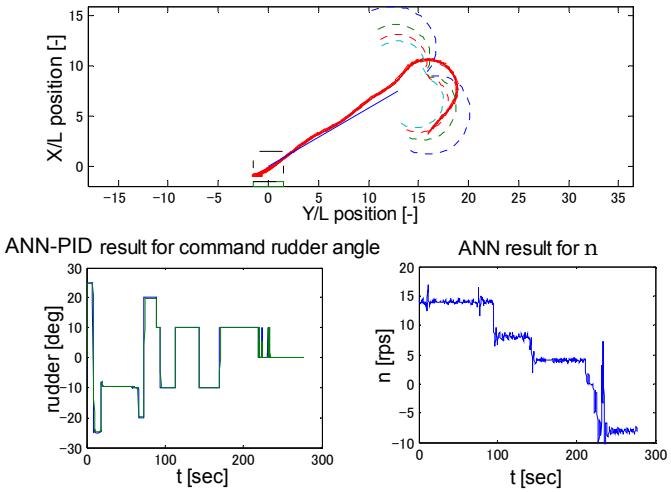

Figure 5.26. Initial heading 39.9º or 399.9º from point desired for 60º on virtual window for rudder constraint ±20º

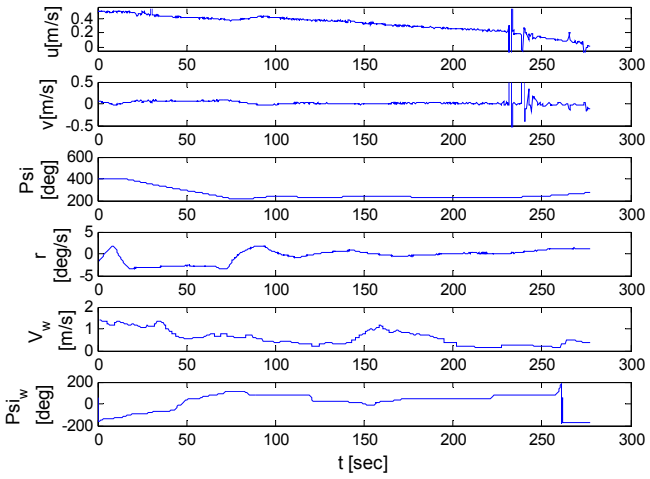

Figure 5.26(cont..). Corresponding details

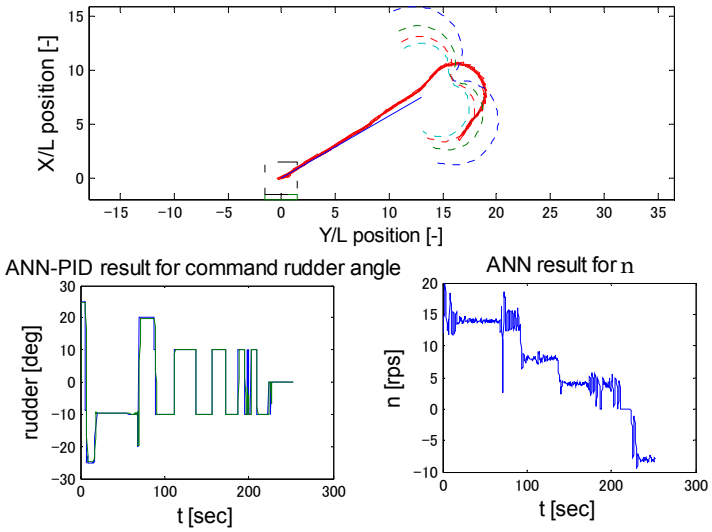

Figure 5.27. Initial heading 32.8º or 392.8º from point desired for 20º on virtual window for rudder constraint ±20º

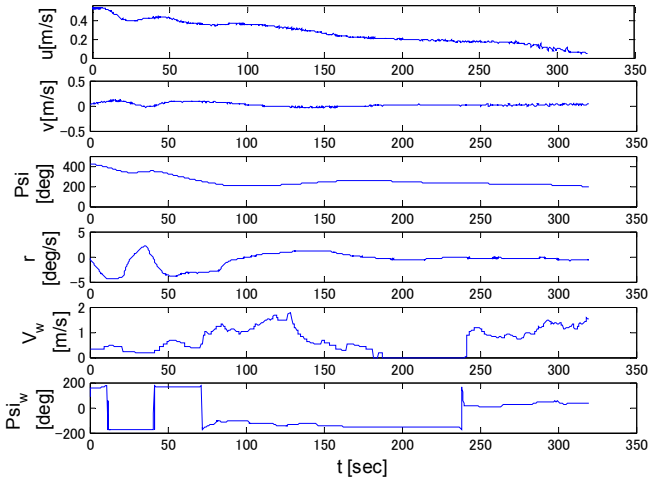

Figure 5.27(cont..). Corresponding details

However, the results are not always so smooth. Figure 5.28 illustrates the result for the ship with initial heading 57.9º, but assumed to start by alerting its heading by +15º. Therefore, it started from a point nearer to heading 72.9º, which was 75º. In addition, considering Figure 5.29, it demonstrates a case for the ship started from a point desired for heading 45º with its actual heading of 31.4º. In both cases, after course changing by the ANN there exists a big gap. However, it was minimised successfully by the PID controller under reasonable wind disturbances. This means, sometimes the ANN

controller may not provide smooth operation as expected, which may lead to some error in ship's positing as well as in heading after course changing. Since it is followed by the PID controller, it is possible to correct such errors in the remaining track keeping stages and the combined controller is sufficient to make sure successful berthing operation even with existing error after course changing. However, the success of berthing largely depends of the existing wind disturbances too. As seen in Figure 5.29, the PID controller succeeded in bringing the ship back to the track. Later on, strong wind after 260 sec altered the ship's course completely during idling and reversing stages.

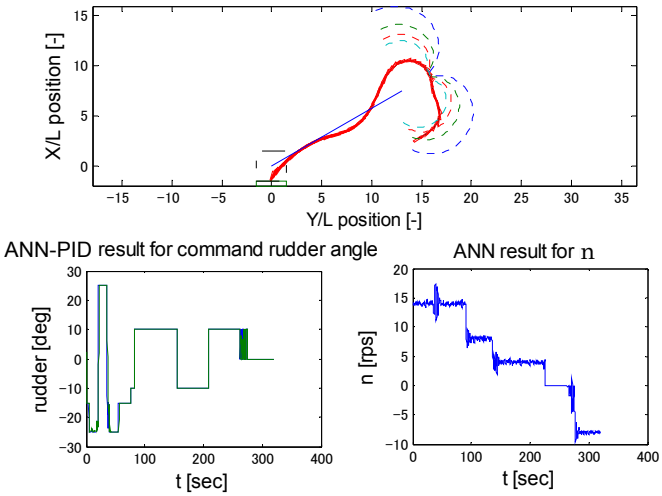

Figure 5.28. Initial heading 57.9º or 417.9º from point desired for 75º on virtual window for rudder constraint ±15º

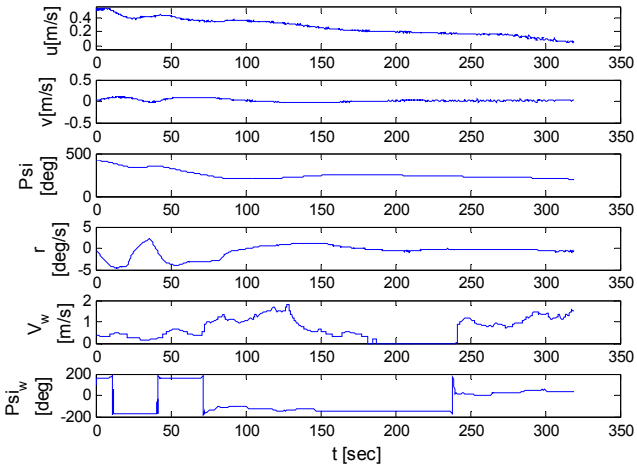

Figure 5.28(cont..). Corresponding details

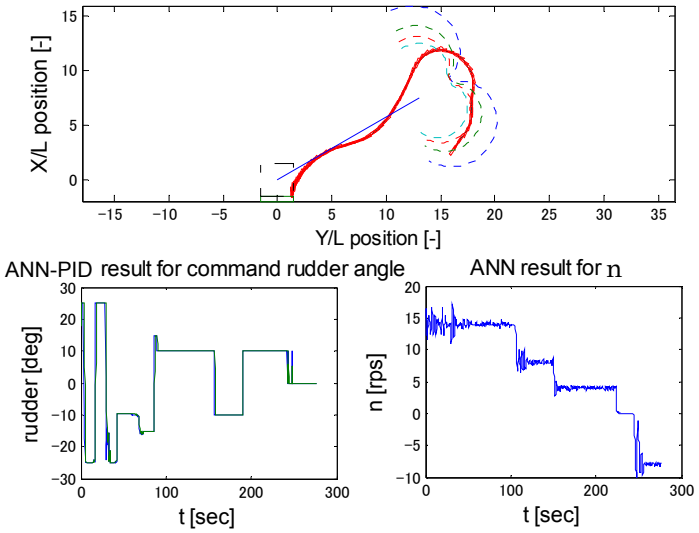

Figure 5.29. Initial heading 31.4º or 391.4º from point desired for 45º on virtual window for rudder constraint ±15º

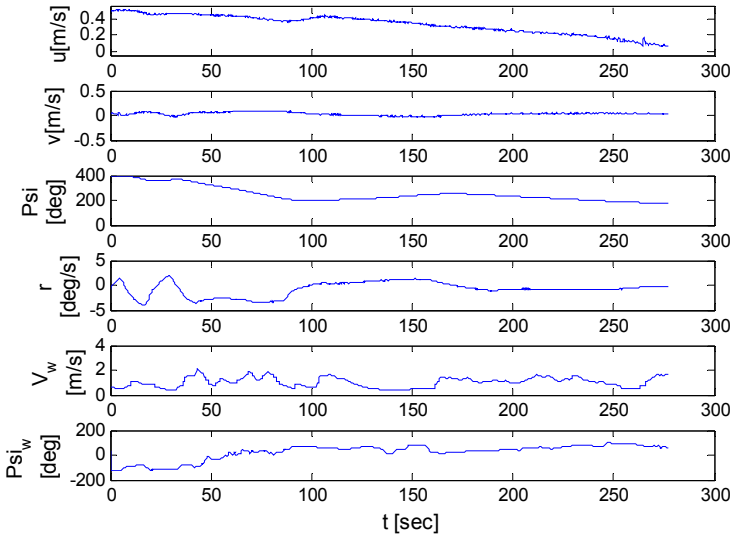

Figure 5.29(cont..). Corresponding details

5.5.2 Experiment for Ship Staring from Mid of Virtual Window for Two Different Rudder Constraints

This type of experiment is carried out for both LHS and RHS approaches. To do such experiment, a separate file containing the midpoints of virtual window for two different rudder constraints is read by the program during autonomous control in order

to sort out the midpoint against its initial heading.

Considering Figure 5.30, the ship started from a point desired for heading 110º on middle of virtual window for rudder constraints ±10º and ±15º. Here, it represents the result for the trajectory that looks like similar to those used as teaching data. Therefore, this result belongs to group 1 as mentioned in section 5.4.1 for LHS approach. The final surge velocity was 0.02 m/s at the end of this experiment.

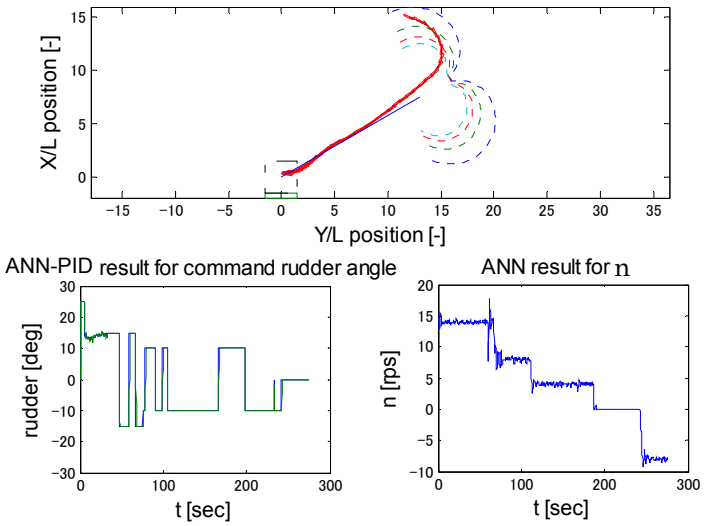

Figure 5.30. Initial heading 110.8º from mid of virtual window for rudder constraints ±10º and ±15º

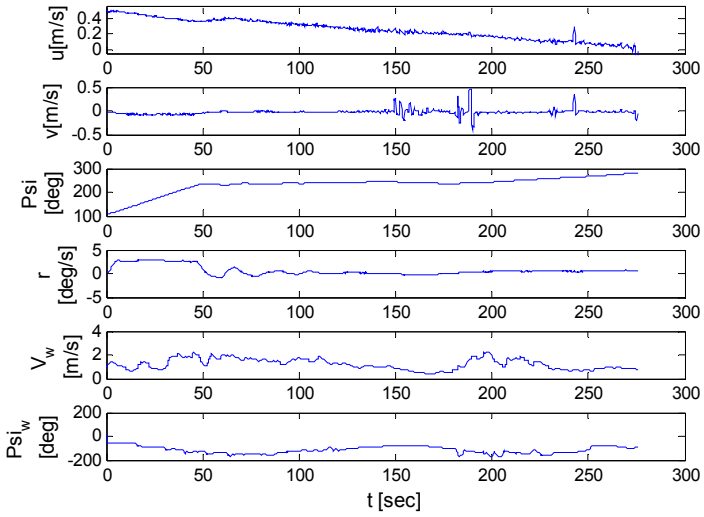

Figure 5.30(cont..). Corresponding details

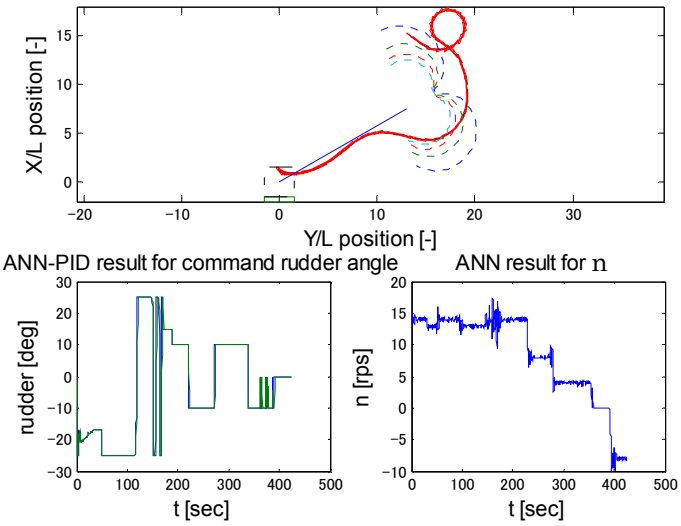

Figure 5.31. Initial heading 128.1º from mid of virtual window for rudder constraints ±10º and ±15º

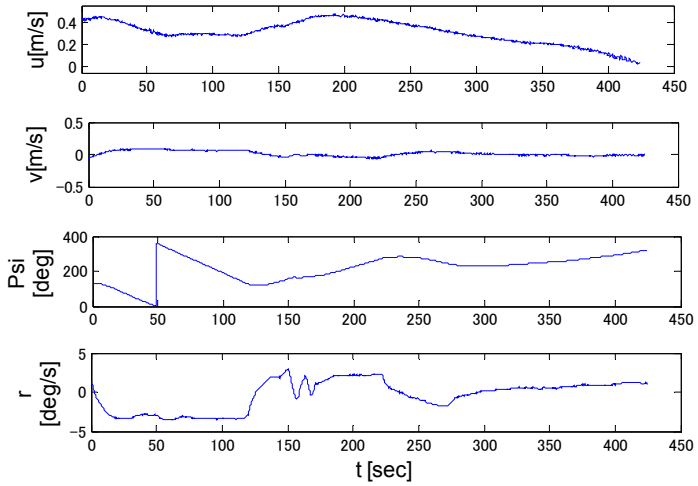

Figure 5.31(cont..). Corresponding details

On the other hand, the rest of the figures show completely different type of trajectories. Two experiment results for the ship started with almost similar initial heading and from mid of virtual window for rudder constraints ±10º and ±15º are shown in Figure 5.31 and 5.32. Here, in both cases, the controller decided to take the port rudder first instead of expected starboard rudder and it continued until the ship made a complete port turn. While continuing with the port tuning, the controller also decided a favourable position to take the starboard rudder and then it started its approach towards

the imaginary line. Thus, these two results belong to group 2 for LHS approach. Here, although the actions of the ANN controller during course changing were almost similar, the responses of the ship were different. This may probably due to existing current and wind disturbances. Unfortunately, due to some error in power system no wind data were logged in during these experiments to prove the above statement.

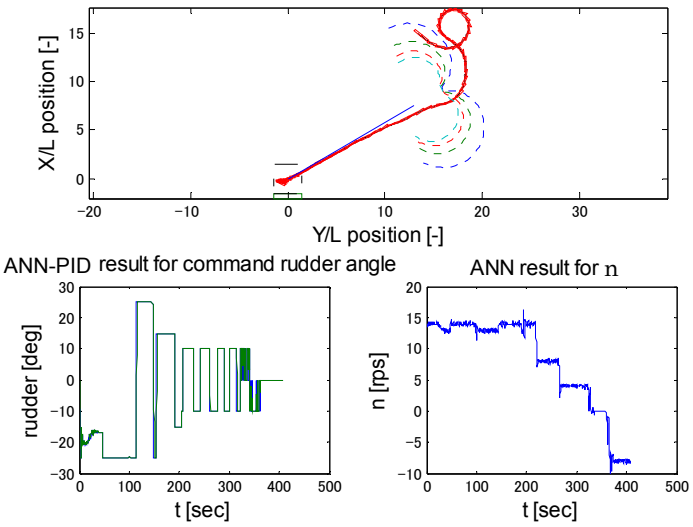

Figure 5.32. Initial heading 128.9º from mid of virtual window for rudder constraints ±10º and ±15º

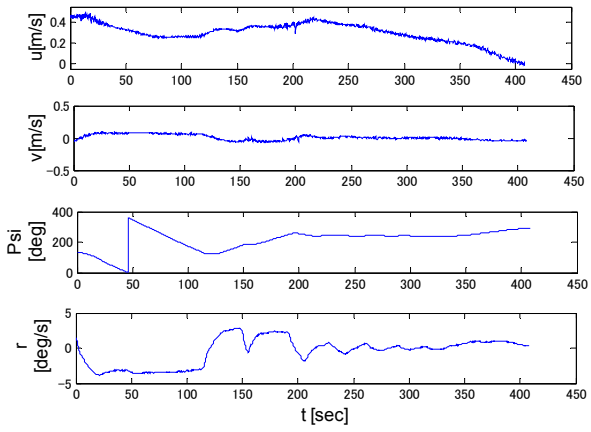

Figure 5.32(cont..). Corresponding details

Considering Figure 5.33, after switching to auto mode the controller took first port rudder to drive the ship far from the imaginary line. Then, followed by starboard rudder, the ship turned towards the approaching line and the controller just kept the track by

proving some bang-bang control like action until the PID controller was activated. Here, due to having sudden wind, the ship just stopped before entering the successful berthing zone and started to drift literally. Unfortunately, for this experiment the wind data are not available due to power problem. Figure 5.34 illustrates another result for the controller that initiated with starboard rudder first, but later on, it suddenly activated port rudder for some time. Such action resulted a larger course changing pattern than expected and the activated PID controller provided necessary corrections for such large existing gap between the ship and the imaginary line to ensure a successful berthing operation. These two types of behaviours of the controller were not observed in previous experiments.

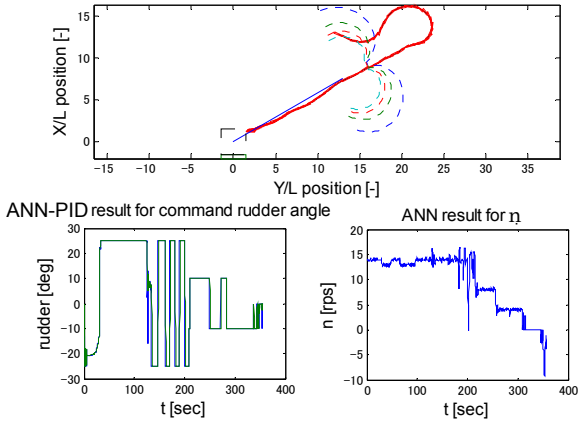

Figure 5.33. Initial heading 116.5º from mid of virtual window for rudder constraints ±20º and ±25º

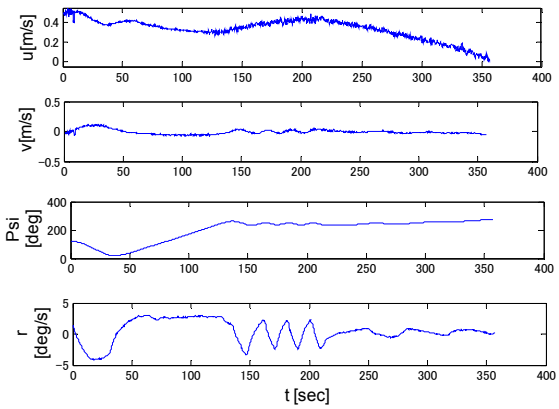

Figure 5.33(cont..). Corresponding details

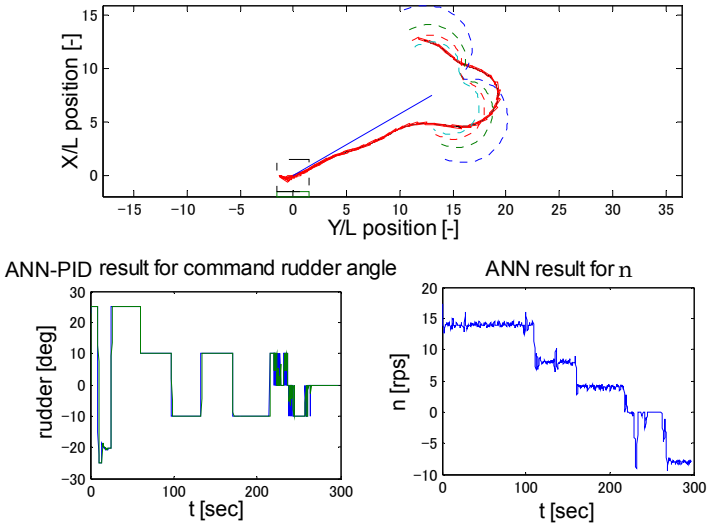

Figure 5.34. Initial heading 108.7º from mid of virtual window for rudder constraints ±20º and ±25º

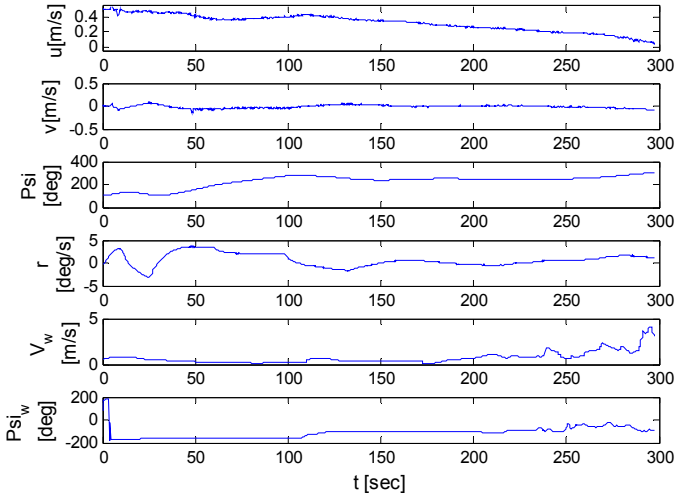

Figure 5.34(cont..). Corresponding details

Figure 5.35 to 5.42 illustrate the result, while using networks for RHS approach. In Figure 5.35, the controller started with a slight kick in the starboard rudder to minimise the existing initial sway velocity and yaw rate. Soon after that, it continued with its expected port rudder and the ship successfully merged with the imaginary line well ahead. Therefore, later on the activated PID controller only kept the track in wind disturbances. Here, sudden gust during reversing stage stopped the ship just after entering the successful boundary zone.

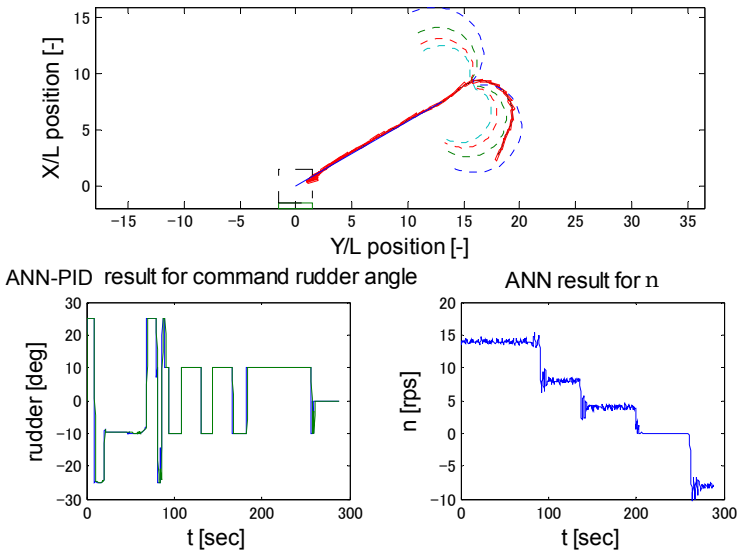

Figure 5.35. Initial heading 19.9º or 379.9º from mid of virtual window for rudder constraints ±10º and ±15º

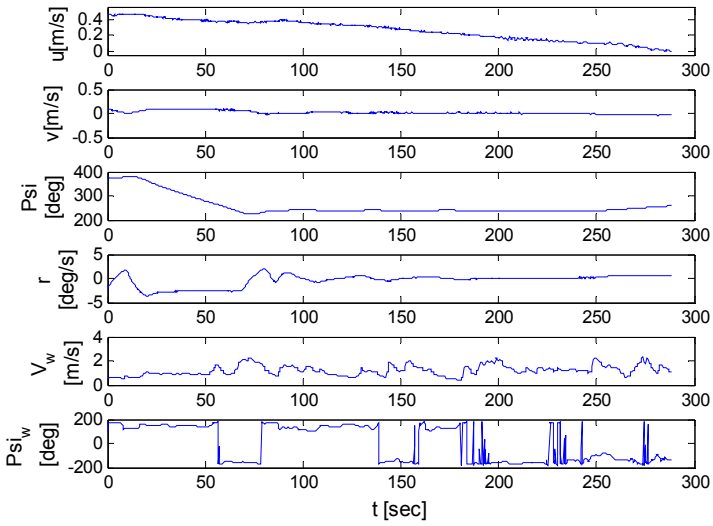

Figure 5.35(cont..). Corresponding details

Figure 5.36 and 5.37 show similar type of trajectories of the ship started from middle of virtual window considering different combinations of rudder constraints. The controller did almost the same action as explained in Figure 5.35. However, the small existing gaps after course changing were successfully minimised by the PID controller during low speed running. All these results belong to group 1 for RHS approach.

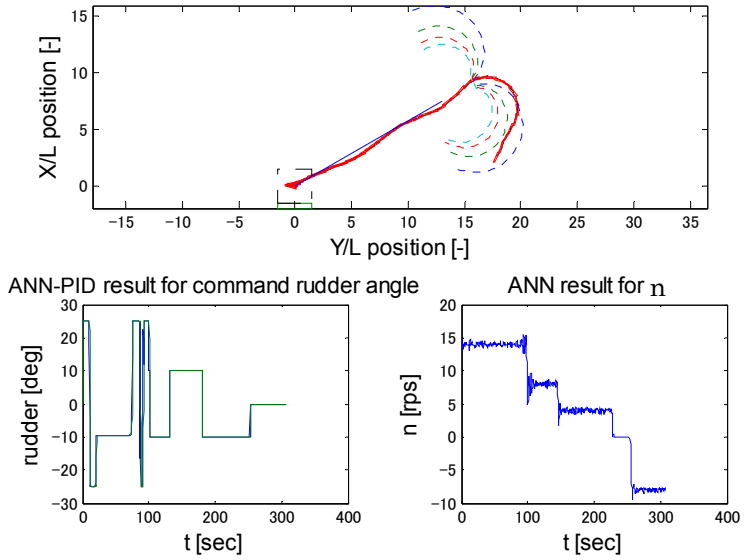

Figure 5.36. Initial heading 26.5º or 386.5º from mid of virtual window for rudder constraints ±10º and ±15º

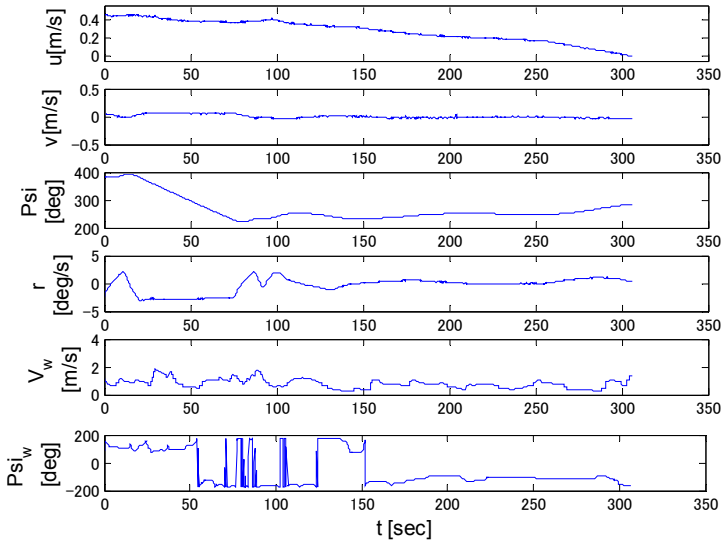

Figure 5.36(cont..). Corresponding details

On the other hand, Figure 5.38, 5.39 and 5.40 illustrate the trajectories of different types that contain larger error in ship position as well as in heading after course changing. This may due to starting from closest point, i.e. mid of ±20º and ±25º or having less option to go for large angle of heading change from such closest point of approach. In spite of that, the PID controller did its best and in all cases ship stopped

successfully within its desired zone. Among the resulting trajectories, the first two may be considered for group 3 due to their 'S' like pattern. On the other hand, Figure 5.40 may belong to group 4 as the ship moved parallel to the imaginary line instead of merging with it.

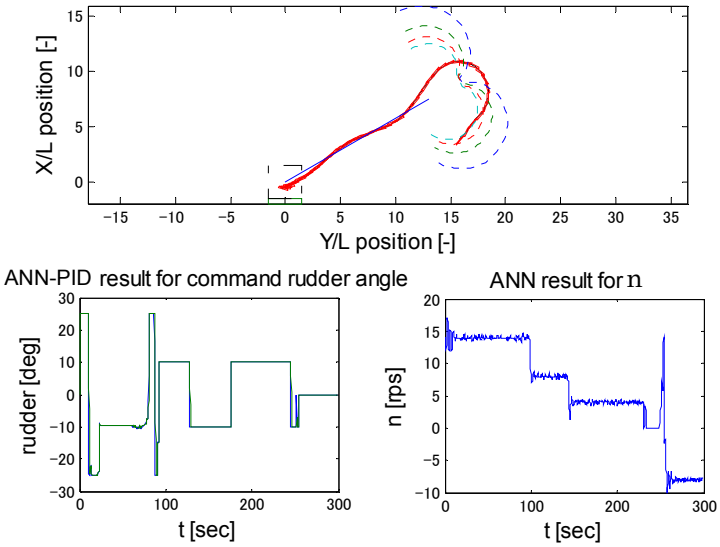

Figure 5.37. Initial heading 37.0º or 397.0º from mid of virtual window for rudder constraints ±20º and ±25º

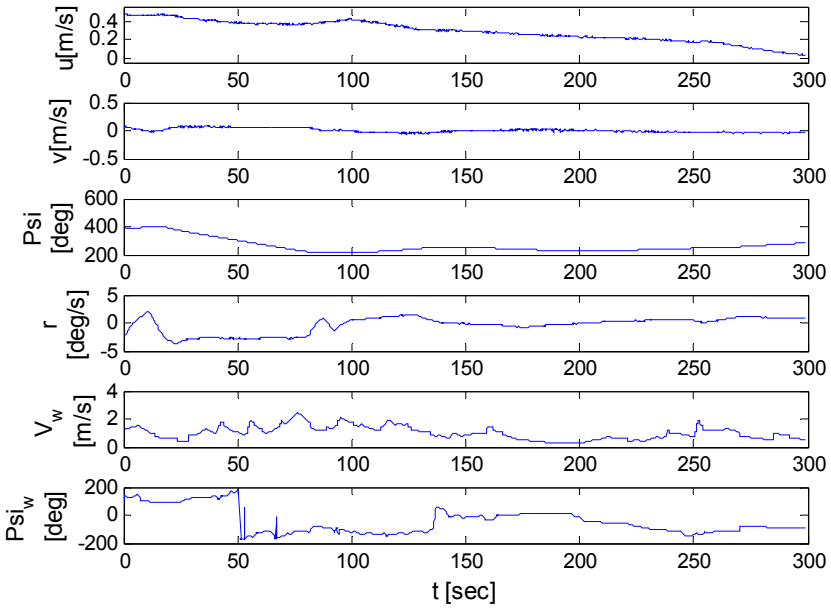

Figure 5.37(cont..). Corresponding details

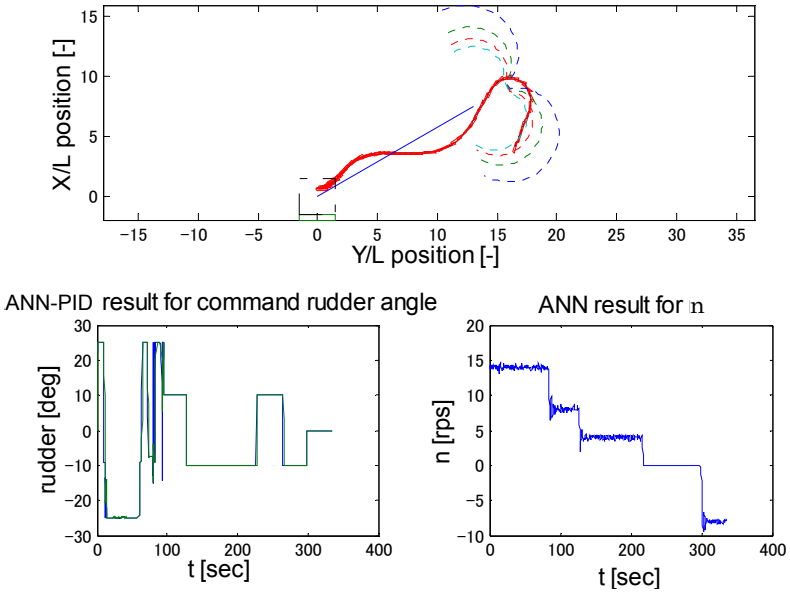

Figure 5.38. Initial heading 18.3º or 378.3º from mid of virtual window for rudder constraints ±20º and ±25º

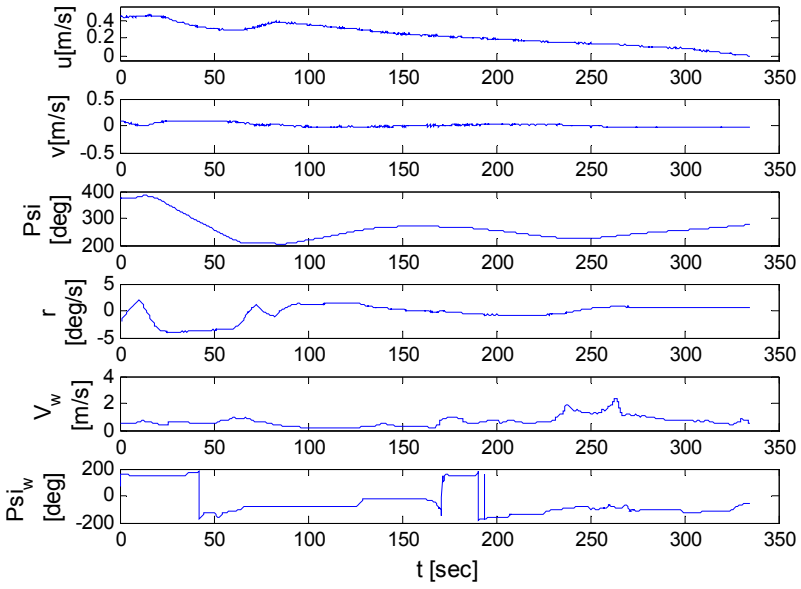

Figure 5.38(cont..). Corresponding details

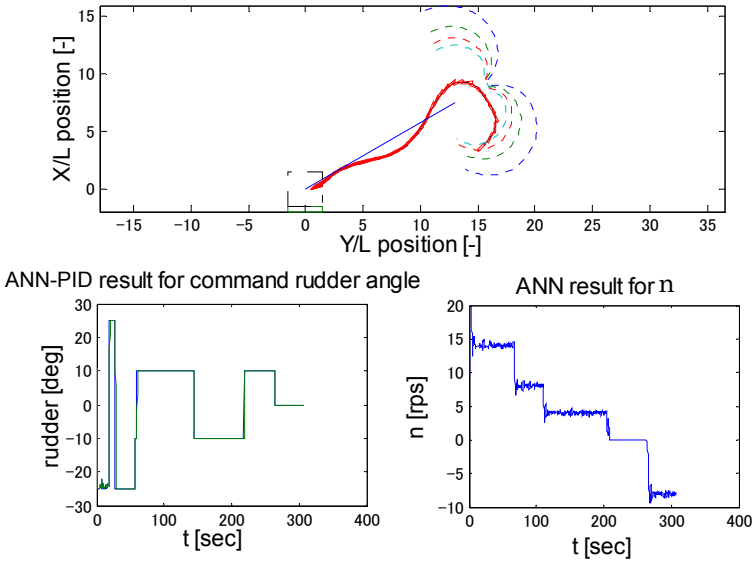

Figure 5.39. Initial heading 42.7º or 402.7º from mid of virtual window for rudder constraints ±20º and ±25º

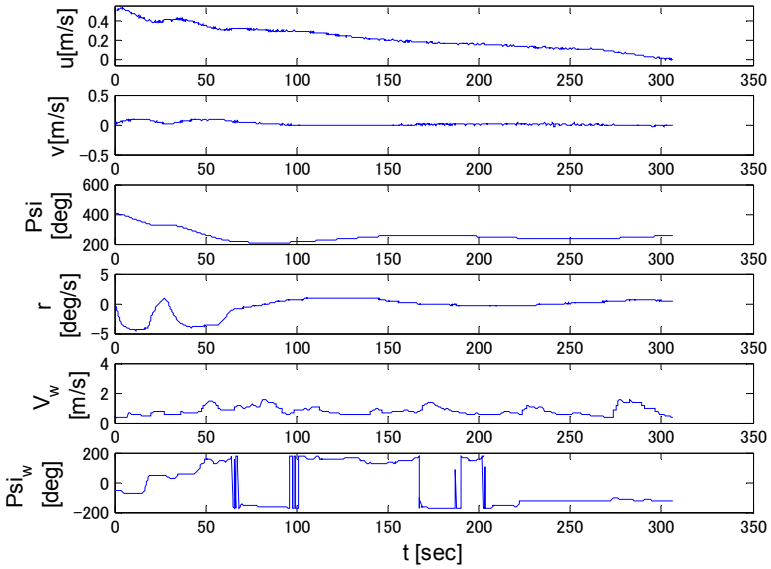

Figure 5.39(cont..). Corresponding details

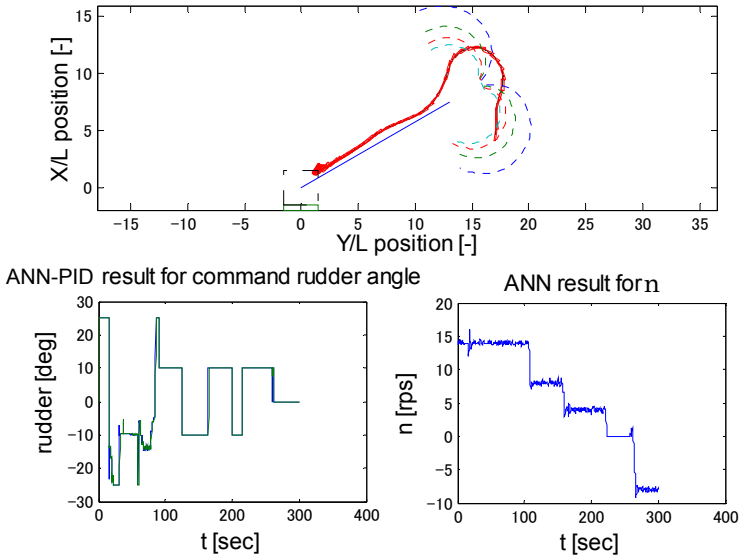

Figure 5.40. Initial heading 3.4º or 363.4º from mid of virtual window for rudder constraints ±20º and ±25º

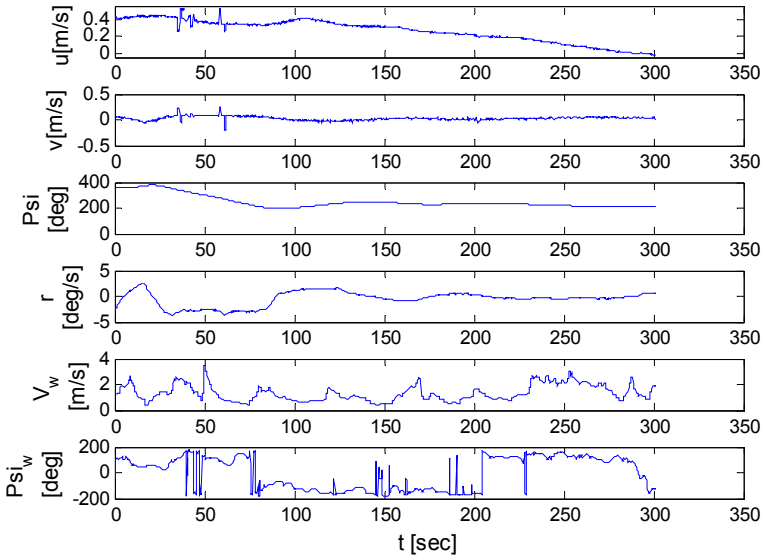

Figure 5.40(cont..). Corresponding details

Few experiments were also carried out considering the ship started from any undesired midpoint of virtual window for two different rudder constraints. Figure 5.41 shows one of such results, where the ship started with its initial heading 37.2º or 397.2º but from a point desired for 45º in mid of virtual window for rudder constraints ±15º and ±20º. Even in such cases, the combined controller has found effective enough to

ensure successful berthing operation. Here, the resulting trajectory belongs to group 1 for RHS approach.

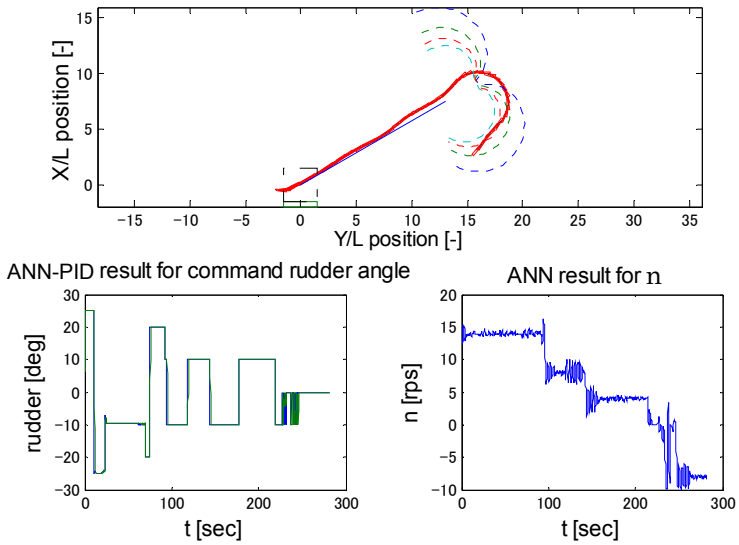

Figure 5.41. Initial heading 37.2º or 397.2º from undesired mid of virtual window for rudder constraints ±20º and ±25º

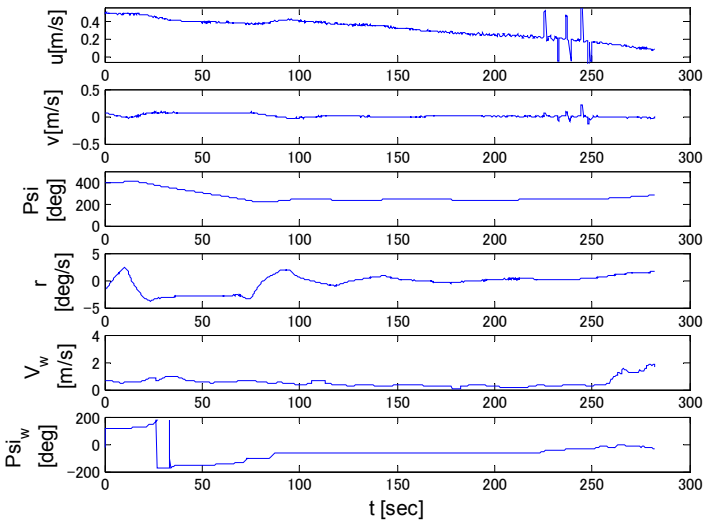

Figure 5.41(cont..). Corresponding details

5.5.3 Experiment for Ship Staring from Arbitrarily Chosen Point

Experiments mentioned in the previous two subsections were done by reading the initial point from a file against the ship's initial heading while switching to auto mode.

Therefore, during those experiments, the ship positions were calculated relative to the sorted out initial point and the program assumed the final goal based on its initial position. However, in a real case for berthing, the ship operator needs to operate the ship for a fixed target port. As a result, later on, the strategy was changed for a fixed-point approach rather than floating one. To do such experiments, there is no need of any file containing the points on virtual window. Like in the real case, the user only needs to navigate the ship to its possible approaching position and switch on to the auto mode. Then, the program will detect the ship position relative to the fixed goal point and the controller will take necessary action to execute the berthing operation. Such experiments are done in several cases where the auto mode is activated considering the ship within constructed virtual window area. Figure 5.42 to 5.45 illustrate such experiment results for RHS approach.

Considering Figure 5.42, the ship with its initial heading 38.9º was started from a point far beyond expected. However, the controller managed quite well to guide the ship up to the fixed goal point and the final surge velocity was less than 0.08 m/s. On contradictory in Figure 5.43, the ship started with almost similar heading and from a nearby point. The controllers also succeeded to guide it up to the desired zone. However, the final surge velocity was much higher than expected due to the late start of reversing.

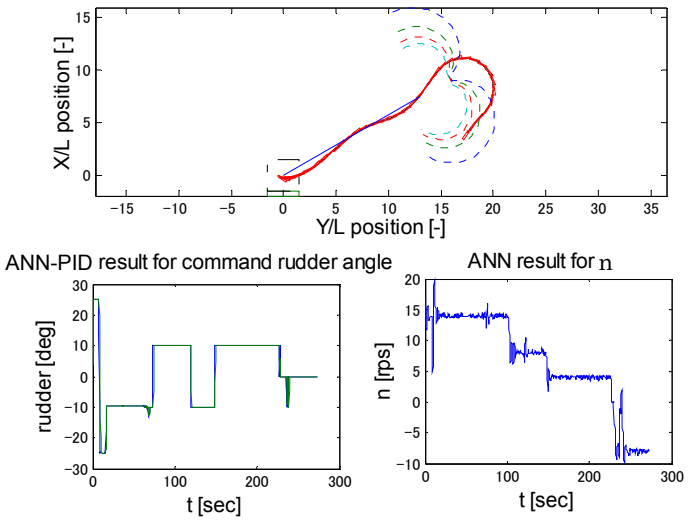

Figure 5.42. Initial heading 38.9º or 398.9º starts from (11.47m, 52.24m)

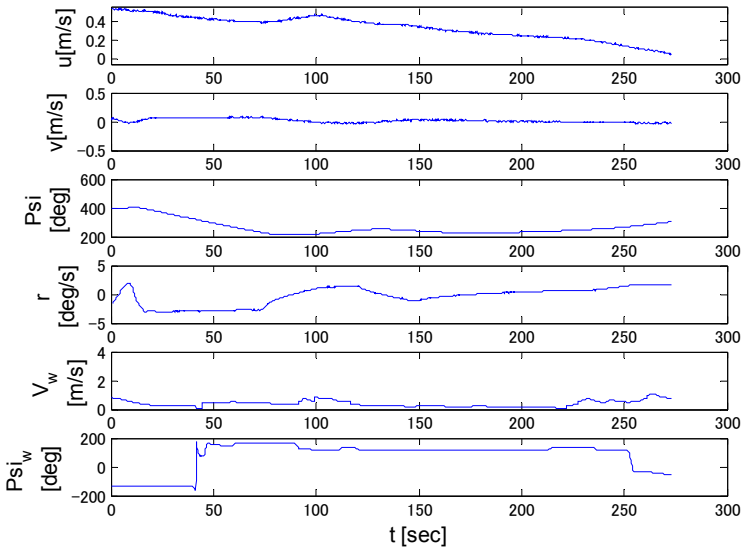

Figure 5.42(cont..). Corresponding details

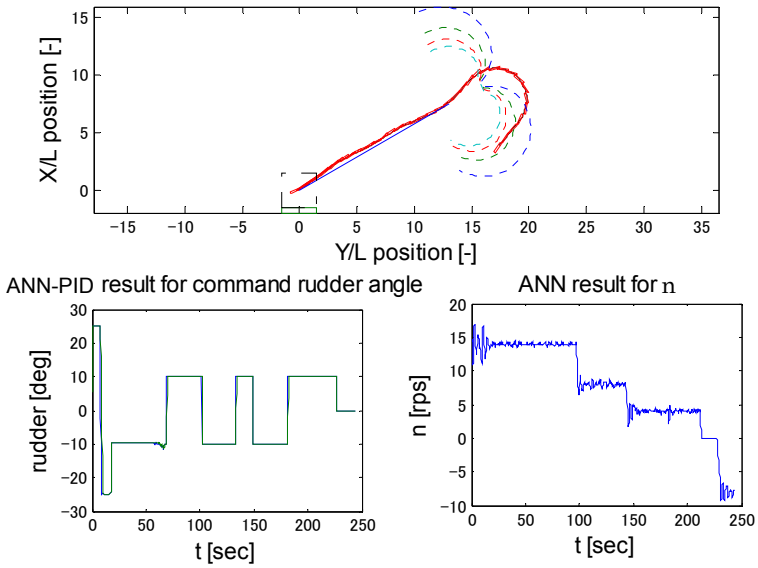

Figure 5.43. Initial heading 38.1º or 398.1º starts from (11.06m, 51.80m)

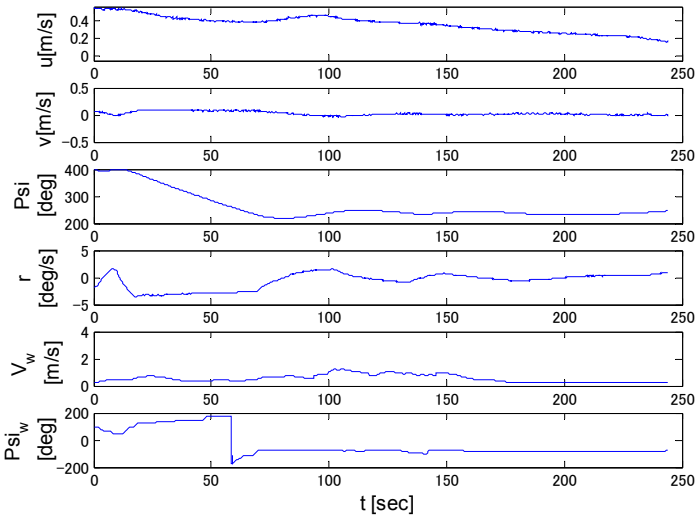

Figure 5.43(cont..). Corresponding details

Figure 5.44 shows the result for ship started with heading 25.2º. Here, the controller executed constant port rudder from the beginning. Therefore, the course changing trajectory looks quite smooth with some error in ship heading. This was corrected later on by the activated PID controller. Some fluctuations in GPS reading during reversing stage remained which made it difficult to guess the final surge velocity after completing the experiment.

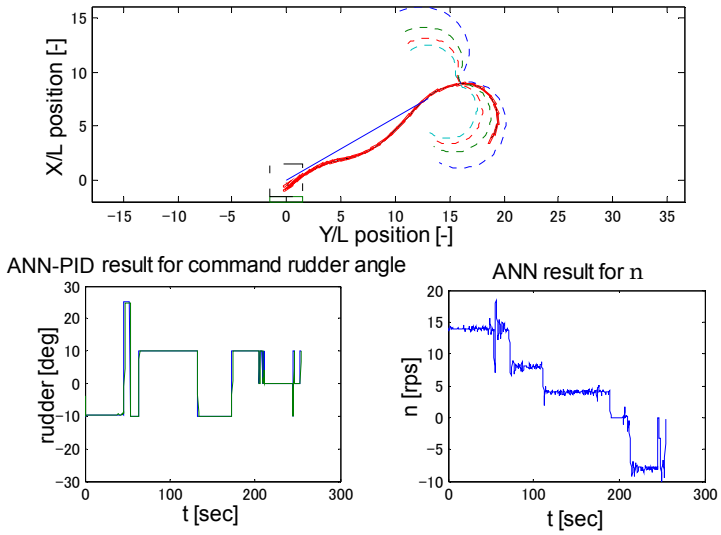

Figure 5.44. Initial heading 25.2º or 385.2º starts from (11.58m, 56.55m)

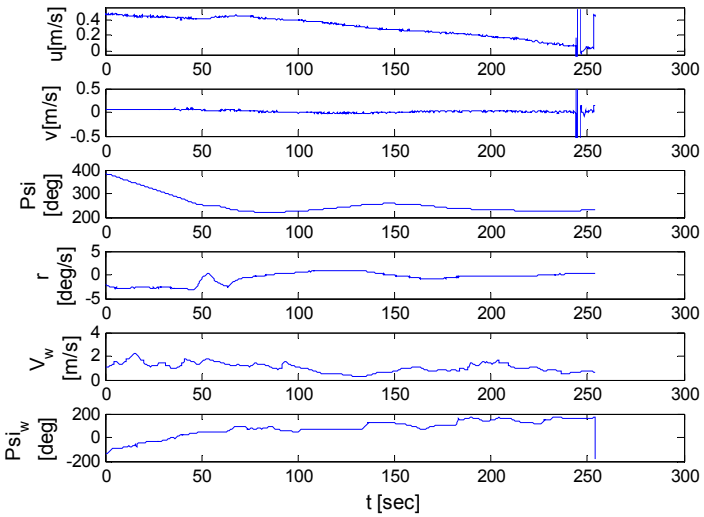

Figure 5.44(cont..). Corresponding details

In Figure 5.45, the ship with its initial heading 60.9º started from an arbitrary point was tested for berthing purpose. Here, the controller initiated with expected port rudder and followed by some bang- bang like control to go some part in a straight course. Then, the ship started its approach towards imaginary line. Due to such action, the ANN controller not only succeeded to merge with the imaginary line well ahead, but also the heading error after course changing was quite reasonable. The final surge velocity after completion of this experiment was less than 0.05 m/s.

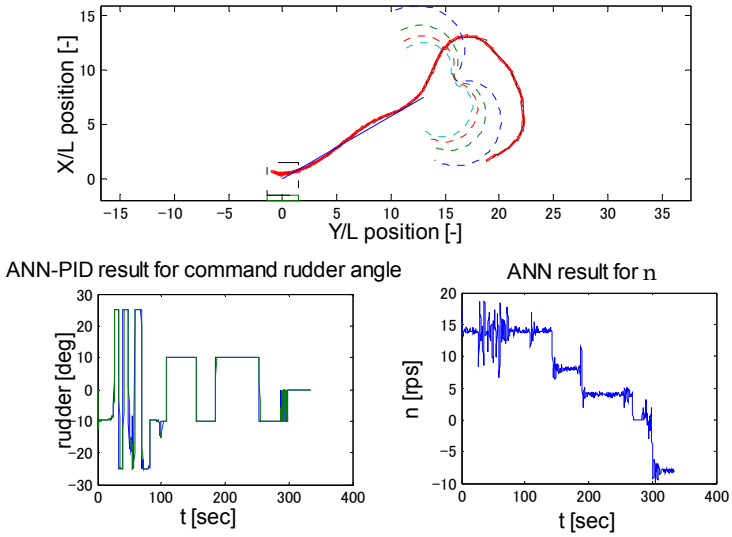

Figure 5.45. Initial heading 60.9º or 420.9º starts from (5.706m, 57.80663m)

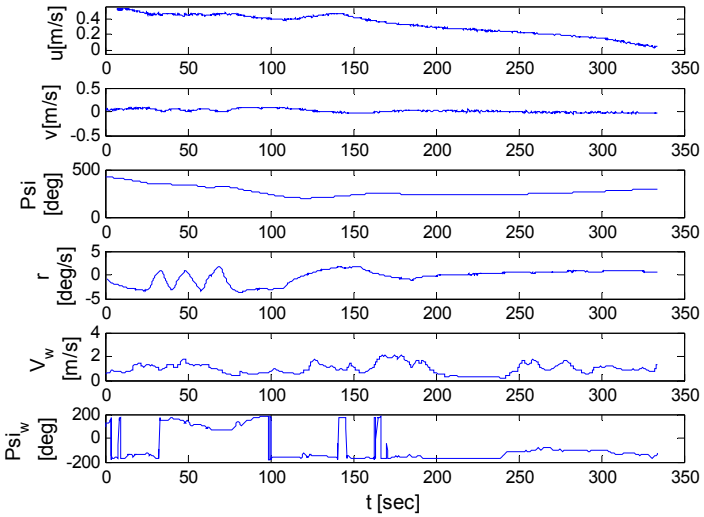

Figure 5.45(cont..). Corresponding details

Figure 5.46 to 5.48 illustrate the results while using the networks for LHS approach. Figure 5.46 shows the results for ship with its initial heading 133.3º started from an arbitrary point within the constructed virtual window area. Here, the trajectory looks similar to those used to train the network and thus belongs to group 1 for LHS approach. However, the controller initiated with a slight kick in port rudder.

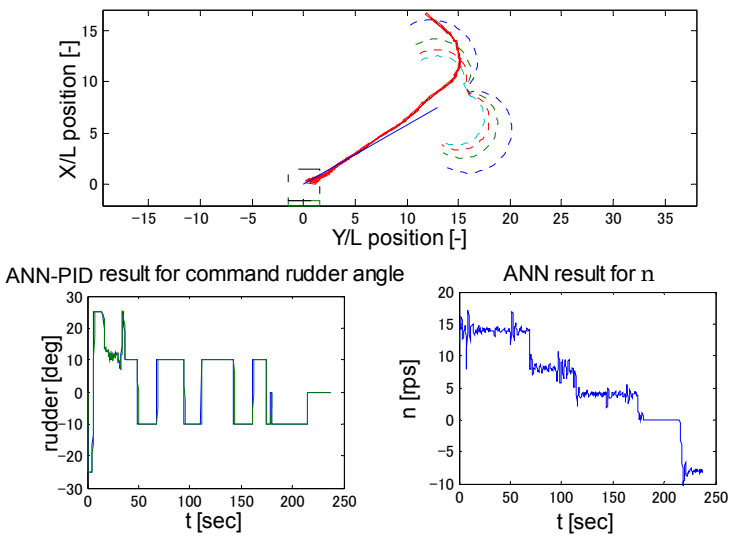

Figure 5.46. Initial heading 133.3º starts from (48.831m, 36.778m)

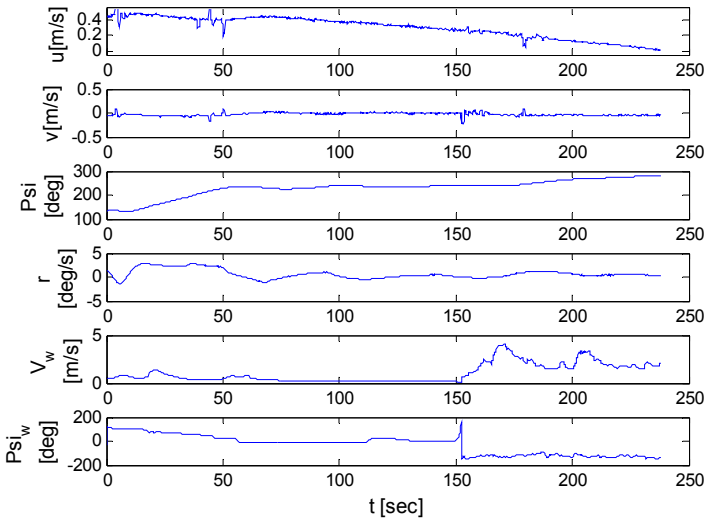

Figure 5.46(cont..). Corresponding details

In figure 5.47, the situation was a little bit different since the ship was planned to start from a point away from the created window. The initial heading was also beyond the range used in teaching data. The purpose of this experiment was to judge the effectiveness of controllers beyond the trained zone i.e. the extrapolation ability. In spite of such situation, ANN managed to merge the ship with imaginary line by taking the maximum allowed starboard rudder i.e. 25º and counter rudder as -25º. For some part, it also behaved like bang-bang control considering rudder ±15º in action. During the low speed running, the wind direction was inconsistent and the velocity was low enough to affect the ship's motion. As a result, after its emergence, the PID controller overtook the ANN and kept the course without that much of difficulty. The final surge velocity was 0.01 m/s but due to sudden high wind near the pier, the ship was literally drifted as shown in the trajectory.

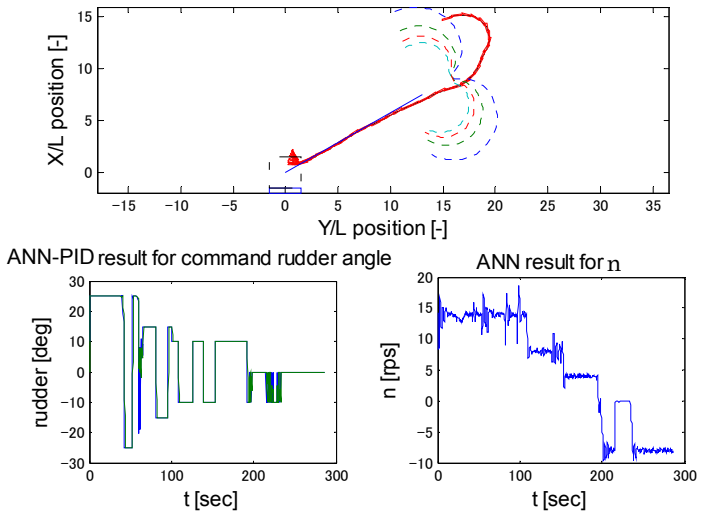

Figure 5.47. Initial heading 73.7º starts from (44.73m, 46.21m)

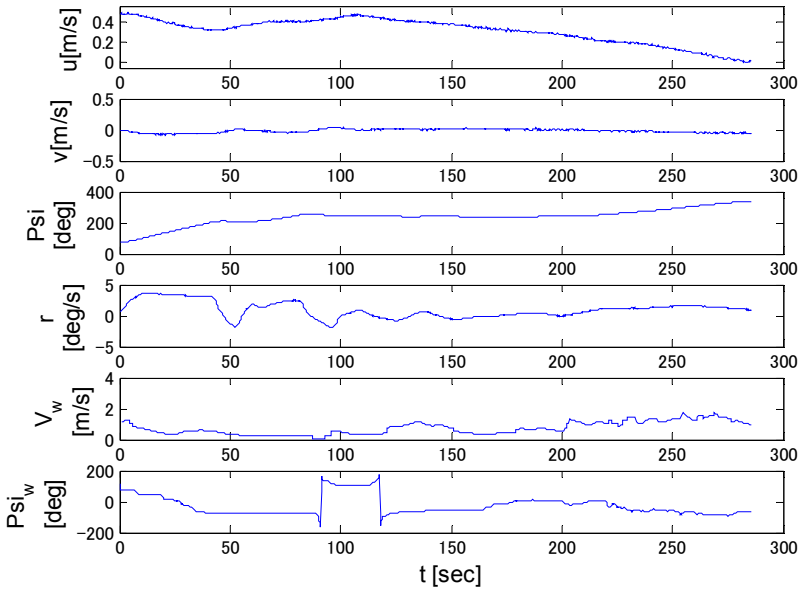

Figure 5.47(cont..). Corresponding details

On the contradictory, Figure 5.48 shows a completely different result. During the experiment, the controller took the port rudder first and continued with it until the ship made a complete port turn. Therefore, the result belongs to group 2 for LHS approach. The final surge velocity during the experiment was nearly zero.

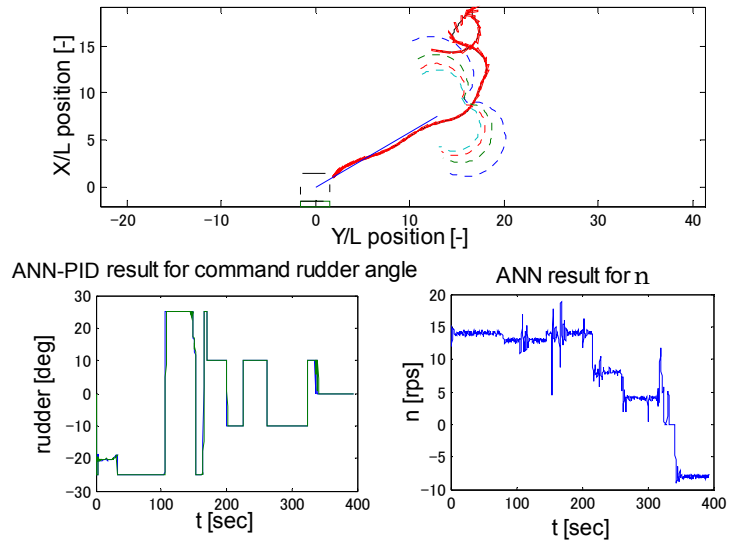

Figure 5.48. Initial heading 99.25º starts from (43.627m, 38.545m)

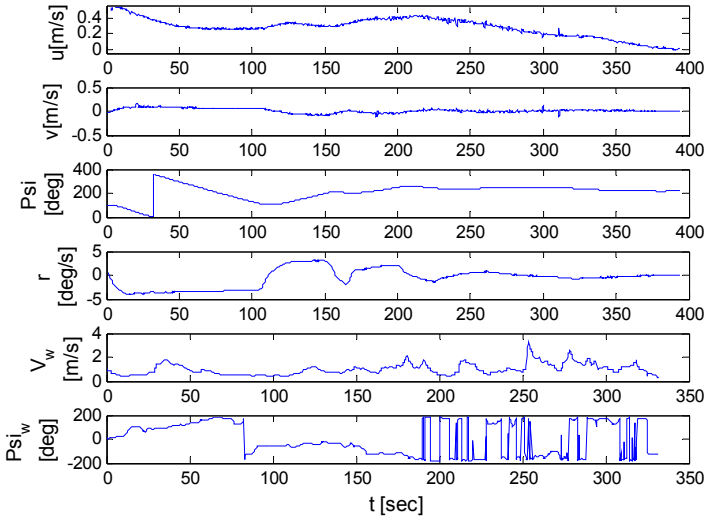

Figure 5.48(cont..). Corresponding details

Finally, all experiment results mentioned in this thesis provide strong evidence that the proposed ANN-PID controller is robust enough to ensure promising results in spite of the ship starting from any unexpected point on virtual window or anywhere within constructed virtual window area. During these experiments, the wind disturbance was one of the key factors to ensure the success of the controller. If the wind blows beyond the permitted limit that is 15 m/s for full scale or 1.5 m/s for model ship, then the results may vary drastically.

Chapter 6 : ANALYSIS OF NETWORK'S BEHAVIOR

In this thesis, the experiment results for automatic berthing are summarised depending on the controller's behaviour. However, to explain why the controller behaves in different ways, especially for rudder output, the network is investigated for different combinations of initial conditions to get the corresponding responses. Usually, the behaviour of the trained ANN controller is largely dependent on the quality and amount of teaching data provided. Moreover, it will also depend on the response of a ship. In this thesis, as inspired by aircraft landing, the ship is objected to make a course change first. Then, it is allowed to go straight following a reference line and decreases its speed. To execute the same berthing for different ports, the available waterways need to be analysed. Then, by setting the reference line at some convenient angle, similar type of teaching data can be created using the proposed technique for different ship. For the port that requires a narrow and complex manoeuvre, the berthing plan may need to modify. However, the optimisation can be utilised for any type of course changing and creation of consistent teaching data. Therefore, the analysed results of network's behaviour mentioned here are not universal. Depending on the berthing plan, the nature of teaching data will change and so do the network's behaviour. Nevertheless, this type of analysis is very important to understand the range of applicability of the ANN controller while facing any unknown and unexpected situation. Similar approach for analysing the network's behaviour can demonstrate the inherent knowledge of trained ANN in any case. By this way, the user can have a fair idea of the network's behaviour well before execution. The following subsections include such analysis results. Similar types of analysis can also be done for ANN trained with a different set of teaching data.

6.1 Network for Left Hand Side (LHS) Approach of Ship

There are necessary nine inputs of the network to calculate the desired rudder angle and among them d_1 and d_2 are position dependent. Thus, several combinations of inputs are possible to observe the network's response. However, the surge velocity, sway velocity and yaw rate are believed to be sensitive enough to analyse the behaviour of

network properly. In this thesis, the ship is expected to start from its desired or nearby point within the constructed virtual window zone. Moreover, such windows also cover varieties of ship's initial heading to start with it. Therefore, in most cases, similar type of response is expected due to the interpolation ability of the neural network for the ship started from its desired starting point. Thus, assuming the ship starts from its expected point, the only option left for the ANN to take the counter rudder at an initial stage would be the existing initial sway velocity and yaw rate. The initial surge velocity may also affect the ANN's decision. Since the ship speeds up using the half-ahead propeller revolution, it is believed that the actual surge velocity during the initial stage would be close to the value used as teaching data.

During the analysis, the initial ship heading is considered as 90º with its corresponding position on virtual window for rudder constraint ±10º. The surge velocity is set to half ahead and the actual rudder angle is set to zero. Considering these four parameters as fixed, different sway velocities and yaw rates are tested for the network's response.

Initially, both the initial sway velocity and yaw rate are set to zero. This is the same condition as used during training net and the network takes expected starboard rudder. During the experiment for LHS approach, the ship is initially commanded to take a starboard turn to enter the window. Thus, while switching to auto mode, the initial sway velocity is likely to have a negative value. Such situation is analysed by considering a gradual increase of the negative value of sway velocity and setting the yaw rate as zero. By doing so, the network has found to take as a usual starboard rudder for small value of sway velocity. It means the network takes the positive rudder i.e. starboard rudder to neutralise the existing negative sway velocity. However, with the increment of sway velocity, such starboard value gradually increases, attains its peak and then starts to decrease. Therefore, after a particular value of sway velocity, the network begins to oppose it by taking the port rudder. Further, the output for the port rudder starts to increase with the increment of sway velocity. Figure 6.1 shows such illustration.

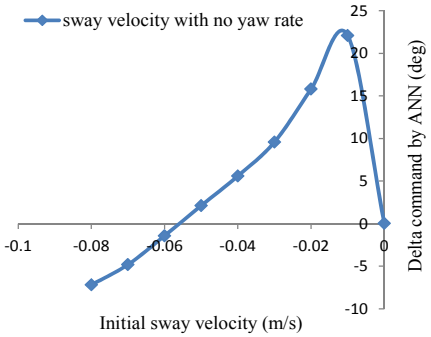

Figure 6.1. δ_{com} by ANN for different sway velocities (LHS)

On the other hand, due to the same reason, the initial yaw rate is likely to have positive value. Such situation is also analysed in a similar way, i.e. by considering a gradual increase of the yaw rate and setting the sway velocity at zero. Then, for any smaller value, ANN has found to oppose the existing yaw rate by taking the port rudder. It means, the controller decides to take negative rudder i.e. port rudder to neutralise the existing positive yaw rate. Such port rudder taken by ANN gradually increases with the increment of yaw rate, attains its peak and then starts to decrease. Therefore, after one particular value, ANN starts to take starboard rudder. That is, instead of opposing, ANN prefers to go with it. This kind of behaviour is just the opposite of varying sway velocity with no yaw rate. Figure 6.2 shows such illustration.

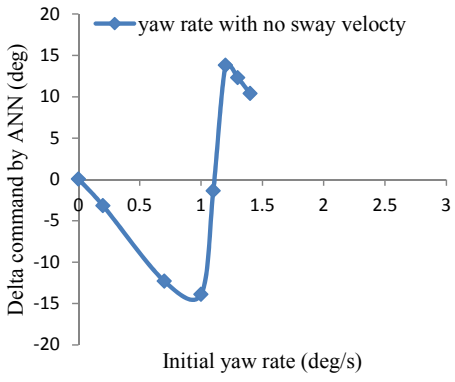

Figure 6.2. δ_{com} by ANN for different yaw rates (LHS)

Since, the mentioned two figures show completely opposite characteristics, therefore it would be interesting to know how the ANN behaves if both of these

parameters have some initial values. To observe such situation, three particular values of sway velocities are selected that are most likely to have as an initial condition during the experiment and vary the yaw rate within considerable region for each sway velocity. The corresponding responses of ANN are shown in Figure 6.3 to 6.5.

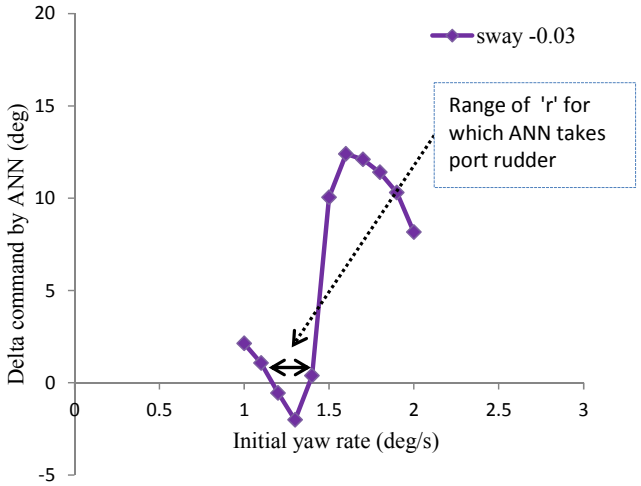

Figure 6.3. ANN's response for varying yaw rate, sway fixed at -0.03 m/s (LHS)

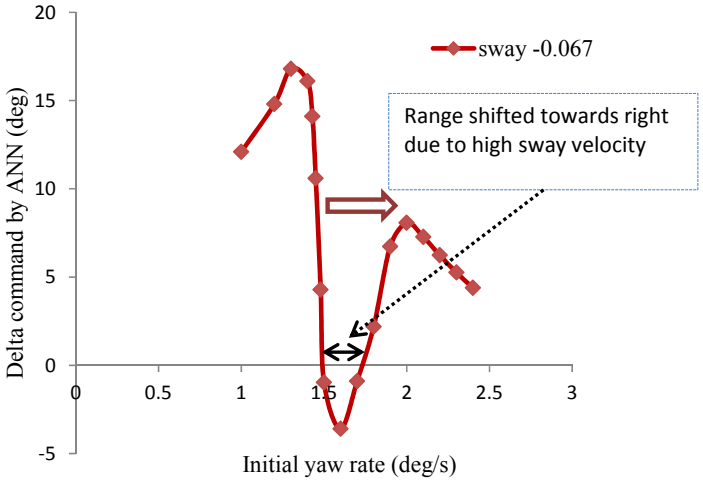

Figure 6.4. ANN's response for varying yaw rate, sway fixed at -0.067 m/s (LHS)

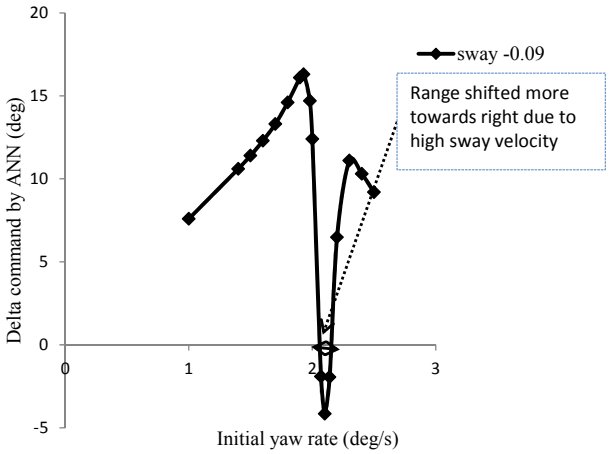

Figure 6.5. ANN's response for varying yaw rate, sway fixed at -0.09 m/s (LHS)

Considering Figure 6.3 to 6.5, the responses are illustrated for varying yaw rate from 1.0 deg/s to 2.4 deg/s. Although in each case, the network possesses a pulsating characteristic, the nature of the curves is almost similar. Here each of the figures show a particular range of yaw rate, for which ANN decides to take the port rudder to oppose the existing sway velocity and yaw rate. Beyond that range, ANN takes the expected starboard rudder for the left hand side approach of ship. Moreover, the defined range of yaw rate gradually shifts towards the right side with the increment of negative sway velocity. This can be ensured by observing the comparison, Figure 6.6, where all four curves for different sway velocities are superimposed. Although these figures are demonstrated considering a particular ship heading and initial position, even upon altering these values, ANN has found to possess similar types of behaviour. In general, it means that if a ship has some drifted sway velocity while entering to the window, then depending on its initial yaw rate ANN may sometimes take the counter rudder before activating its expected rudder action.

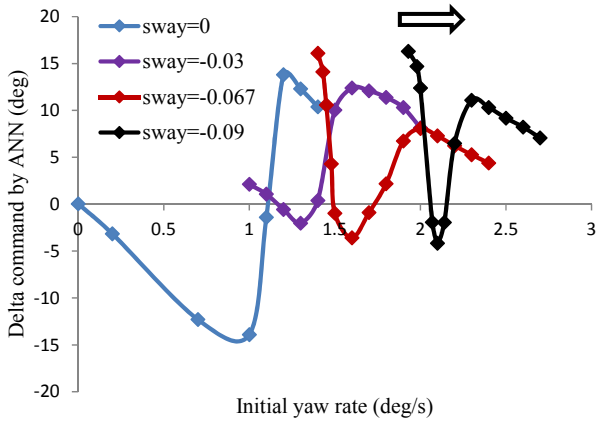

Figure 6.6. Comparison of ANN's response (LHS)

In case of surge velocity, ANN always takes the starboard rudder for the ship starts with a little bit slower velocity than the half ahead. However, the calculated rudder gradually increases with the decrement of initial surge velocity. Figure 6.7 illustrates such demonstration.

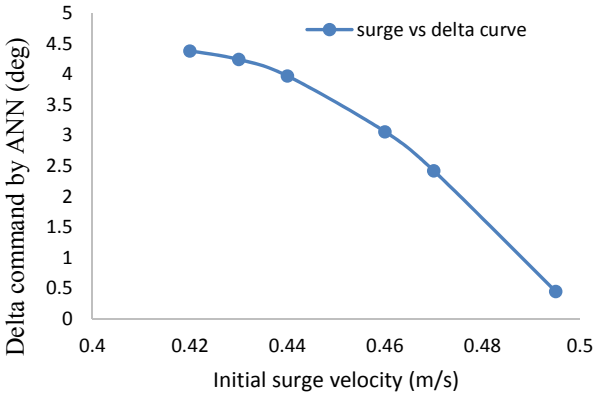

Figure 6.7. Comparison of ANN's response (LHS)

6.2 Network for Right Hand Side (RHS) Approach of Ship

In this thesis, the network used for the right hand side approach is different from that of left hand side. Therefore, a separate analysis is also needed for such case. Considering the teaching data for RHS approach, total 32 starting points are included for the ship's initial heading -270° or 90°, 60°, 30°, 0° or 360°, 330°, 300°, 270° and 250°/255°/260°/265°. On the other hand, the teaching data for LHS approach involved

24 starting points for the ship heading 90°, 120°, 150°, 180°, 210° and 230°/225°/220°/215°. Therefore, the number of teaching data for RHS approach is larger than that of LHS. Moreover, the ship's behaviour for port and starboard turning are also not symmetric due to the hydrodynamic properties of the ship. As a result, the networks are not expected to behave in a similar way.

During the analysis, the initial ship heading is considered as 425º or 65º with its corresponding position in virtual window for rudder constraints ±10º. The surge velocity is also set to half ahead and the actual rudder angle is set to zero. Considering these four parameters as fixed, different sway velocities and yaw rates are tested for the network's response like as for LHS approach.

Initially, both sway velocity, yaw rate are set to zero, and the ANN takes expected port rudder to start its approach for RHS. However, this time during the experiment, the ship is initially commanded to take a port turn to enter the window. Thus, while switching to auto mode, the initial sway velocity is likely to have positive value. Such situation is analysed by considering a gradual increase of the positive sway velocity and setting the yaw rate as zero. Then, with a slight increment of sway velocity, the ANN has found to take its maximum port rudder. It means, the network takes the negative rudder i.e. port rudder to neutralise the existing positive sway velocity. For RHS approach, this maximum value remains almost constant with the increment of sway velocity. Therefore, the network never opposes the existing sway velocity if there is no yaw rate. This type of behaviour is very smooth and not the same as found in LHS approach. This might be due to having a larger amount of teaching data for better learning while training net. Figure 6.8 shows such illustration.

On the other hand, due to the mentioned reason, the initial yaw rate is likely to have negative value. Such situation is also analysed in a similar way, i.e. by considering a gradual increase of the negative value of the yaw rate and setting the sway velocity at zero. Then, for any smaller value, ANN has found to oppose the existing yaw rate by taking the starboard rudder. It means, the controller decides to take positive rudder i.e. starboard rudder to neutralise the existing negative yaw rate. After a particular value of yaw rate, the starboard rudder taken by ANN gets almost constant that does not change much for further increment of yaw rate. Figure 6.9 shows such illustration.

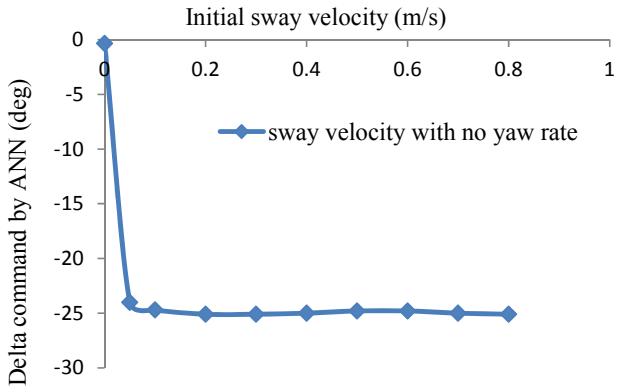

Figure 6.8. δ_{com} by ANN for different sway velocities (RHS)

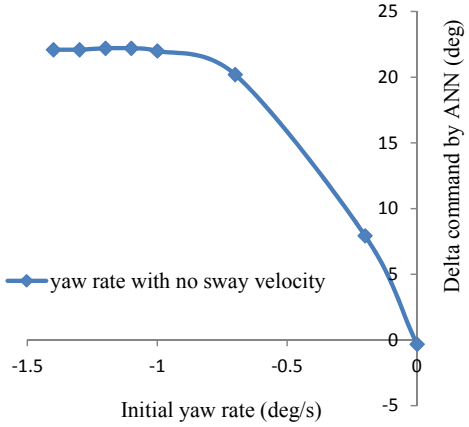

Figure 6.9. δ_{com} by ANN for different yaw rates (RHS)

Since the above two figures show completely opposite characteristic, therefore same as LHS approach, it would be interesting enough to analyse the network's behaviour for different combination of sway velocity and yaw rate. This time, the same three values of sway velocities are selected as LHS approach, but with opposite sign and the behaviour of ANN for variable yaw rate is observed. Figure 6.10 to 6.12 show the corresponding responses of ANN.

Considering Figure 6.10, since the sway velocity is low enough, it does not have that much effect on ANN's behaviour. As a result, the effect of having an initial yaw rate is more prone than having any low sway velocity in RHS approach. The ANN takes the port rudder only for small values of yaw rate. Otherwise, irrespective of any higher

values of yaw rate as an initial condition, ANN always takes the starboard rudder.

On the other hand, with the increment of sway velocity as found in Figure 6.11 and 6.12, the graph is gradually pulled down due to the effect of sway velocity. It means more part of it goes to port side. Such figures show that the effect of having high sway velocity is dominant for small yaw rate. However, later on with the increment in yaw rate, the curve turns toward the positive value and ANN starts to take starboard rudder. Each time with the increment of sway velocity, the graph is also little bit shifted towards the left. As a result, the value of yaw rate for which ANN alters its behaviour gradually increases. This can be ensured by observing the comparison Figure 6.13, where all four curves for different sway velocities are superimposed. Finally, the analysis of the network for RHS approach can be concluded in a similar way as for LHS approach. Thus, if a ship has a low initial sway velocity while entering to the window, then in most cases the ANN will take the starboard rudder to oppose the expected turn except for low existing yaw rate.

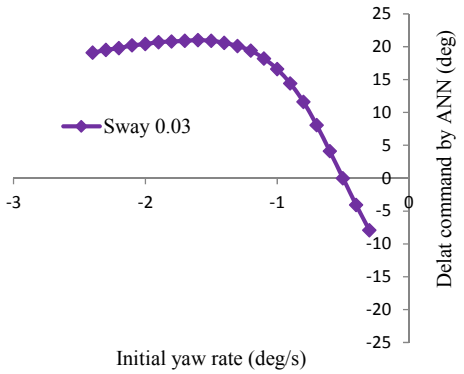

Figure 6.10. ANN's response for varying yaw rate, sway fixed at 0.03 m/s (RHS)

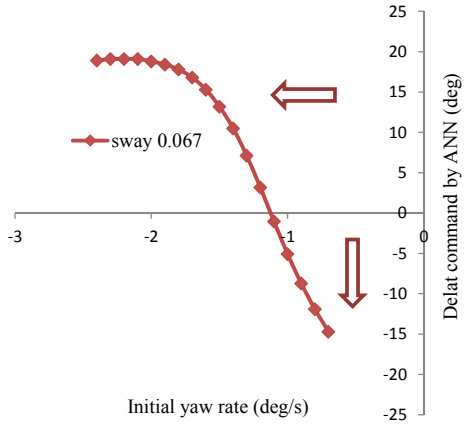

Figure 6.11. ANN's response for varying yaw rate, sway fixed at 0.067 m/s (RHS)

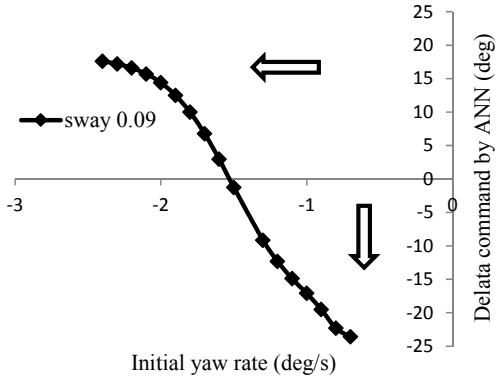

Figure 6.12. ANN's response for varying yaw rate, sway fixed at 0.09 m/s (RHS)

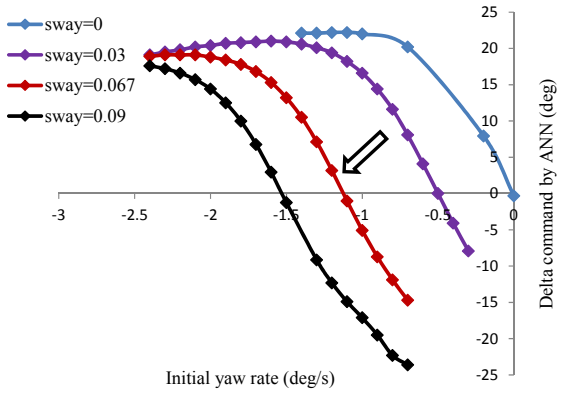

Figure 6.13. Comparison of ANN's response (RHS)

Regarding the ANN's response for varying surge velocity, ANN always takes expected port rudder irrespective of any initial surge velocity. However, the port rudder taken by ANN gradually increases with the decrement of surge velocity. Figure 6.14 illustrates such demonstration.

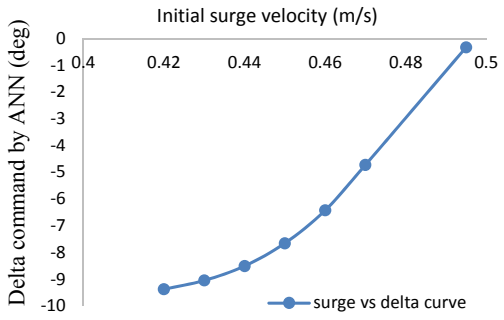

Figure 6.14. Comparison of ANN's response (LHS)

Here, the analysis of the network's behaviour mainly demonstrates how the network behaves depending on existing initial sway velocity and yaw rate. Therefore, no matter how such initial sway velocity or yaw rate results from. In this thesis, it results due to the execution of turning motion before switching to auto mode. Usually, in real ship cases or in different experiment sites, it is extremely difficult to maintain a straight course in the presence of environmental disturbances. Therefore, some amount of sway velocity or yaw rate exists in such cases too. Thus, the network will behave in a similar way in other experiment sites depending on the existing initial conditions.

Chapter 7 : AUTOMATIC TUG ASSISTANCE

After the ship successfully stops within the surrounded area of berthing goal point as shown in Figure 3.1, the final step is to align it with actual pier. Usually in the harbour area, a big ship with single rudder-single propeller often requires a set of adequate thrust devices or tugs assistance with exactly taken into account the surge, sway and yaw rate to execute such crabbing motion. The number of tugs involves in such operation depends on the size of the ship as well as existing wind disturbances. The effect of wind varies with its relative direction and the speed of the ship. Although it might appear logical that the effect of wind on a tanker stopped in the water would cause the bow to swing towards the wind, it is difficult to predict the effect of wind on other ships like partially loaded container ship. To understand the behaviour of a stopped ship under wind disturbances, it is necessary to have an idea about the centre of lateral resistance and the point of influence of wind. A brief description of these can be found in master's guide to berthing (37) and also given as follows:

The centre of lateral resistance: The point of influence of underwater forces acting on hull to resist the wind-induced motion is known as the centre of lateral resistance (CLR). Therefore, CLR is the point on the underwater hull at which the total hydrodynamic force can be considered to act. In case of ship with motion, it is usual to consider the pivot point (P) rather than CLR when discussing the effects of wind. On the other hand, a stopped ship does not have a pivot point. Therefore, in such cases CLR should always be used.

The point of influence of wind: This is the point (W) on above-water structure of ship upon which the total wind force can be considered to act. This point is not fixed like ship's centre of gravity (CG). Moreover, the point of influence of wind moves depending on the profile of the ship exposed to the wind. Thus, W will be close to the mid-length when a ship's beam is facing to the wind. On the other hand, it may move slightly forward or aft depending on the superstructure position of the ship.

In order to consider the effect of wind while executing the crabbing motion, W must be viewed in relation to CLR. A ship under wind disturbances, always wants to settle into

an equilibrium position where the pivot point and the point of influence of wind are in alignment. If a stopped ship faces the wind on its beam, W will be close to the mid-length of the ship. Similarly, the CLR will also at its mid-length. The difference between the two points produces a small moment, and the ship will turn towards the wind with its head facing to it. As the ship continues to turn, W also starts to move until it is close to the CLR. Therefore, the couple reduces gradually to zero and the ship settles on its heading. Figure 7.1 illustrates such phenomenon.

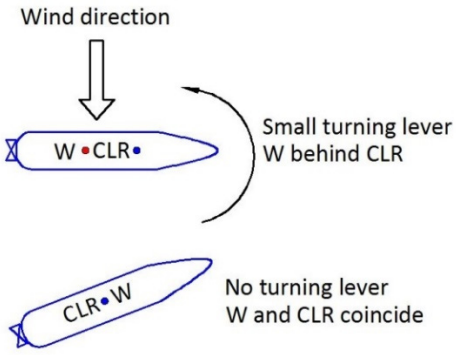

Figure 7.1. Wind effect on a stopped ship

In this thesis, while starting the crabbing motion, the ship might have some forward speed. Therefore, the ship Esso Osaka with its pivot (P) forward of midship will experience a large lever with the point W at midship. The resultant force will cause the ship's head to turn to the wind as shown in Figure 7.2.

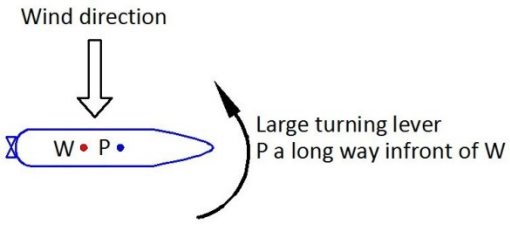

Figure 7.2. Wind effect with forward motion

Therefore, allocation of side thrusts under gust wind disturbances is very difficult. Bui *et al* (38) solved such thrust allocation problem by using the redistributed pseudo inverse approach to determine the thrust and direction of each individual tugboat. The

main goal of that approach was to minimise the power supplied to the tugboat. However, this thesis deals with the side thrusts that act perpendicular to the ship hull and for simplicity the pulsating nature of thrust output is ignored. At first, to develop a controller for side thrusts, ANN has been tried in a similar way as explained by Tran and Im (22) under no wind condition. However, considering wind that is mostly unpredictable, there is no other easy way to maintain consistency in teaching data that is very important to ensure the effectiveness of the trained ANN controller. As a result, simple but effective PD controller has been chosen over ANN in such cases under wind disturbances. Moreover, to control the forward motion, especially in wind, longitudinal trust is also involved. The methodologies considered while designing the PD controllers are heading angle correction in terms of minimising the difference between the X-coordinate value of fore and aft peak of ship, surge and sway velocity control, ship position control and reverse thrust when almost reaching the destination i.e. making the sway velocity minimum as possible. The following expressions describe the PD controllers used for automatic thrust generation in lateral and longitudinal direction.

if $\Psi < 270^0$ *and dis_fore>dis_rev*

$$\begin{aligned} T_{fore} &= C_1 * (\mathrm{X}_{fore} - 1.5 - X_{fore}) + C_2 * \mathrm{sway} \\ T_{aft} &= C_1 * (\mathrm{X}_{fore} - 1.5 - X_{fore}) + C_2 * \mathrm{sway} + C_3 * \mathrm{diff} \end{aligned} \tag{7.1}$$

if $\Psi > 270^0$ *and dis_aft>dis_rev*

$$\begin{aligned} T_{fore} &= C_1 * (\mathrm{X}_{aft} - 1.5 - X_{aft}) + C_2 * \mathrm{sway} + C_3 * \mathrm{diff} \\ T_{aft} &= C_1 * (\mathrm{X}_{aft} - 1.5 - x_{aft}) + C_2 * \mathrm{sway} \end{aligned} \tag{7.2}$$

if $\Psi < 270^0$ *and dis_fore<dis_rev*

$$\begin{aligned} T_{fore} &= C_1 * (-1.5 - X_{fore}) + C_2 * \mathrm{sway} \\ T_{aft} &= C_1 * (-1.5 - X_{fore}) + C_2 * \mathrm{sway} + C_3 * \mathrm{diff} \end{aligned} \tag{7.3}$$

if $\Psi > 270^0$ *and dis_aft<dis_rev*

$$\begin{aligned} T_{fore} &= C_1 * (-1.5 - X_{aft}) + C_2 * \mathrm{sway} + C_3 * \mathrm{diff} \\ T_{aft} &= C_1 * (-1.5 - X_{aft}) + C_2 * \mathrm{sway} \end{aligned} \tag{7.4}$$

Longitudinal thrust

$$T_{long} = C_4 * surge + C_5 * \mathrm{Ypos} + C_6 * \mathrm{distance} \tag{7.5}$$

where, Ψ is ship heading, X_{fore} and X_{aft} are x-coordinate of ship's fore and aft peak respectively, *diff* is $abs(X_{fore}-X_{aft})$, *distance* is the perpendicular distance of ship's CG from the actual pier, *dis_fore* and *dis_aft* are perpendicular distance of ship's fore and aft peak respectively from the actual pier, *dis_rev* is the perpendicular distance from the actual pier to start reverse thrust, Y_{pos} is the y-coordinate of ship's CG in the earth fixed coordinate, C_1~C_6 are the coefficients.

Considering Equation 7.1 and 7.2 for providing side thrusts, first part belongs to a constant value irrespective of ship position to withstand the wind force up to 1.5 m/s. The second part is for controlling the sway velocity and the third part activates if a correction for ship heading is needed. On the other hand, if the ship reaches the zone to provide reverse side thrusts as given by Equation 7.3 and 7.4, the first part is no longer constant rather increases the thrust value gradually with the decrement of the distance value to minimise the sway velocity upon reaching the pier. Other parts remain same. Here, the value of *dis_rev* depends on the steady sway velocity while approaching to the pier using side thrusters in presence of wind disturbances form different direction. Considering longitudinal thrust given in Equation 7.5, the first part is for controlling forward velocity. The second part is for controlling ship position in longitudinal direction and the third part is for controlling thrust value with respect to ship's distance from actual pier. Then, by combining the proposed controller for side thrusters with the existing ANN-PID controller, simulations are done in the different unknown situation.

7.1 Simulations for Berthing Manoeuvre Including Thrusters

The effectiveness of ANN-PID controller to stop the ship around the berthing goal point has already been verified for several known and unknown situations. Depending on the controller's action and presence of wind disturbances, a ship may have different termination points as well as different surge, sway velocities and yaw rates. Therefore, the compatibility of the newly developed PD controller for side thrusters needs to be tested for the exiting ANN-PID controller. In this thesis, the side thrusters are activated if surge velocity is less than 0.05 m/s or as the ship approaches the berthing goal point (0, 0). The following figures demonstrate the total automatic berthing process, including

the thrusters to align the ship with actual pier. Considering these figures, the ship having different initial heading is tested for different arbitrary point within constructed virtual under maximum allowable wind disturbances that is 1.5 m/s.

Figure 7.3 to 7.5 show the result for ship starting with initial heading 180º from three different starting points. Wind disturbances are also considered from three different directions. Therefore, while staring the side thrusters, the termination state of the ship is different in each case. As seen in Figure 7.3, wind from 315º results a slight clockwise turn during the idling and reversing stages. At last, the surge velocity goes down to 0.05 m/s, the thrusters are activated to guide the ship up to the actual pier and align with it. Finally, the berthing operation ends with surge velocity -0.02m/s, sway velocity -0.016 and final ship heading 266º.

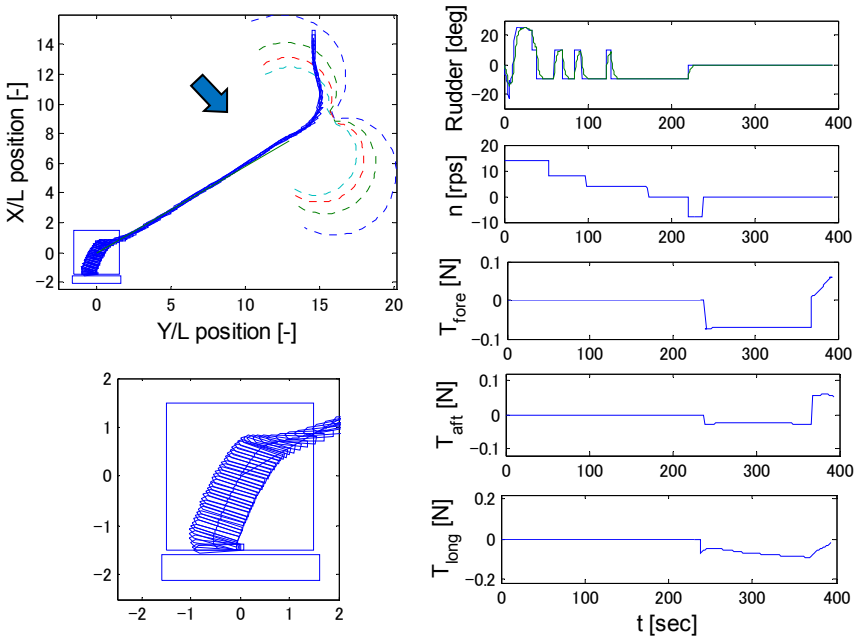

Figure 7.3. Berthing with thrusters, initial heading 180.0º starts from (43m, 44m)

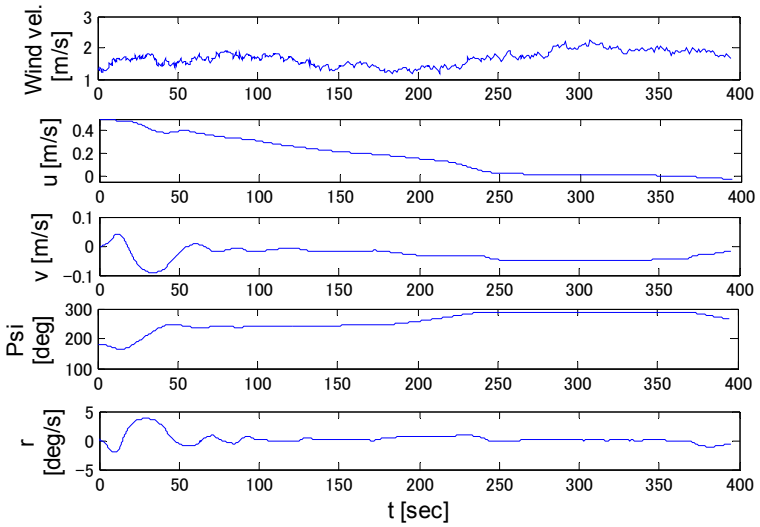

Figure 7.3(cont..). Corresponding details

On the other hand, Figure 7.4 is tested for wind from 135º that is just opposite as mentioned in Figure 7.3. Therefore, the ship tends to make sight anticlockwise turn during its idling stage. This also brings the ship close to the berthing goal point with a relatively high velocity as compared to Figure 7.3. From that state, the thrusters are activated. Here, the reverse thruster in longitudinal direction plays an important role in reducing the surge velocity. Finally, the berthing ends with surge velocity -0.026 m/s, sway velocity almost 0m/s and ship heading 270º.

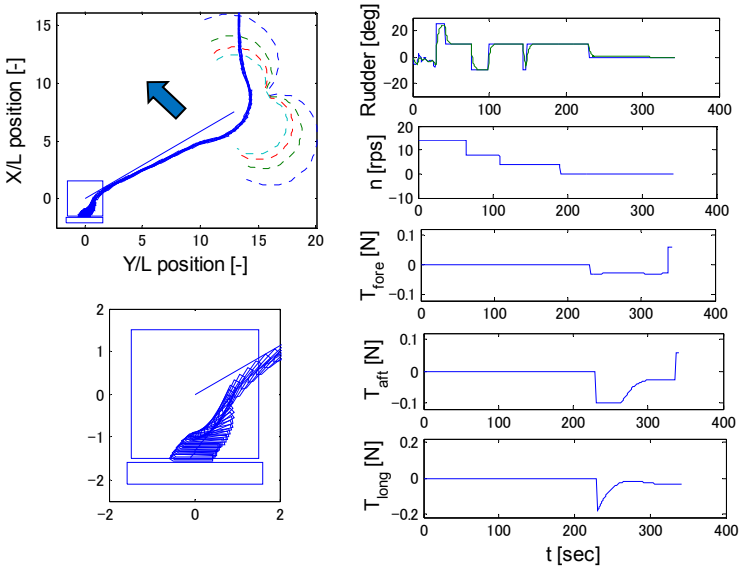

Figure 7.4. Berthing with thrusters, initial heading 180.0º starts from (47m, 40m)

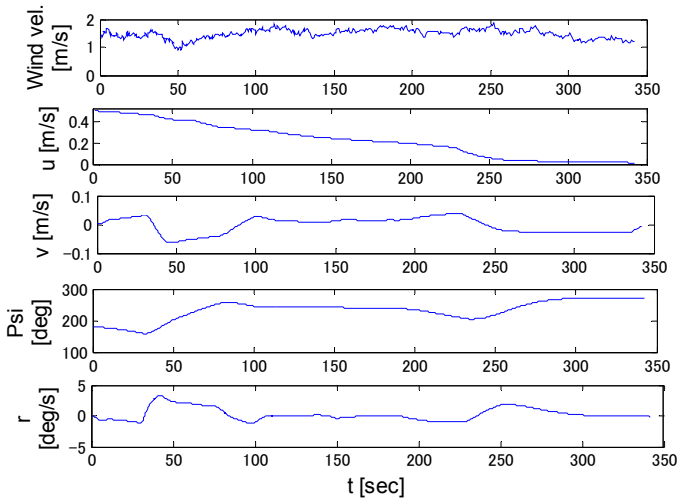

Figure 7.4(cont..). Corresponding details

Figure 7.5 shows the result of the following wind. Due to the wind, although the ANN controller executes reversing well before, the velocity drop was insufficient. Therefore, soon after the ship crosses the (0, 0) point, the thrusters are activated. Here, the maximum reverse thrust in longitudinal direction becomes necessary for some short duration to reduce the ship's speed within the controllable range. At the same time, the literal thrusters also provide the necessary amount of thrusts to align the ship with pier. Finally, the simulation ends with surge velocity -0.04 m/s, sway velocity -0.028 m/s and the ship heading ends with 285.5º.

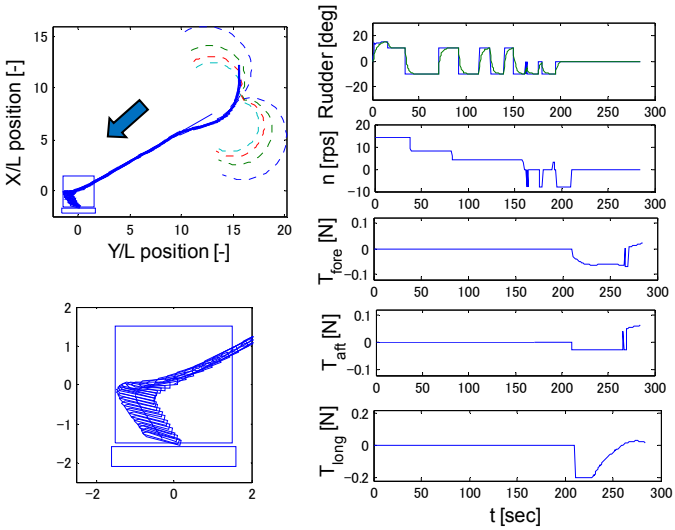

Figure 7.5. Berthing with thrusters, initial heading 180.0º starts from (35m, 47m)

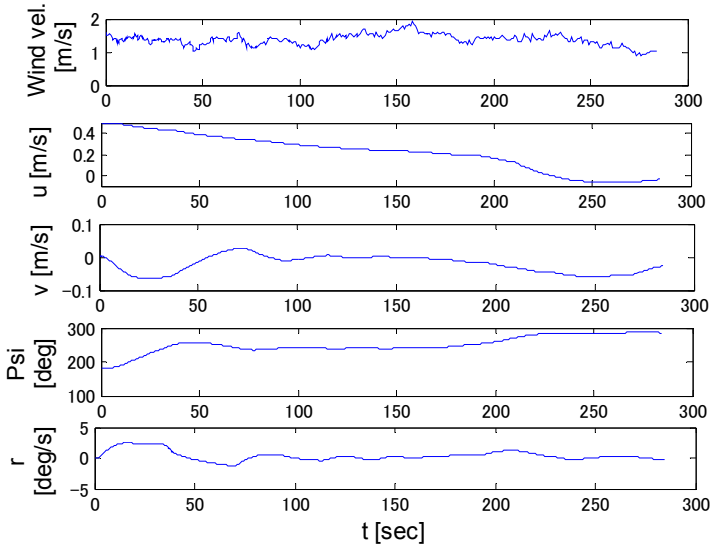

Figure 7.5(cont..). Corresponding details

Figure 7.6 and 7.7 show the results for ship starting with initial heading 220º from two different starting points. Considering Figure 7.6, the controllers for thrusters successfully manage to maintain the ship heading against the wind during execution of the crabbing motion. However, the ship takes a long time to reach the pier as sway velocity is relatively low due to the opposite wind direction and there is barely needed for any longitudinal thruster for position alignment. Here, the ship's final surge velocity is almost zero with sway velocity 0.005m/s and heading 269º.

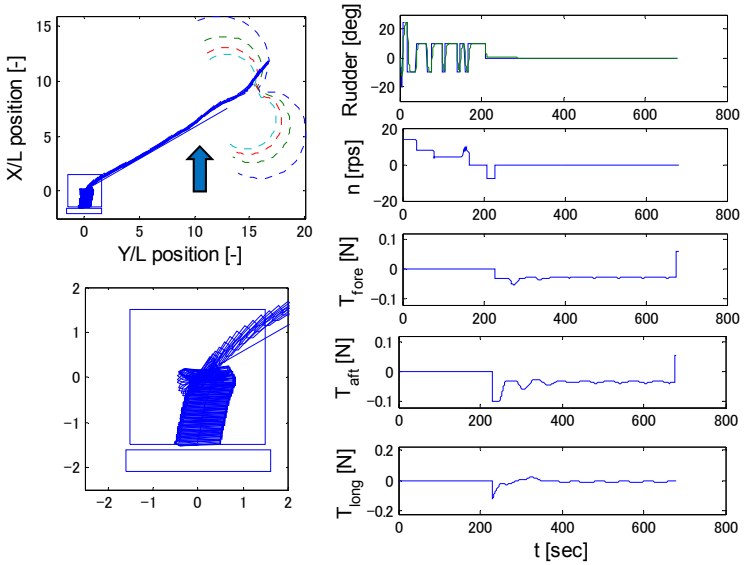

Figure 7.6. Berthing with thrusters, initial heading 220.0º starts from (34m, 49m)

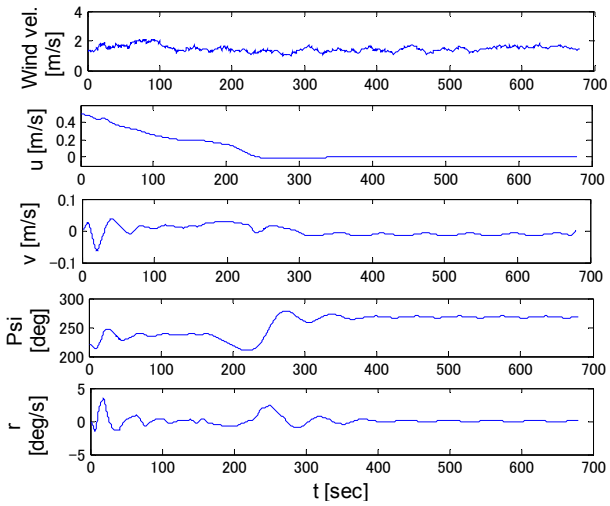

Figure 7.6(cont..). Corresponding details

In Figure 7.7, the following wind is considered again. However, this time an average wind of 1.0 m/s is taken into count. A difference in the final ship state before activating the thrusters' controllers is clearly visible as compared to Figure 7.5 with higher wind velocity. The simulation result shows that the ship is close to the goal point when the thrusts are activated. Therefore, with the activation of reverse longitudinal thrust together with the lateral thrusts, the ship successfully reaches the pier. Here, the final surge velocity is almost zero. However, the sway velocity is -0.01 m/s and heading 272.4º.

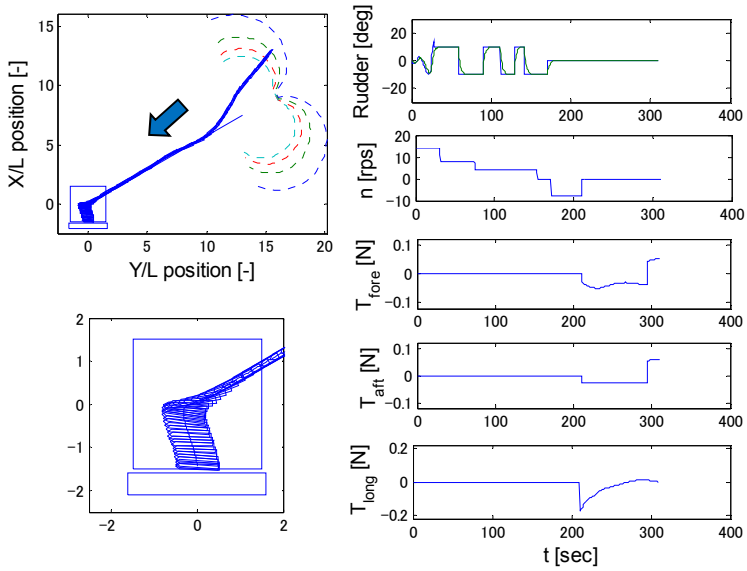

Figure 7.7. Berthing with thrusters, initial heading 220.0º starts from (38m, 46m)

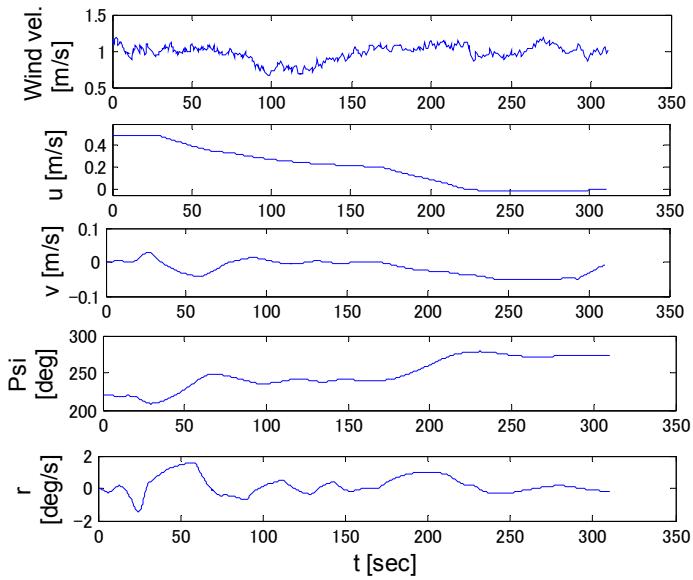

Figure 7.7(cont..). Corresponding details

Figure 7.8 and 7.9 show the result for ship started with heading 270º from two different initial positions. Here, the controllers are tested for two opposite wind directions. Figure 7.8 shows the result for wind from 90º. This brings the ship little bit closes to the pier while activating the thrusters. Therefore, the reverse thrust is needed to adjust the longitudinal position of the ship. Finally, the simulation ends with surge velocity almost zero, sway velocity -0.01m/s and heading angle 273º.

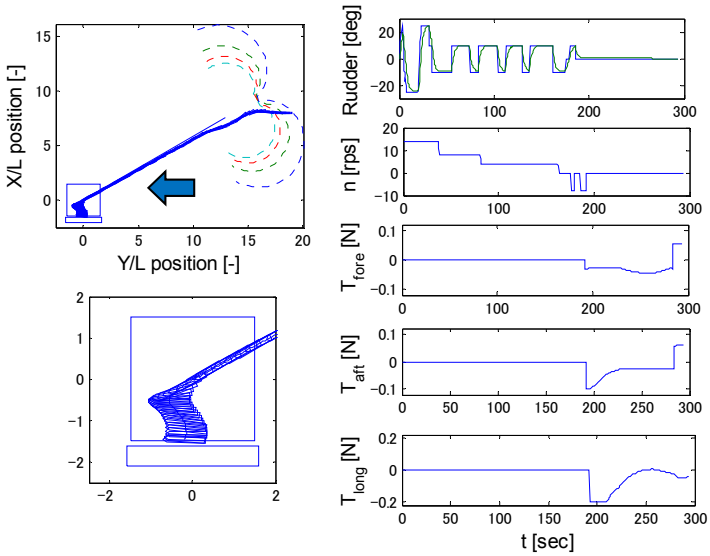

Figure 7.8. Berthing with thrusters, initial heading 270.0º starts from (24m, 56m)

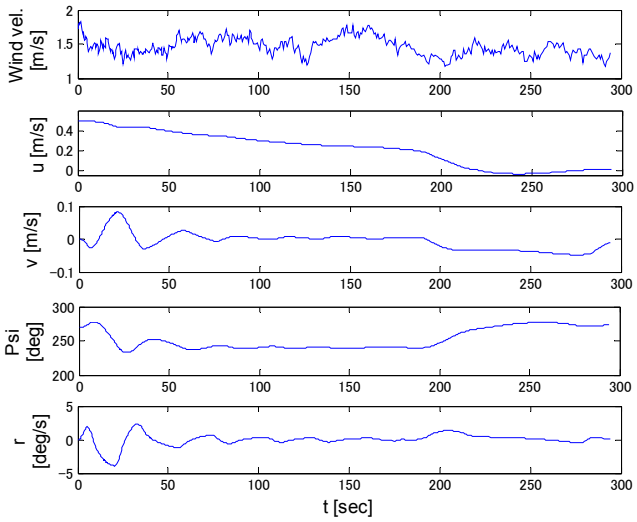

Figure 7.8(cont..). Corresponding details

On the other hand, in Figure 7.9 the wind from 270º stops the ship just after entering the assumed berthing zone. Therefore, the forward longitudinal thrust is needed to move the ship further and at the same time lateral thrusts to align it with pier. Here, the final surge velocity is -0.022 m/s. However, the sway velocity is almost zero with heading 275º.

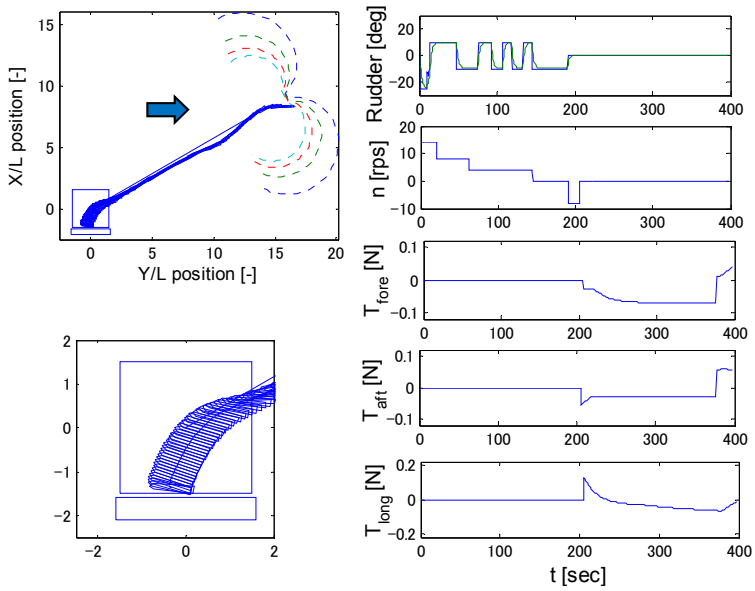

Figure 7.9. Berthing with thrusters, initial heading 270.0º starts from (25m, 48m)

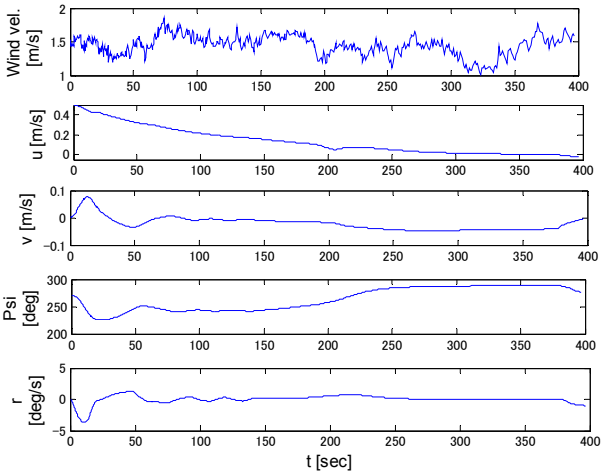

Figure 7.9(cont..). Corresponding details

Figure 7.10 and 7.11 show the result for ship starting with heading 360º from two different initial points. Here, the controller is tested in the wind from 0º and 225º, respectively. Figure 7.10 shows the result where the downward wind tends to generate a lever in a clockwise direction during the crabbing motion. To oppose it, the controller adjusts the lateral thrusts acting on the fore and aft part of the ship to provide a counter lever as well as to continue with the crabbing motion. The longitudinal thruster also plays a vital role for the position alignment of the ship. Finally, the simulation ends with surge velocity -0.055 m/s, sway velocity -0.011 m/s and heading angle 276.5º.

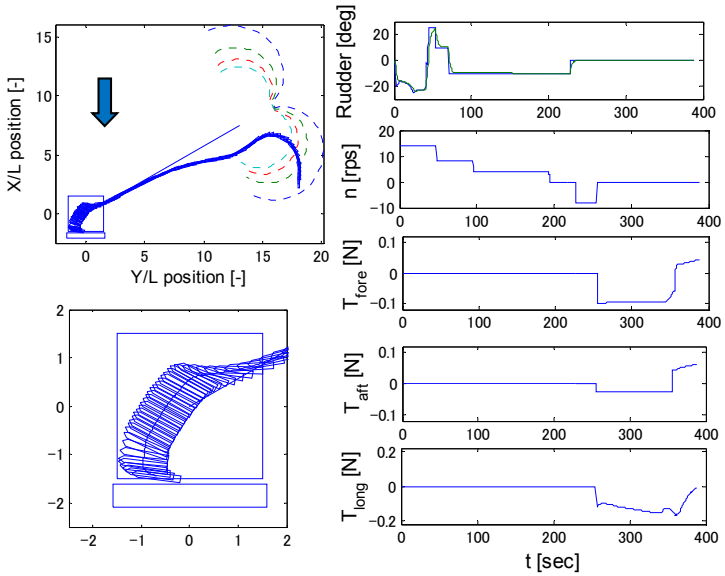

Figure 7.10. Berthing with thrusters, initial heading 360.0º starts from (8m, 54m)

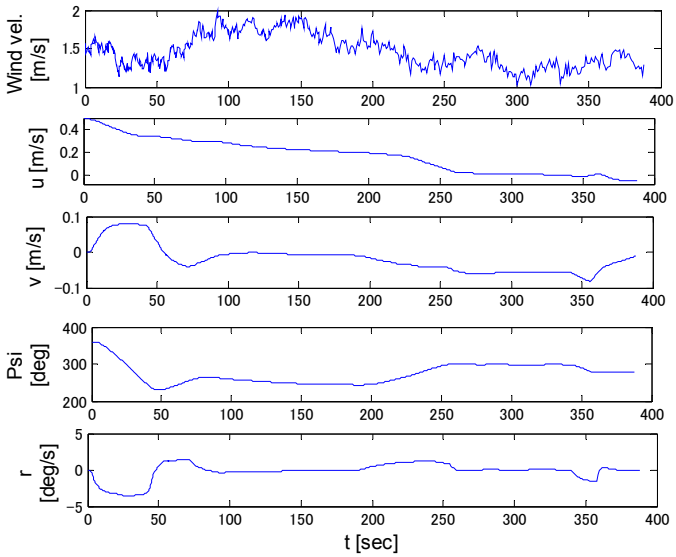

Figure 7.10(cont..). Corresponding details

Figure 7.11 shows the result for wind almost opposing to the straight running along the imaginary line. Therefore, during reversing the surge velocity drops to 0.05 m/s before crossing the berthing goal point. Then, the thrusters are activated to guide it up to the actual pier with almost zero longitudinal thrust value. Finally, the ship stops with almost zero surge and sway velocity and heading 277.6º.

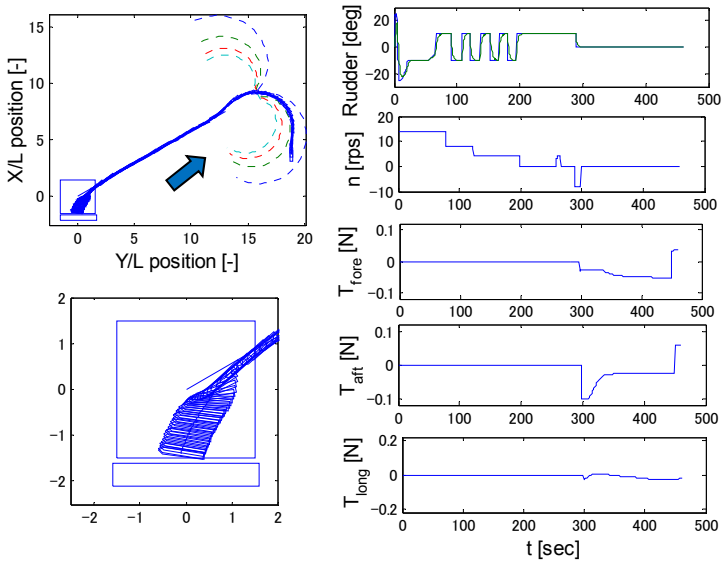

Figure 7.11. Berthing with thrusters, initial heading 360.0º starts from (11m, 57m)

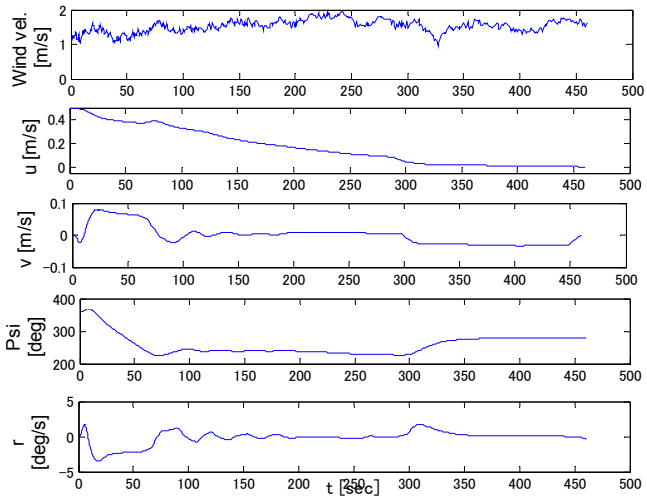

Figure 7.11(cont..). Corresponding details

7.2 Simulations with Experiment End Conditions

The PD controlled thrusters are also tested for different experiment end conditions. First row of Figure 7.12 shows the experiment result that belongs to group 2 for LHS approach. Here, the ship deviates due to sudden gust wind and stops just before entering the berthing zone. Then, by considering the final state of that experiment as initial conditions for the controller, the simulation is done as shown in the second row of Figure 7.12.

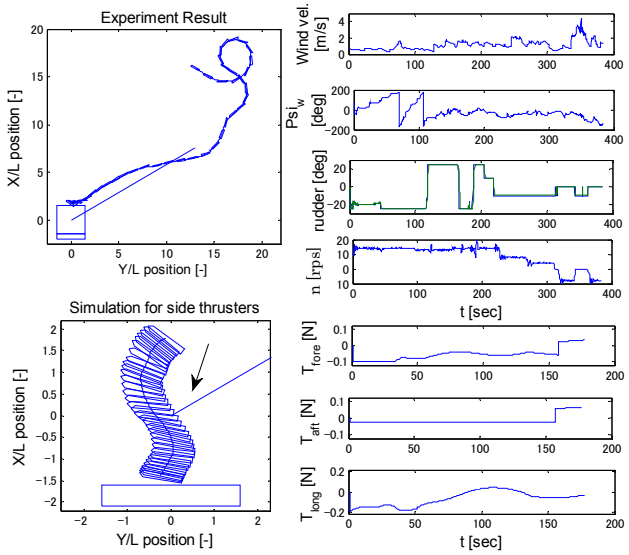

Figure 7.12. Simulation with experiment end conditions, initial heading 360.6º for thrusters

Here, the simulation is done for the ship's initial heading 360.6º (found as final heading after the experiment). Other initial conditions are also kept same as found in experiment end conditions. Maximum allowable wind is considered from an average direction as found in that experiment. Since the ship stops outside the desired berthing zone, the controller needs to maintain the crabbing motion for a long lateral distance. Moreover, it also needs to correct the large heading error. However, the simulation shows satisfactory result and it ends with almost zero surge and sway velocity with final heading 280º.

First row of Figure 7.13 shows the experiment result where the ship comes closer to the pier with final heading 250.8º. From that state, the simulation for the thrusts is investigated under maximum wind velocity and average wind direction as found in the experiment. Such simulation result is shown in the second row of Figure 7.13. Finally, the ship stops with almost zero surge and sway velocity with final heading 274º.

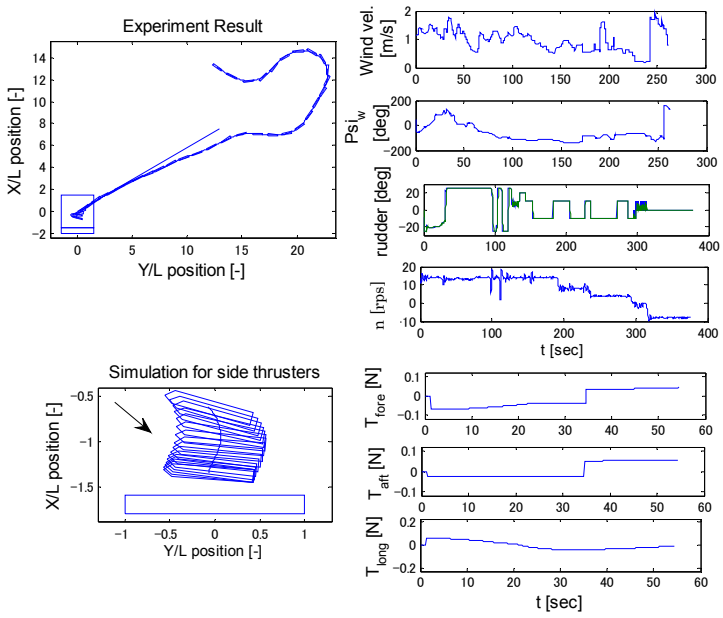

Figure 7.13. Simulation with experiment end conditions, initial heading 250.8º for thrusters

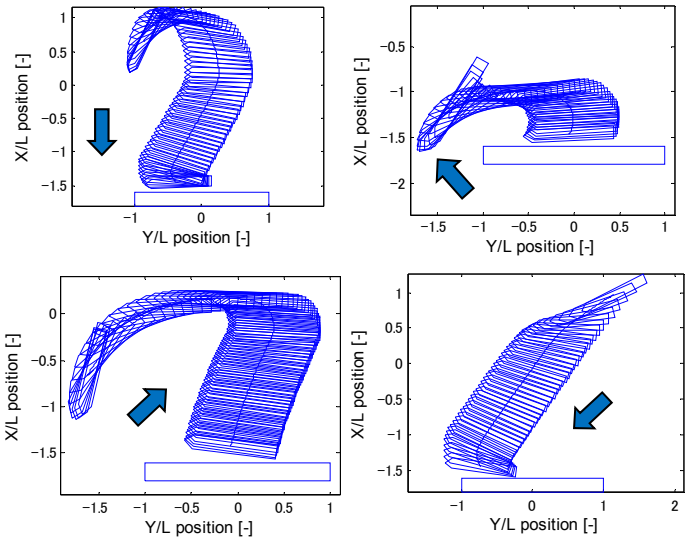

Figure 7.14. Simulations start with different experiment end conditions

Figure 7.14, shows more simulation results tested for experiment end conditions where the ship has different heading angles for corrections as well as different endpoint. Wind from different directions is also investigated. Irrespective of that, the PD controller seems effective enough to guide the ship successful up to the pier in each case. Only for following wind, it poses some difficulties for heading angle correction.

Chapter 8 : WAYPOINT CONTROLLER

In this thesis, the ship with particular heading is expected to start its berthing approach from a desired point on virtual window. Several simulations and experiment results also show that the controller works effectively while starting from an unexpected point. However, starting from its nearby desired point is always preferable to guarantee the successful berthing. To do this, it is necessary to follow a planned path for every ship to approach the set point on virtual window. This planned path may include both course changing and path keeping. Therefore, proper timing of the rudder angle change as well as to take the counter rudder to overshoot the existing sway velocity and yaw rate is always a crucial matter for the ship operators. To assist the ship operators regarding this matter, a number of proposals exits based on PID controller (39) or optimum regulator. However, in this chapter, a Fuzzy reasoned waypoint controller is discussed. The control laws used here is similar to collision avoidance rules mentioned by Hasegawa (24, 25, and 26). However, instead of collision risk, the nearness is reasoned by the fuzzy controller.

8.1 Navigation Path Planning

Navigation path planning is done based on the given set points called waypoints (WP) to be passed. These points are usually selected at the turning points. Then, the path is planned normally directing to the next point (WP) to be passed. However, near the turning point, the fuzzy reasoning system will decide to choose the appropriate course defined by the next two WPs as following equation:

$$\psi_I = \psi_1 + (\psi_2 - \psi_1) * CDH \tag{8.1}$$

where, ψ_I is order of course change, ψ_1 is course of the shortest path to the next WP, ψ_2 is course of the shortest path to the second next WP and CDH is the reference degree to the second next WP ($0 \le CDH \le 1$), calculated by fuzzy.

Figure 8.1 shows the course changing command near a course changing point (WP).

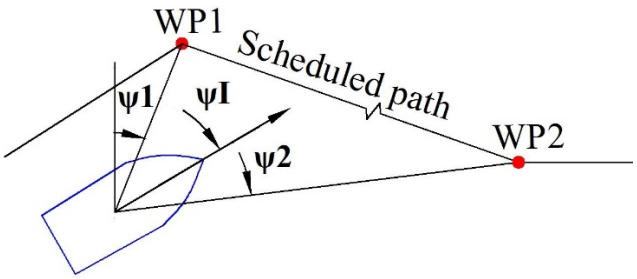

Figure 8.1. Course command near a course changing point

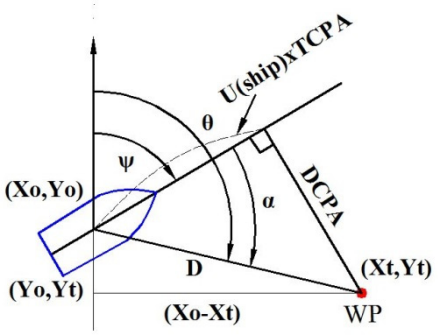

Figure 8.2. Bearing relation between ship and waypoint

In this thesis, to judge the nearness of the waypoint, TCPA (time to closest point of approach) and DCPA (distance of the closest point of approach) are used for fuzzy reasoning. Figure 8.2 shows the bearing relationship between the ship and waypoint. According to the figure, the distance between the ship and nearest waypoint is calculated as follows:

$$D = \sqrt{((Xo - Xt)^2 + (Yo - Yt)^2} \tag{8.2}$$

Then, the following calculations are done to get the bearing angle of waypoint from the ship.

$$\theta = a\tan 2\frac{(Yt - Yo)}{(Xt - Xo)} \tag{8.3}$$

$$\alpha = \theta - \psi \tag{8.4}$$

where, ψ is ship heading, θ is encountering angle of way point from vertical axis and α is bearing angle of waypoint from the ship. Here, if the value of ψ, θ or α becomes negative, then 2π is added to make to them positive.

Finally, DCPA and TCPA are calculated using the following two equations.

$$DCPA = D\left|\sin\alpha\right| \tag{8.5}$$

$$TCPA = \frac{D\cos\alpha}{U_{ship}} \tag{8.6}$$

Another important point to be considered is the scale effect. There should be some difference on the nearness between a large ship and a small one. Therefore, the following equations are used for non-dimensionalised TCPA and DCPA. The nearness is then reasoned from $DCPA'$ and $TCPA'$ instead of *DCPA* and *TCPA*.

$$DCPA' = \frac{DCPA}{L} \tag{8.5}$$

$$TCPA' = TCPA\frac{U_{ship}}{L} \tag{8.6}$$

Membership function of $TCPA'$, $DCPA'$ and *CDH* are given in Figure 8.3 and the control rules to reason *CDH* is shown in Table 8.1. Here, the rules are considered similar to collision avoidance, i.e. "if *DCPA* is very short and *TCPA* is also very short, then *CDH* is very big". It means, if the ship is very far from second next waypoint, then the command course will consider only for the next waypoint. However, with the increase of nearness the command course will modify by considering both next and second next waypoint.

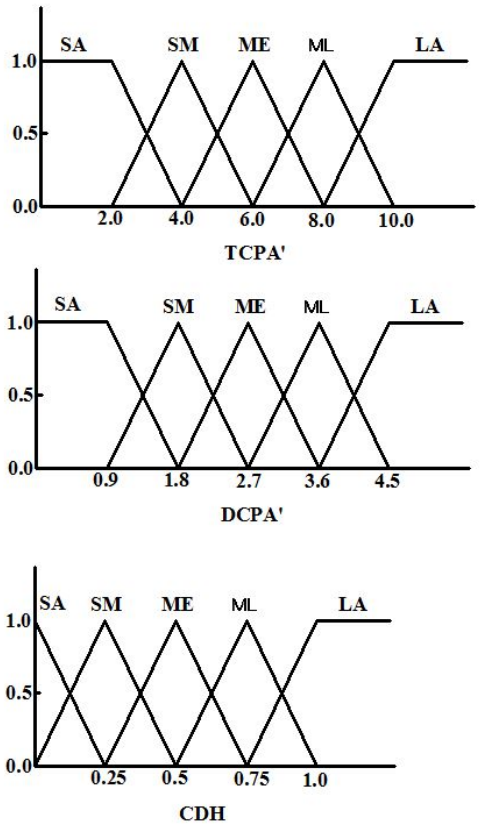

Figure 8.3. Membership functions for course changing algorithm

Table 8.1. Control rules for course changing algorithm

		TCPA’				
		SA	SM	ME	ML	LA
DCPA’	SA	LA	ML	ME	SM	SA
	SM	ML	ME	SM	SA	SA
	ME	ME	SM	SA	SA	SA
	ML	SM	SA	SA	SA	SA
	LA	SA	SA	SA	SA	SA

After deciding the appropriate course by fuzzy reasoning, the course is corrected using a PD controller. Equation 8.7 shows the PD controller used here to correct the heading.

$$\delta_{order} = K_p(\psi_I - \psi) - K_d\dot{\psi}$$
$$\Rightarrow if \begin{cases} \delta_{order} \geq 25^0, \delta_{order} = 25^0 \\ \delta_{order} \leq -25^0, \delta_{order} = -25^0 \end{cases} \quad (8.2)$$

where, ψ_I is desired heading calculated by fuzzy reasoning, ψ is ship's current heading, $\dot{\psi}$ is the yaw rate, K_P is proportional gain and K_D is differential gain.

8.2 Simulation Results

Using the waypoint controller, simulations are done for different sets of waypoints. These are illustrated in the following figures. Here it is noted that, the waypoint controller considers next and second next waypoints one at a time. Therefore, one extra waypoint is always needed to go up to the desired set goal point.

Figure 8.4 shows the result for the set of waypoints that is placed at an angle -45º. Initially, considering the nearness of the waypoints, fuzzy reasoned desired course does not change much. Therefore, the command rudder is also zero. Soon after that, desired heading starts to change gradually and the PD controller decides to take rudder. The maximum nearness is judged by fuzzy after 80 sec and the PD takes its maximum allowable rudder. Then, fuzzy reasons the desired heading for the next pair of waypoint. Since this pair is set on the same line, the ship finally merges with that line. The simulation is done under average gust wind of 1.5 m/s from 45º.

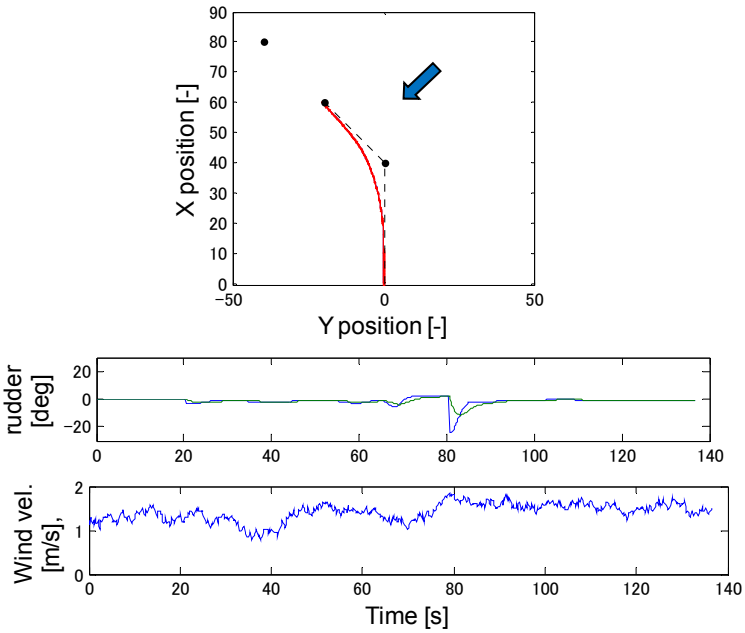

Figure 8.4. Waypoints set at -45º, controller under wind of 1.5m/s from 45º

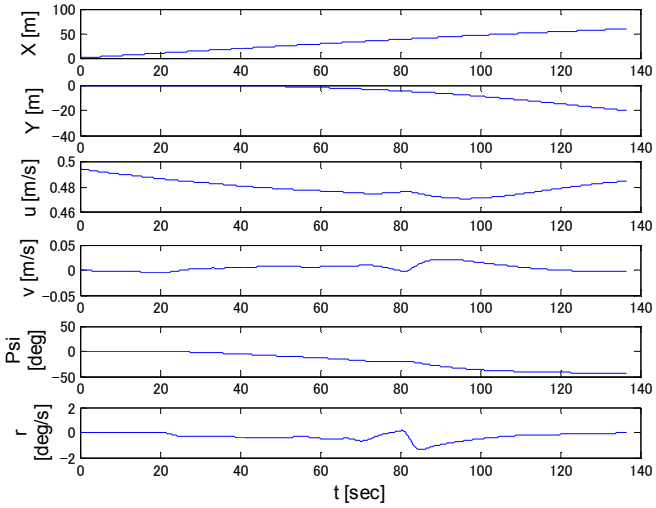

Figure 8.4(cont..). Corresponding details

Figure 8.5 shows the result for the set of waypoints that is placed at an angle on 60º. Since the first waypoint has the same coordinate as mentioned in Figure 8.4, initially the reasoned desired heading remains similar to initial heading. Then, similar to Figure 8.4, depending on the nearness the desired heading is modified and the PD controller corrects the existing error under wind disturbances from 270º. Finally, the ship aligns with the line passes through the next pair of waypoints.

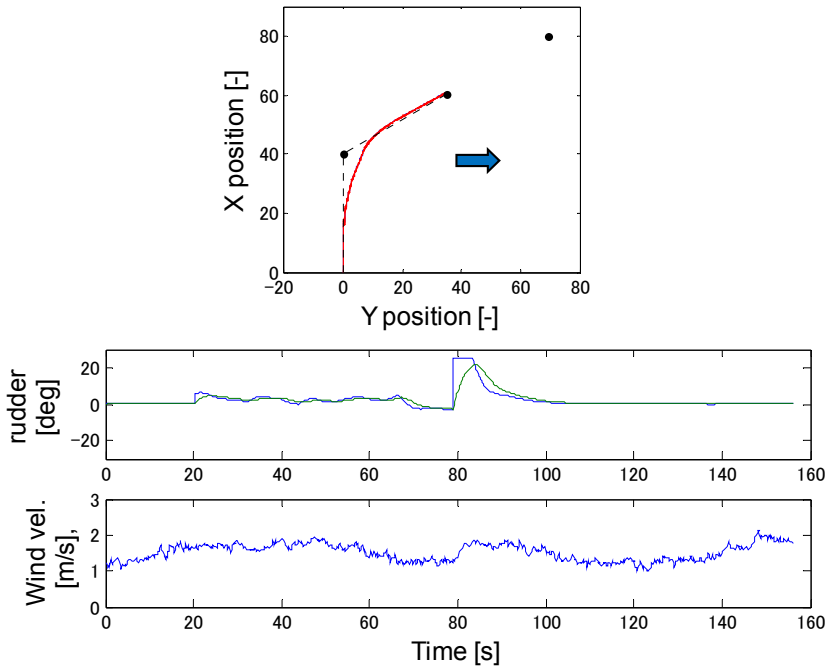

Figure 8.5. Waypoints set at 60º, controller under wind of 1.5m/s from 270º

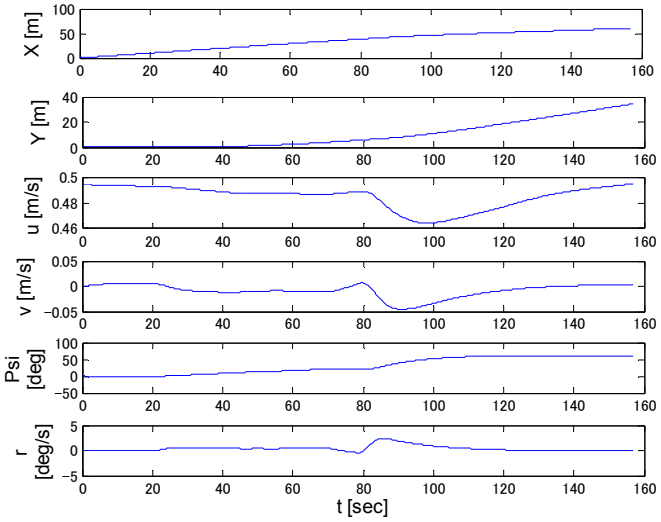

Figure 8.5(cont..). Corresponding details

Figure 8.6 shows the result for the set of waypoints that is placed to execute both starboard and port turn of the ship. Here, fuzzy reasons the desired heading and PD controller decides the rudder command. The resulting trajectory seems quite satisfactory. The simulation is considered under wind of 1.5 m/s from 135º.

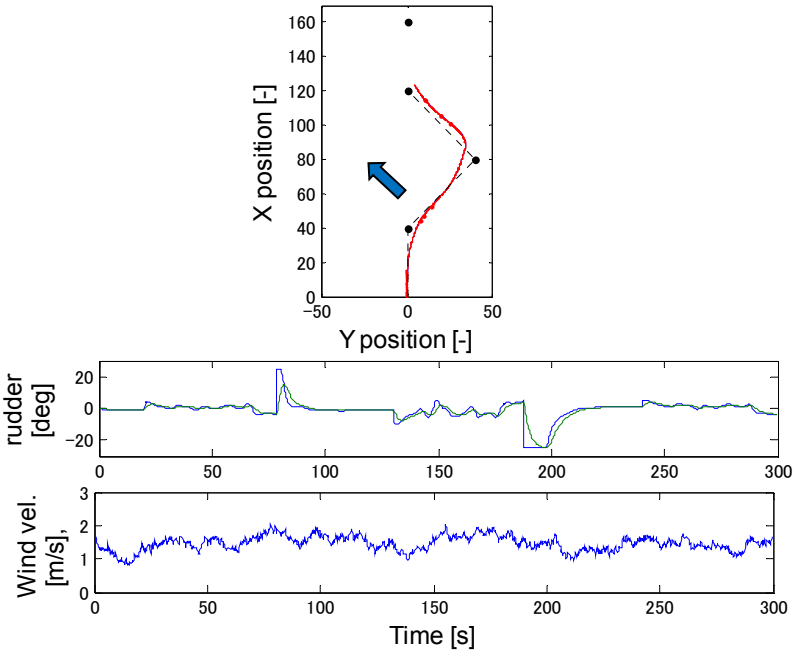

Figure 8.6. Waypoints set to starboard and port turn, controller under wind of 1.5m/s from 135º

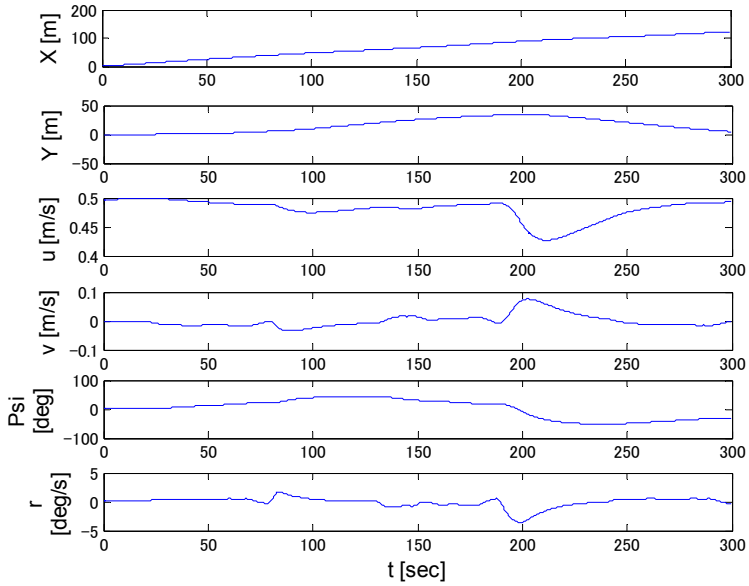

Figure 8.6(cont..). Corresponding details

After getting promising result, the controller is tested for bringing the ship from its current state to a set point on virtual window. Considering the experiment field, the controller is planned to guide the ship from the pier to the point on virtual window following some pre-set waypoints. So, it will be used instead of manually driving the ship up to its starting point. Before doing the experiments, simulations are done to

justify the effectiveness of waypoint controller. Figure 8.7 and 8.8 show such results.

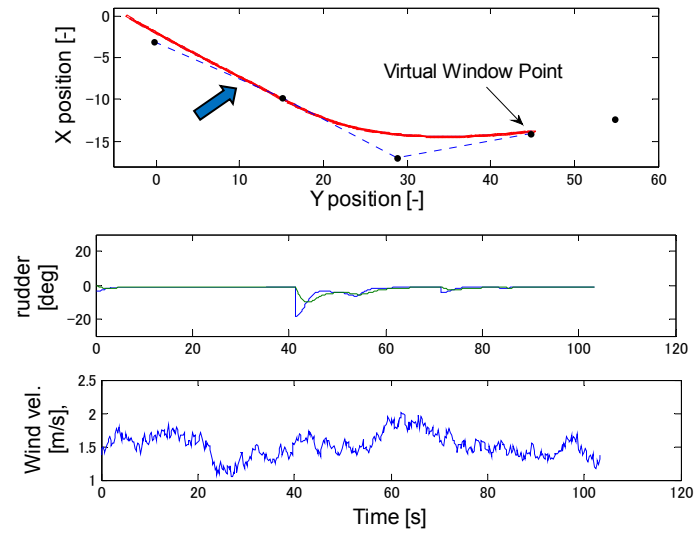

Figure 8.7. Waypoint controller, initial heading 120º for set point on virtual window (-14.15m, 44.82m)

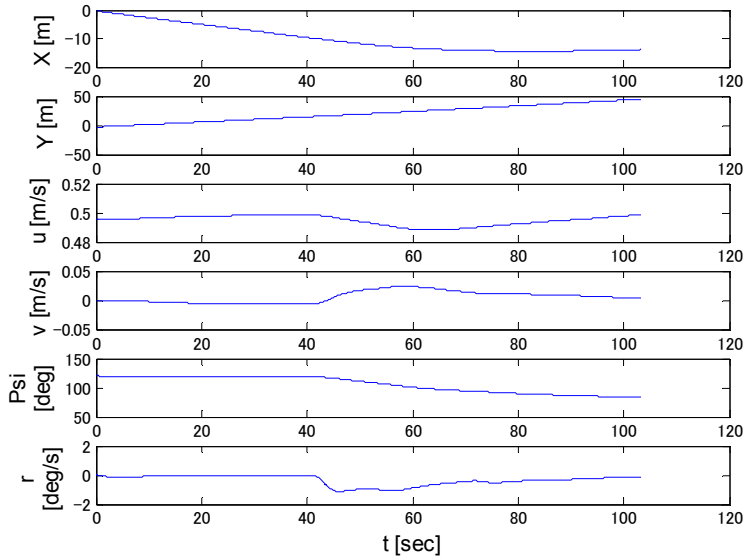

Figure 8.7(cont..). Corresponding details

Considering Figure 8.7, the waypoints are set for a target point desired for heading 50º on virtual window for rudder constraint ±20º. The initial heading to start the simulation is set as 120º. Then, depending on the nearness of the waypoints, the desired heading is determined and the rudder command is activated. Here, the first two

waypoints are set in a line to make the ship heading parallel to it. After passing the second waypoint, the ship will adjust its course and try to pass nearby of set goal point. The last two waypoints are again set in one line to make the final heading parallel to it. Although the figure shows the ship successfully attains the nearby goal point, there remains some error in the heading. Such error can be fixed by adjusting the position of last two waypoints. The simulation is done for wind 1.5 m/s from 225º.

Figure 8.8 shows the result for another set of waypoints. The simulation is done for initial heading 130º under wind of 1.5 m/s from 315º. In the following wind, the PD controller compensates the heading error from the beginning. Then, it changes the course gradually depending of desired course as determined by fuzzy reasoning. Here the ship appears very close to the target point. However the error in ship heading remains.

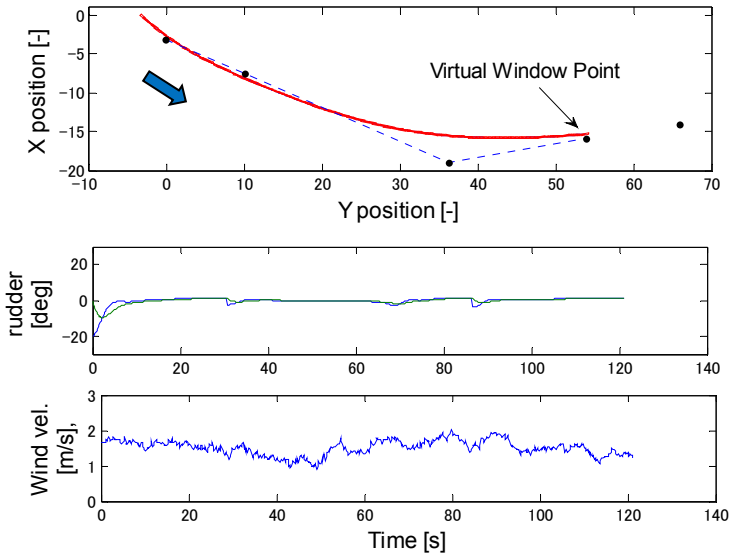

Figure 8.8. Waypoint controller, initial heading 130º for set point on virtual window (-15.81m, 53.8m)

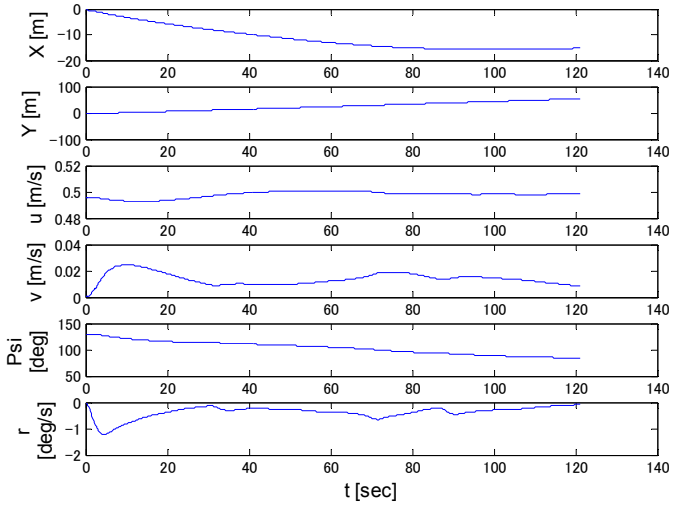

Figure 8.8(cont..). Corresponding details

The ANN-PID controller proposed in this thesis, is already verified for its robustness. Therefore, even some error remains in heading as well as position after the guidance by the waypoint controller, the ANN-PID controller is expected to deal with it. Therefore, such compatibility is then tested for automatic ship berthing experiment.

8.3 Compatibility Test for Ship Berthing Experiment

Experiments are done for different target points on virtual window considering the ship's different initial heading. The compatibility is then tested for the waypoint controller and ANN-PID controller for berthing. The following figures show such illustrations.

Figure 8.9 shows the result for the ship started with initial heading 69.9º. Then, a set of waypoints was used to guide it using the waypoint controller up to an arbitrary point. The last pair of waypoints was aligned to make the ship heading 50º. Using the fuzzy reasoned waypoint controller, finally the ship succeeded to reach close to the target goal with heading 47.2º. After crossing the y-coordinate of the set goal point, the ANN-PID controller was activated for berthing by taking the current state as input for it. Then, the controller guided the ship up to the pier by providing necessary command for rudder and propeller revolution outputs, respectively. The experiment ended with surge

velocity 0.05m/s and heading 252.8º.

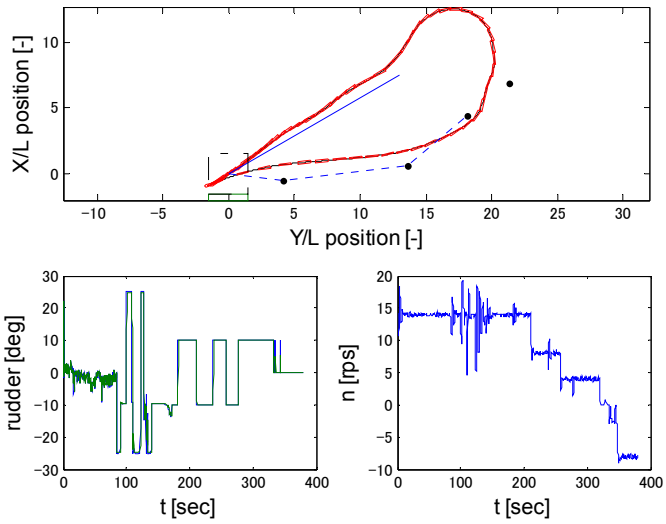

Figure 8.9. Target (54.52m, 13.22m) with heading 50º, Achieved (54.45m, 11.29m) with heading 47.2º

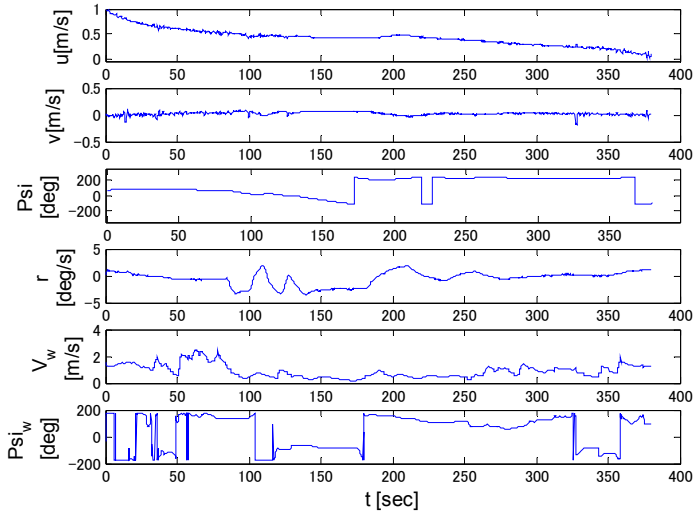

Figure 8.9(cont..). Corresponding details

Considering Figure 8.10, same set of waypoints is tested for initial heading 83.9º. With this initial heading, the ship followed the waypoints smoothly and succeeded to reach the goal point with less than one-meter accuracy. Then, the ANN-PID was activated and the ship started its starboard turn to merge with the imaginary line. At last, sudden gust during idling and reversing stages distracted the ship from its actual course

and the experiment ended with surge velocity 0.035m/s and heading 277.5º.

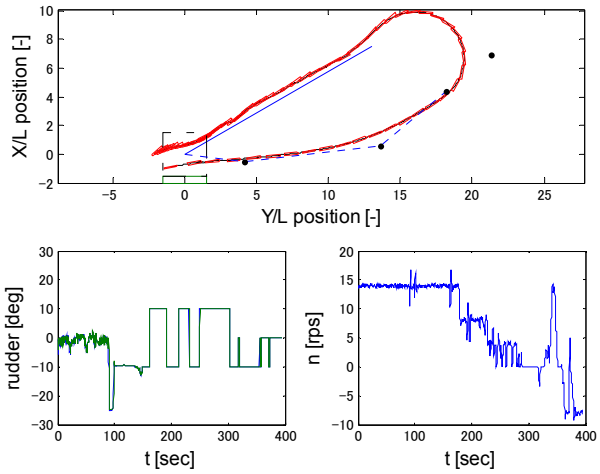

Figure 8.10. Target (54.52m, 13.22m) with heading 50º, achieved (54.45m, 12.31m) with heading 46.1º

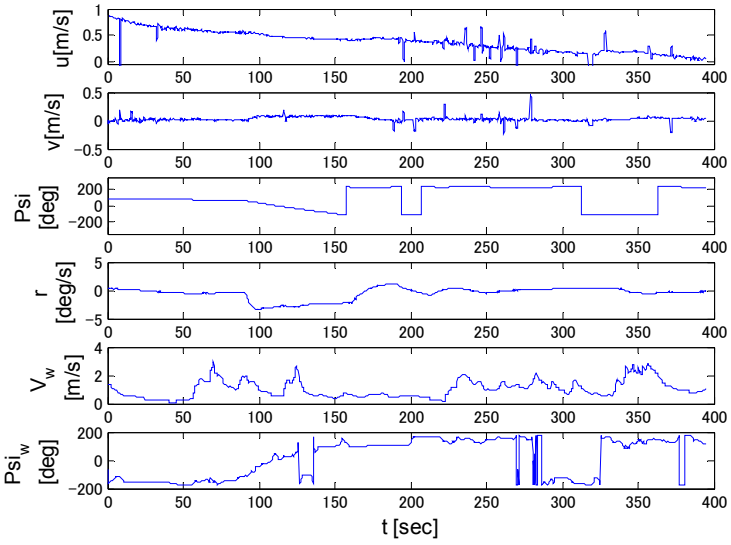

Figure 8.10(cont..). Corresponding details

Figure 8.11 shows the result for a new set waypoint tested for initial heading 69.2º. Due to having an improper heading angle, the ship was able to follow the waypoints at the beginning. However, later on it manages to pass nearby the set goal point. The error in the ship heading and the position was quite reasonable. From that state, the ANN-PID controller started to guide the ship up to the desired berthing zone. The final surge

velocity was 0.018m/s and the heading was 218.8º.

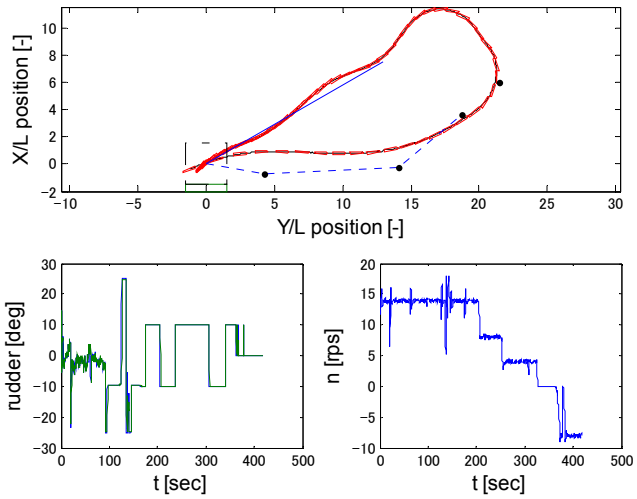

Figure 8.11. Target goal (56.15m, 10.97m) with heading 50º, achieved (55.93m, 9.47m) with heading 56.65º

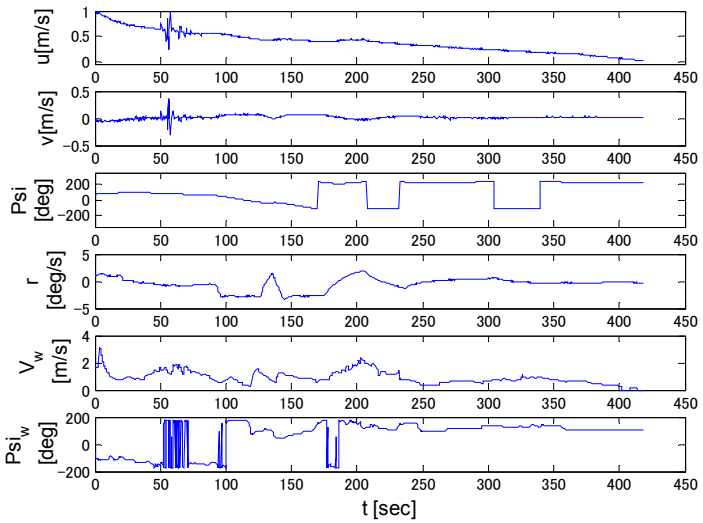

Figure 8.11(cont..). Corresponding details

Figure 8.12 shows the set of waypoints for a target point on virtual window that is desired for heading 50º on ±20º. During the experiment, the ship stared with its initial heading 58.5º. Therefore, similar to Figure 8.8, the controller took large distance and time to minimise the heading error. Finally, the ship reached close to the target pint with reasonable heading. From that state, the ANN-PID controller guided the ship for

automatic berthing and stopped it within the assumed successful zone. The final surge velocity was -0.02 m/s and heading was 296.8º.

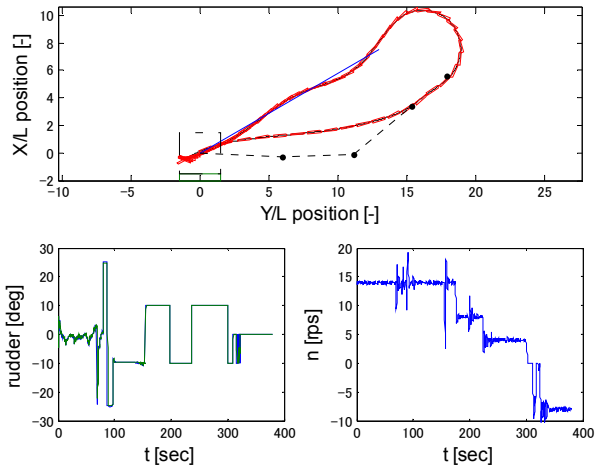

Figure 8.12. Target point on virtual window (45.89m, 10.16m) with heading 50º, achieved (45.83m, 10.13m) with heading 51.61º

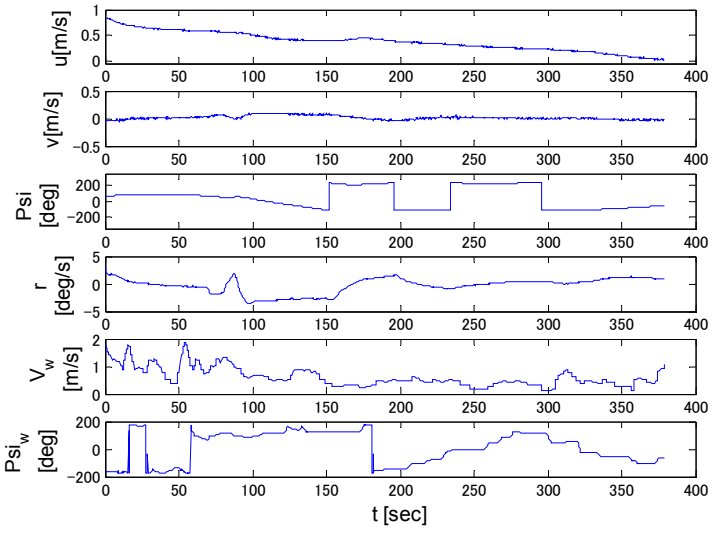

Figure 8.12(cont..). Corresponding details

Figure 8.13 shows another set of waypoints for heading 50º on virtual window for rudder constraint ±15º. Ship started with heading 58.5º was then tested for the auto guidance using the waypoint controller. Here, due to the large gap between the current and desired heading, the controller took some time to adjust the course following the

waypoint. At last, it reached close to the set goal with reasonable heading. After that, similar to other figures the ANN-PID was used for automatic ship berthing. In this experiment, the final surge velocity was 0.035m/s and heading was 277º.

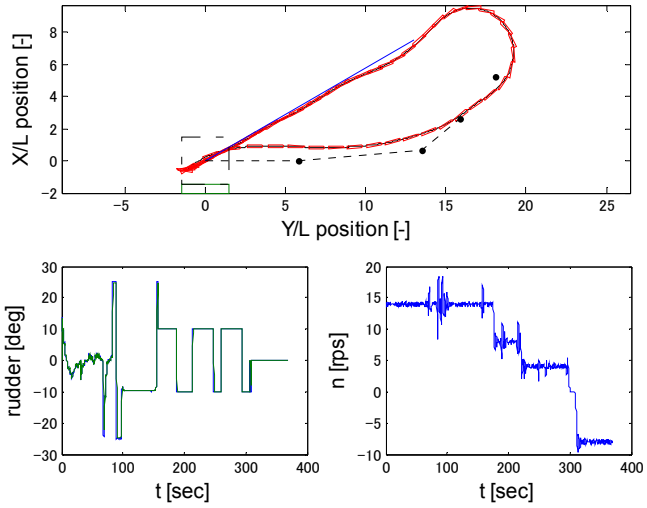

Figure 8.13. Target point on virtual window (47.52m, 7.91m) with heading 50º, achieved (47.74m, 8.24m) with heading 51.01º

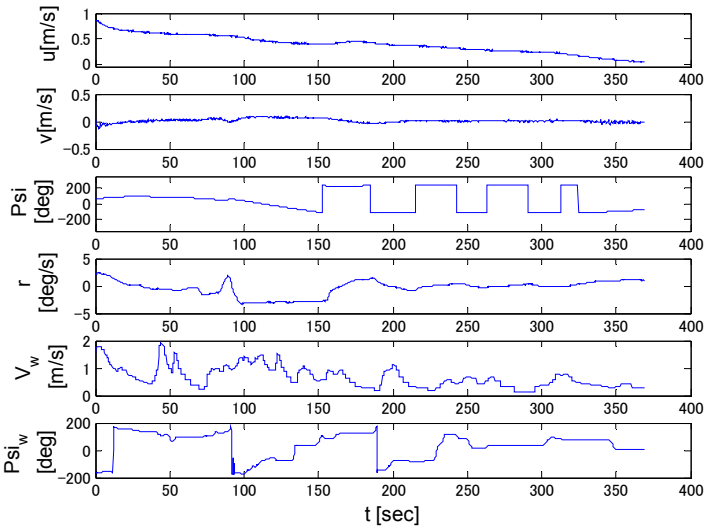

Figure 8.13(cont..). Corresponding details

Finally, the mentioned simulation and experiment results establish a clear idea about the compatibility of the waypoint controller and ANN-PID controller for total berthing process.

Chapter 9 : CONCLUSIONS & FUTURE WORKS

9.1 Conclusions

This thesis starts with an intention to bring automatic berthing in real ship operation. To do that, creating consistent teaching data for better learning of ANN controller is considered as a prime concern. Using nonlinear programming (NLP) method, the problem is solved and a set of consistent teaching data is ensured that contains not only variations in ship heading and starting point but also in operating rudder angle. Then, instead of centralised controller, two separate ANNs are trained for rudder and propeller revolution outputs. Further on, simulations and experiments are conducted for the Esso Osaka model ship. The behaviour of the network for rudder is analysed and automatic side thrusters are discussed for final alignment of the ship with the actual pier. Waypoint controller for guiding the ship up to the desired starting point is also considered. The major concluding remarks for each chapter are summarised as follows:

In Chapter 2, to predict the hydrodynamic behaviour of the subject ship, a modified version of MMG model is used. To validate the model for speed prediction, speed tests are performed for different propeller revolution and compared with the simulation results. Although the experiment results tend to diverge with the increment of propeller revolution, such divergence is well within acceptable limit until half ahead i.e. propeller rps 14. Turning tests are also performed to validate the model for course changing prediction. The tests are performed and compared with the simulation results for four different rudder angles, considering both port and starboard turn. These four specific rudder angles are selected as constraints for the construction of virtual window. Each of such comparison includes not only the turning trajectory, but also non-dimensionalised surge velocity and yaw rate distribution. At last, satisfactory results are ensured based on such comparisons.

In Chapter 3, a new way of creating teaching data using nonlinear programming (NLP) method is proposed to ensure consistency. Then, by using the technique of repeated optimisation, a concept named ‘virtual window’ is introduced. The concept of

virtual window enables the teaching data to include not only variations in the ship's initial heading angle and position but also in operating rudder angle. In order to consider wind disturbances during berthing, gust wind instead of uniform wind takes into account. During low speed running along the reference line after course changing, PID controller with rudder restriction ±10º is proposed to cope with the existing wind disturbances. Then, to learn the complex input-output relationship, two separate double hidden layered feed-forward nets are used instead of centralised one for rudder and propeller revolution outputs, respectively with minimum MSE value. In this thesis, the trained network for rudder after course changing is supposed to be followed by a feedback PID controller for track keeping. Thus, in terms of rudder command, it would be a combined effort of ANN-PID controller. On the other hand, proper speed control throughout the whole berthing process is only decided by the separately trained ANN for propeller revolution.

In Chapter 4, the proposed ANN-PID controller is verified to prove its combined effectiveness for both teaching and non-teaching data. The controller is tested in completely different situations than used in the training session, where the wind from eight different directions with maximum velocity (1.5 m/s for model and 15 m/s for full scale) is considered. Different gusts for same average velocity are investigated to verify the controller's workability and found satisfactory. In case of severe wind near pier, the ANN-PID controller is again proved by investigating different initial heading angles and positions. To judge the robustness of controller, ship starting from undesired point is tested under different wind disturbances. Here, the starting point is considered as any undesired point on virtual window, middle of virtual window for two different rudder constraints or any arbitrarily chosen point within the constructed virtual window zone. In each case, the ANN-PID controller behaves intelligently. However, some errors remain in the desired ship heading and positing after course changing that are corrected later on by the activated PID controller during low speed running. Therefore, the overall combined effort ensures successful berthing. At last, Monte Carlo simulations are performed to analyse the stability of the closed loop system and success rate while using the proposed controller. Three success indexes are chosen as: non-dimensionalised distance from target goal point, heading error and surge velocity for further analysis.

After getting the satisfactory percentage of success, automatic ship berthing experiment is planned and executed as a next step of this thesis.

Chapter 5 includes the experiment result for both LHS and RHS approaches. Initially, the experiments are done by considering the ship started from its desired points on virtual window. While performing the experiments for the left hand side approach, the ANN has found to behave in some particular ways depending on different initial conditions or wind disturbances. Therefore, the results are gathered in some groups depending on the similarities of network's behaviour or the resulting trajectory pattern. This thesis includes three different groups of experiment results based on current available experiment data for LHS approach. The experiments for the right hand side approach are also conducted with separately trained neural networks. Considering the results, the controller has also found to behave in some particular ways, but different from that of LHS approach. Due to having a windy experiment day, the controller is also tested for its behaviour under the wind beyond the permitted limit. This thesis includes four of such groups where the results belong to each do not guarantee a successful berthing. However, similarities in resulting trajectories are clearly visible. Later on, the experiments are also carried for ship starting from undesired point on virtual window, middle of virtual window for any two rudder constraints and at last from any arbitrary point. Although the experiments are done for unexpected staring points, the controller behaves almost in a similar way as for virtual window points. Most of the experiment results are found successful within the considerable wind disturbance that is 1.5 m/s. However, sudden gusts during step deceleration also alter the original course of the ship.

In Chapter 6, the network's response for rudder angle output is analysed for different initial conditions. The analysis shows that the response of the network for RHS approach is smoother than that of LHS approach. This is probably due to having more varieties of teaching data in RHS approach and thus better learning of the network. The initial surge velocity has found to play no role to alter the ANN's initial behaviour in both LHS and RHS approaches. Therefore, even the initial velocity deceases while switching to auto mode, ANN always takes the expected rudder for its corresponding approach. Although, the angle taken by ANN increases with decrease in surge velocity.

For LHS approach, there is always a range of yaw rate for which ANN takes the port rudder for any existing sway velocity. This range of yaw rate gradually shifts towards the right with the increment of sway velocity. For RHS approach, the network for rudder output does not have any pulsating responses like in LHS approach. Therefore, for small initial sway velocity, ANN always takes the starboard rudder to oppose the possible initial yaw rate. With the increment of sway velocity, the effect of having sway velocity dominates and it pulls the curve towards downside. This makes the ANN to take the expected port rudder for small value of initial yaw rate. However, with the increment of such initial sway velocity, the curve continues to be pulled down and shifted towards the left hand side.

In Chapter 7, since the existing ANN-PID controller is designed to stop the ship at some safe distance, the newly developed PD controlled thrusters are discussed under wind disturbances to couple with the existing controller to finally aligning the ship with pier. In order to ensure proper control of the crabbing motion, two sides and one longitudinal thruster are proposed for Esso Osaka, single rudder-single propeller ship. Then, the simulations are done to test the compatibility of these two controllers for ship's different initial headings and arbitrary starting points. Maximum allowable wind from eight different directions is considered to judge its effectiveness. Several experiment results are tested with their end conditions to judge the capability of the developed controller to finally aligning the ship with actual pier. Although most cases ensure successful berthing, the following wind possesses some difficulties in heading error correction.

In Chapter 8, a waypoint controller based on fuzzy reasoning is discussed to guide the ship from its current state to a set point on virtual window. Initially, different set of waypoints is tested. Then, the experiments are carried out for some pre-set waypoints and different initial headings. The results show that the ship approaches the goal point with reasonable accuracy and then the ANN-PID controller is activated to guide it up to the pier under existing wind disturbances.

9.2 Future Works

The proposed ANN-PID controller is tested for Monte Carlo simulations and found 91.45% success for arbitrarily chosen samples. During such investigation, some cases are found when the controller confuses to guide the ship and thus starts to rotate it repeatedly. This is due to some bugs that remain during training the network. However, it is possible reduce the percentage of unsuccessful cases by including those initial headings and stating positions into the teaching data and train the network again. This would be done as a future work of this thesis.

The PD controlled side thrusters are tested in simulations only. Therefore, using air fans attached on board, experiments for the developed PD controller would be possible in future to validate it with the exiting ANN-PID controller as a final approach to berth.

BIBLIOGRAPHY

1. Yamato, H. *et al*. September, 1990. Automatic Berthing by Neural Controller. *Proc. Of Ninth Ship Control Systems Symposium*, vol. 3, pp.3.183-201.
2. Fujii, T. and Ura, T. 1991. Neural-Network-Based Adaptive Control Systems for AUVs. *Journal of Engineering Applications of Artificial Intelligence*, vol. 4, pp.309-318.
3. Cui, X. *et al*. 1992. Application of Neural Networks to Temperature Control in Thermal Power Plants. *Journal of Engineering Applications of Artificial Intelligence*, vol. 5, pp.527-538.
4. Lee, T. H. *et al*. 1994. A Neural Network based Model Reference PID-like Controller for Process Control. *Journal of Engineering Applications of Artificial Intelligence*, vol. 7, pp.677-684.
5. Zeng, G. M. *et al*. 2003. A Neural network Predictive Control System for paper Mill wastewater Treatment. *Journal of Engineering Applications of Artificial Intelligence*, vol. 16, pp.121-129.
6. Zhau *et al*. 2009. Neural Network Model-based Automotive Engine Air/Fuel Ratio Control and Robustness Evaluation. J*ournal of Engineering Applications of Artificial Intelligence,* vol. 22, pp.171-180.
7. Aoyama, A. *et al*. 1995. A Fuzzy Neural-Network Approach for nonlinear Process Control. *Journal of Engineering Applications of Artificial Intelligence*, vol. 5, pp.486-498.
8. Di, L. *et al*. 2001. Neural-Network-based Self-Organized Fuzzy Logic Control for Arc Welding. *Journal of Engineering Applications of Artificial Intelligence*, vol. 14, pp.115-124.
9. Ponce, A.N. *et al*. 2004. Neural Networks for Self-tuning Control Systems. *Journal of Acta Polytechnica Hungarica*, vol. 44, pp.49-52
10. Zilkova, J. *et al*. (2006). Nonlinear System Control Using Neural Networks. *Journal of Acta Polytechnica Hungarica*, vol. 3, pp.85-94.
11. Zhang, S. and Ren, G. September, 2006. Design of Robust Fuzzy Controller for Ship Course-Tracking based on RBF Network and Backstepping Approach.

Journal of Marine Science and Application, vol. 5, No. 3, pp.05-10.

12. Liu, C. *et al*. September, 2014. Trajectory Tracking of Underactuated Surface Vessels based on Neural Network and Hierarchical Sliding Mode. *Journal of marine Science and Technology*. DOI: 10.1007/s00773-014-0285-y
13. Yang, Y. *et al*. October, 2014. Robust Adaptive NN-Based Output Feedback Control for a Dynamic Positioning Ship Using DSC Approach. *Science China, Information Sciences*, vol. 57, pp.102803:1-102803:13.
14. Hasegawa, K. and Kitera, K. September, 1993. Automatic Berthing Control System using Network and Knowledge-base. *Journal of Kansai Society of Naval Architects of Japan*, vol. 220, p.135-143. (in Japanese)
15. Im, N.K. and Hasegawa, K. September, 2001. A Study on Automatic Ship Berthing Using Parallel Neural Controller. *Journal of Kansai Society of Naval Architects of Japan*, vol. 236, pp. 65-70.
16. Im, N.K. and Hasegawa, K. March, 2002. A Study on Automatic Ship Berthing Using Parallel Neural Controller (2nd Report). *Journal of Kansai Society of Naval Architects of Japan*, vol. 237, pp.127-132.
17. Im, N.K. *et al*. November, 2007. An Application of ANN to Automatic Ship Berthing using Selective Controller. *Journal on Marine Navigation and safety of Sea Transportation*, vol. 1, pp.101-105.
18. Nguyen, P.H. *et al*. October, 2007. Automatic Berthing Control of Ship using Adaptive Neural Network. *International Symposium on Electrical & Electronics Engineering*. HCM City, Vietnam.
19. Ohtsu, K. *et al*. 2007. Minimum Time Ship Manoeuvring Method Using Neural Network and Nonlinear Model predictive Compensator. *Journal of Control Engineering Practice*, vol. 15, issue 6, pp.757-765.
20. Xu, G. and Hasegawa, K. 2012. Automatic Berthing Using Artificial Neural Network on Teaching data Generated by Optimal Steering. *Conference at The Japan Society of Naval Architects and Ocean Engineers*, vol.14. pp.295-298.
21. Kose, K. *et al*. December, 1986. On a Computer Aided Manoeuvring System in Harbours. *Journal of Society of Naval Architects of Japan*, vol. 160, pp.103-110. (in Japanese)

22. Nakata, M. and Hasegawa, K. 2003. A Study on Automatic Berthing Using Artificial Neural Network- Verification of Model Ship Berthing Experiments. *Journal of Kansai Society of Naval Architects of Japan*, vol. 240, pp. 145-150.
23. Tran, V.L. and Im, N.K. 2012. A Study on Automatic Berthing with Assistance of Auxiliary Devices. *Journal of Naval Architecture and Ocean Engineering*, vol. 4, pp.199-210. Korea.
24. Hasegawa, K. *et al.* December, 1986. Ship Auto-Navigation Fuzzy Expert System (SAFES), *Journal of Society of Naval Architects of Japan*, pp.445-452.
25. Hasegawa, K. September, 1990. Automatic Navigator-Included Simulation for Narrow and Congested Waterways. *Proc. of Ninth Ship Control Systems Symposium*, vol.2, pp.110-134.
26. Hasegawa, K. October, 1993. Knowledge-Based Automatic Navigation System for Harbour Manoeuvring. *Proc. of tenth Ship Control system Symposium*, vol.2, pp.67-90.
27. Ahmed, Y.A. 2012. Automatic Ship Berthing using Artificial Neural Network based on Virtual Window Concept in wind Condition. *Master Thesis paper, Osaka University*.
28. The Specialist Committee on Esso Osaka. 2002. Final Report and Recommendations to the 23rd ITTC. *Proceedings of the 23rd ITTC*, Vol. 2, pp.573-609.
29. Ueda, N. and Ueno, M. A. March, 1982. A comparative Study on Experimental Results for Manoeuvring Hydrodynamic Coefficients (in Japanese). *Bachelor Thesis paper, Osaka University*.
30. Fujiwara, T. *et al*. 1998. Estimation of wind forces and moment acting on ships. *Journal of the Society of Naval Architecture of Japan* , vol. 183, pp.77-90.
31. Davenport, A.G. 1967. The Dependence Wind Loads on Meteorological Parameters. *Proc. Of Conference on Wind Effects on Buildings and Structures*.
32. Okazaki, T. and Ohtsu, K. 2008. A Study on Ship Berthing Support System. *IEEE International Conference on System, Man and Cybernetics*, pp.1522-1527.
33. More, J. June,1977. The Lavenberg-Marquardt Algorithm: Implementation and Theory. *Conference on Numerical Analysis,* Dundee, UK.
34. Endo, M. and Hasegawa, K. August, 2003. Passage Planning System for Small

Inland Vessels Based on Standard Paradigms and Manoeuvres of Experts. *MARSIM'03*, vol._, pp.RB-19-1-RB-19-9.

35. Yoshimura, Y. and Nomoto, K. November, 1978. Modeling of Manoeuvreing behaviour of Ships with a propeller Idling, Boosting and Reversing. *Journal of the Society of Naval Architects of Japan,* vol. 144, pp.57-69.
36. Im, N.K. and Seo, J.H. March, 2010. Ship Manoeuvring Performance Experiments using a Free Running Model Ship. *Journal on Marine Navigation and Safety of Sea Transportation*, vol. 4, pp.29-33.
37. A Master's Guide to Berthing, Berthing in Wind. Source: http://www.shipinspection.eu/index.php/the-mariner-s-handbook/a-master-s-guide-to-berthing/item/462-berthing-in-wind
38. Bui, V. P. *et al*. October, 2010. Modelling and Control Allocation for Ship Berthing System Design. *International Conference on Control, Automation and Systems,* pp.195-200.
39. Tzeng, C.Y. *et al*. October, 2006. Autopilot Design for Track-keeping and Berthing of a Small Boat. *IEEE International Conference on System, Man and Cybernetics*, pp.669-674.

LIST OF TABLES

LIST OF FIGURES

ACKNOWLEDGEMETS

I would like to express my sincere gratitude to my supervisor Prof. Kazuhiko Hasegawa for accepting me as a graduate student in the Department of Naval Architecture and Ocean Engineering, Osaka University. This research would not be possible without his valuable advice, patient guidance, enthusiastic encouragement and useful critiques.

I also gratefully acknowledge Prof. Naomi Katou and Associate Prof. Naoya Umeda for kindly agreeing to be the members of the reviewing committee for this thesis.

It is also a great pleasure to express my gratitude to Dr. Makino for his views and suggestions regarding this thesis and helping to meet with tug masters to know valuable parameters and way of operating tugs. I am thankful to Prof. Wakabayashi at Kobe University to allow me to ride on Fukaye Maru to observe its berthing operation. Special thanks to Dr. Amin Osman to make me understand about the basic things of manoeuvring and also Dr. Kyoung Gun Oh for helping me to know about the free running experiment.

Throughout my entire stay in Hasegawa laboratory, I have met with many students studied in Master and Bachelor courses. Many of them helped me with the daily necessities and doing free running experiments. Without their help, the experiments would not be possible. I would like to thank all members of Hasegawa Laboratory, especially Mr. Zobair, Ms. Jyotsna, Mr. Usada, Mr. Kayaida, Mr. Sakai and Mr. Fujimoto for supporting me and make my stay happier.

I am thankful to the Ministry of Education, Science and Culture (MEXT), Government of Japan for providing me the opportunity to study at Osaka University and get generous financial support throughout my study.

There is a small Bangladeshi community at Osaka University who always helps and supports each other. I would like to thank all the members of this community for the pleasant moments that they share with my family.

I really would like to share the accomplishment of this thesis with my lovely wife, Sofia Akter Noor, who supported me during my research with endless patience and sacrifices.

Finally, on a personal note, I would like to express my heartfelt thanks to my creator Allah for helping me to complete my PhD degree successfully. I know he will continue his blessings for my upcoming future. I am also grateful to our parents for their endurance, support and prayers. I would not be able to achieve anything in my life without them.

LIST OF PUBLICATIONS

Journal papers

1. **Ahmed, Y. A.** and Hasegawa, K. November, 2013. Automatic Ship Berthing using Artificial Neural Network Trained by Consistent Teaching Data using Non-Linear Programming Method. *Journal of Engineering Applications of Artificial Intelligence*, vol. 26, issue 10, pp.2287-2304.
2. **Ahmed, Y. A.** and Hasegawa, K. September, 2015. Consistently Trained Artificial Neural Network for Automatic Ship Berthing Control. *Conference and Journal of Marine Navigation and Safety of Sea Transportatio*n.

Conference Proceedings

1. **Ahmed, Y. A,** and Hasegawa, K. September, 2012. Automatic Ship Berthing using Artificial Neural Network Based on Virtual Window Concept in Wind Condition. *Proc. of the 13th IFAC Symposium on Control in Transportation Systems*, pp.359-364. Sofia, Bulgaria.
2. **Ahmed, Y. A.** and Hasegawa, K. September, 2013. Implementation of Automatic Ship Berthing using Artificial Neural Network for Free Running Experiment. *Proc. of the 9th IFAC Conference on Control Applications in Marine Systems*, vol. 9, pp.25-30, Osaka, Japan.
3. **Ahmed, Y. A.** and Hasegawa, K. August, 2014. Experiment Results for Automatic Ship berthing using Artificial Neural Network Based Controller. *The 19th World Congress of International Federation of Automatic Control*, pp. 2658-2663. Cape Town, South Africa.
4. **Ahmed, Y. A.** and Hasegawa, K. December, 2014. Artificial Neural Network based Automatic Ship Berthing Combining PD Controller Side Thrusters. *The 13th International Conference on Control, Automation, Robotics and Vision*, pp.1304-1309, Singapore.

Seminar

1. **Ahmed, Y. A.** and Hasegawa, K. 2013. Automatic Ship Berthing Experiment using Artificial Neural Network Based on Virtual Window Concept. *The 16th Academic Exchange Seminar between Osaka University and Shanghai Jiao Tong University*.

Appendix A: MANOEUVRING MATHEMATICAL GROUP (MMG) MODEL

A.1 Hydrodynamic Forces and Moment Acting on a Hull

The hydrodynamic forces and moment acting on the hull during manoeuvring are usually expressed as a combination of linear and non-linear terms. The hydrodynamic forces and moment, considering advance and astern motions can be described by the following equations.

(i) Advance (u>0)

$$\begin{aligned} X_H &= \frac{\rho}{2} LdU^2 \left(X_{uu}\acute{}(0) + X_{\beta\beta}\acute{}\beta\acute{}^2 + X_{\beta r}\acute{}\beta\acute{}\dot{r}\acute{} + X_{rr}\acute{}\dot{r}\acute{}^2 + X_{\beta\beta\beta\beta}\acute{}\beta\acute{}^4 \right) \\ Y_H &= \frac{\rho}{2} LdU^2 \{ Y_{\beta}\acute{}\beta + Y_{\dot{r}}\acute{}\dot{r}\acute{} + Y_{\beta\beta}\acute{}\beta\acute{}|\beta| + Y_{rr}\acute{}\dot{r}\acute{}|r| + (Y_{\beta\beta r}\acute{}b + Y_{\beta rr}\acute{}\dot{r}\acute{})\beta\dot{r}\acute{} \} \\ N_H &= \frac{\rho}{2} LdU^2 \{ N_{\beta}\acute{}\beta + N_{\dot{r}}\acute{}\dot{r}\acute{} + N_{\beta\beta}\acute{}\beta\acute{}|\beta| + N_{rr}\acute{}\dot{r}\acute{}|r| + (N_{\beta\beta r}\acute{}b + N_{\beta rr}\acute{}\dot{r}\acute{})\beta\dot{r}\acute{} \} \end{aligned} \tag{A.1}$$

(ii) Astern (u<0)

$$\begin{aligned} X_H &= \frac{\rho}{2} LdU^2 (X'_{vrs} v'r' + X'_{uus}|u'|u') \\ Y_H &= \frac{\rho}{2} LdU^2 (Y'_{vr} + Y'_{rs} r' + Y'_{rrs}|r'|r' + Y'_{\beta r}|\beta_{NL}\cos(\beta_{NL})|r') \\ N_H &= \frac{\rho}{2} \mathrm{L}^2 dU^2 (N'_{vr} + N'_{rs} r' + N'_{rrs}|r'|r' + N'_{\beta\beta rs}(\beta_{NL}\cos(\beta_{NL}))^2 r' \\ &\quad + N'_{\beta rrs}|\beta_{NL}\cos(\beta_{NL})r'|r') \end{aligned} \tag{A.2}$$

Where,

If $|\beta| \leq \frac{\pi}{2}$

$$\beta_{NL} = \beta \tag{A.3}$$

If $|\beta| > \frac{\pi}{2}$,

$$\beta_{NL} = (\pi - |\beta|)sin(\beta) \tag{A.4}$$

Here, Y'_{vr} is calculated as follows:

If $|\beta| \leq C_{y1}$

$$Y'_{vr} = C_{y1}\beta|\beta| + C_{y1}\beta \tag{A.5}$$

If $|\beta| > C_{y1}$ *and* $|\beta| \leq C_{y2}$

$$Y'_{vr} = C_{y3}\beta|\beta| + C_{y4}\beta + sgn(\beta) \tag{A.6}$$

If $|\beta| > C_{y2}$

$$Y'_{vr} = C_{y6}|\beta - sgn(\beta)\pi|(\beta - sgn(\beta)\pi) + C_{y7}(\beta - sgn(\beta)\pi) \tag{A.7}$$

N'_{vr} is calculated as follows:

If $|\beta| \leq C_{n1}$

$$N'_{vr} = C_{n1}\beta|\beta| + C_{n1}\beta \tag{A.8}$$

If $|\beta| > C_{n1}$ *and* $|\beta| \leq C_{n2}$

$$N'_{vr} = C_{n3}\beta|\beta| + C_{n4}\beta + sgn(\beta) \tag{A.9}$$

If $|\beta| > C_{n2}$

$$N'_{vr} = C_{n6}|\beta - sgn(\beta)\pi|(\beta - sgn(\beta)\pi) + C_{n7}(\beta - sgn(\beta)\pi) \tag{A.10}$$

.

A.2 Propeller Thrust

Propeller thrust can be described by longitudinal force of a propeller. The following expression is used to calculate propeller thrust.

(i) Advance (n>=0)

$$X_P = \rho {D_P}^4 n^2 (1-t) K_T$$
$$Y_P = 0 \qquad \text{(A.11)}$$
$$N_P = 0$$

Where,

$$\mathrm{K_T(J)} = \mathrm{C_1 J} + C_2 \mathrm{J} + \mathrm{C_3 J}^2 \qquad \text{(A.12)}$$
$$J = u_P/(nD_P) \qquad \text{(A.13)}$$
$$u_P = u(1-w_P) \qquad \text{(A.14)}$$
$$1 - w_P = (1-w_{P0}) + \tau|v' + x'_P r'| + C'_P (v' + x'_P r')^2 \qquad \text{(A.15)}$$

(ii) Astern (n<0)

$$X_P = \rho X^*_P D_P^2 (nD_P)^2$$
$$Y_P = \frac{\rho}{2} Y^*_P L d (nD_P)^2 \qquad \text{(A.16)}$$
$$N_P = \frac{\rho}{2} N^*_P L^2 d (nD_P)^2$$

X force is divided depending on the advance coefficient J_S as follows:

$$J_S = \frac{u}{nD_P} \qquad \text{(A.17)}$$

If $J_S \geq 0$

$$X^*_P = C_4 + C_5 J_S \qquad \text{(A.18)}$$

If $J_{St'} < J_S < 0$

$$X_P^* = C_6 \tag{A.19}$$

If $J_S < J_{St'}$

$$X_P^* = C_8 + C_7 J_S \tag{A.20}$$

Y force and N moment are divided as follows:

If $J_{syn0} < J_S < J_{syn}$

$$\begin{aligned} Y_P^* &= A_1 + A_2 J_S \\ N_P^* &= B_1 + B_2 J_S \end{aligned} \tag{A.21}$$

If $J_S < J_{syn}$

$$\begin{aligned} Y_P^* &= A_3 + A_4 J_S \\ N_P^* &= B_3 + B_4 J_S \end{aligned} \tag{A.22}$$

If $J_S > J_{syn0}$

$$\begin{aligned} Y_P^* &= A_5 \\ N_P^* &= B_5 \end{aligned} \tag{A.23}$$

A.3 Rudder Force and Moment

The hydrodynamic forces and moment generated by rudder angle can be expressed by using rudder normal force and rudder angle as follows:

(i) Advance (*n*>=0)

$$X_R = -\frac{\rho}{2} L d U^2 (1 - t_R) F_N \sin\delta \tag{A.24}$$

$$Y_R = -\frac{\rho}{2} LdU^2(1 + a_H)F_N \cos\delta$$

$$N_R = -(\frac{\rho}{2} Ld^2U^2)(x_R + a_H x_H)F_N \cos\delta$$

where,

$$F_N = \frac{A_r}{Ld} f {U_R}^2 sin\alpha_R \quad \text{(A.25)}$$

$$f = \frac{6.13\lambda}{\lambda + 2.25} \quad \text{(A.26)}$$

$${U_R}^2 = (1 - w_R)^2\{1 + Cg(s)\} \quad \text{(A.27)}$$

$$g(s) = \frac{\eta K(2 - (2 - K)s)s}{(1 - s)^2} \quad \text{(A.28)}$$

$$\eta = D_P/h_R \quad \text{(A.29)}$$

$$K = 0.6(1 - w_P)/(1 - w_R) \quad \text{(A.30)}$$

$$s = 1.0 - (1 - w_R)Ucos\beta/nP \quad \text{(A.31}$$

$$w_R = w_{R0}w_P/w_{P0} \quad \text{(A.32)}$$

$$\alpha_R = \delta - \gamma\beta'_R \quad \text{(A.33)}$$

$$\beta'_R = \beta - 2x_R r' \quad \text{(A.34)}$$

(ii) Astern (n<0)

$$X_R = 0$$
$$Y_R = 0 \quad \text{(A.35)}$$
$$N_R = 0$$

A.4 All Hydrodynamic Derivatives

Hydrodynamic derivatives regarding hull, propeller and rudder for both forward and astern motion are given in Table A.1

Table: A.1 Hydrodynamic derivatives

m'	*0.2709*	m'_x	*0.02*	m'_y	*0.2224*	I'_{zz}	*0.0172*
J'_{zz}	*0.00821*	X'_{uu}	*-0.02639*	$X'_{\beta r}$	*0.191559*	$X'_{\beta\beta\beta\beta}$	*0.2751225*
X'_{rr}	*0.012856*	$X'_{\beta\beta}$	*0.022823*	X'_{vrs}	*0.495*	X'_{uus}	*-0.03189*
Y'_{β}	*0.3039*	Y'_{r}	*0.0908104*	$Y'_{\beta\beta}$	*0.5454883*	$Y'_{\beta\beta r}$	*0.214706*
Y'_{rr}	*-0.000143*	$Y'_{\beta rr}$	*0.332125*	Y'_{rs}	*0.0519*	Y'_{rrs}	*0.32*
N'_{β}	*0.112252*	N'_{r}	*-0.063663*	$N'_{\beta\beta}$	*0.051978*	$N'_{\beta\beta r}$	*-0.27805*
N'_{rr}	*0.0027571*	N'_{brr}	*-0.02597*	N'_{rs}	*-0.0365*	N'_{rrs}	*-0.016*
$N'_{\beta\beta rs}$	*-0.111*	$N'_{\beta rrs}$	*-0.0855*	C_{y1}	*0.393*	C_{y2}	*0.404*
C_{y3}	*-0.632*	C_{y4}	*1.99*	C_{y5}	*-0.609*	C_{y6}	*-0.393*
C_{y7}	*-0.404*	C_{n1}	*-0.0671*	C_{n2}	*0.123*	C_{n3}	*0*
C_{n4}	*-0.126*	C_{n5}	*0.166*	C_{n6}	*0.1108*	C_{n7}	*0.0802*
t	*0.2*	w_{P0}	*0.4710*	x'_P	*-0.5*	C_1	*0.32*
C_2	*-0.2466*	C_3	*-0.2668*	C_4	*-0.146*	C_5	*0.28*
C_6	*-0.257*	C_7	*0.51*	C_8	*-0.14*	τ	*1.45*
C'_P	*-0.359*	A_1	*-7.9e-5*	A_2	*7.99e-3*	A_3	*-4.93e-3*
A_4	*-5.87e-3*	A_5	*-5.58e-4*	B_1	*3.5e-5*	B_2	*-3.17e-3*
B_3	*1.96e-3*	B_4	*2.33e-3*	B_5	*2.25e-4*	$J_{St'}$	*-0.6*
J_{syn}	*-0.35*	J_{syn0}	*-0.06*	t_R	*0.2173*	a_H	*0.398*
x_R	*-0.82*	x_H	*-0.442*	A_r/Ld	*1/59.1*	λ	*1.599*
h_R	*0.1278*	w_{R0}	*0.1792*	γ_{port}	*0.19*	γ_{stbd}	*0.23*

Appendix B: FUJIWARA WIND MODEL

The coefficients mentioned in Equation 2.2 can be defined as follows:

$$\begin{aligned} C_X &= X_0 + X_1 cos\psi_{RW} + X_3 cos3\psi_{RW} + X_5 cos5\psi_{RW} \\ C_Y &= Y_1 sin\psi_{RW} + Y_3 sin\,3\psi_{RW} + Y_5 sin5\psi_{RW} \\ C_N &= N_1 sin\psi_{RW} + N_2 sin2\psi_{RW} + N_3 sin3\psi_{RW} \end{aligned} \tag{B.1}$$

where,

$$Relative\ wind\ direction, \psi_{RW} = \text{atan}\left(\frac{U_{WR}}{V_{WR}}\right) \tag{B.2}$$

$$X_0 = x_{00} + x_{01}\frac{BH_{BR}}{A_T} + x_{02}\frac{C}{H_C} + x_{03}\frac{A_{OD}}{L^2} \tag{B.3}$$

$$\begin{aligned} X_1 = x_{10} + x_{11}\frac{A_L}{LB} + x_{12}\frac{LH_C}{A_L} + x_{13}\frac{LH_{BR}}{A_L} + x_{14}\frac{A_{OD}}{A_L} + x_{15}\frac{A_T}{LB} + x_{16}\left(\frac{A_T}{L^2}\right)^{-1} \\ + x_{17}\left(\frac{H_C}{L}\right)^{-1} \end{aligned} \tag{B.4}$$

$$\begin{aligned} X_3 = x_{30} + x_{31}\left(\frac{LH_{BR}}{A_L}\right)^{-1} + x_{32}\frac{A_L}{A_T} + x_{33}\frac{LH_C}{A_L} + x_{34}\frac{A_{OD}}{A_L} + x_{35}\frac{A_{OD}}{L^2} + x_{36}\frac{C}{H_C} \\ + x_{37}\frac{C_{BR}}{L} \end{aligned} \tag{B.5}$$

$$X_5 = x_{50} + x_{51}\left(\frac{A_{OD}}{A_L}\right)^{-1} + x_{52}\frac{C_{BR}}{L} + x_{53}\frac{A_L}{LB} \tag{B.6}$$

$$Y_1 = y_{10} + y_{11}\frac{C_{BR}}{L} + y_{12}\frac{C}{L} + y_{13}\left(\frac{A_{OD}}{A_L}\right)^{-1} + y_{14}\frac{C}{H_C} + y_{15}\left(\frac{BH_{BR}}{A_T}\right)^{-1} \tag{B.7}$$

$$Y_3 = y_{30} + y_{31}\frac{A_L}{LB} + y_{32}\frac{LH_C}{A_L} + y_{33}\frac{C_{BR}}{L} + y_{34}\left(\frac{H_{BR}}{B}\right)^{-1} + y_{35}\frac{A_{OD}}{A_L} + y_{36}\left(\frac{BH_{BR}}{A_T}\right)^{-1} \tag{B.8}$$

$$Y_5 = y_{50} + y_{51}\frac{A_L}{LB} + y_{52}\left(\frac{H_{BR}}{L}\right)^{-1} + y_{53}\frac{C_{BR}}{L} + y_{54}\left(\frac{A_T}{B^2}\right)^{-1} + y_{55}\frac{C}{L} + y_{56}\frac{LH_C}{A_L} \tag{B.9}$$

$$N_1 = n_{10} + n_{11}\frac{C}{L} + n_{12}\frac{LH_C}{A_L} + n_{13}(\frac{A_L}{A_T})^{-1} + n_{14}\frac{C}{H_C} + n_{15}\frac{A_L}{LB} + n_{16}\ \frac{A_T}{L^2} + n_{17}\,(\frac{A_T}{B^2})^{-1} + n_{18}\,\frac{C_{BR}}{L} \tag{B.10}$$

$$N_2 = n_{20} + n_{21}\frac{C_{BR}}{L} + n_{22}\frac{C}{L} + n_{23}(\frac{A_{OD}}{A_L})^{-1} + n_{24}\ \frac{A_T}{B^2} + n_{25}(\frac{H_{BR}}{L})^{-1} + n_{26}\ (\frac{BH_{BR}}{A_T})^{-1} + n_{27}\ \frac{A_L}{LB} + n_{28}\ \frac{A_L}{L^2} \tag{B.11}$$

$$N_3 = n_{30} + n_{31}\frac{C_{BR}}{L} + n_{32}(\frac{BH_{BR}}{A_T})^{-1} + n_{33}\ \frac{A_L}{A_T} \tag{B.12}$$

To calculate the above coefficients, necessary parameters are given in Table B.1.

Table. B.1 Coefficient of independent variables

m=		**0**	**1**	**2**	**3**	**4**	**5**	**6**	**7**	**8**
C_X	X_{0m}	-0.330	0.293	0.0193	0.682					
	X_{1m}	-1.353	1.70	2.87	-0.463	-0.570	-6.640	-0.0123	0.0202	
	X_{3m}	0.830	-0.413	-0.0827	-0.563	0.804	-5.67	0.0401	-0.132	
	X_{5m}	0.0372	-0.0075	-0.103	0.0921					
C_Y	y_{0m}	0.684	0.717	-3.22	0.0281	0.0661	0.298			
	y_{1m}	-0.40	0.282	0.307	0.0519	0.0526	-0.0814	0.0582		
	y_{3m}	0.122	-0.166	-0.0054	-0.0481	-0.0136	0.0864	-0.0297		
C_N	n_{0m}	0.299	1.71	0.183	-1.09	-0.0442	-0.289	4.24	-0.0646	0.0306
	n_{1m}	0.117	0.123	-0.323	0.0041	-0.166	-0.0109	0.174	0.214	-1.06
	n_{3m}	0.0230	0.0385	-0.0339	0.0023					